



Cape Peninsula
University of Technology

**AN ANALYSIS AND IMPROVEMENT OF SELECTED FEATURES OF POWER
QUALITY OF GRID-TIED ALTERNATIVE ENERGY SYSTEMS**

by

GUNJAN GUPTA

Thesis submitted in fulfilment of the requirements for the degree

Doctor of Technology: Electrical Engineering

in the Faculty of Engineering

at the Cape Peninsula University of Technology

Supervisor: Prof. Wilfred Fritz

Co-supervisor: Prof. Mohamed Tariq Kahn

Bellville

April 2018

CPUT copyright information

The dissertation/thesis may not be published either in part (in scholarly, scientific or technical journals), or as a whole (as a monograph), unless permission has been obtained from the University

DECLARATION

I, **Gunjan Gupta**, declare that the contents of this thesis represent my own unaided work, and that the thesis has not previously been submitted for academic examination towards any qualification. Furthermore, it represents my own opinions and not necessarily those of the Cape Peninsula University of Technology.



Signed

10 April 2018
Date

LIST OF PUBLICATIONS

Journal Publications

- 1 **Gupta, G.**, Fritz, W., M.T.E. Kahn: *Enhancement in Distribution Power Quality Using D-STATCOM with Phase Faults*. International Journal of Applied Engineering Research, ISSN 0973-4562 Volume 12, Number 21 (2017) pp. 11441-11446.
- 2 **Gupta, G.**, Fritz, W., M.T.E. Kahn: *A Comprehensive Review of DSTATCOM: Control and Compensation Strategies*. International Journal of Applied Engineering Research ISSN 0973-4562 Volume 12, Number 12 (2017) pp. 3387-3393.

Conference Publications

- 3 **Gupta, G.**, Fritz, W. (2016): *Probabilistic Model for Residential Load Profiles and Power Quality Improvement*. In the Proceedings of the Domestic use of energy DUE2016 Conference at the Cape Peninsula University of Technology, Cape Town, South Africa, 29-31 March 2016: 50-54. ISBN 978-0-9946759-0-3.
- 4 **Gupta, G.**, Fritz, W. (2016): *Power Quality Monitoring by Advanced Mathematical Tools: A Survey*. In the Proceedings of the 1st IEEE International Conference on Power Electronics. Intelligent Control and Energy Systems (ICPEICES-2016), 4-6 July 2016. ISBN 978-1-4673-8587-9.
- 5 **Gupta, G.**, Fritz, W. (2016): *Voltage Unbalance for Power Systems and Mitigation Techniques a Survey*. In the Proceedings of the 1st IEEE International Conference on Power Electronics. Intelligent Control and Energy Systems (ICPEICES-2016), 4-6 July 2016. ISBN 978-1-4673-8587-9.
- 6 **Gupta, G.**, Fritz, W. (2017): *Control algorithms for a three-phase Shunt Compensator – A comparative study*. In the Proceedings of the 3rd IEEE International Conference on Computational Intelligence and Communication Technology (IEEE-CICT 2017), 9-10 February 2017. ISBN 978-1-5090-6218-8.
- 7 **G. Gupta**, W. Fritz and M.T.E. Kahn. *Power Quality and Power Control of a Wind Turbine Utilizing a STATCOM*. 25th Southern African Universities Power Engineering Conference SAUPEC 2017, poster paper.

- 8 **G. Gupta**, W. Fritz and M.T.E. Kahn. *Comprehensive Study of Improvement of Power Quality Parameters of Grid Tied Alternative Systems using DSTATCOM*. 25th Southern African Universities Power Engineering Conference SAUPEC 2017, poster paper.

ABSTRACT

Electrical energy can be easily used and converted to other forms of energy for various applications. Technological advancement increases the dependency on electricity to a great extent. Various internal and external factors are responsible for the bad quality of power in power systems. The performance of the system is greatly affected by the presence of harmonics, as well as voltage and frequency variations, which leads to the malfunctioning of the device and decline of power quality and supply at load side. The reactive power compensation is carried out for better power quality.

The literature survey is done to find the best and efficient scheme for reactive power compensation and mitigation of various power quality problems. The devices which are used to measure various power quality factors are discussed. Various mitigating schemes are surveyed in order to compensate reactive power and to improve the power quality at the distribution end.

The integration of the most widely used renewable energy, wind energy in the distribution system creates technical issues like stability of the grid, harmonic distortion, voltage regulation, active and reactive power compensation etc. which are restricted to IEC and IEEE standards. One of the topics this thesis addresses is regulation in the reactive power generated along with voltage regulation by using an effective power electronics device known as a STATCOM. The main power quality factors like overvoltage and voltage flickers are mitigated by establishing STATCOMs in small wind farms. The wind farms are equipped with three wind turbines. These three wind turbines found in the wind farm can be operated together or one after another with an introduced delay.

A glitch in even a little piece of a power grid can result in loss of efficiency, income and at times even life. In this manner, it is basic to outline a system which can distinguish the faults of the power system and take a faster response to recover it back to required reactive power. Two devices STATCOM and D-STATCOM are used for this purpose in this thesis.

The D-STATCOM circuit and operating principle are also discussed in thesis. Different topologies of D-STATCOM discussed with their benefits and shortcomings. The voltage, current and hybrid technologies of D-STATCOM are also discussed.

In this thesis, the following novel work have been done along with verification of already available work in literature. These are:

1. A 3-phase fault introducing block is used on a distribution line. The block can introduce fault(s) in any of the three phases A, B, or C. The D-STATCOM is used to compensate the reactive power on the line due to introduced faults.
2. A small distribution grid is used with a single feeder and four distribution points. The position of STATCOM is fixed and the loads considered are of variable nature like industrial unit, University etc.
3. This work in (2) is further extended by using a STATCOM of 50% KVA and with droop control. The distributed energy resources (DERs) are also used on the line and STATCOM is used for compensation.
4. The STATCOM is used for reactive power compensation when wind farms are used to provide energy to distribution lines. The STATCOM is used both in series and parallel.
5. The verification of already available work is also done, which compares the performance of D-STATCOM and Static VAR Compensation (SVC) for reactive power compensation.

A steady transmission of power is required on transmission line, the occurrence of faults results in error or failure of steady transmission. To address this problem an efficient device, a D-STATCOM, is used for both voltage and reactive power compensation in distribution grids for better power quality. The reactive power compensation is one of the important parameter to improve the power quality at the distribution end. The faults are introduced in all phases together, two phases at a time or single phase. The use of D-STATCOM compensates voltage and reactive power. A breaker circuit with extra load is also introduced in the distribution line, the load presence is dynamic. The D-STATCOM compensates by absorbing or supplying reactive power. The MATLAB/Simulink environment is used for providing compensation using D-STATCOM in presence of the faults introduced in different phases and extra load in presence of a circuit-breaker. The 25 kVA, 100 MVA distribution is studied in the presence of faults in 3-phases.

A STATCOM can also be used to control power system voltages. The STATCOM is also used for providing compensation of reactive power on the distribution line. The STATCOM is placed at different points along the line, in the presence of light and heavy loads as well as power factor correction capacitors and the consideration for droop control. A MATLAB/Simulink-based model is used for simulation. The result shows that a shunt-

connected STATCOM gives better voltage control than the STATCOM connected in series at the end of the feeder.

The work done in the thesis uses STATCOM phasor model for distribution line with wind energy and distribution line with different loads connected along the line. The D-STATCOM is used for lines with breaker circuit and in presence of faults. The reactive power compensation is addressed along with voltage compensation which are not addressed together in literature.

The work improves the reactive power compensation capability of the grid with stability. The used compensating devices provides compensation using control strategies which are less complex and cost effective. The point of common coupling (PCC) of the device STATCOM or D-STATCOM emanates as an important factor which influences reactive power performance of the grid. With increase in distance from PCC the reactive power compensation of these devices decreases.

ACKNOWLEDGEMENTS

I would like to thank my supervisors Prof. Wilfred Fritz and Prof. Mohamed Tariq Kahn for their incredible support and huge understanding and efficiency. I am extremely privileged to have this done due to such supervision and assistance. Without them, I would not have accomplished this.

DEDICATION

I would like to dedicate this thesis to a very special person, my husband, Dr. Vipin Balyan, for his continued and unfailing love, support and understanding during my pursuit of Ph.D degree that made the completion of thesis impossible. I greatly value his contribution and deeply appreciate his belief in me. I extend my dedication to my little boy, Advik, for abiding my ignorance and the patience he showed during my thesis writing.

GLOSSARY

APF	Active Power Filter
BESS	Battery Energy Storage System
BP	Back Propagation
BPFF	Back Propagation Feed Forward
BSS	Battery Storage System
CO ₂	Carbon-di-oxide
CSC	Convertible Series Compensator
CTF	Character Of Triangle Function
DC	Direct Current
DE	Diesel Engine
DER	Distributive Energy Resource
Dev.	Deviation
DFIG	Doubly Fed Induction Generator
DG	Distribution Grid
DSP	Digital Signal Processor
DSP	Digital Signal Processor
DSTATCOM	Distribution Static Compensator
D-STATCOM	Distribution Static Synchronous Compensator
DT-CWT	Dual Tree Complex Wavelet Transform
DVR	Dynamic Voltage Restorer
EPLL	Enhanced Phase Locked Loop
FFRLS	Variable Forgetting Factor Recursive Least Square
FRC	Fully Rated Converter
FSIG	Fixed Speed Induction Generator
GCT	Gate commutated Thyristor
GW	Giga Watts
HPF	High Pass Filter
HVDC	High Voltage Direct Current
IAG	Isolated Asynchronous Generator
IG	Induction Generator
IGBT	Insulated Gate Bipolar Transistor

ILST	Improved Linear Sinusoidal Tracer
InC	Incremental Conductance
IPFC	Inter-Phase Power Flow Controller
IRPT	Instantaneous Reactive Power Theory
KIMEL	Kernel Incremental Meta-learning Algorithm
KV	Kilo Volt
kW	Kilo Watts
kWh	Kilo Watt Hours
LMS	Least-mean-square
LPF	Low Pass Filter
Max.	Maximum
MEPLL	Modified Enhanced Phase Locked Loop
MHP	Micro-Hydro Power Turbine
MISCT	Modified Instantaneous Symmetrical Component Theory
MLANN	Multilayer Artificial Neural Network
MMC	Modular Multilevel Converter
MOSFET	Metal Oxide Field Effect Transistor
MPPT	Maximum Power Point Tracking
MW	Mega Watts
NN	Neural Network
OPEC	Organization of Petroleum Exporting Countries
p.u	Per unit
PEF	Percentage Error Feedback
PFC	Power Factor Correction
PI	Proportional and Integral
PLL	Phase Locked Loop
PMSG	Permanent Magnet Synchronous Generator
PQ	Power Quality
PV-UPQC	Photo-Voltaic Unified Power Quality Conditioner
PWM	Pulse Width Modulation
RAD	Round Adaptive Detection
RTRL	Real Time Recurrent Learning
SAPF	Shunt active power filter
SCIG	Squirrel Cage Induction Generator
SCR	Silicon-controlled rectifier
SECS	Solar Energy Conversion System
SEIG	Self-Excited Induction Generator

SM	Sub Module
SMES	Super Conducting Magnetic Energy Storage
SMPS	Switched Mode Power Supply
SOGI-Q	Second Order Generalized Integer Quadrature
SPLL	Software Phase Locked Loop
SPS	Sim Power System
SRF	Synchronous Reference Frame
SSSC	Static Synchronous Series Controller
SSTS	Solid State Transfer Switch
STATCOM	Static Synchronous Compensator
SVC	Static VAR (Volt-Ampere Reactive) Compensator
SyRG	Synchronous Reluctance Generator
TCPST	Thyristor Control Phase Shifting Transformer
TCSC	Thyristor Controlled Series Compensator
THD	Total Harmonic Distortion
UPFC	Unified Power Flow Controller
VFC	Voltage Frequency Controller
VFIMD	Variable Frequency Induction Motor Drive
VSC	Voltage Source Converter
VSI	Voltage Source Inverter
VSS-FXLMS	Variable Step size Filtered-X Least Mean Square
WT	Wind Turbine

TABLE OF CONTENTS

DECLARATION.....	ii
LIST OF PUBLICATIONS.....	iii
ABSTRACT.....	v
ACKNOWLEDGEMENTS.....	vii
DEDICATION.....	viii
GLOSSARY.....	ix
LIST OF FIGURES	xix
LIST OF TABLES	xxiv
CHAPTER ONE: INTRODUCTION TO POWER QUALITY.....	1
1.1 Introduction.....	1
1.2 Structure of the thesis.....	2
1.3 Problem statement.....	3
1.4 Background	3
1.4.1 Power quality and related standards.....	3
1.4.2 Power Quality monitoring and evaluation.....	5..
1.5 Power Quality problems.....	7
1.5.1 Transients.....	7
1.5.2 Long-duration voltage variations	10
1.5.3 Short-duration voltage variations	11
1.6 Voltage Unbalance	14
1.7 Waveform distortion.....	15
1.7.1 DC offset	16
1.7.2 Harmonics	16
1.7.3 Inter-harmonics.....	17
1.7.4 Notching	17

1.7.5	Noise	18
1.8	Solution of Power Quality improvement in power systems	20
1.8.1	FACTS (Flexible Alternating Current Transmission System).....	21
1.8.2	Custom Power Devices	23
1.9	Objectives of the research	25
1.10	Literature Survey	25
1.11	Research Questions	39
1.11.1	Which strategies help to achieve better Power Quality?	39
1.11.2	How is a DSTATCOM a better device than other available custom devices?..	39
1.11.3	How can basic DSTATCOM be refined to achieve good power quality at the distribution end?	39
1.11.4	Is there any Software or Hardware implementation? What is the measure that the actual problem is solved?.....	39
1.11.5	What will be done if the chosen approach does not work properly?	40
1.12	Research Design and Methodology	40
1.13	Significance of research.....	40
1.14	Expected outcomes, results and contributions of research	41
2	CHAPTER TWO: MEASUREMENT OF POWER QUALITY PROBLEMS.....	42
2.1	Introduction.....	42
2.2	Organization of the chapter.....	42
2.3	Power quality measurement devices	43
2.4	Wiring and grounding testers	43
2.4.1	Multimeters.....	45
2.4.2	Digital meters.....	46
2.4.3	Oscilloscopes	46
2.4.4	Disturbance analysers	47
2.4.5	Spectrum and harmonic analysers.....	48
2.4.6	Combination disturbance and harmonic analysers.....	50
2.4.7	Flicker meters	51
2.5	Future applications	52
2.5.1	Industrial power quality monitoring applications	52

2.5.2	Power system performance assessment and benchmarking	53
2.5.3	Applications for system maintenance, operations, and reliability.....	53
2.6	Summary and future direction.....	54
3	CHAPTER THREE: MITIGATION TECHNIQUES.....	57
3.1	Introduction.....	57
3.2	Organization of the chapter.....	57
3.2.1	Voltage sag mitigation	57
3.2.2	Micro-interruptions and long interruptions mitigation	68
3.2.3	Voltage spikes mitigation	70
3.2.4	Voltage swell mitigation	71
3.2.5	Voltage fluctuation mitigation	76
3.2.6	Harmonic Distortion Mitigation	83
3.2.7	Conclusion.....	86
4	CHAPTER FOUR: DSTATCOM AND ITS OPERATING PRINCIPLE	90
4.1	Introduction.....	90
4.2	Organization of the chapter.....	90
4.3	DSTATCOM and its operating principles	90
4.3.1	Transformer unbalances and non-linear loads.....	95
4.3.2	Ripple filter	97
4.3.3	AC inductor.....	97
4.4	DSTATCOM topologies	97
4.5	Three-Phase Three-Wire DSTATCOM	98
4.5.1	Non-isolated VSC-Based DSTATCOMs	99
4.5.2	Isolated VSC-Based DSTATCOMs.....	99
4.6	Three-Phase Four-Wire DSTATCOM	99
4.6.1	Non-isolated VSC without Transformers.....	100
4.6.2	Non-isolated three-Leg VSC with Transformers.....	100
4.6.3	Non-isolated Two-Leg VSC With Transformers	101
4.6.4	Isolated Three Single-Phase VSCs.....	103

4.6.5	Isolated Three-Leg VSC with Transformers:	103
4.6.6	Isolated Two-Leg VSC with Transformers.....	103
4.7	Modes of control of DSTATCOM	103
4.8	Classification according to Mitigated PQ problems	105
4.8.1	Voltage control strategies	105
4.8.2	Current Control Strategies	108
4.8.3	Inverter Technologies for DSTATCOM	109
4.8.4	Voltage and Current Control Strategies	112
4.8.5	Artificial Neural Networks.....	112
4.9	Conclusion.....	113
5	CHAPTER FIVE: GRID-CONNECTED ALTERNATIVE SYSTEMS AND REACTIVE POWER COMPENSATION USING STATCOM.....	115
5.1	Introduction.....	115
5.2	Organization of the chapter.....	116
5.3	Renewable Energy Systems Connected to Grid	116
5.4	Equipment Required for Grid-Connected Systems.....	117
5.5	Types of Grid-tied Systems.....	117
5.5.1	Solar PV Systems.....	117
5.5.2	Wind Turbines	118
5.6	Advantages of grid-tied systems	120
5.7	Wind as a source of energy	120
5.8	Wind Farms	122
5.9	Wind Energy-generating Systems.....	124
5.9.1	Power in Wind Turbines.....	124
5.10	Advantages and disadvantages of wind power	128
5.10.1	Wind power advantages	128
5.10.2	Wind power disadvantages.....	129
5.11	Classification of wind turbines.....	129
5.11.1	Wind Turbines power capacities	129
5.11.2	Geared drive and direct drive wind turbines.....	130

5.11.3	Grid-connected and off-grid wind turbines	130
5.12	Wind energy and power quality concerns	130
5.13	STATCOM and power quality improvement.....	131
5.14	Reactive Power Compensation.....	132
5.15	STATCOM and FSIG Stability.....	134
5.16	Transmission Cost of Wind Farm.....	136
5.17	Distribution grids variations with injection of wind energy.....	137
5.17.1	Effect of voltage flicker or fluctuations.....	138
5.17.2	Voltage above limits.....	138
5.17.3	Power loss.....	141
5.18	Distribution grid power compensation	141
5.18.1	STATCOM operating principle	142
5.18.2	Use of STATCOM.....	143
5.18.3	Distribution grid, STATCOM, and wind turbines model	143
5.19	Simulation results	144
5.19.1	STATCOM in series.....	144
5.19.2	STATCOM in parallel.....	144
5.20	Conclusion.....	144
6	CHAPTER SIX: MODELLING AND SIMULATION	145
6.1	Introduction.....	145
6.2	Description of DSTATCOM average model	146
6.2.1	Simulation.....	148
6.3	DSTATCOM with a three phase breaker.....	152
6.4	STATCOM Phasor model	156
6.4.1	Dynamic response	156
6.4.2	Fault condition and performance comparison of STATCOM with SVC.....	158
6.5	Power grid simulation model description.....	162
6.5.1	Single source system.....	164
6.5.2	STATCOM fixed-positions	165
6.5.3	STATCOM droop control	175

6.5.4	System with distributed energy resources.....	175
6.6	Conclusion.....	179
7	CHAPTER SEVEN: CONCLUSIONS AND FUTURE WORK	181
7.1	Objective-Specific Conclusions.....	181
7.1.1	Objective 1	182
7.1.2	Objective 2	183
7.1.3	Objective 3	183
7.1.4	Objective 4	184
7.2	Statistical Conclusion.....	185
7.3	Future Work.....	187
	REFERENCES.....	188
	APPENDIX A.....	203
	APPENDIX B.....	211

LIST OF FIGURES

Figure 1.1: Power quality evaluation procedure.....	6
Figure 1.2: Power quality problems.....	7
Figure 1.3: Current impulsive transient due to lighting	8
Figure 1.4: Oscillatory transient occurrence due to switching of back-to-back capacitor	9
Figure 1.5: Long duration voltage variations.....	11
Figure 1.6: Momentary interruption in three-phase “root mean square” voltages	12
Figure 1.7: Voltage sag associated with S-L-G faults	13
Figure 1.8: Voltage swell associated with S-L-G fault.....	14
Figure 1.9: Voltage unbalance	15
Figure 1.10: DC offset.....	16
Figure 1.11: Harmonics	17
Figure 1.12: Notching	18
Figure 1.13: FACTS and custom power devices.....	21
Figure 1.14: FACTS controller	22
Figure 2.1: Wiring and grounding tester	44
Figure 2.2: Graphics-based analyser output.....	48
Figure 2.3: Fast Fourier Transform waveforms	49
Figure 2.4: A power quality monitoring instrument capable of monitoring disturbances, harmonics on both utility systems and end-user systems.....	51
Figure 2.5: Flicker curves from IEEE standards 141 and 519	52
Figure 3.1: Direct AC-AC converter technology	58
Figure 3.2: AC chopper across line (a-b) in phase of a sag supporter	59
Figure 3.3: Prototype model of AC-chopper-based DVR	59
Figure 3.4: 8-switch conditioner using hybrid filter	61
Figure 3.5: Simulation results of the 8-switch conditioner with 3-phase voltage sag (a) DC link (b) grid and (c) load	62
Figure 3.6: ASD Typical topology	63
Figure 3.7: Series Voltage Compensator Square Wave Inverter	64
Figure 3.8: Control panel with an ASD and an induction motor	65
Figure 3.9: Interior of the test control panel with an ASD and induction motor.....	66
Figure 3.10: Compensated DSTATCOM circuit diagram.....	67
Figure 3.11: Equivalent circuit of single-phase DSTATCOM	67
Figure 3.12: Typical MV distribution grid	69
Figure 3.13: Probability density function of net present value using monte-carlo simulation.....	69

Figure 3.14: Voltage spikes recorded at the PV array terminal during inverter morning start-up	70
Figure 3.15: Frequency Dependent Surge Arrester	72
Figure 3.16: Schematic diagram of zig-zag transformer	73
Figure 3.17: Basic configuration of autotransformer	74
Figure 3.18: Voltage swell mitigation device	75
Figure 3.19: Simplified circuit diagram of SSC	75
Figure 3.20: Detailed single-phase model of SSC	76
Figure 3.21: Electrical system configuration	77
Figure 3.22: Power system single line diagram	78
Figure 3.23: Control block diagram for voltage fluctuation compensation	79
Figure 3.24: Flowchart of the proposed balancing theorem	80
Figure 3.25: Maximum normalised upper arm energy with respect to the weighting factor, k	81
Figure 3.26: Prototype MMC model	82
Figure 3.27: Structure of current compensation scheme	84
Figure 3.28: Block diagram for the control circuit.....	85
Figure 3.29: ML-ANN Scheme	86
Figure 4.1: DSTATCOM schematic diagram.....	91
Figure 4.2: A DSTATCOM with a single-phase power system.....	92
Figure 4.3: Operational characteristics of the shunt compensator (a) V-I (b) V-Q	93
Figure 4.4: Single line diagram of the DSTATCOM.....	94
Figure 4.5: Equivalent circuit of the DSTATCOM	96
Figure 4.6: Phasor diagram (a) lagging operation (b) leading operation	96
Figure 4.7: (a) Classification of 3-phase 3-wire DSTATCOM, (b) 3-leg topology of the 3-phase three-wire DSTATCOM, (c) 2-leg with split capacitor, (d) 3 single-phase topology, (e) isolated 3-leg VSC, and (f) isolated 2-leg VSC.....	98
Figure 4.8: Classification of 3-phase 4-wire DSTATCOM.....	99
Figure 4.9: D-STATCOM 3-phase and 4-wire configurations (a) 4-leg VSC (b) 3-leg VSC and split capacitors (c) Neutral terminal at the DC bus and 3-leg VSC (d) 3-DC capacitors and 3-leg VSC.....	101
Figure 4.10: D-STATCOM 3-phase and 4-wire configurations including non-isolated VSC utilizing transformers (a) zig-zag transformer and 3-leg VSC (b) star delta transformer and 3-leg VSC (c) T-connected transformer and 3-leg VSC (d) star hexagon transformer and 3-leg VSC (e) zig-zag transformer and 2-leg VSC (f) T-connected transformer and 2-leg VSC (g) star hexagon transformer and 2-leg VSC	102
Figure 4.11: D-STATCOM 3-phase and 4-wire configurations including isolated VSC utilizing transformers (a) zig-zag transformer and 3-leg VSC (b) star delta transformer	

and 3-leg VSC (c) T-connected transformer and 3-leg VSC (d) star hexagon transformer and 3-leg VSC (e) zig-zag transformer and 2-leg VSC (f) star delta transformer and 2-leg VSC (g) T-connected transformer and 2-leg VSC (h) star hexagon transformer and 2-leg VSC (i) hexagon transformer and 2-leg VSC.....104

Figure 4.12: Vectors of different DSTATCOM modes (a) Capacitive mode (b) Inductive mode (c) Active power release (d) Active power absorption..... 105

Figure 4.13: DSTATCOM structure for HV distribution system 109

Figure 4.14: DSTATCOM (3-phase 3-leg inverter with a single DC capacitor)..... 110

Figure 4.15: Split capacitor based DSTATCOM 110

Figure 4.16: Independent single phase inverter with single DC capacitor based DSTATCOM 111

Figure 4.17: 3-phase 4-leg inverter based DSTATCOM..... 111

Figure 5.1: World’s net electricity generation from renewable energy 115

Figure 5.2: Grid-tied solar kit layout and components..... 118

Figure 5.3: Grid-tied wind generation system..... 119

Figure 5.4: Global cumulative wind power capacity..... 121

Figure 5.5: Wind Turbine Dimensions Evolution 124

Figure 5.6: Wind turbine of horizontal axis 125

Figure 5.7: Illustration of power coefficient/tip-speed ratio curve, C_p/λ 127

Figure 5.8: Power curve for a 2MW wind turbine..... 128

Figure 5.9: STATCOM arrangement. (a) STATCOM connection; (b) vector diagram .. 133

Figure 5.10: A large FSIG-based wind farm connected to the system with a STATCOM 133

Figure 5.11: System voltage without STATCOM..... 134

Figure 5.12: With STATCOM: (a) RMS voltage at point of connection (b) supplied reactive power 135

Figure 5.13: Simulink distribution grid model 138

Figure 5.14: Voltages at buses B1, B2 and B3 for series and parallel connection of STATCOM..... 139

Figure 5.15: Reactive power generated by STATCOM (a) series connection and (b) parallel connection 140

Figure 5.16: Series connection of STATCOM for 15 seconds simulation (a) wind speed (b) reactive power generated by STATCOM..... 142

Figure 6.1: DSTATCOM average model..... 147

Figure 6.2: DSTATCOM current with controller set to Q regulation.....150

Figure 6.3: Reactive power of DSTATCOM controller set to Q regulation 150

Figure 6.4: Reactive power at bus B3 with DSTATCOM controller set to Q regulation

.....	151
Figure 6.5: Voltage at bus B3 with DSTATCOM controller set to Q regulation.....	151
Figure 6.6: A 25kV distribution network with D-STATCOM connected in parallel with variable load.....	152
Figure 6.7: A 25kV distribution network with D-SATCOM connected in parallel with breaker circuit before load	153
Figure 6.8: DSTATCOM current in circuit with variable load at bus B3 and an extra load with breaker	154
Figure 6.9: Voltage at bus B1 in circuit with variable load at bus B3 and an extra load with breaker	154
Figure 6.10: Voltage at bus B1 in circuit with variable load at bus B3 and an extra load with breaker	155
Figure 6.11: Active power in circuit with variable load at bus B3 and an extra load with breaker.....	155
Figure 6.12: Reactive power in circuit with variable load at bus B3 and an extra load with breaker.....	156
Figure 6.13: Power grid for STATCOM phasor model	157
Figure 6.14: Dynamic response measured voltage and reference voltage.....	159
Figure 6.15: Dynamic response: measured reactive power and reference power	159
Figure 6.16: SVC Power System with Faults.....	160
Figure 6.17: Measured voltage v_m on STATCOM and SVC fault.....	161
Figure 6.18: Measured reactive power on STATCOM and SVC fault.....	161
Figure 6.19: Inductance and resistance on transmission line.....	163
Figure 6.20: Simulated power distribution grid	163
Figure 6.21: Voltage in steps of 10m from the PCC along the distribution line for 100, 200 and 315 kVA systems without STATCOM, with STATCOM at PCC, and STATCOM at final DP.....	166
Figure 6.22: STATCOM response for load change from no load to full load at PCC(DP1) and DP5	167
Figure 6.23: Estimated reactance measured for 100, 200 and 315 kVA systems for different frequencies or band of frequencies.	167
Figure 6.24: Reactive current injected response for both states of STATCOM controller tuned and untuned for a 100 kVA system	168
Figure 6.25: Reactive current injected response for both states of STATCOM controller (tuned and untuned) for a 200 kVA system.....	168
Figure 6.26: Reactive current injected response for both states of STATCOM controller (tuned and untuned) for a 315 kVA system.....	169

Figure 6.27: Reactive current injected response for both states with power factor correction capacitors (PFC) and without PFCs for a 100kVA system.....	169
Figure 6.28: Reactive current injected response for both states with power factor correction capacitors (PFC) and without PFCs for a 200 kVA system.....	170
Figure 6.29: Reactive current injected response for both states with power factor correction capacitors (PFC) and without PFCs for a 315 kVA system.....	171
Figure 6.30: Voltage in steps of 10m from the PCC along the distribution line for 100, 200 and 315 kVA systems without STATCOM, with STATCOM at PCC and with STATCOM at the last DP with droop control.....	172
Figure 6.31: Voltage in steps of 10m from the PCC along the distribution line for 100, 200 and 315 kVA systems without STATCOM, with STATCOM at PCC and with STATCOM at the last DP with light loads and a distributed energy source of voltage source type connected at the DP5	173
Figure 6.32: Voltage in steps of 10m from the PCC along the distribution line for 100, 200 and 315 kVA systems without STATCOM, with STATCOM at PCC, with STATCOM the last DP, and a distributed energy source of voltage type for heavily loads	174
Figure 6.33: Voltage in steps of 10m from the PCC along the distribution line for 100, 200, and 315 kVA systems without STATCOM, with STATCOM at PCC, and with STATCOM at the last DP and a distributed energy source of current type for light loads.....	176
Figure 6.34: Voltage in steps of 10m from the PCC along the distribution line for 100, 200 and 315 kVA systems without STATCOM, with STATCOM, with STATCOM at PCC, and with STATCOM at the last DP and a distributed energy source of current type for heavy loads.....	178

LIST OF TABLES

Table 1.1: Important standard organizations	5
Table 1.2: Categories of oscillatory transients	9
Table 1.3: Power quality problems, causes, effects and characteristics	19
Table 1.4: Classification of custom power devices	23
Table 1.5: Custom power devices, advantages, and disadvantages.....	24
Table 1.6: Literature survey	26
Table 2.1: Different approaches for measuring voltages and currents using multimeters	46
Table 2.2: Types of power quality variations	55
Table 3.1: Simulation condition	82
Table 5.1: Applications of wind turbine.....	123
Table 6.1: Maximum load of the system associated with each distribution point for 100, 200 and 315 systems in kVA	164

CHAPTER ONE

INTRODUCTION TO POWER QUALITY

1.1 Introduction

The aim of this thesis is to discuss and improve the power quality problems in grid-tied alternative systems at the distribution end. Another aim is to emphasize the improvement of selected issues of power quality (PQ) which renewable energy systems are facing. The most important factor is to deal with the electrical power quality issues and maintain it according to certain standard limits. If the PQ is poor and unmaintained, it results in faulty machine operation, interrupted production, grid instability, etc. due to deterioration of voltage and current parameters. The most common power quality problems and their effect on the sensitive equipment are voltage spikes, voltage dips, under voltages, frequency variations, power sag, electrical line noise, brownouts, etc. The main aim of this study is to develop the most efficient method to mitigate certain PQ issues in grid-tied systems.

The work done in this thesis is the reactive power compensation by employing STATCOM and DSTATCOM in distribution grids. The reactive power is a local phenomenon in the grid. The reactive power, if not compensated directly influence grid stability. STATCOM and DSTATCOM are employed due to their fast response in compensating reactive power which otherwise will result in PQ problems and will influence grid stability too. The STATCOM and DSTATCOM ability to support voltage and cost is also less as compared to other devices in literature.

In this thesis, work available in literature is improved by introducing reactive power variation due to the occurrence of faults and three phase breaker circuit. Then, this reactive power is compensated with the help of DSTATCOM. A verification of phasor model of STATCOM dominance over Static VAR Compensator (SVC) model in presence of a fault breaker circuit is done, which is available in literature.

The work is extended further by the use of STATCOM to regulate reactive power of a distribution grid when wind farms are used as a renewable energy source. A small distribution grid is assumed considering practical situations with a single feeder and four distribution points. These distribution points can be small home complex network, rural stations, industrial unit or

a University with residential facility etc. The system is considered to be linear with fixed STATCOM positions near point of common coupling (PCC) and at the end of the line.

The work is further extended by using a STATCOM with kVA rating 50% of the system rating and a droop control of 5%. The influence of distributed energy resources (DERs) on the performance of impedance algorithm and STATCOM is also checked by placing two DERs.

1.2 Structure of the thesis

Chapter ONE expands on the research problem, statement of the problem, and the background of the research problem. The source of PQ concerns, several techniques to improve PQ, and customer load profiles are discussed thoroughly. Research objectives and several research questions are mentioned. This chapter also briefs the research design and methodology as well as the limitations of the research. Furthermore, this chapter presents the summary of the significance of the research, including expected outcomes and results.

Chapter TWO provides the reader with a roadmap of devices such as multimeters, oscilloscopes, disturbance analyzers, spectrum analyzers, flicker meters, and energy monitors, which are used to measure various power quality problems.

Chapter THREE describes the different techniques to reduce power quality problems at the distribution end. Various techniques and components such as direct AC-AC converter, eight switch power conditioner, DSTATCOM, etc. are discussed to mitigate various power quality problems like voltage sag, voltage swell, voltage flicker, micro-interruptions and long interruptions, and harmonic distortion.

Chapter FOUR introduces the readers to the functioning of the shunt compensator and its characteristics. Various topologies of DSTATCOM such as three-phase three-wire DSTATCOM and three-phase four-wire DSTATCOM are also mentioned in detail in this chapter.

Chapter FIVE presents information on the enhancement of power quality using STATCOM. The grid-connected alternative systems are discussed in this chapter as well as wind energy

systems. Also, the power quality parameter, namely reactive power, is compensated using STATCOM in wind turbines.

Chapter SIX covers the utilization of DSTATCOM and STATCOM for compensation of reactive power. DSTATCOM is placed at different positions and on different types of distribution lines to get the desired power quality. Simulations are done in various grid-tied alternative systems with voltage and current control. The DSTATCOM average model is discussed and the simulations are done to compensate the reactive power in distribution grids.

The overall conclusion is made in Chapter SEVEN.

1.3 Problem statement

A shunt capacitor and DSTATCOM (Distributed Static Compensator) is employed to reduce the effect of PQ problems in grid-tied alternative systems at the distribution end. The reactive power compensation is done by placing DSTATCOM at different positions and on different types of distribution lines in order to get the desired power quality at the distribution end. The PQ is maintained to meet customer expectations and confidence.

1.4 Background

This section briefs on the definition of PQ and its related standards. The procedure of PQ evaluation is discussed afterward.

1.4.1 Power quality and related standards

1.4.1.1 Definition of power quality

Since the 1980's, PQ has originated as one of the most prolific jargons in the power industry. Electric PQ is a feature of power engineering that came into the picture since power systems originated. PQ has marked an important place in the systems which deal with high power, semiconductor based switches as well as transmission and sub-transmission networks. Generally, a sinusoidal voltage of frequency 50 Hz or 60 Hz with described magnitude is used to operate AC power systems. Modern power systems engineering deals with energy efficiency problems like accuracy in sinusoidal waveforms, problems due to voltage and current variations, and other AC waveform distortions.

Any deviation in frequency or magnitude of the required waveform is a PQ problem.

According to IEEE 1110, "PQ is the formation of powering and grounding sensitive electronic equipment in a standardized manner which is required for the proper operation of the equipment"(Zaveri et al., 2011). The main aim of it is to maintain voltage or current of the system as a pure sinusoidal wave with 1 p.u magnitude at 1 p.u frequency. The phase shift of the adjacent phases of a three-phase system must be 120° .

In other words, it is basically any problem in power systems manifested in voltage, current, or frequency deviations that result in faulty operation of customer's equipment.

OR

It is simply the interaction of electricity in consumer devices. If the electrical equipment is performing correctly, the power quality is good, and if it malfunctions during normal operation, power quality is poor.

OR

The composition of voltage and current quality can simply be referred to as power quality i.e. degree of any deviation from the standard voltage and frequency.

Power Quality = Voltage Quality + Current Quality

Based on these definitions: **POWER QUALITY = RELIABILITY**

The main aim of power quality is to minimise the incurred losses and also to maintain unity power factor in the system.

1.4.1.2 Standards

First and foremost, the question arises: "why do we need standards?" These standards are the guidelines or reference point from which the quality of the products is measured or characterized by the consumers using them in their everyday lives. PQ standards provide guidelines which assure compatibility of end users with the applied system. It can be used by researchers, scientists, and designers to improve the power quality.

These are categorized as Generic standards, Product standards, and Network standards. "Generic standards" are the generalized standards to which all electrical equipment should conform to. The "Product standards" cover specific product guidelines where a generic

standard application is not appropriate, and the “Network standards” cover the entire range of low and high-frequency disturbances.

Table.1.1 shows some of the standards and organizations. It is very difficult to define PQ by a certain parameter, but applying certain standards and specifications allows compatibility between manufacturer and customer (Bollen et al., 2009). On the other hand, imposing incorrect or incompatible standards lead to financial loss and hours of wasted discussion.

1.4.2 Power Quality monitoring and evaluation

There are several conditions in which PQ should be monitored, for instance, if any PQ problem is encountered at the distribution side, if any process requires a high level of PQ validation, or if sensitive equipment is connected. It is important for the device to be connected to a network or to be electrically close to affected loads and distribution loads. There are several equipment which can be used to monitor PQ faults, such as voltage dip, harmonic level, transients, and flickers.

Cost-effective equipment must be used in order to meet the demands of the customer. “Portable PQ monitor/analyser” is used for on-the-spot analysis in three-phase systems, while “Fixed PQ monitor/analyser” is used for long-time monitoring and can be linked to personal computers for immediate read-outs. “Networked-array of PQ” is used for centralized uninterrupted monitoring of the network.

Table 1.1: Important standard organizations

Adapted from (Bollen et al., 2009)

Organizations	Abbreviation	Types of Standards
American National Standard Institute	ANSI	Steady state voltage ratings (ANSI C84.1) IEC documentations
Institute of Electrical & Electronic Eng.	IEEE	Standards catalog Student bearers
Computer & Business Equipment Manufacturers Association	CBEMA	Equipment guides

Electric Power Research Institute	EPRI	Newsletter on PQ standards
National Electrical Manufacturers Association	NEMA	Equipment Standards
National Institute for standards and Technology	NIST	Standards general information
National Fire Protection Association	NFPA	Protection from lighting
Underwriters	UL	Laboratory safety standard

Customer needs, expectations, and confidence are important factors in terms of PQ. The flowchart in Figure 1.1 shows how to evaluate Power Quality.

The first step in evaluating PQ is to identify the problem category, for example, the voltage regulation, voltage sag and swell, flicker, transients, and harmonic distortion, etc. The causes of the problem are then characterized. Then, collection of data and measurements are processed (Zaveri et al., 2011). The third step is to identify a range of solutions relating to utility transmission and the distribution system, the end-user customer system, equipment design, and specifications. The modelling and analysis procedure is further evaluated. Finally, there is an evaluation of possible solutions in order to reach the optimum solution.

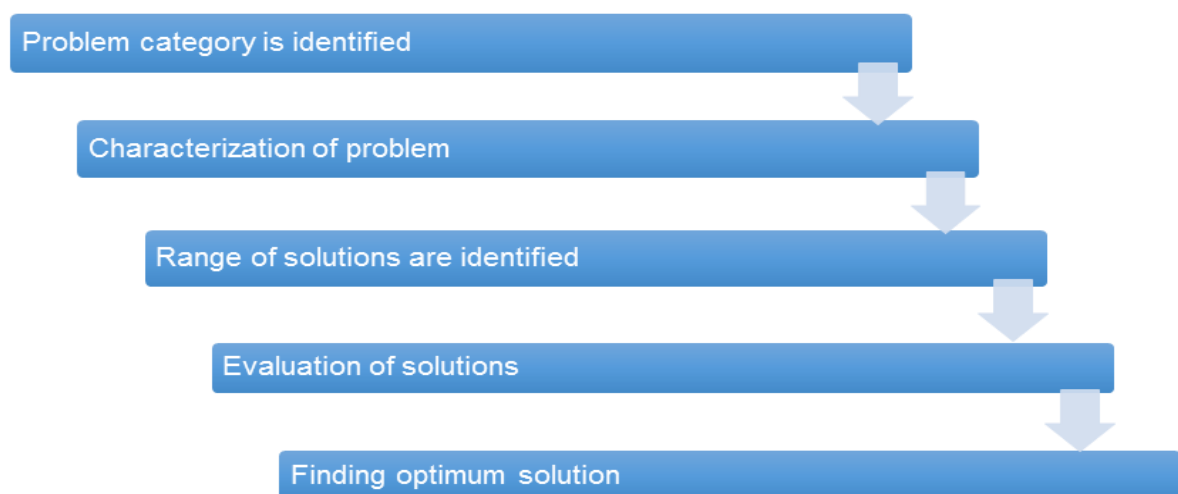


Figure 1.1: Power quality evaluation procedure

Adapted from (Zaveri et al., 2011)

1.5 Power Quality problems

In the present era, nobody can imagine life without electronic devices. In order to meet the growing necessity of microprocessors in equipment, adjustable speed devices (ASD's), technology equipment, and energy efficient LED lightning are being used. There is a major change in the nature of electric loads. These loads are the major concerns of power quality problems. Machinery or appliances can fail or be permanently damaged due to power problems. PQ problems are broadly classified as transients, long and short duration voltages, voltage unbalances, and waveform distortion as shown in Figure 1.2. These PQ problems are discussed in detail below.

1.5.1 Transients

The transients are used in the analysis of power systems related to an event, which is undesirable and momentary in nature. Generally, transients can be found in all types of electrical and communication circuits. They are deviations in the AC sine wave which appear for a very short duration. They are undesirable events typically lasting from a fraction of milliseconds to a few nanoseconds, thus, are momentary in nature. An electrical transient can be described as a unidirectional impulse of positive or negative polarity, or a momentary increase of voltage and/or current in an electrical circuit. The transients can be broadly classified into two categories: impulsive transients and oscillatory transients.

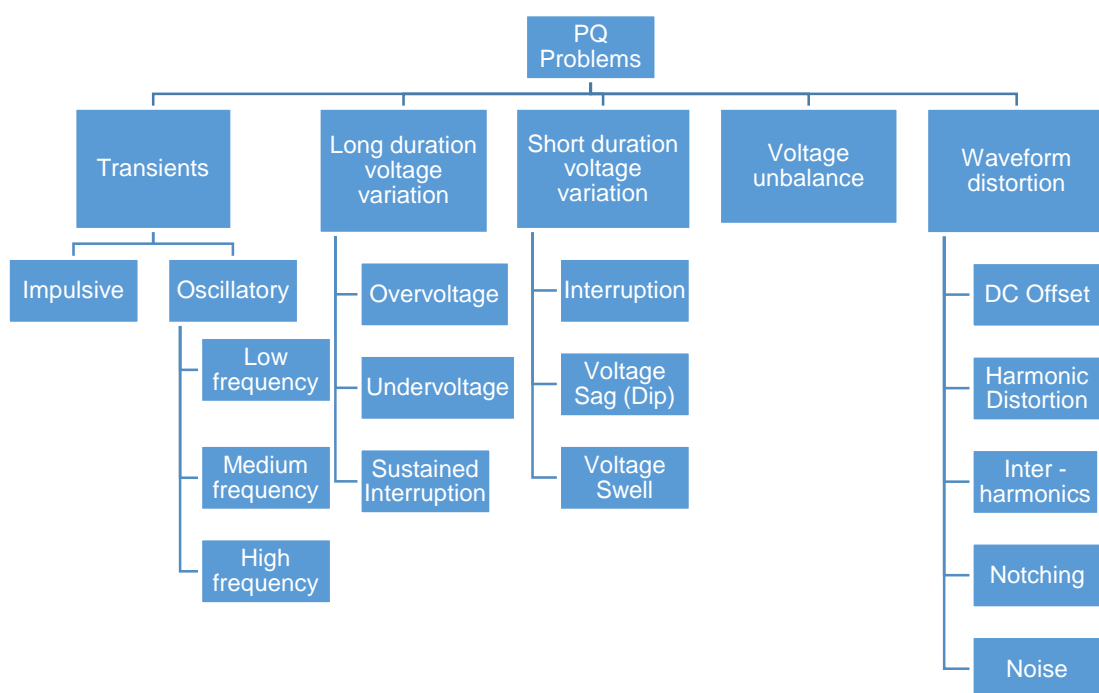


Figure 1.2: Power quality problems

Adapted from (Shawon et al., 2016)

1.5.1.1 Impulsive Transient

These transients are sudden frequency changes in the steady-state condition of either the voltage, the current, or both. They are unidirectional in polarity without affecting power and are normally characterized by peak magnitude and rise time duration. The typical causes of impulsive transients are lightning and electrostatic discharge. The voltage transients which arises due to lighting are higher in magnitude, with small duration, and low energy levels. Figure 1.3 shows the impulsive transient caused by lightning.

1.5.1.2 Oscillatory Transient

An oscillatory transient is also a sudden frequency variation in the steady-state condition of voltage, current, or both, that includes both positive and negative polarity values without affecting power (Acha et al., 2002). The switching of the capacitor is the main cause of oscillatory transient. The oscillatory transients are usually characterized by their spectral content, duration of appearance, and magnitude. They are categorized in terms of their frequency as mentioned below in Table 1.2.

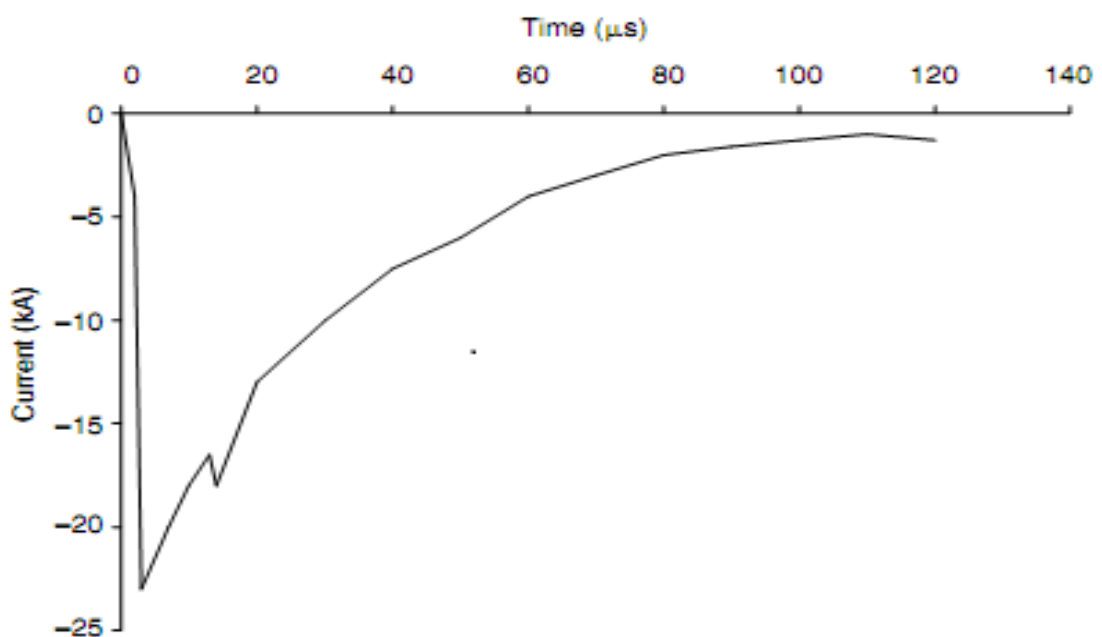


Figure 1.3: Current impulsive transient due to lightning

Adapted from (Shawon et al., 2016)

Table 1.2: Categories of oscillatory transients

Adapted from (Zaveri et al., 2011)

FREQUENCY RANGE	OSCILLATORY TRANSIENTS	TYPICAL DURATION
< 5 kHz	Low frequency	0.3 to 50 ms
5 – 500 kHz	Medium Frequency	20 μ s
500 kHz – 5 MHz	High frequency	5 μ s

The low-frequency oscillatory transient, which is the most common transient, is generally the result of capacitor bank energization or Ferro resonance of an unloaded transformer. Figure 1.4 shows the oscillatory transient occurrence due to switching of the back-to-back capacitor.

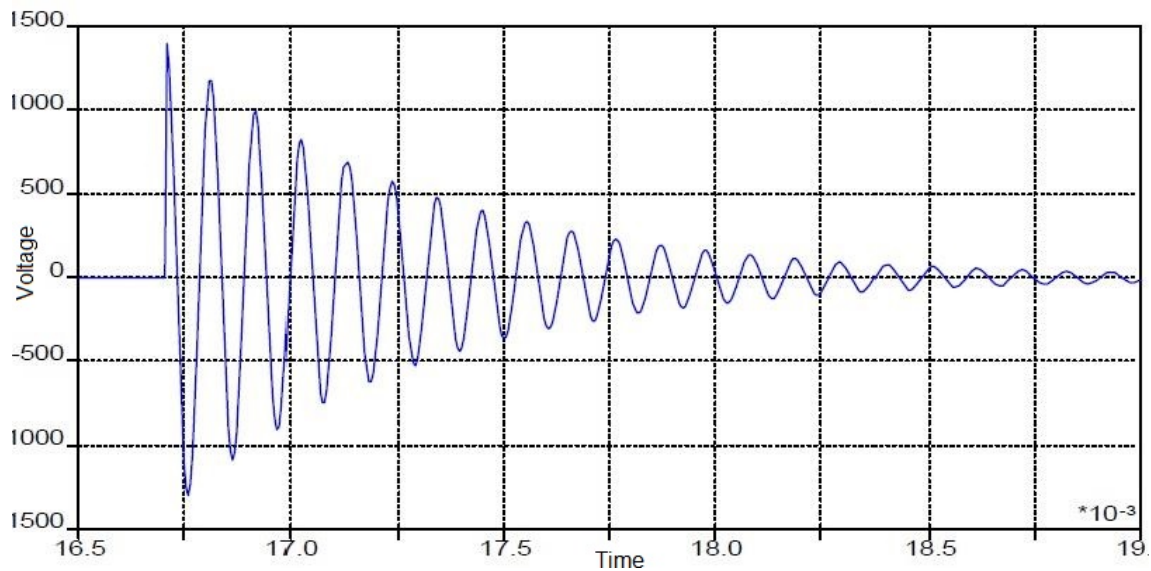


Figure 1.4: Oscillatory transient occurrence due to switching of back-to-back capacitor

Adapted from (Agarwal et al., 2016)

1.5.2 Long-duration voltage variations

The long-duration voltages are *RMS* deviations at power frequencies that occur for a time duration greater than a minute. The ANSI C84.1 specifies a certain limit for long duration voltage. If it exceeds for more than one minute, it is considered to be “long duration voltage“, which can be classified as overvoltage, undervoltage, and sustained interruption.

1.5.2.1 Overvoltage

An overvoltage is an increase in the root mean square AC voltage with a value of more than 110 percent at the power frequency. It occurs for a time duration greater than one minute. The overvoltage is mainly due to energization of the capacitor bank or load switching. The overvoltage occurs either due to weak system voltage regulations or inadequate voltage controls. It can also appear due to transformers incorrect tap settings. Overvoltage is shown in Figure 1.5.

1.5.2.2 Undervoltage

An undervoltage is a percentage reduction in the root mean square AC voltage that is less than 90 percent at the power frequency for a time duration longer than one minute. The main causes of undervoltage are switching events which are exactly the opposite of the events that result in overvoltages. The switching on or off of a load and a capacitor bank respectively can result in an undervoltage until the voltage regulators of the system can regulate the voltage to an acceptable level. Overloaded circuits may also result in undervoltages. The term brownout is usually used to explain the retained periods of undervoltage considered as a special utility dispatch method to decrease the power demand. However, there is no proper definition of brownout and the term does not provide the same clarity as undervoltage does when describing a disturbance. It is shown in Figure 1.5.

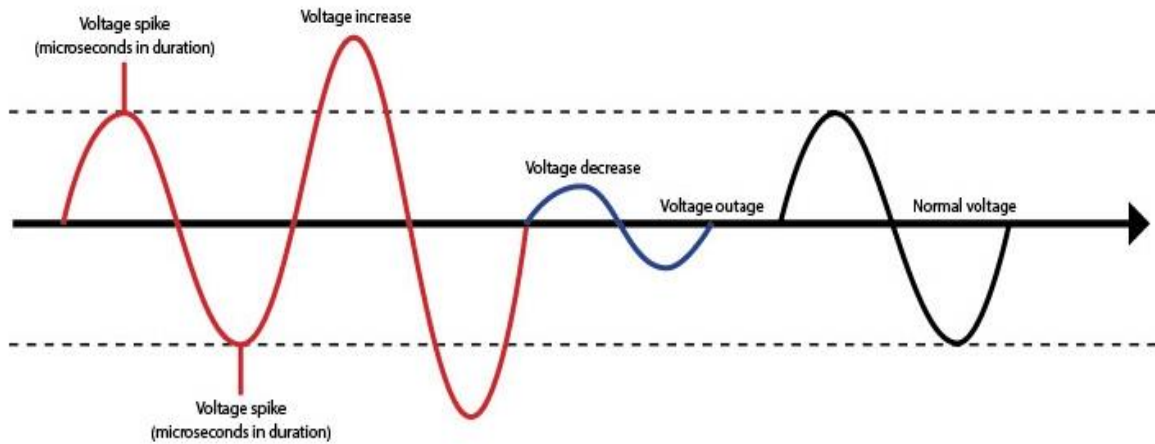


Figure 1.5: Long duration voltage variations

Adapted from (Bollen, 2000)

1.5.2.3 Sustained Interruption

If the supply voltage value is zero for more than a minute, the long duration of voltage disparity is assumed to be a sustained interruption. Sustained interruption can also be described as when the supply voltage is absent for long periods as shown in Figure 1.5. The voltage interruptions that appear for more than a minute are usually permanent and need human intervention in order to mitigate damage occurred to the system (Bollen, 2000). The sustained interruption is usually a reference to a particular power system phenomenon and usually has no relation with the power outage. The utilities often describe outage or interruption similarly for the purpose of reliability reporting. However, this creates confusion in the mind of end-users who consider an outage as a type of interruption in power which results in the shutdown of a process, which is smaller and is only for one-half of a cycle.

1.5.3 Short-duration voltage variations

According to IEC standards, “the voltage variations that arise due to fault conditions, large load energization, and loose connections in the power wiring are considered as short duration voltage variations”. The location of fault and system conditions decides the damage caused by the fault. It can result in loss of voltage for the entire duration (interruptions), the voltage may drop temporarily (voltage sags), or the voltage may rise (voltage swells).

1.5.3.1 Interruptions

An interruption is a condition when the current in the load or the supply voltage falls below 0.1 p.u for a maximum time period that is less than a minute. These are caused due to faults in the power system and failed equipment. The interruptions are usually calculated considering their duration as the magnitude of voltage is less than 0.1 times of nominal. The interruption duration which arises on the utility system by fault is determined by the utility protective devices. The instantaneous breaking of the circuit usually limits the interruptions that are caused by non-persistent faults which are less than thirty cycles. Figure 1.6 shows the three-phase instant interruption caused due to a fault and next, the circuit- breaking operation. The delayed breaking of the circuit for the protective device may cause an instant or short term interruption. The time duration of an interruption due to equipment failure or inappropriate connections can be inconsistent.

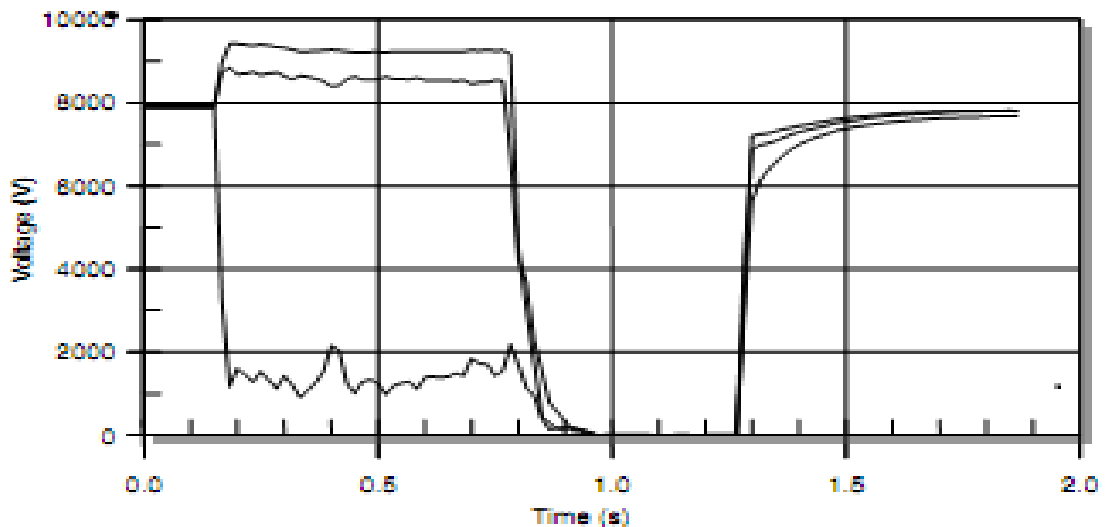


Figure 1.6: Momentary interruption in three-phase “root mean square” voltages

Adapted from (Badoni et al., 2016b)

1.5.3.2 Voltage Sag

The voltage sag is also known as the “voltage dip”. This is a short duration in which the *RMS* voltage decreased due to reasons such as overload, short circuits, or the starting of electric motors. A voltage sag occurs due to the *RMS* voltage falling between 10% to 90% of nominal voltage for one and a half cycles to a minute. Figure 1.7 shows the voltage sag related with the single line to ground (SLG) fault on the same substation from another feeder (Bollen, 2000). However, the voltage sag observed by the end-user is dependent on other factors like:

- Service voltage level
- Fault types
- Number of delta-wye transformations
- Wye-delta transformations between the customer and fault.

1.5.3.3 Voltage Swell

The voltage swell is the opposite of a voltage sag or dip. This occurs when *RMS* voltage increase above 110% of nominal voltage for a time duration of less than a minute. The voltage swells are also defined as "momentary overvoltage".

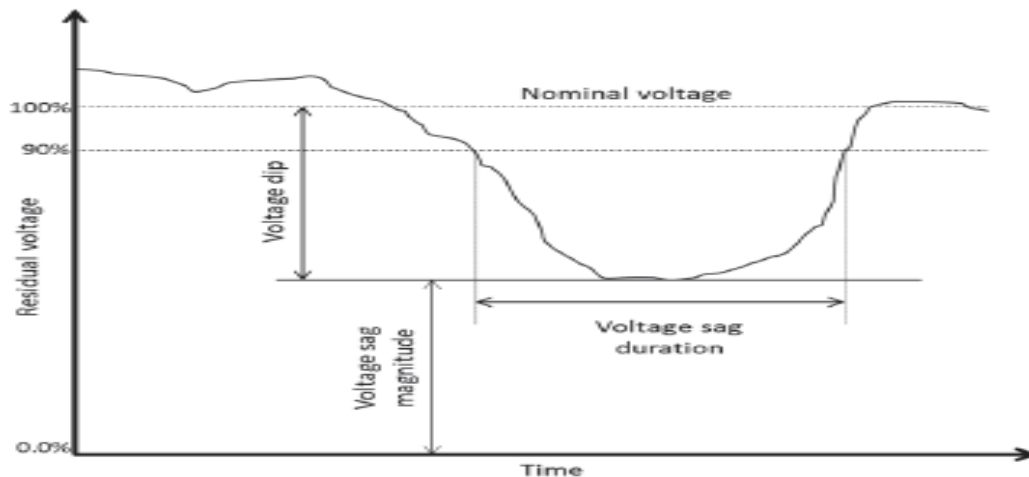


Figure 1.7: Voltage sag associated with S-L-G faults

Adapted from (Bollen, 2000)

The voltage swells are mainly related to fault conditions in the system - much like the voltage sags - but they appear rarely. This is specifically correct for systems which are not grounded or delta systems with floating conditions where the instant variation in ground reference causes a voltage increase on the phases without ground. Figure 1.8 shows when a voltage swell appears as a result of a single line-to-ground (SLG) fault on the system, resulting in an instant increase in voltage which is temporary on the phases which are not faulty, which ends with the fault. The voltage swells may also result due to the de-energization of the load with higher value. The abrupt interruption in current can result in a very large voltage change according to the given equation $V = L \frac{di}{dt}$, where L is the line inductance and $\frac{di}{dt}$ is rate of change of the

current with respect to time. Besides this, a large capacitor bank may also result in the voltage swell, although it usually results in an oscillatory transient.

The effect of the voltage swells is more disastrous even though the effects of voltage sag are easily detectable. Voltage swells may result in failure of the components on the equipment's power supplies. Although the effect is gradual in nature, it is an accumulative effect. The voltage swells can result in overheating which may lead to a complete shutdown. Overheating can arise due to control problems and hardware failure in the electronics equipment, which are usually sensitive, and can get damaged if prone to voltage swell.

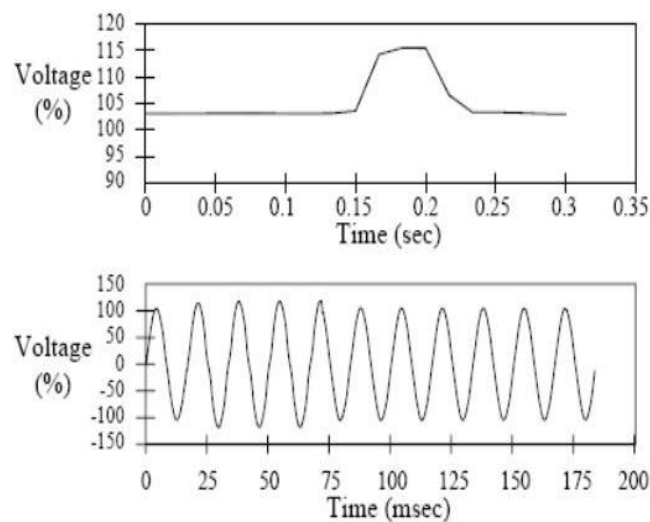


Figure 1.8: Voltage swell associated with S-L-G fault

Adapted from (Singh & Jain, 2015)

1.6 Voltage Unbalance

The voltage unbalance is also known as “voltage imbalance”. The voltage unbalance is defined as the ratio of the maximum deviation from the average of the three-phase voltages or currents with the average of the three-phase voltages or currents as in Equation (1.1). Initially the voltage unbalances in no-load conditions is usually less than or equal to 3%.

$$\% \text{ voltage unbalance} = \frac{V_{maxdif} - V_{av3ph}}{V_{av3ph}} \times 100\% \quad (1.1)$$

Where, $V_{max\ dif}$ = phase voltage different from average of three phases

$V_{av\ 3ph}$ = Average voltage of three phases

For the case when voltage unbalance is greater than 1%, motor will be derated. The voltage unbalances condition is shown in Figure 1.9. The utility can also generate the unbalanced voltages which might arise due to equipment's malfunctioning such as blown capacitor fuses, open delta transformers, and open-delta regulators(Singh, Jayaprakash & Kothari, 2009b). Open delta equipment are more prone to the voltage unbalance compared to closed delta equipment since they use two phases to carry out their transformations. The voltage unbalance can also result due to non-uniform load distribution in single phase between the 3-phases and results in voltage unbalance of less than 2%. In addition to this, there are conditions of voltage unbalances greater than 5% which results due to single phasing in the lateral feeder of the utility's distribution because of overloading of one phase or a fault due to a blown fuse.

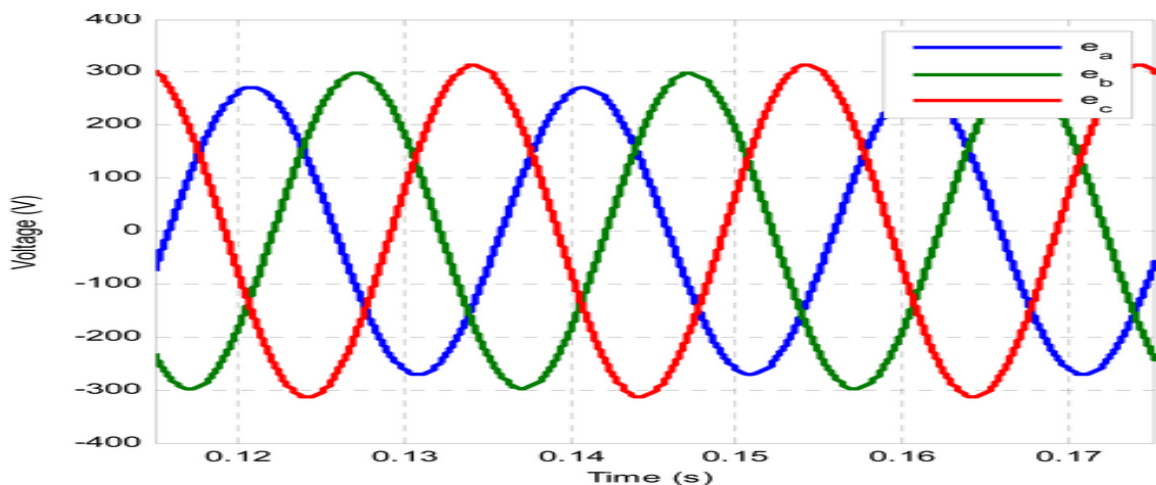


Figure 1.9: Voltage unbalance

Adapted from (Singh, Jayaprakash & Kothari, 2009b)

1.7 Waveform distortion

The waveform distortion is a deviation from an ideal sine wave of power frequency primarily characterized by the insubstantial content of the deviation. There are broadly five types of waveform distortion like inter-harmonics, DC offset, harmonics, notching, and noise. These are outlined in detail below.

1.7.1 DC offset

The DC voltage or current presence in an AC power system is defined as DC offset. The main causes of waveform distortion are lack of symmetry of electronic power converters or geomagnetic disturbance. Figure 1.10 shows DC offset condition.

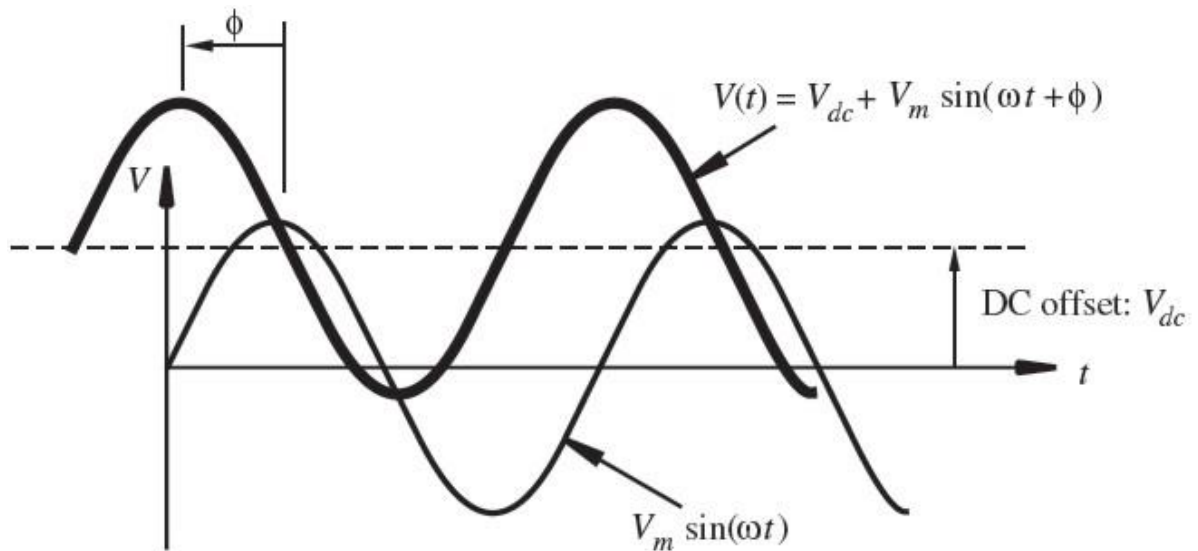


Figure 1.10: DC offset

Adapted from (Singh, Jayaprakash & Kothari, 2009b)

1.7.2 Harmonics

The harmonics are voltages or current at those frequencies which are integer multiples of fundamental frequency 50 or 60 Hz. The harmonics joins with fundamental voltage or current and generates distorted waveforms. Harmonic distortion is caused due to power system loads and the nonlinear nature of the devices. The distortion levels in harmonics are described by the complete harmonic spectrum with magnitudes and phase angles of each individual harmonic component as shown in Figure 1.11. The total harmonic distortion (THD) is calculated as the effective value of harmonic distortion.

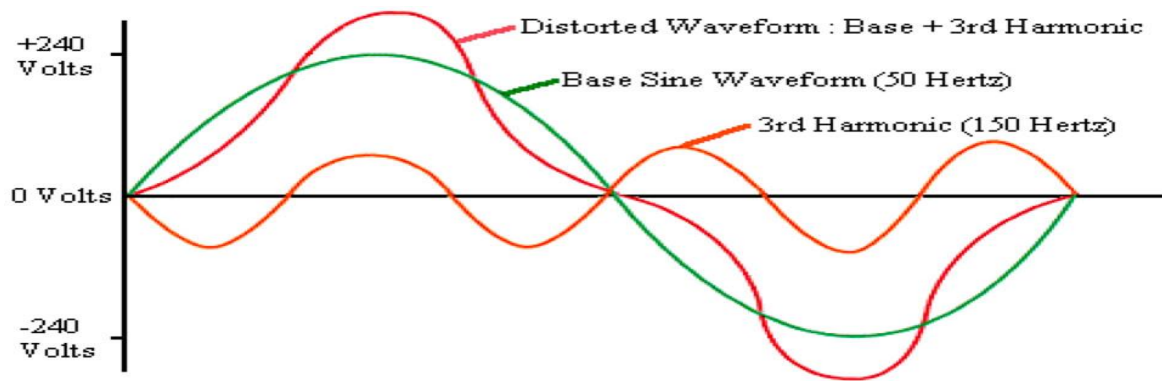


Figure 1.11: Harmonics

Adapted from (Singh, Jayaprakash & Kothari, 2009b)

The total harmonic distortion is expressed in percent or DB and is calculated as in Equation (1.2).

$$THD = \frac{\sqrt{V_2^2 + V_3^2 + V_4^2 + \dots}}{\sqrt{V_1^2 + V_2^2 + V_3^2 + \dots}} \quad (1.2)$$

1.7.3 Inter-harmonics

The voltage or currents with frequency components which are non-integer multiples of the fundamental frequency at which the supply systems operate, (50 or 60 Hz), is termed as inter-harmonics. Their appearance can be in any form as a wideband frequency spectrum or as discrete frequencies. The main sources of them are cyclo-converters, static frequency converters, induction furnaces and arcing devices.

1.7.4 Notching

This is a voltage disturbance that occurs periodically and is caused when current is regulated from one phase to another under the normal operation of power electronic devices as shown in Figure 1.12. It appears continuously and can be characterized by the harmonic spectrum of the affected voltage. The frequency component associated with notching can be quite high.

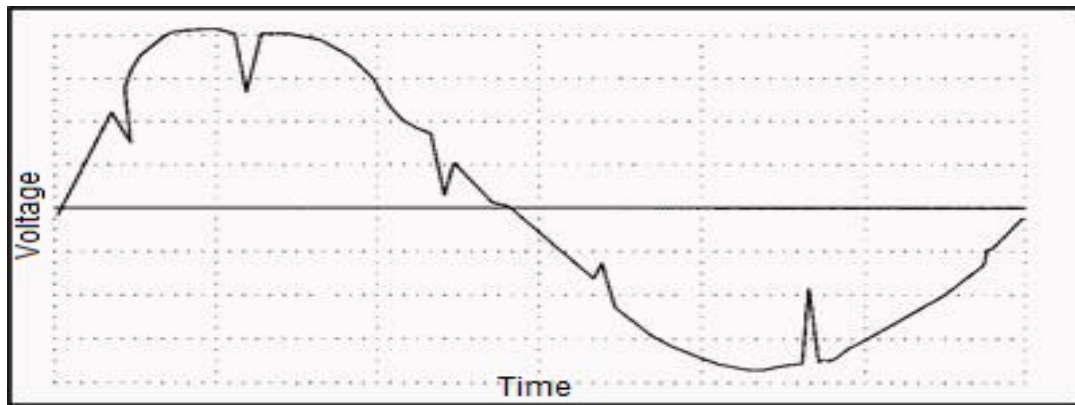


Figure 1.12: Notching

Adapted from (Singh, Jayaprakash & Kothari, 2009b)

1.7.5 Noise

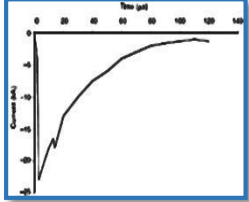
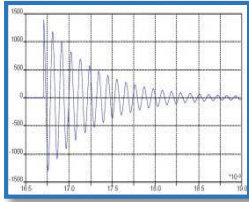
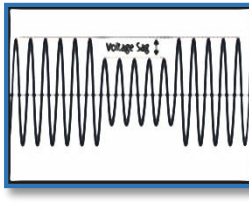
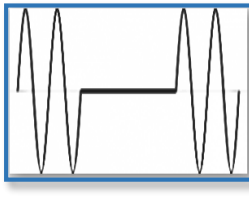
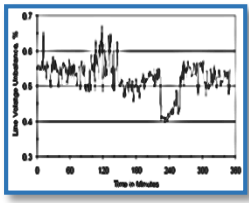
The noise is unwanted electrical disturbance with information which is lower than 200 kHz. Noise problems are becoming more prevalent with improper grounding. In order to reduce the effect of noise these points needs to be followed:

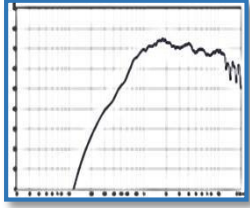
- Filters need to be installed properly.
- Use proper grounding techniques.
- Isolate the transformers.
- In order to mitigate the impact of electrical noise, use line conditioners.
- Separate data and power lines at a certain distance.
- Use twisted pair and data cables which are shielded.
- Sensitive electronic equipment and large electromagnetic interference sources need to be separated properly.

The table below provides an overview of the common Power Quality problems, their causes, characteristics, and consequences.

Table 1.3: Power quality problems, causes, effects and characteristics

Adapted from (Bollen, 2000)

PQ Problems	Definition	Causes	Effects	Characteristics
Impulsive Transient	Sudden, on-power frequency change in the steady state condition of voltage, current or both (unidirectional in polarity)	Lighting, High Frequency	Excitation of Power system resonance circuits	
Oscillatory Transient	Sudden, non-power frequency change in the steady state condition of voltage, current or both (bi-directional in polarity)	Capacitor switching	Sub transmission and distribution system affected	
Voltage Sag (Dip)	Decrease in between 0.1 and 0.9 p.u in RMS voltage or current for 0.5 cycle to 1 min	System faults, energization of heavy loads, Starting of large motors	Loss of efficiency and tripping of contractors	
Voltage Swell	Increase in between 1.1 and 1.8 p.u in RMS voltage or current for 0.5 cycles to 1 min	Transformer unregulation, Heavy load energization	Flickering of screens and lightings, data loss	
Voltage Unbalance	Max. dev. From the avg. of 3-phase voltages or currents divided by avg. of 3-phase voltages or currents	Blown fuses in one phase of a 3-phase capacitor bank	Existence of negative sequence in three phase induction machines	

Harmonic Distortion	Occurs from non-linear characteristics of devices and loads on the power system	Nonlinear loads, SMPS	Resonance and electromagnetic interference	
----------------------------	---	-----------------------	--	---

1.8 Solution of Power Quality improvement in power systems

The power system can be defined as an integration of electrical components which are used to generate, transmit, distribute and utilize electric power. Therefore, with the above mentioned PQ problems, the electrical device may fail or lead to complete shutdown. These problems can lead to the following conditions:

- Memory loss
- Uninterrupted power supplies
- Glitches
- Non-periodic flickering of light
- Demand more current to maintain output power
- Tripping of sensitive devices

The three main places of bad power quality origination based on utilities are:

- **Supply Generation Point:** Some power quality problems originate at the generating station due to poor maintenance, bad planning, load transferring, and constraints related to expansion and scheduling.
- **The Transmission System:** Some power quality problems originate in the transmission system, such as interruptions (due to galloping), voltage spikes, transient overvoltage (due to lightning), voltage dips (due to faults), etc. FACTS devices are implemented to deal with these PQ problems related to the transmission system.
- **The Distribution System:** Typical PQ problems originate in the distribution system like interruptions, voltage dips, overvoltages, voltage spikes, and energizing of transformers. Custom Power devices are used to deal with this category of problems.

Therefore, solutions to these problems should be developed for optimum efficiency.

1.8.1 FACTS (Flexible Alternating Current Transmission System)

Hingoreni (1988) first defined the concept of FACTS and FACTS Controllers. It is a technology-based concept which allows dynamic and flexible control over active and reactive power flow in transmission systems. The impedance of transmission lines, voltage, and phase angle are the control variables on which FACTS work. FACTS and customer power devices are listed in Figure 1.13.

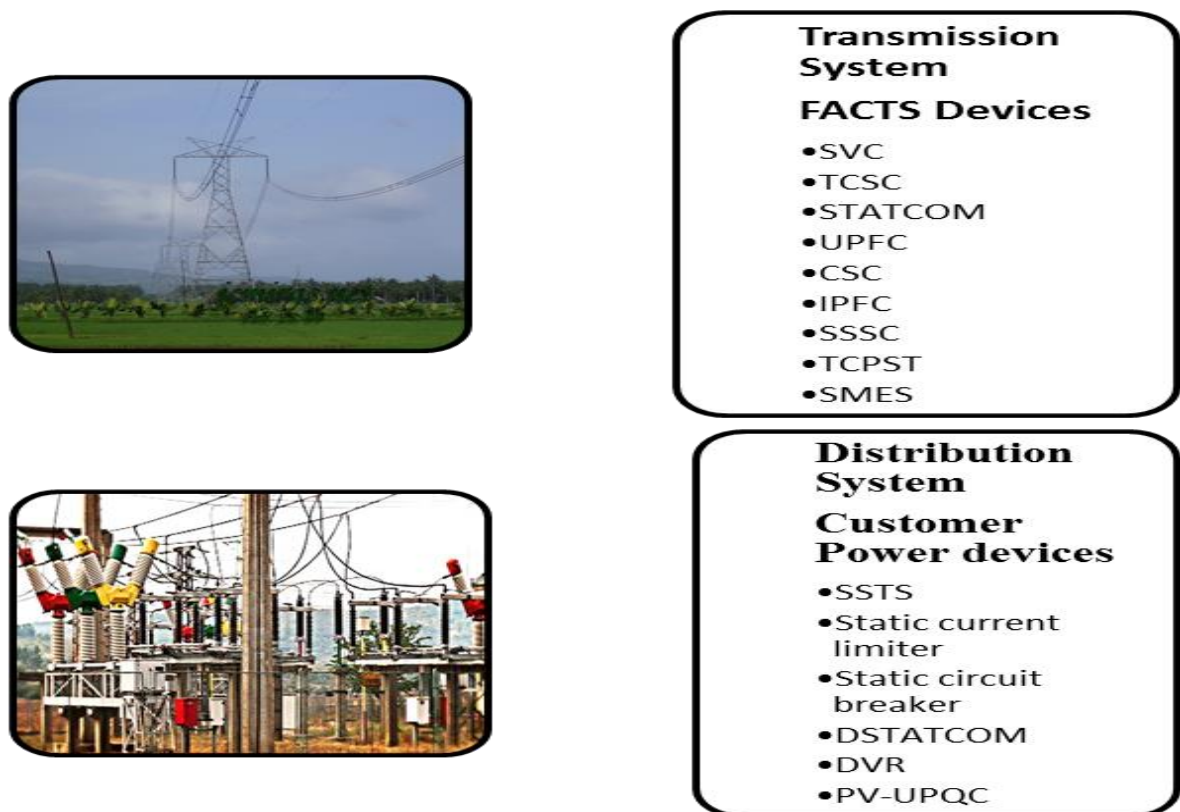


Figure 1.13: FACTS and custom power devices

Adapted from (Transmission, 2007)

The FACTS are classified into four categories, according to the way they are connected to the system, as listed below and are shown in Figure 1.14.

- Series Controllers (TCSC, SSSC)
- Shunt Controllers (TCR, SVC, STATCOM)
- Combined Series-Series Controllers (IPFC)
- Combined Series-Shunt Controllers (TCPST, UPFC)

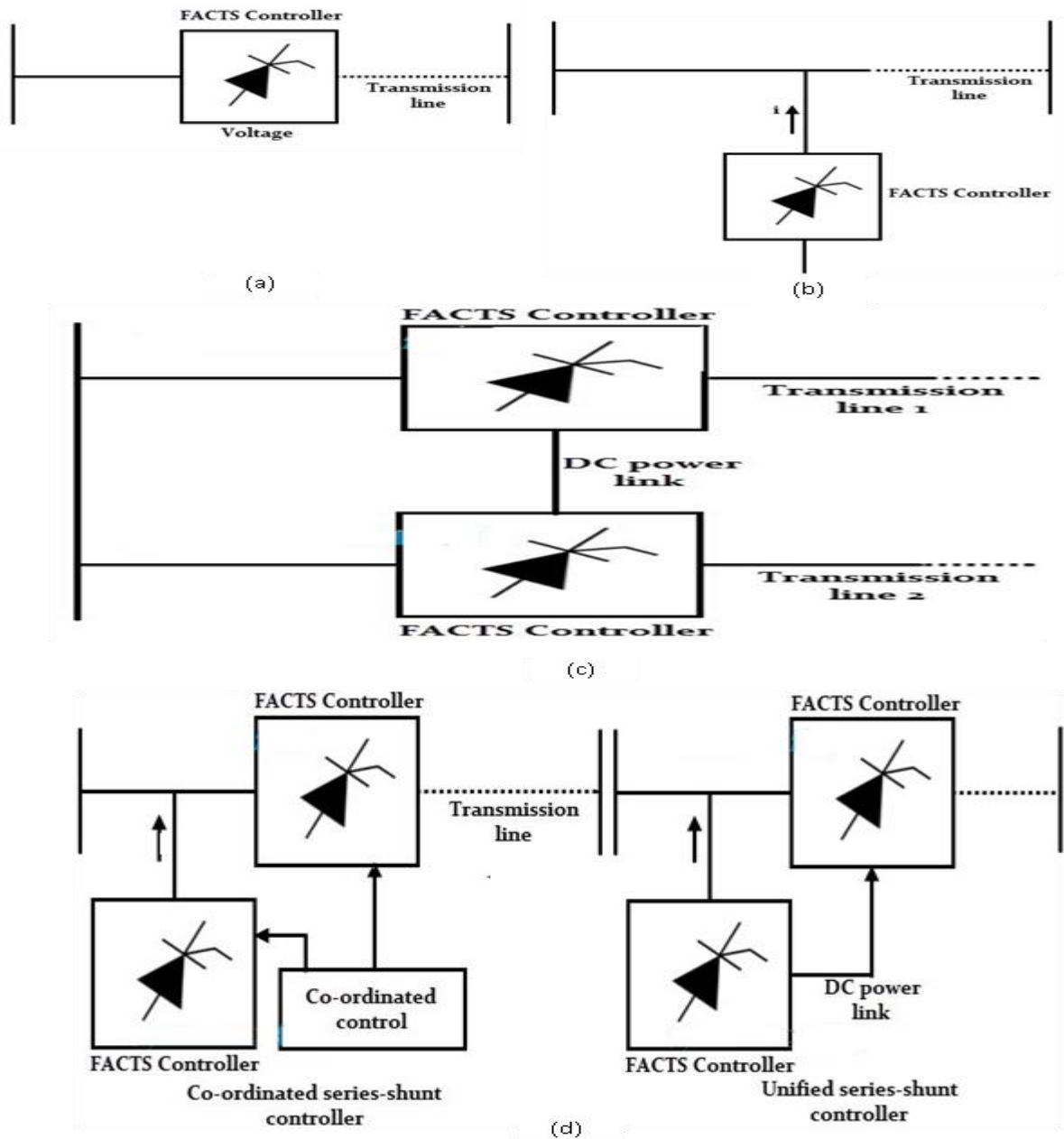


Figure 1.14: FACTS controller
 Adapted from (Transmission, 2007)

Although, FACTS and FACTS controllers are performing well in improving power quality, they need improvement in the following areas:

- There is no clear and understandable explanation of the device configurations required and use for compensating or reducing a particular distribution line problem.

- There is a great possibility of uncertainties with the transmission systems while dealing with long-term projects.
- A very high degree of errors arise when FACTS encounter multiple operational problems.
- There is a lack of economic assessments of FACTS projects for utility and transmission systems.

Currently, researchers are endeavoured to find new algorithms to improve the stability of the system and power quality. However, a lot of work is required in this area to reach the desired goals.

1.8.2 Custom Power Devices

Just like FACTS, these are used to enhance power quality at the transmission side. Similarly, custom power devices increase the quality and reliability of power at distribution end by enhancing power transfer volume and stability. Consequently, the user end will get fewer power interruptions, less harmonic distortion and phase unbalances, almost no flicker, and supply voltage frequency will be in the prescribed range. Custom power devices can be classified as shown in Table 1.4.

Table 1.4: Classification of custom power devices

Adapted from (Saggu, 2015)

Converter based classification	Topology based classification	Supply system based classification
<ul style="list-style-type: none"> • VSI • SSI 	<ul style="list-style-type: none"> • Shunt connection (DSTATCOM) • Series connection (DVR) • Series + shunt connection (UPQC) 	<ul style="list-style-type: none"> • Two-wire compensating devices • Three-wire compensating devices • Four-wire compensating devices

Table 1.5 shows the basic custom power devices and their components, as well as the advantages and disadvantages.

Table 1.5: Custom power devices, advantages, and disadvantages

Adapted from (Saggu, 2015)

Custom Power Devices	Components used	Advantages	Disadvantages
VSI	Diode rectifier, DC voltage bus and large DC capacitor	<ul style="list-style-type: none"> • Most popular as it can be extended to multilevel and chain converters. • Better steady-state performance 	<ul style="list-style-type: none"> • High switching loss • High total loss
CSI	SCRs and GCTs	<ul style="list-style-type: none"> • Low switching loss 	<ul style="list-style-type: none"> • Poor power factor • Harmonic distortion
DSTATCOM	Power generator, capacitor bank, reactor bank and self-controlled thyristor exchange capacitors	<ul style="list-style-type: none"> • Less harmonics • Nominal cost 	<ul style="list-style-type: none"> • Low speed of operation • Only reactive power
DVR	Energy storage unit, inverter circuit, filter unit and series-injecting transformer	<ul style="list-style-type: none"> • High rating • Active & reactive power • High speed of operation 	<ul style="list-style-type: none"> • High cost
UPQC	HPF & LPF, DC Capacitor, series & shunt transformer, two IGBTs	<ul style="list-style-type: none"> • Fastest of all • Very fewer harmonics • Mitigate almost all PQ problems 	<ul style="list-style-type: none"> • Complex construction • Very high cost

1.9 Objectives of the Research

Once 2007, ESKOM urges all customers to partner with them to save electricity. This ensures adequate and sufficient space for planned maintenance and better power quality. This thesis focusses on the custom power device, DSTATCOM (Distribution static compensator), as it is a boon in the power industry for regulation of line voltage at the point of common coupling. It can mitigate various power quality parameters, such as reactive power compensation or harmonics elimination. The main research objectives are given below:

- To have a better knowledge on power quality, power quality problems affecting distribution grids, devices and instruments used to measure power quality and the various methods to mitigate power quality problems.
- To have a better understanding on the voltage and control methods of one of the efficient power electronic device, DSTATCOM, for compensating reactive power.
- To develop a model with STATCOM injected on a distribution grid in presence of wind power for regulating reactive power and to demonstrate the method using MATLAB/Simulink environment.
- To develop an AC voltage control strategy for DSTATCOM and STATCOMs installed on distribution networks to compensate reactive power and to demonstrate the method using MATLAB/Simulink environment.

1.10 Literature Survey

Table.1.6 shows the literature survey of various papers on DSTATCOM, the improvement and application of DSTATCOM on residential and industrial loads, as well as various power quality parameters which are mitigated using these proposed designs.

Table 1.6: Literature survey

Serial Number	Mitigated Parameters	PQ	Algorithm/topology/converter	Applications	Components/ Equipment	Software	References
1	Harmonic distortion, load balancing, terminal voltage regulation at PCC		LMF adaptive filtering algorithm	Single-stage 3-phase grid integration of SPV system	SPV array, VSC, 3-phase grid	MATLAB/ Simulink	(Agarwal et al., 2016)
2	Load balancing, reactive power compensation, harmonics suppression		Interior point optimization-based control algorithm	3-phase DSTATCOM	3-phase VSC, 3-leg uncontrolled rectifier	MATLAB/ Simulink	(Singh, Arya, et al., 2016)
3	Harmonics compensation, power factor correction, load balancing, voltage regulation		ANFIS-LMS- based control algorithm	3-phase DSTATCOM (shunt compensator)	VSC(6 IGBTs)	MATLAB/ Simulink	(Badoni et al., 2016a)
4	Harmonics elimination, reactive power compensation		Wiener-filter and LMS-based control algorithm	3-phase SAPF	3-phase 3-leg VSC, 6 IGBTs	MATLAB/ Simulink	(BADONI et al., 2016)

5	Harmonics spectra, load balancing	LMS-LMF based control algorithm	DSTATCOM in 3-phase distribution system	DC bus capacitors, ripple filters	MATLAB/ Simulink, SPS	(Srinivas et al., 2016)
6	THD, load unbalancing	DT-CWT-based control algorithm	DSTATCOM in distribution system	VSC, interfacing inductors, IGBTs	MATLAB/ Simulink, SPS	(Kumar et al., 2017)
7	Voltage control, harmonics elimination, power factor improvement, load balancing, load compensation	Adaline-based control algorithm	PMSG based 3-phase loads	IGBTs, 3-leg VSC	MATLAB/ DSP	(Singh & Niwas, 2016)
8	Load balancing, harmonics elimination, reactive power compensation	MPPT algorithm	Standalone SPV-diesel battery hybrid system	DC-DC boost converter, BESS	MATLAB/ Simulink	(Philip et al., 2015)
9	Harmonics, reactive power compensation, load unbalancing	Adaptive, recursive inverse-based control algorithm	3-phase SAPF	VSC, 3-phase uncontrolled diode bridge rectifier	MATLAB/ Simulink	(Singh, Badoni, et al., 2016)

10	Reactive power compensation, harmonics elimination, load balancing	Sliding mode controller algorithm	DSTATCOM	PI controller	MATLAB/Simulink	(Kant et al., 2016)
11	Harmonics elimination	Hybrid standalone power generation system using MHP, SCIG & SPV	Residential green buildings	3-phase VSC,BESS	MATLAB/Simulink	(Rezkallah et al., 2015)
12	Reactive power compensation, harmonics elimination, load balancing	KIMEL-based algorithm	DSTATCOM	3-leg VSC, 3-phase diode rectifier	MATLAB/Simulink, SPS	(Kant et al., 2014)
13	Neutral current compensation, reactive power compensation, harmonics current, load balancing	Current sensor less control algorithm	DSTATCOM in 3-phase distribution system	Harmonics filters, VSC	MATLAB/Simulink	(Kant et al., 2014)
14	Terminal voltage control, harmonics elimination, load balancing	ILST-based control algorithm	PMSG-based DG (single-phase loads)	3-phase PMSG, Diesel engine, 3-leg VSC, star-connected RC filter	MATLAB/Simulink	(Bhim Singh, Jain, et al., 2014)

15	Harmonics elimination, power factor correction	Notch-Filter based control algorithm	Malfunction DSTATCOM	3-phase VSC, 2 IGBTs & a capacitor at DC link	MATLAB/ Simulink	(Jain et al., 2015)
16	Harmonics injection into the grid, reactive power compensation, load unbalancing	RTRL-based control algorithm	Control of DSTATCOM	3-phase 3-leg VSC, 6IGBTs	MATLAB/ Simulink, SPS	(Badoni et al., 2016b)
17	Harmonics suppression, load balancing, voltage regulation	Adaptive-neural network based control algorithm	Distributed power generation system	DSTATCOM, SyRG system with BESS	MATLAB/ Simulink	(Singh, Jayaprakash, Kumar, et al., 2011)
18	Reactive power compensation, PCC voltage regulation, harmonics suppression	Adaptive control algorithm	Wind-diesel standalone micro grid	Permanent magnet brushless generators, BSS	MATLAB/ Simulink, SPS	(Pathak et al., 2014)
19	Reactive power compensation, load balancing, harmonics elimination	Discrete-derivative control technique (Anti-Hebbian control algorithm)	DC-link voltage in shunt-compensator	Proportional Integral controller	MATLAB/ Simulink, SPS	(Ahmad et al., 2016)

20	Harmonics mitigation, reactive power compensation, power factor correction	PEF-based control algorithm	Single-phase malfunction SECS	DC link voltage structure	MATLAB	(Jain & Singh, 2015a)
21	Harmonics elimination, reactive power compensation, load balancing, voltage regulation	VFFRLS-based control algorithm	DSTATCOM for 3-phase distribution system	VSC	MATLAB/ Simulink	(Badoni et al., 2016a)
22	Harmonics elimination, load balancing	Adaptive theory-based notch filter algorithm	Diesel-generator set based standalone supply system	Diesel engine, 3-phase wound field synchronous generator, 4-leg VSC	MATLAB/ Simulink	(Jain et al., 2015)
23	Harmonics elimination, reactive power compensation, grid currents balancing	InC based MPPT algorithm	3-phase grid supportive kind of PV generation system	Boodt converter, grid interfaced VSC	MATLAB/ Simulink	(Jain & Singh, 2015b)

24	Harmonics elimination, reactive power compensation	PLL-less control algorithm	Single-phase single-stage malfunction grid interfaced SPV system	DC link of VSC & PI controller	MATLAB	(Cupertino et al., 2011)
25	Harmonics elimination, load balancing	VSS-FXLMS-based control algorithm	Wound field synchronous generator based diesel generator	Diesel engine, 3-leg VSC with a capacitor	MATLAB/ Simulink	(Bhim Singh, Niwas, et al., 2014)
26	Load unbalancing, harmonics elimination	VFC (VFIMD-based control algorithm)	SEIG in a standalone micro hydro power generating system	DSTATCOM & direct torque controlled VFIMD	MATLAB	(Chilipi et al., 2014)
27	Reactive power compensation, harmonics elimination, load balancing, neutral current reduction	NN-based load conductance control algorithm	DSTATCOM in a 4-wire distribution system	VSC, "T" connected transformer	TMS 320F240 DSP Processor	(Arya & Singh, 2014)
28	Reactive power compensation, voltage regulation	Voltage estimators based voltage sensorless control algorithm	DSTATCOM for a 3-phase 4-wire	LPF, a ripple filter and one single tuned HPF	MATLAB/ Simulink	(Arya, Singh, Chandra, et al., 2014)

			distribution system			
29	Harmonics elimination, load balancing, voltage regulation, reactive power compensation	InC based EPLL algorithm	Wind-DG microgrid	PMBLDCG based power generator and DG driven SyRG	MATLAB/ Simulink, SPS	(Pathak et al., 2015)
30	Harmonics elimination, load balancing, reactive power compensation	Learning based anti-Hebbian control algorithm	3-phase VSC based DSTATCOM	DSP	MATLAB/ Simulink, SPS	(Arya, Singh, Chandra, et al., 2014)
31	Load balancing, harmonics elimination, neutral current compensation, voltage regulation, power factor correction	MISCT-based control algorithm	SPV power generating system	4-leg VSC	MATLAB/ Simulink, SPS	(A. K. Verma et al., 2014)
32	Harmonics elimination, load balancing,	BP control algorithm	3-phase DSTATCOM	DSP, shunt passive ripple filter	MATLAB/ Simulink, SPS	(Singh & Arya, 2014)

	reactive power compensation					
33	Neutral current elimination, reactive power compensation, harmonics elimination, load balancing	Hyperbolic tangent function-based LMS control algorithm	3-phase 4-wire DSTATCOM	3-leg VSC, zig-zag transformer	dSPACE-1104	(Dube et al., 2014)
34	Load balancing, harmonics elimination, power factor correction	EPLL based control algorithm	Double stage solar PV grid	DC-DC boost converter, interfacing inductors and DC bus capacitor	MATLAB	(A. Verma et al., 2014)
35	Harmonics suppression, load unbalance	D-Q theory based control algorithm	Wind energy conversion system & a DG-DG set of a standalone hybrid system	DC-DC boost converter, VSC	MATLAB/ Simulink, SPS toolbox	(Reddy & Reddy, 2012)
36	Harmonics suppression, load balancing, voltage regulation	Adaptive neural network based control algorithm	3-phase 3-wire SyRG system with a battery energy storage system	3-leg VSC based DSTATCOM	TMS320F240 DSP	(Arya et al., 2015)

37	Voltage control, harmonics mitigation	Adaline-based control algorithm	2-winding asymmetric single phase SEIG	Speed governor controlled diesel/biogas engine	DSP implementation, MATLAB	(Kalla et al., 2014)
38	Harmonics mitigation, grid currents balancing	ILST-based CTF based control methodology	Single-stage 3-phase grid connected SPV system	3-phase VSC	MATLAB/ Simulink, SPS	(Bhim Singh, Jain, et al., 2014)
39	Voltage control, load balancing, neutral current compensation, harmonics elimination	CTF based control methodology	SPV-DG-BESS	SPV array, diesel driven PMSG, BESS	MATLAB/ Simulink, SPS	(Philip et al., 2015)
40	Load balancing, harmonics elimination, neutral current compensation, voltage regulation, power factor correction	MEPLL control algorithm	Grid interfaced SPV power generation system	3-leg VSC	MATLAB/ Simulink, SPS	(A. Verma et al., 2014)
41	Grid currents balancing, reactive power	RAD based algorithm	3-phase single-stage multitasking	3-leg VSC	MATLAB/ Simulink, SPS	(Jain & Singh, 2014)

	compensation, harmonics elimination		grid tied SECS			
42	Load balancing, harmonics current mitigation	LMS algorithm	DSTATCOM	VSC & PI controller	MATLAB/ DSP-dSPACE DS 1104	(Srinivas et al., 2016)
43	Harmonics elimination, power factor improvement, load balancing, load compensation	Adaline-based control algorithm	PMSG based DG using 3- phase 3-wire DSTATCOM	3-leg VSC, PWM current controller, 3- phase induction motor	MATLAB/ DSP-dSPACE DS 1104	(Singh & Niwas, 2014)
44	Grid currents balancing, reactive power compensation, harmonics elimination, neutral current mitigation	SOGI-Q based algorithm	3-phase multifunctional grid connected SECS	Boost converter, 4- leg VSC	MATLAB	(Jain & Singh, 2015b)
45	Reactive power compensation, load balancing, harmonics elimination	Composite observer based control technique	Distributed power generation system	DSTATCOM	DSP-dSPACE DS 1104	(Singh & Raj Arya, 2013)

46	Harmonics elimination, load leveling, reactive power compensation	BPFF control scheme	Wind-DG hybrid configuration	VSC as VFC, PMBLDC, Boost converter	MATLAB/SPS	(Pathak et al., 2014)
47	Loads balancing, harmonics elimination, reactive power compensation	Hyperbolic tangent function-based LMS algorithm	PMSG-based DG for standalone supply system	PMSG, DE, DSTATCOM, BESS	MATLAB/MATLAB/DSP-dSPACE DS 1104	(Dube et al., 2014)
48	Load leveling and balancing, harmonics elimination, neutral current compensation	LPF based control algorithm	IAG based isolated asynchronous standalone generator wind energy conversion system	3-leg IGBT-based VSC, Interfacing inductors, scaling circuits	MATLAB	(Sharma & Singh, 2014)
49	Reactive power compensation, voltage regulation, power factor correction, load balancing, load harmonics	LMS-based NN control algorithm	Grid interfaced SPV generating system	DC-DC boost converter, 4-leg VSC, 4-wire distribution system	MATLAB/Simulink	(B Singh et al., 2014)

	current elimination					
50	Reactive power compensation	Simple-peak detection control algorithm	3-phase, 4-wire DSTATCOM	LPF & voltage unit vector	MATLAB	(Arya, Singh & Jain, 2014)
51	Harmonics elimination, load balancing, power factor correction	EPLL-based control algorithm	3-phase DSTATCOM	DSP, ripple factor	MATLAB/ Simulink, DSP-dSPACE DS 1104	(Singh & Arya, 2013b)
52	Harmonics elimination, reactive power compensation, load balancing	Variable step projection learning affine control algorithm	VSC based shunt compensator	Small shunt passive ripple filter, 3-phase thyristor based controller rectifier	MATLAB/ Simulink	(Singh, Arya, et al., 2013)
53	Load balancing, grid currents balancing	SPV power generation system based on IRPT	3-phase 4-wire distribution system	PV array, a DC-DC boost converter, a 3-leg VSC, isolated 4-D transformer	MATLAB/ Simulink	(Singh, Shahani, et al., 2013)
54	Neutral current compensation, reactive power compensation, load balancing,	Kurtosis driven variable learning adaptive filter	VSC based DSTATCOM	Self-sustaining DC bus, shunt passive ripple filter	MATLAB/ Simulink	(Arya & Singh, 2013a)

	harmonics elimination					
55	Harmonics elimination, load balancing, reactive power compensation	Composite-observer based control algorithm	3-leg VSI based DSTATCOM	VSI, interfacing inductors	DSP-dSPACE DS 1104	(Singh & Raj Arya, 2013)
56	Load balancing, reactive power compensation, harmonics elimination	CTF based control algorithm	3-phase DSTATCOM	Multipliers, LPF, Summers	MATLAB/ Simulink	(Arya & Singh, 2012)
57	Harmonics elimination, load compensation, load balancing, voltage regulation	SRF theory based controller	IG based DG set for small standalone supply systems	BESS, DSTATCOM(3- leg VSC with T-Transformer)	MATLAB/ Simulink	(Singh & Niwas, 2012)
58	Harmonics elimination, reactive power compensation	SPLL-based control algorithm	3-phase DSTATCOM	3-leg VSC, IGBT	MATLAB/ Simulink, SPS	(Singh & Arya, 2012)

1.11 Research Questions

The cost associated with the poor power quality can be tremendous. It can be due to factors like voltage sags, voltage swells, and harmonic distortion, etc. Custom power devices developed significantly in recent years due to the great demand in electricity consumption, and the need to save electricity and improve power quality. One of these efficient devices is DSTATCOM. The research questions which come to mind are as follows:

1.11.1 Which strategies help to achieve better Power Quality?

The consumption of reactive power is the main cause of poor power quality. DSTATCOM is the compensating device to control the flow of reactive power in the distribution system. The STATCOM is used for compensation of transmission systems.

1.11.2 How is a DSTATCOM a better device than other available custom devices?

The main advantages of DSTATCOM and STATCOM are simple configuration, less response time, and reduced harmonics. In terms of improving power quality, it is one of the fastest and efficient custom power devices available.

1.11.3 How can basic DSTATCOM be refined to achieve good power quality at the distribution end?

DSTATCOM can be used in different modes to achieve desired power quality parameters. This includes cascaded DSTATCOM, multilevel DSTATCOM, and the genetic and fuzzy logic control algorithm for DSTATCOM. The proportional and integral controllers are often used to control the operation of DSTATCOM.

1.11.4 Is there any Software or Hardware implementation? What is the measure that the actual problem is solved?

Use of software programs in the simulation of DSTATCOM or STATCOM is extremely important for development and understanding of power electronics-based technology. Software implementation on MATLAB/Simulink environment is done to run the circuits. Impedance and voltage reduction measurements, response of PV inverters, and energy stabilizing elements are some of the key deciding factors that ensure the goal of improving power quality is reached.

1.11.5 What will be done if the chosen approach does not work properly?

Other custom devices will be used in addition to DSTATCOM and STATCOM to get better results in reactive power compensation.

1.12 Research Design and Methodology

The investigation method is briefly outlined below.

- Studies of:
 - Mitigation methods for various PQ problems
 - FACTS and custom power devices
 - Grid tied renewable systems
 - DSTATCOM
 - STATCOM
 - Voltage and current control of DSTATCOM and STATCOM
- Parameters to be focused:
 - Reactive power compensation
 - Voltage flicker
- Mathematical modelling:
 - Simulation of structured DSTATCOM using MATLAB/Simulink environment
 - Simulation of structured STATCOM using MATLAB/Simulink environment

1.13 Significance of research

This research is significant in increasing transmittable power in AC Power systems. Fixed switched capacitors are employed to increase efficiency. DSTATCOM provides reactive power absorption completely by means of voltage and current waveforms that are electronically processed. It provides quick response time, maximum voltage reduction in flicker and fluctuations, and excellent dynamic characteristics. Furthermore, this research is significant to the power industry since energy consumption reduction methods is a crucial need of the modern era due to the government imposing heavy taxes and penalties on customers who use excessive energy..

The following stakeholders benefitted from the research:

- ESKOM
- CPUT
- Students at CPUT obtained training in energy grid-tied systems
- Industry such as industrial plants using arc furnaces
- Distribution system applications where there is a need to reduce PQ parameters

1.14 Expected outcomes, results and contributions of research

The expected outcomes and contributions that are wished to be achieved for distribution lines are:

- Software to verify structured DSTATCOM and STATCOM
- Reduced complexity of distribution lines.
- Lowest kilovolt ampere rating of compensation device
- Least number of semiconductor devices
- Compensation of reactive power
- Regulation of amplitude of voltage under varying loads
- Compensation of load and compensator currents at PCC

CHAPTER TWO

MEASUREMENT OF POWER QUALITY PROBLEMS

2.1 Introduction

Power quality problems are detrimental to a fully-functioning power system. Power quality phenomenon exists on a long range of frequencies, ranging from overvoltages, which are very fast transients that last a microsecond, to outages that last for hours or days. The steady-state phenomenon like harmonic distortion is also considered a power quality problem. The extensive variety of problems that can affect power quality greatly influences the development of equipment and standard measurement procedures.

Dealing with power quality problems require obtaining useful information in the form of data at an appropriate location and in a particular period of time. That is why, instrument selection is an important factor in terms of obtaining the appropriate data. It is important that the instruments which ensemble any application is used since the network will not be able to recognize if the wrong equipment is utilized.

The information about the location where power quality needs to be measured and the duration are also important factors. Once the data is collected, information is extracted from it to find out the cause of the power quality problem. This approach requires someone who is equipped with hands-on experience regarding the power system and the affected equipment. The data which a faulty instrument provides must be sorted to extract useful information from it in order to obtain a solution. Sometimes problems are not singular, and may in fact be a combination of problems which will need to be sorted out by a combination of solutions to obtain the desired end output.

2.2 Organization of the chapter

Various devices for measuring power quality are discussed. Various devices such as multimeters, digital meters and oscilloscopes are then mentioned in the next section. Various analysers such as conventional analysers, graphic based analyser, spectrum analysers, and harmonic based analysers are discussed afterwards. Flicker meters are also mentioned. The chapter concludes on the future scope of these measurement devices.

2.3 Power quality measurement devices

Power quality measurement devices are wiring and grounding test devices such as:

- Multimeters
- Oscilloscopes
- Disturbance analysers
- Spectrum analysers and harmonic analysers
- Combination disturbance and harmonic analysers
- Flicker meters
- Energy monitors

Selecting an instrument depends on the type of analysis, therefore, before selecting an instrument some other important factors must be considered:

- Number of channels
- Temperature specifications of the instrument
- Input voltage range
- Ruggedness of the instrument
- Power requirements
- Input isolation (isolation between input channels and from each input to ground)
- Ability to measure three-phase voltages
- Ability to measure currents
- Ease of use
- Housing of the instrument
- Documentation
- Communication capability
- Analysis software

2.4 Wiring and grounding testers

The wiring or grounding within the end-user premises is one of the main reasons for power quality problems. An easy way of identifying these problems is the visual inspection of lines, wires, connecting points, and panel boxes (Sedinin & Rogulin, 2012). Additionally, there are special test devices that can detect wiring and grounding problems. The device is shown in Figure 2.1.

Requirements for a wiring and grounding test device include:

- Recognition of isolated ground in shorts and neutral ground in bonds.

- Ground and neutral impedance measurement.
- Recognition of open grounds, neutrals, or hot wires.
- Recognition of hot, neutral, or ground reversals.



Figure 2.1: Wiring and grounding tester

Adapted from (Sedinin & Rogulin, 2012)

The testers for 3-phase wiring must be able to indicate the phase rotation and different phase-to-phase voltages. These circuits are very simple and useful in providing an excellent test for circuit functioning. Many wiring and grounding problems can be identified at the site of end-users without employing expensive instrumentation monitoring devices or equipment.

2.4.1 Multimeters

Wiring plays an important role. When the wiring test output provides a positive response, it is important to check frequently. After checking the robustness of the wiring, the levels of voltage and current in the facility should also be checked. Using these methods, unbalances between circuits can be detected, including problems such as overloading, undervoltage, and overvoltage. A multimeter can be used to detect these problems. The signals which are checked includes:

- Phase to ground voltages
- Phase to neutral voltages
- Neutral to ground voltages
- Phase to phase voltages for 3-phase system
- Phases of currents
- Neutral currents

The most important aspect that needs to be considered for the selection and use of a multimeter is the procedure of circulation. Most meters are calibrated to provide an RMS indication of the measured signal (Sedinin & Rogulin, 2012). Some other approaches are also used in order to find the RMS value. The three most common approaches are:

- **Peak method:** The signals are usually sinusoidal. The meter finds the *RMS* value by dividing the peak value of the signal by the square root of 2 i.e. 1.414.
- **Averaging method:** The meter finds the average value of the rectified signal. This average value of a clean sinusoidal signal (i.e. signal with constant frequency) is proportional to the *RMS* value.
- **True RMS:** When a voltage is applied across a resistance, it results in heating. The *RMS* value of the signal is a measure of this heating. The actual *RMS* value can be detected using a thermal detector. Recent developments in the digital world brought about modern digital meters which does a digital calculation to find the *RMS* value. The square of the signal is done on a sample-to-sample basis for a period. Then, the square root of the result is calculated.

The results of these approaches is the same for a sinusoidal signal without distortion. These methods provide different results for distorted signals. The distortion levels appear very often, especially for neutral and phase current on the premises. Table 2.1 provides a useful overview of the different approaches that can be used.

Table 2.1: Different approaches for measuring voltages and currents using multimeters

Adapted from (McGranaghan & Santoso, 2007)

Name	Meter type		
	True RMS	Peak Method	Average
	Circuit Type		
	RMS Converter	Peak	Sine wave average
Sine Wave	100%	$100\sqrt{2}$	100/1.11
Square Wave	100%	$82\sqrt{2}$	110/1.11
Triangle Wave	100%	$121\sqrt{2}$	96/1.11
ASD Current	100%	$127\sqrt{2}$	86/1.11
PC Current	100%	$184\sqrt{2}$	60/1.11
Light Dimmer	100%	$113\sqrt{2}$	84/1.11

2.4.2 Digital meters

Photographs can be useful in providing precise information. The people who conduct the measurements are likely to get diverted while trying to make an instrument work properly and do tests. The human memory is also prone to get confused and forget the vast amount of measurements taken at a time. The solution to this is the use of modern digital cameras during field measurements. The photographs can be used to document tests. The exposure in the picture can be varied accordingly to aid inspection. Some of the items which can be recorded photographically while doing field measurements are:

- Nameplates of the transformers, motors, etc.
- Setup of the facility.
- Connection of transducer and probe.
- Waveform displayed on instruments.
- Substations, arrangements of switch gear, etc.
- Electrical components and equipment dimensions, size, and weight.

2.4.3 Oscilloscopes

An oscilloscope is an important equipment piece for real-time tests. The oscilloscope shows the variation of current and voltage waveforms that are tested. The voltage and current waveforms displayed can provide information without having performed the detailed harmonic analysis. By inspecting the magnitude and waveform shapes of the voltage and current,

distortion and problems like pulse shape can be detected. Oscilloscopes are available in different models and ranges. Digital oscilloscopes are useful to store data for later use or comparison. The oscilloscopes can be used for calculation of energy, analysis spectrum with the help of waveforms. Furthermore, digital oscilloscopes can analyse data with the help of computer software (McGranaghan & Santoso, 2007).

In recent years, oscilloscopes are available as hand-held instruments which can display waveforms and process signals. These oscilloscopes are useful due to their portable nature. These oscilloscopes can be operated like a volt-ohm-meter (VOM), but with extra information. These are best suited for the initial survey of any industrial unit.

2.4.4 Disturbance analysers

Disturbance analysers and monitors belong to the category of equipment developed particularly for measuring power quality. These are capable of measuring a vast variety of disturbances which may occur in the power system, for example, short duration transients, long duration outages, and undervoltages. By setting the thresholds, these instruments can record disturbance for a period of time. The information regarding disturbances are usually stored on paper tape. However, due to recent developments many instruments are coming with attachment capability that allows recording on discs. They fall under the two categories explained below.

2.4.4.1 Conventional analysers

The conventional analysers records events with information about overvoltage and undervoltage. It also outlines the magnitude and duration of voltage sags, voltage surges, and transients, etc.

2.4.4.2 Graphic-based analysers

Graphic-based analysers can save the detailed information normally generated by conventional analysers. Information regarding actual waveform can also be printed. Information provided by conventional analysers cannot determine the characteristics of a disturbance or a transient. For example, the peak and duration cannot describe an oscillatory transient. Therefore, it is very crucial to have the waveform capture capability of a graphics based disturbance analyser. This can be used for the analysis of a power quality problem as shown in Figure 2.2. A conventional disturbance monitor is cheaper and easier to use for initial checks of the location where a problem occurred.

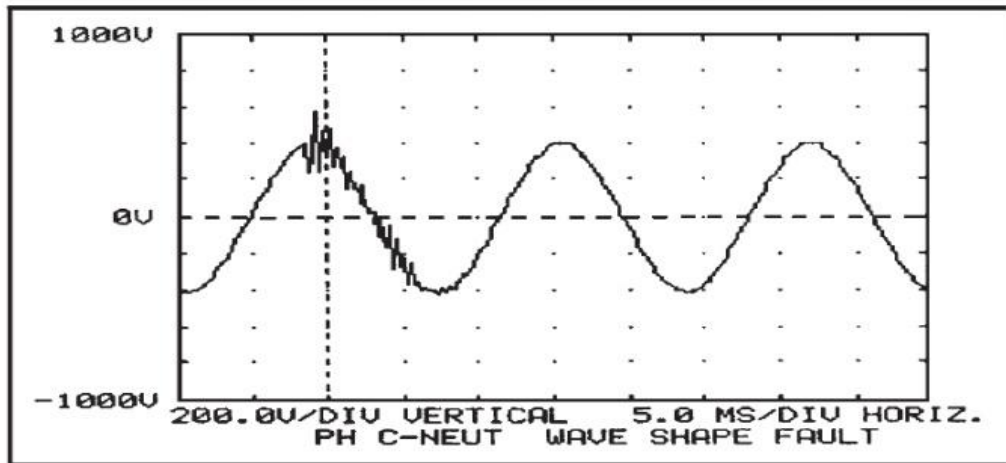


Figure 2.2: Graphics-based analyser output

Adapted from (Meyer et al., 2009)

2.4.5 Spectrum and harmonic analysers

Spectrum and harmonic analysers can display captured harmonic waveforms on the screen. They are used for calculating the K factor to derate transformers and total harmonic distortion (THD) in percentage with respect to fundamental. They are capable of measuring the frequency spectrum, i.e., the harmonic frequency corresponding to the current and voltage up to the 5th harmonic.

The harmonic frequency can either be displayed as a bar graph or as numerical values of the signal. It can be used for measuring the voltage or current of a single-phase or a three-phase. The power factor is a measurement of how much of the total power is being used for useful work efficiently, and can be measured using these analysers. A beneficial feature is the fact that these analysers can store data for more than a week, allowing time for the data to be transferred to a PC.

Spectrum and harmonic analysers are powerful tools in the analysis of harmonic power quality problems. In order to find out the low-order harmonics, powerful analysers with add-on modules are used for Fast Fourier Transform (FFT) (Golkar, 2004). To improve the frequency resolution, we must extend the recording time. It is calculated as shown in Equation 2.1.

$$\Delta f = \frac{1}{T} = \frac{F_s}{N} \quad (2.1)$$

The lowest frequency tested is 0 Hz, the DC component; and the highest frequency is the Nyquist frequency ($\frac{F_s}{2}$). The waveforms are shown in Figure 2.3.

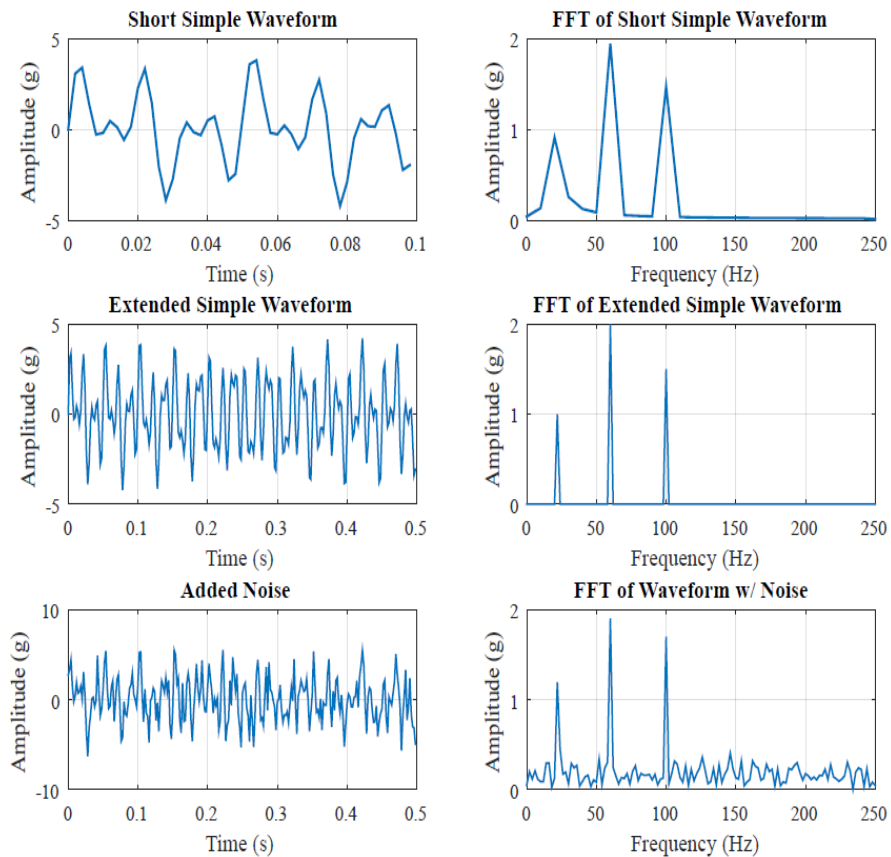


Figure 2.3: Fast Fourier Transform waveforms

Adapted from (Golkar, 2004)

Some of the important capabilities that harmonic measurements must include are:

- Simultaneous measurement of both voltage and current, for harmonic power flow information.
- For individual harmonic components the analyzer must be capable of measuring both magnitude and phase angle which is also required for calculations of power flow.
- Capability of high sampling rate and a 60 Hz fundamental sampling interval.

- Capable of adjusting according to harmonic distortion levels as harmonic levels varies with load and system conditions variation.

For harmonic analysis, the instruments must fulfil the conditions mentioned below.

2.4.5.1 Simple meters

A portable meter is ideal as it is lightweight and easy to carry to the problem location for a quick check of the harmonic levels. The market currently has several portable meters available. These instruments come with their own advantages and disadvantages in term of operation and design (Bingham, 2008). A microprocessor-based circuit is generally used by these devices in order to perform the necessary calculations for determining the individual harmonics up to the 50th harmonic. They can also provide *RMS* value, THD, and the telephone influence factor (TIF). Few devices have the ability to calculate harmonic powers both in magnitudes and phases, as well as the ability to upload stored waveforms and calculations to a computer.

2.4.5.2 General-purpose spectrum analysers

Spectrum analysis is performed on waveforms. These instruments are designed for a wide variety of applications and are termed as general signal analysis instruments. The benefit associated with these instruments is that they are equipped with very powerful capabilities at a reasonable cost, as they are manufactured and designed targeting a bigger market. Furthermore, they are not limited to applications only related to power systems. The drawback associated with them is that they are not designed specifically for sampling power frequency waveforms. As a result, attentive measures needs to be taken to gain an accurate harmonic analysis.

2.4.5.3 Special purpose power system harmonic analysers

Some instruments are specifically designed for harmonic analysis of power systems. They use the FFT with sampling rates especially designed for detecting power signals harmonic components. These devices can be left in the field and are equipped with communication capability from a remote area.

2.4.6 Combination disturbance and harmonic analysers

These instruments are more recent and combines the harmonic sampling and energy monitoring functions along with complete disturbance monitoring functions. The output is based on graphics and the data is collected remotely into a central database through phone

lines. Data can be analysed statistically. The data is readily available in the form of spreadsheets as an input as well as different processors (Bollen, 2000).

This type of analyser is shown in Figure 2.4. This instrument is designed for both utility and applications for end user. It can be enclosed and clamped on utility poles for outdoor installations. It is able to monitor 3-phase voltages and currents with neutrals together, which is a necessary component for detecting power quality problems (Parle et al., 2001). This instrument does the acquisition of raw data and stores the data in internal memory which can then be downloaded from a remote location. The downloaded data is analysed in offline mode using power software that can provide a wide variety of outputs.

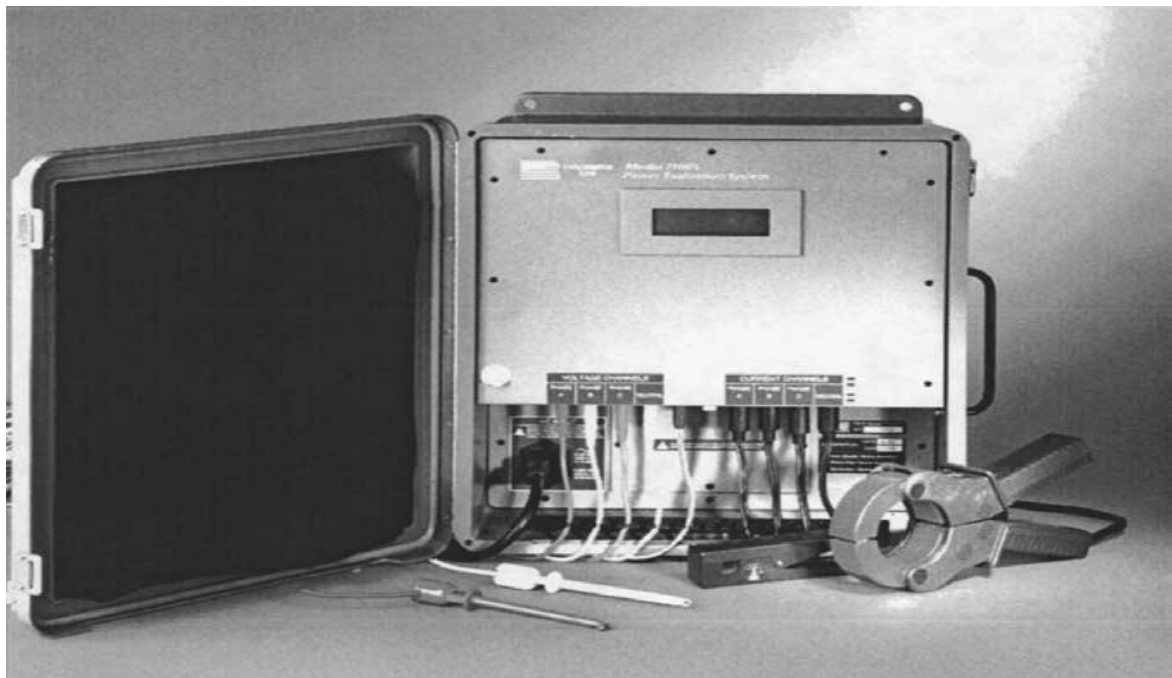


Figure 2.4: A power quality monitoring instrument capable of monitoring disturbances, harmonics on both utility systems and end-user systems

Adapted from (Parle et al., 2001)

2.4.7 Flicker meters

Flicker can be measured by a wide variety of approaches that range from utilizing very simple *RMS* meters that include flicker curves, to elaborate flicker meters that use specifically tuned filters and statistical analysis to evaluate the level of voltage flicker. Various approaches for measuring flicker are discussed below (Shea, 2004).

2.4.7.1 Flicker standards

There are IEEE standards that address flicker standards. IEEE Standards 141-19936 and 519-19927 both have flicker curves which work as utility guidelines for evaluating the severity of the flicker in the system. Standards 141 and 519 flicker curves are shown in Figure 2.5. Some other countries follow a standard approach of IEC standards when measuring flicker. The IEC flicker meter is used in Europe as a standard. The method as defined in IEC Standard 61000-4-158 (formerly IEC 868) is a very extensive approach for measuring flicker. In order to account for the differences of 120 V and 230 V systems, IEEE in recent times have adopted the IEC standards by adding an extra curve.

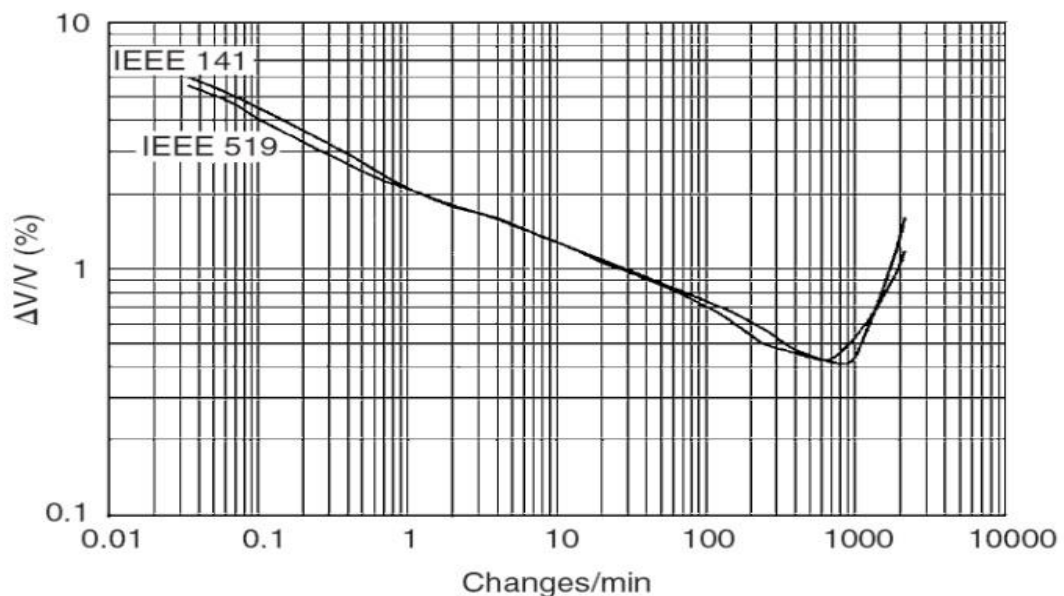


Figure 2.5: Flicker curves from IEEE standards 141 and 519

Adapted from (Shea, 2004)

2.5 Future applications

There are many applications for the concept of intelligent power quality monitoring. Some of which are listed in this section.

2.5.1 Industrial power quality monitoring applications

- Energy demand profiling with methods that save energy and reduce demand through the use of better appliances or reduced circuitry.

- Harmonic evaluation to determine transformer loading concerns, harmonics sources, errors which might result in failure of converters, and resonance concerns which are related to power factor correction.
- Evaluation of voltage sag to locate the sensitive equipment and possible opportunities for process ride.
- Power factor correction evaluation to locate the proper operation of capacitor banks, switching and resonance concerns, as well as the minimization of electric bills by optimizing the performance of the system.
- Motor starting evaluation to identify switching problems, inrush current concerns, and the operation of protection devices.
- Short-circuit protection evaluation to check for the proper operation of protective devices.

2.5.2 Power system performance assessment and benchmarking

- Analysis of steady-state power quality parameters for performance trends, correlation with system conditions, and identifying the conditions which require attention.
- Evaluation to locate the reasons for voltage sags in transmission or distribution as well as classifying these events for analysis.
- Characterisation of capacitor switching to locate the source of the transient, identify the capacitor bank, and classify events for analysis and database management.
- Calculations of performance and reporting back to the system for benchmarking and system maintenance.

2.5.3 Applications for system maintenance, operations, and reliability

- **Locating faults:** This can reduce the response time for repairing circuits considerably and also locates problem conditions which result in multiple faults over a period of time in a location.
- **Capacitor bank performance evaluation:** Use of smart applications can easily locate fuse blowing, failures, switching problems, and resonance problems.
- **Voltage regulator performance evaluation:** This evaluation is necessary to locate unusual operations, including arcing and regulation problems.
- **Distributed generator performance evaluation:** Smart systems should easily identify interconnection problems like protective device coordination, harmonic injection, or islanding.

- **Incipient fault identifier:** Research has shown that cable and arrester faults are often preceded by current discharges which start to appear weeks before the actual failure.
- Transformer loading evaluation to identify loss of life in transformers that may arise due to loading. Harmonic loading impacts are included in the calculations.
- Evaluating feeder breaker performance to locate coordination problems.

2.6 Summary and future direction

In recent times, power quality monitoring is becoming an integral part of general distribution system monitoring as well as an important customer service requirement. Power generating companies now include power quality monitoring along with energy management monitoring, evaluation of protective device operation, and distribution automation functions. The companies must provide the power quality information through the intranet. This information must be available to customers for appliance or equipment protection.

Power quality information should be analysed and summarised in a form that gives priority to the expenditures of the system as well as ensuring that customers can understand it. This clearly signifies that power quality indices must focus on sensitivity of customer equipment.

Information received from monitoring power quality can be used to improve the efficiency and reliability of the system with respect to customers. In terms of power quality research, there are advantages associated with all involved parties, from companies to consumers. Research regarding this is still in progress and is geared towards improved capabilities and applications for power quality monitoring.

Table 2.2: Types of power quality variations

Adapted from (McGranaghan, 2001)

Power quality variation Parameters	Monitoring Requirements	Requirements for analysis and display
Voltage: Regulation and unbalance	<ul style="list-style-type: none"> • 3-phase voltages • magnitude of <i>RMS</i> value • Continuous monitoring within a period with samples max./min./avg. • Currents for response of equipment 	<ul style="list-style-type: none"> • Moving • Statistical evaluation of voltage and unbalance levels
Harmonic distortion	<ul style="list-style-type: none"> • 3-phase voltages and currents • Waveform Characteristics • Minimum 128 samples/cycle • Sampling of all voltages and currents synchronised together • Sampling characteristics configurable 	<ul style="list-style-type: none"> • Individual waveforms and their FFTs • Harmonic levels trends (Total harmonic distortion and individual harmonics) • Statistical characteristics of harmonic levels • Evaluation of neutral conductor loading issues • Evaluation with respect to standards (e.g., IEEE 519, EN 50160)
Voltage sag, swells, and short duration interruptions	<ul style="list-style-type: none"> • For each event that is captured, 3-phase voltages and currents • Configurable thresholds of triggering events • Events characteristics with actual voltage and current waveforms, as well as plots of <i>RMS</i> value vs time • 1 cycle resolution of <i>RMS</i> value 	<ul style="list-style-type: none"> • plots of waveform and <i>RMS</i> vs time with the pre and post event information • Detailed evaluation of the reason of each event • Voltages and currents to evaluate load interaction issues • Plots of magnitude duration with equipment ride through characteristics • Summary of statistical performance using bar charts for benchmarking • Power conditioning equipment performance evaluation during events

Transients

- 3 phase voltages and currents with complete waveforms
- Minimum of 128 samples per cycle for events from the power supply system (e.g., capacitor switching)
- Thresholds configurable for triggering
- Triggering based on waveform variations, not just peak voltage
- Waveform plots
- Evaluation of event causes (e.g., capacitor switching uplink or downlink from monitor)
- Correlation of events with switching operations
- Statistical summaries of transient performance for benchmarking

CHAPTER THREE

MITIGATION TECHNIQUES

3.1 Introduction

Factories with automation make use of power electronics to aid in process control. This equipment includes AC drives, DC drives, computers, and PLCs. Faults in power systems cause process interruptions related to factors such as costs and production. Therefore, it is important to mitigate these faults at each stage for better efficiency.

3.2 Organization of the chapter

Many compensating techniques have been developed to mitigate various faults. Some techniques from the literature has been extracted, such as the direct AC-AC converter method, eight-switch power conditioner method, and the SW-SVC method. Furthermore, the use of DSTATCOM is discussed in order to mitigate voltage sag at the distribution end. In the next section, mitigation of micro-interruptions and long interruption are emphasised.

Customer-based approach and probabilistic life cost are two techniques that are discussed. Thereafter, voltage spikes mitigation is discussed in detail. AC photo-voltaic models and MV spark gap operation is surveyed in terms of enhancing power quality. The use of a zig-zag transformer, autotransformer with random hysteresis voltage control, and an SSC is surveyed to mitigate voltage swell. The next section provides detail on voltage fluctuation mitigation. STATCOM modelling, arc furnace strategy, and balancing theorem are then discussed. Lastly, active power controller methods and power electronic interfaces to mitigate harmonic distortion are discussed.

3.2.1 Voltage sag mitigation

Voltage sag is generally caused by excessive network loading. Different techniques which are used for mitigation are mentioned below.

3.2.1.1 Direct AC to AC converter

The direct AC-AC converter is one of the most efficient technology available for use. The conventional DVR (Dynamic Voltage Restorer) topologies are not preferred due to having DC links. Topologies without DC links are more convenient as they do not require a storage device

(Jothibasu & Mishra, 2015). Figure 3.1 depicts a schematic diagram of the proposed topology including a detailed phase-a sag supporter.

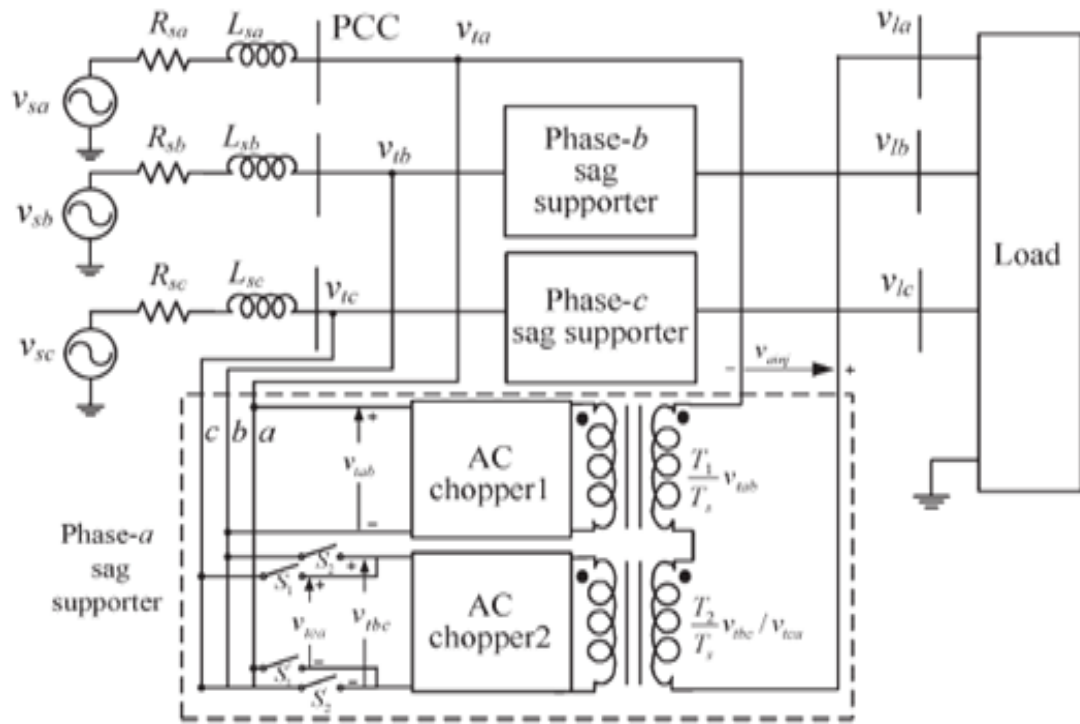


Figure 3.1: Direct AC-AC converter technology

Adapted from (Jothibasu & Mishra, 2015)

The voltage sag supporter is connected between the PCC and the load. In case of a voltage dip at a point of common coupling, the voltage required in series of the supplied voltage is injected by the corresponding sag supporter. This is done for the desired voltage across the load. In Figure 3.2, the topology uses the interphase AC-AC topology for phase compensation (Jothibasu & Mishra, 2015), together with 1 sag supporter, 2 choppers, and 1 isolation transformer in each phase. The isolation transformer's secondary winding is always connected and is used to sum and inject the choppers output voltages.

Figure 3.3 shows the prototype model of the AC-chopper based DVR.

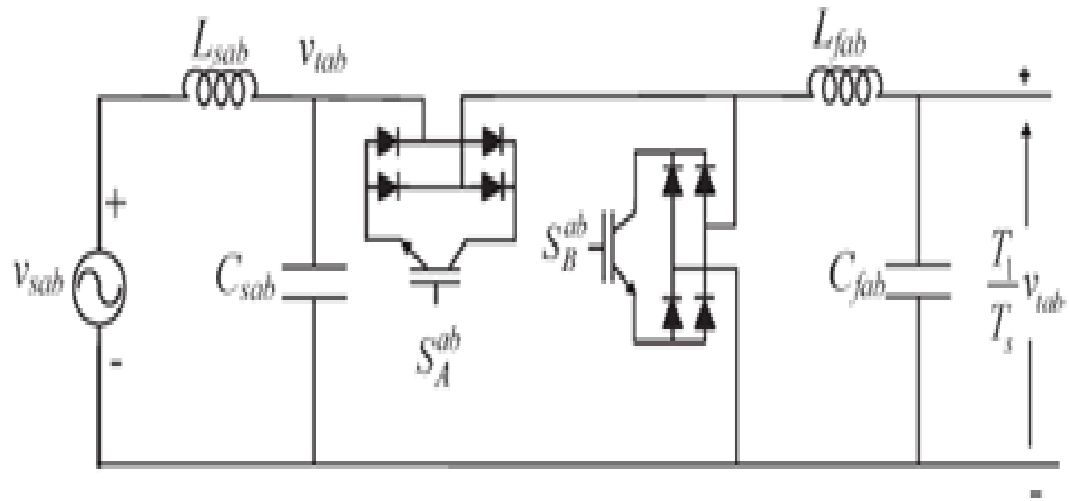


Figure 3.2: AC chopper across line (a-b) in phase of a sag supporter
Adapted from (Jothibasus & Mishra, 2015)

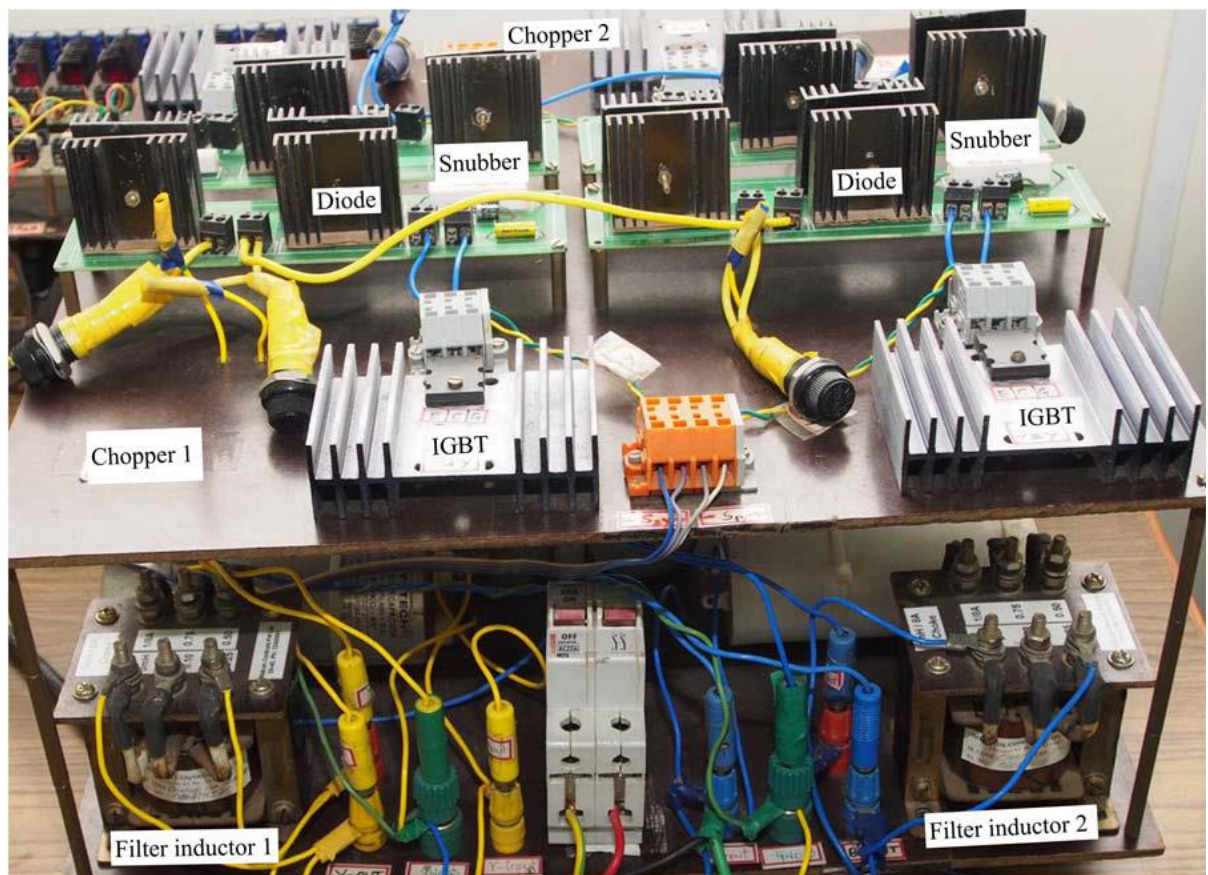


Figure 3.3: Prototype model of AC-chopper-based DVR
Adapted from (Jothibasus & Mishra, 2015)

3.2.1.2 Eight-switch power conditioner

A converter which uses nine switches has been proposed in the literature and is considered for many applications. This is used as a replacement of the dual bridge converter in which bridges are connected back-to-back.

The main benefit which the 9 switch converter has over a dual bridge converter is the number switches; the dual bridge converter uses 12 switches while the proposed converter uses 9 switches, as the name indicates. The 9-switch converter lacks in terms of attaining the total output, as it depends on the phase shift between its two terminals.

The overall power quality can be improved via the use of a properly designed control scheme to justify the use of a 9-switch converter as a power conditioner. The cost of a 9 switch converter is less due to the switches being reduced by 3. Additionally, an eight-switch converter is also given below which composes a unit for mitigation of voltage sag. For current harmonic compensation, another unit is used.

The use of a hybrid filter with the shunt converter is shown in Figure 3.4. The duty cycles D_A and D_R of switches S_A and S_R (Cavalcanti et al., 2015) can be determined by equation (3.1) and (3.2).

$$D_A = \frac{1}{2} + \frac{V_A}{V_{DC}} \quad (3.1)$$

$$D_R = \frac{1}{2} - \frac{V_R}{V_{DC}} \quad (3.2)$$

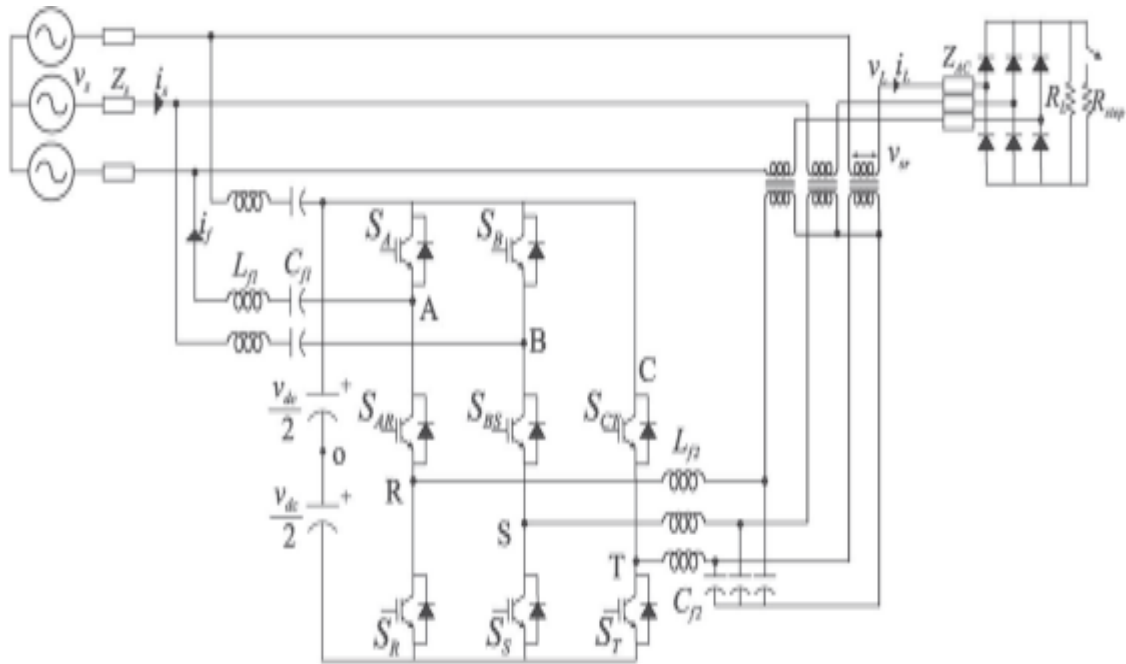


Figure 3.4: 8-switch conditioner using hybrid filter

Adapted from (Cavalcanti et al., 2015)

V_A and V_R are the reference voltages imposed at output terminal A and R respectively. There are two controls used in an 8-switch conditioner: series control and shunt control. The series converter complementary duty cycle can be obtained by scaling the duty cycles used in Equation (3.3) and (3.4).

$$\bar{D}_{Rseries} = M_{series} \bar{D}_R \quad (3.3)$$

$$\bar{D}_{Rseries} = M_{series} \left(\frac{V_R}{V_{DC}} + \frac{1}{2} \right) \quad (3.4)$$

The series converter is only responsible for injecting fundamental voltages and is designed for voltage sag mitigation. The experimental results of the filter is shown in Figure 3.5.

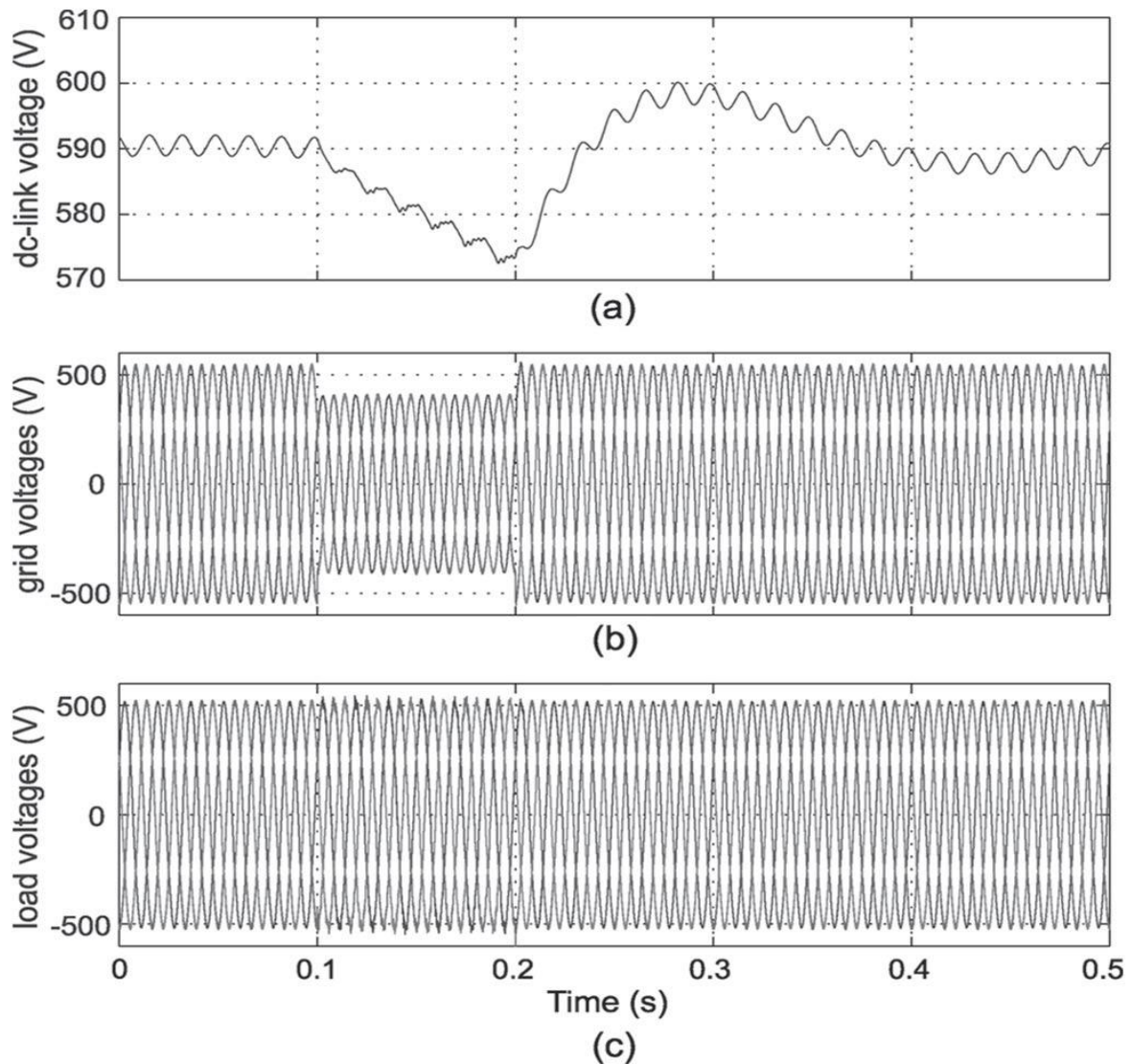


Figure 3.5: Simulation results of the 8-switch conditioner with 3-phase voltage sag (a) DC link (b) grid and (c) load

Adapted from (Cavalcanti et al., 2015)

3.2.1.3 Square Wave Series Voltage Compensator (SW-SVC)

Voltage sag is a major power quality issue. The traditional method to keep industrial processes safe from voltage sags is the utilisation of a large series voltage compensator (SVC) such as the DVR. SVCs are the best solution, however, they come at a higher cost. Sometimes, the overall cost of the process is far lesser than the cost of SVCs. It is therefore better to look for options with similar characteristics but at a lesser cost.

For example, adjustable speed drives (ASDs) comes with embedded protection functions which can mitigate voltage sags. The other cost-effective solution is to protect the contactors and power line carriers with low-power single-phase square wave SVCs. Combining these two can provide considerable improvement of the protected process ride through capability.

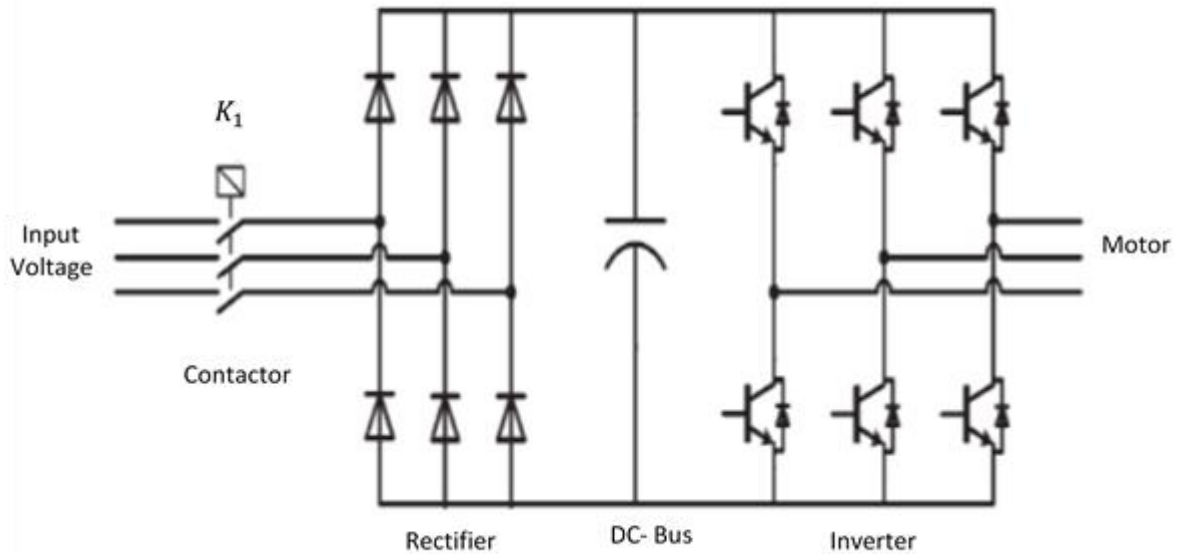


Figure 3.6: ASD Typical topology

Adapted from (Pires et al., 2015)

ASD is an electronic device which mitigates voltage sags. The topology of ASD is shown in Figure 3.6. A square-wave voltage is injected during the voltage sag generated by a line frequency amplitude modulated voltage inverter. During overload condition, this injected voltage sums up with the remaining voltage, eventually leading to the protection of the sensitive loads. Figure 3.7 shows the series voltage compensation (Pires et al., 2015).

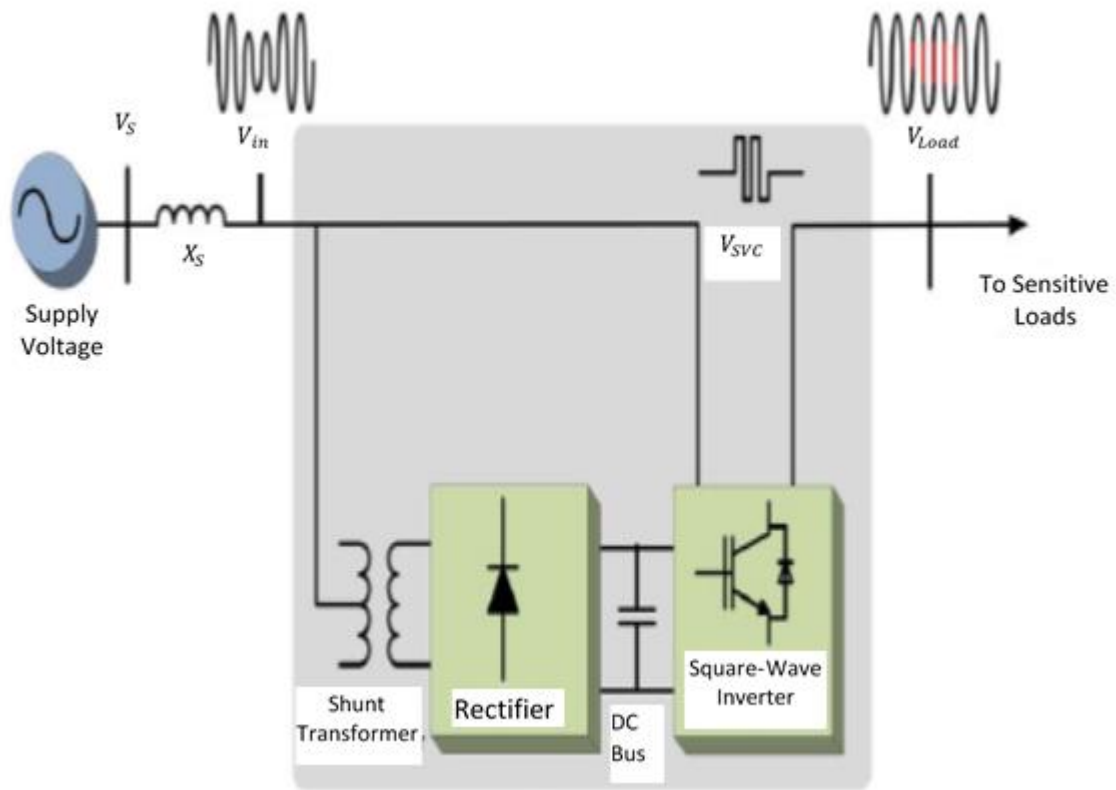


Figure 3.7: Series Voltage Compensator Square Wave Inverter
 Adapted from (Pires et al., 2015)

Figure 3.8 and Figure 3.9 depicts the test drive set. The test drive has an induction motor with the rating 220 V, 1.5 hp, and 1700 rpm. It also includes a mechanical load emulator eddy current brake Figure 3.8. The ASD is connected to the supply with the help of a connector as shown in Figure 3.9.

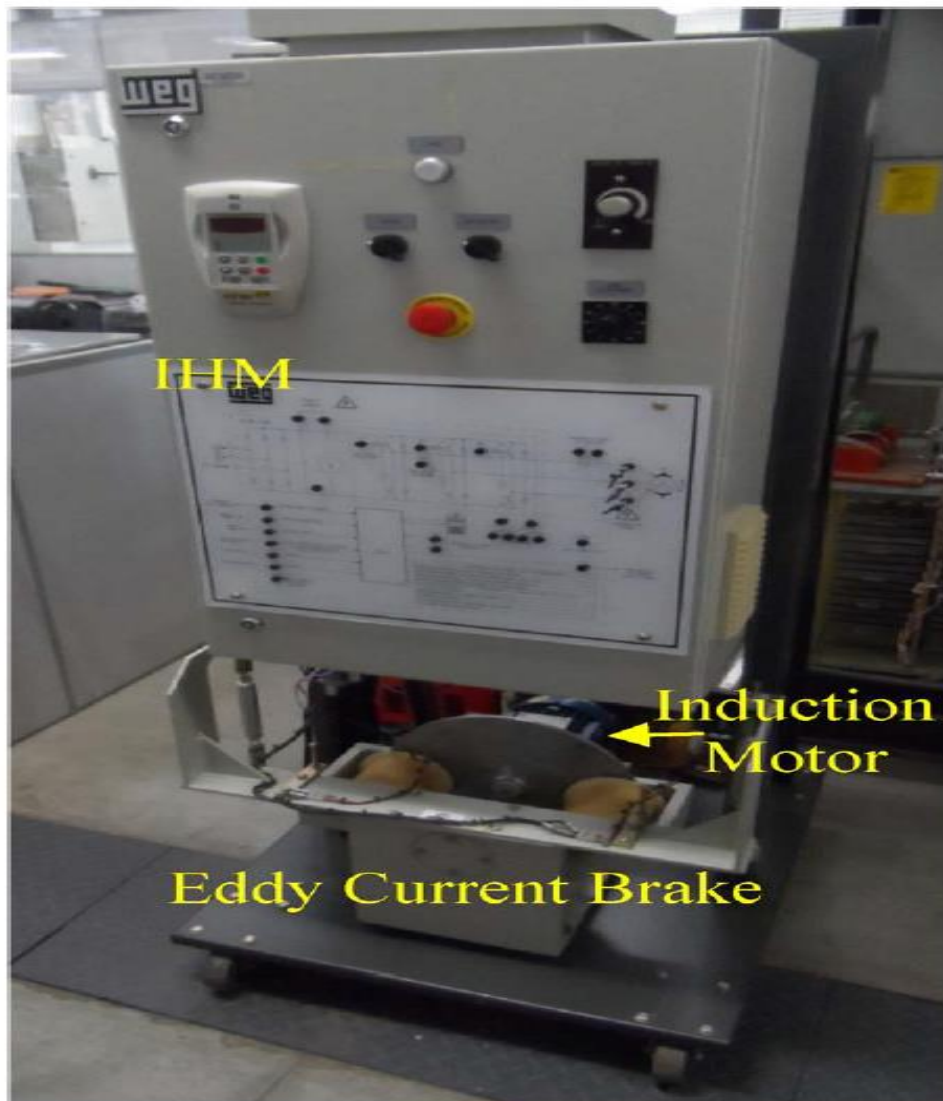


Figure 3.8: Control panel with an ASD and an induction motor

Adapted from (Pires et al., 2015)



Figure 3.9: Interior of the test control panel with an ASD and induction motor

Adapted from (Pires et al., 2015)

3.2.1.4 Distribution Static Compensator (DSTATCOM)

The DSTATCOM is covered in Chapter 5. The circuit diagram of DSTATCOM is shown in Figure 3.10, which uses 3-point-phase 4-wire, and 2-level neutral clamped voltage source inverter (Mishra et al., 2003). Figure 3.11 shows a single phase equivalent representation of Figure 3.10. “ u ” is a switching function and can have the value of either $+1$ or -1 , depending on its switching state. The filter inductance, resistance, and shunt capacitor are denoted by

L_f , R_f , and C_{fc} respectively. The shunt capacitor is used to eliminate high frequency components.

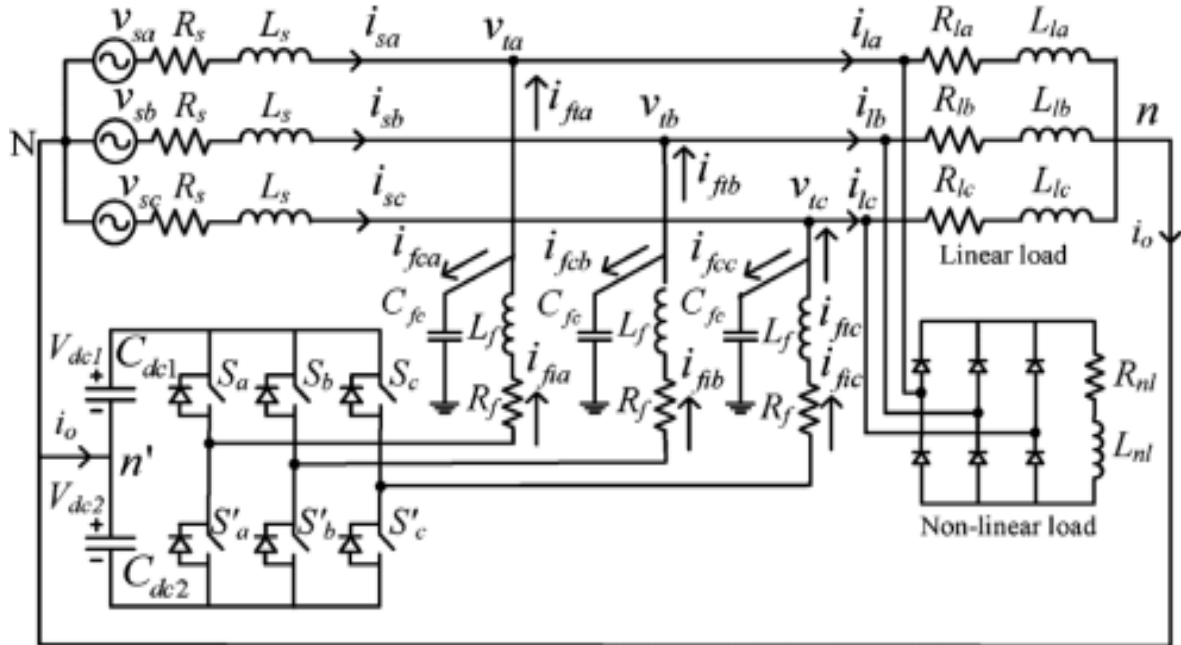


Figure 3.10: Compensated DSTATCOM circuit diagram

Adapted from (Mishra et al., 2003)

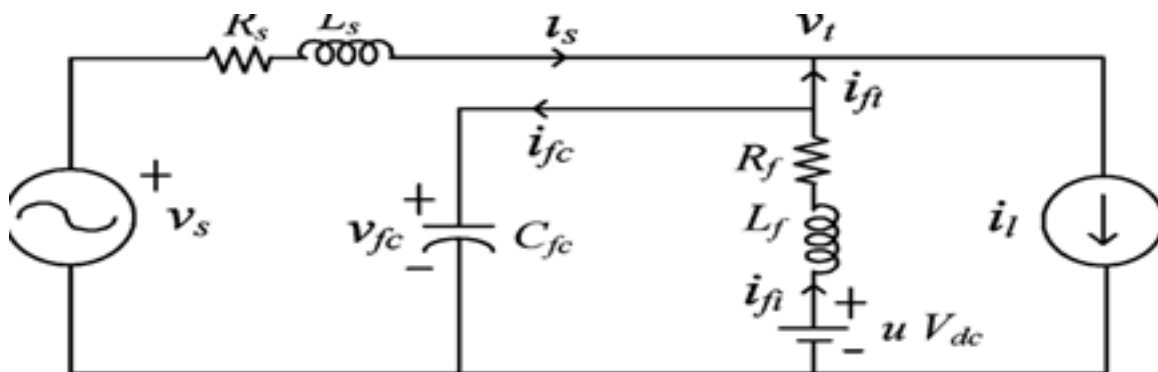


Figure 3.11: Equivalent circuit of single-phase DSTATCOM

Adapted from (Mishra et al., 2003)

3.2.2 Micro-interruptions mitigation

Micro-interruptions are commonly caused by insulation failure and lightning. Some probabilistic models are discussed to mitigate micro-interruptions. Voltage dips and interruptions leads to major economic damage including market and client loss. Therefore, it would be beneficial to find alternative methods of optimal mitigation. Some theories are discussed below.

3.2.2.1 Customer-based approach

In order to maintain customers, energy providers must reduce problems such as voltage dips and interruptions. Selecting the most cost-effective mitigation method is potentially challenging due to the varying characteristics of devices as well as variations in nature. There is inconsistency between industrial selection approaches and theoretical approaches. An optimal mitigation approach which is close to both is defined and applied to a practical example.

In Figure 3.12, a typical medium voltage (MV) distribution grid is shown. The interruption cost is very high and the installation rated power is typically from 40 to 400 KVA. The industrial plant is connected to the public grid on an open ring structure in a strongly meshed grid rated power. The reliability data at the connection point to the public grid can be viewed from literature (Girbau-Llistuella et al., 2017). The results of this approach is easy to understand and can also be used when comparing the performance of other mitigation approaches.

3.2.2.2 Probabilistic life-cycle cost

There are several kinds of custom power solutions which affects the life cycle cost analysis. In Qdo et al., (2009), cost analysis using either deterministic or probabilistic approaches is done. With the deterministic approach, both input variables and outcomes are deterministic numbers, however, they can give misleading outputs. The probabilistic approach is more comprehensive and accurate due to the use of the Monte Carlo Simulation. This method was therefore used for 10,000 iterations. The Probability Density Function (PDF) is shown in Figure 3.13. This provides better idea of the advantages that can be achieved by installing the device.

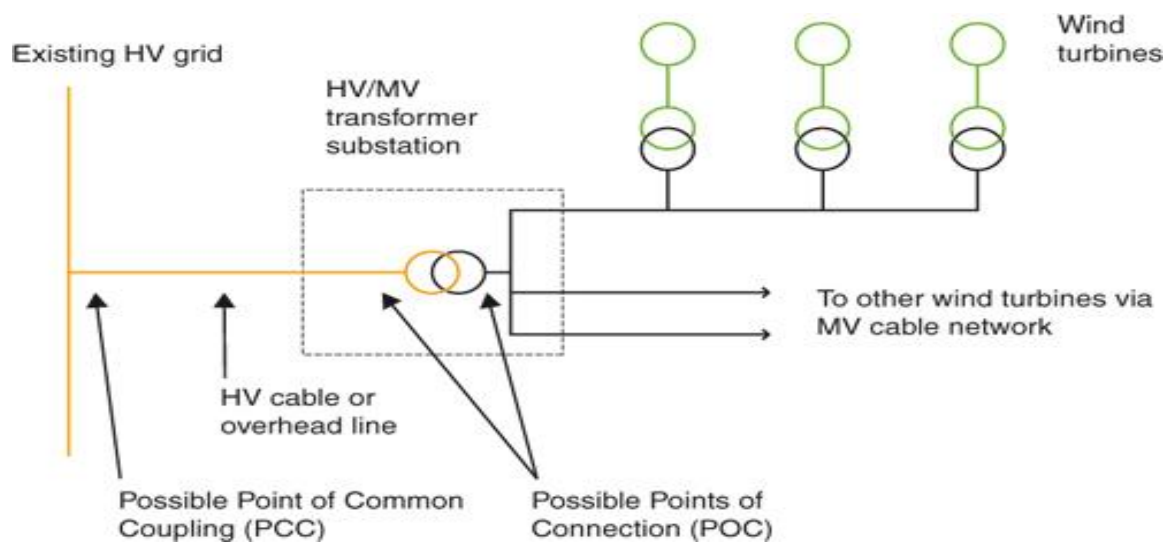


Figure 3.12: Typical MV distribution grid

Adapted from (Van Hertem et al., 2007)

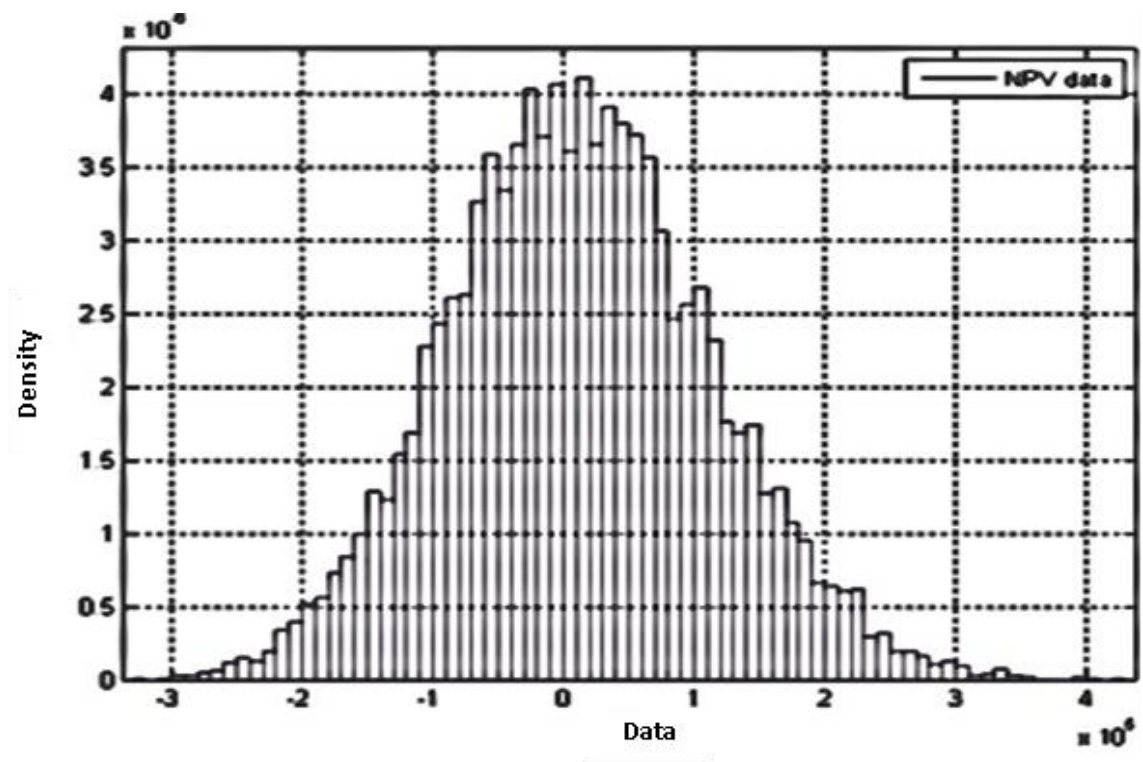


Figure 3.13: Probability density function of net present value using monte-carlo simulation

Adapted from (Qdo et al., 2009)

3.2.3 Voltage spikes mitigation

Voltage spikes are generally caused by lightning and the disconnection of heavy loads. Various models have been used to mitigate fluctuations, some of which are discussed below.

3.2.3.1 AC Photovoltaic (PV) models

One means to mitigate the spikes is to reduce the parasitic inductance, however, this is not a practical approach. AC PV models can be used, because micro-inverters are clamped directly on the module, thereby eliminating the DC wires, with too much of the parasitic inductance. One way is to eliminate the repeated switching in the mornings and in the evenings. For this, the voltage threshold needs to be set. Voltage spikes can also be eliminated by using DC side relays that are switched at zero currents. Figure 3.14 shows the voltage spikes during the inverter's morning start-up. The effect of spikes on the DC side relays is always a point of concern (Vangala et al., 2008).

Finally, it can be deduced that micro-inverters in AC PV arrays do not suffer from this problem because a properly mixed and balanced module connected to a micro-inverter must have a negligible parasitic inductance.

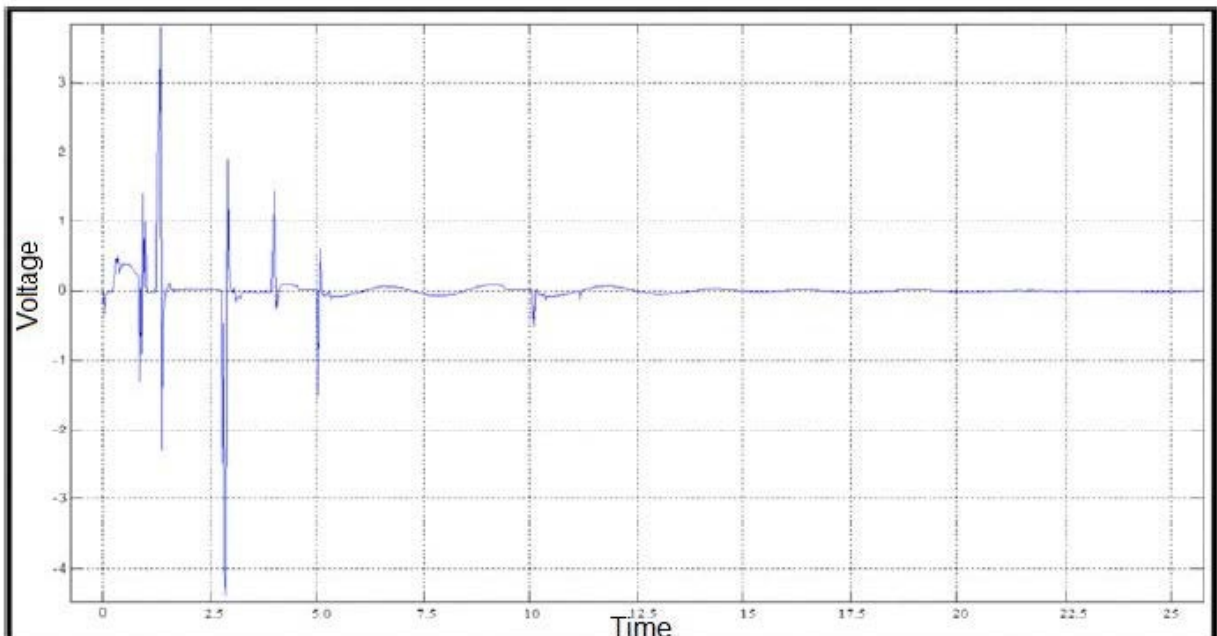


Figure 3.14: Voltage spikes recorded at the PV array terminal during inverter morning start-up

Adapted from (Vangala et al., 2008)

3.2.3.2 Medium voltage (MV) spark gap operation

Spark gaps are often used to protect small distribution transformers. Due to the steep voltage changes in the secondary side, an overvoltage is coupled with the ignition of the spark gap. The customer socket can be influenced by this overvoltage. The breakdown of MV spark gaps is studied in this sub section in which an impulse is superimposed on AC voltage. In order to study the propagation of overvoltage to the low-voltage side, a high frequency and detailed transformer model is used.

In Sabiha & Lehtonen (2010), MV spark gaps breakdown probability is modelled first under an impulse voltage superimposed on AC voltage. This model is then utilised to determine single-phase, double-phase and three-phase spark gap breakdown possibilities for the conditions when lightning induces the overvoltage. A high frequency transformer model is used to study the overvoltages and effects using the transformer.

The distribution transformer model with MV spark gap and low voltage (LV) network are used in a single circuit to study the performance of LV network under lightning-induced overvoltages.

The use of a low-voltage surge arrester (SA) at the secondary terminals of the distribution transformer are explored for the mitigation of transferred overvoltage. When a SA is used at the transformer secondary side, it can protect the customer load from the overvoltage which is transferred through the distribution transformer. The model which is used is the Frequency Dependent model as shown in Figure 3.15.

In this model, non-linear V-I characteristics of an arrester is represented with two sections of non-linear resistance, A_0 and A_1 . The (R-L) filter has considerable impedance for fast front surges. To conclude, the LV network can be protected by installing a SA in the beginning in order to block or reduce the effect of the overvoltages before it can reach the customer utility.

3.2.4 Voltage swell mitigation

Voltage swells are generally caused by ground faults that affect the power system. They can lead to overheating, tripping, or even the complete failure of an industrial unit or equipment, such as motor drives and control relays. There are many techniques which can be employed to mitigate this power quality problem.

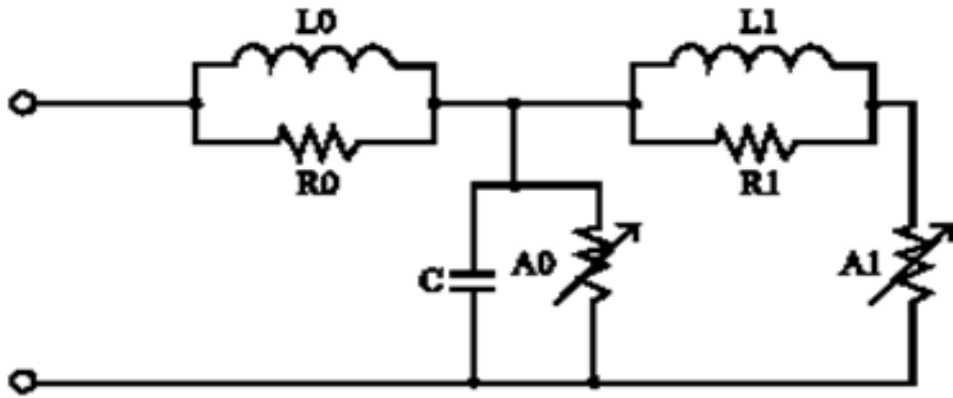


Figure 3.15: Frequency Dependent Surge Arrester

Adapted from (Sabiha & Lehtonen, 2010)

3.2.4.1 Zig-zag transformer

The benefit of using a voltage swell compensator, which is based on a switched autotransformer by random hysteresis voltage control, is that for every phase a single controlled switch is used without storing any energy. In addition, the control scheme distributes the load voltage harmonic spectrum and leads to the reduction of total harmonic distortion (THD).

A 3-phase zig-zag winding transformer connected across a 3-phase star load can be used to mitigate voltage swell across any single phase of the load at a time. The circuit diagram of this technique is shown in Figure 3.16. The combination of the transformer and the load receives power from a contractor, R . The star point of the load is connected to the neutrals of both the supply and zig-zag transformer. (Basu & Hafidz, 2008).

In Figure 3.16, when a voltage swell exists in any one phase at a time, the disturbance is sensed by a voltage sensitive relay which opens the faulty phase contractor to create a single phasing condition of the 3-phase supply. Simultaneously, the extra connection of R is closed for providing the connection between the transformer and supply neutrals. The effect of voltage swell in single-phase is almost negligible when the load is connected as shown in Figure 3.16.

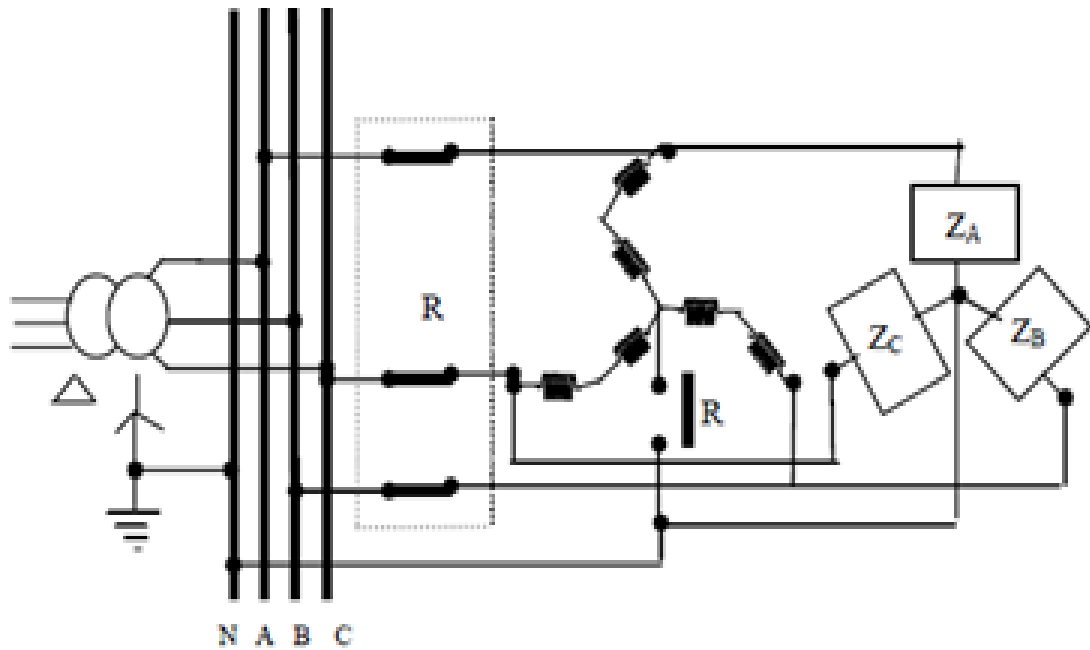


Figure 3.16: Schematic diagram of zig-zag transformer

Adapted from (Basu & Hafidz, 2008)

3.2.4.2 Autotransformer with Random Hysteresis Voltage Control

Dynamic voltage restorer (DVR) and STATCOM are normally utilised as solutions for voltage sag and swell. The modelling and analysis of a PWM switched autotransformer is presented as a device which can be used as a mitigation method for voltage sag and swell disturbances. This system requires less switching devices and is a better compensator compared to commonly used compensators. This compensator limits the load voltage THD in the presences of disturbance. This compensator can also keep the real load and reactive powers constant.

The literature presents another voltage swell compensator which is constructed on a switch autotransformer by random hysteresis voltage control. The benefit of using this compensator is that a single controlled switch is used in each phase without any energy storages. Figure 3.17 shows this compensation scheme. It consists of a single IGBT switch used in a bridge configuration, a thyristor bypass switch, output filters, an autotransformer, and the system controller (Mehranfar et al., 2011).

The four power diodes denoted as D1, D2, D3, and D4 are connected to the IGBT switch (SW), controlling the direction of power flow which is connected in the AC voltage controller configuration shown in Figure. 3.18.

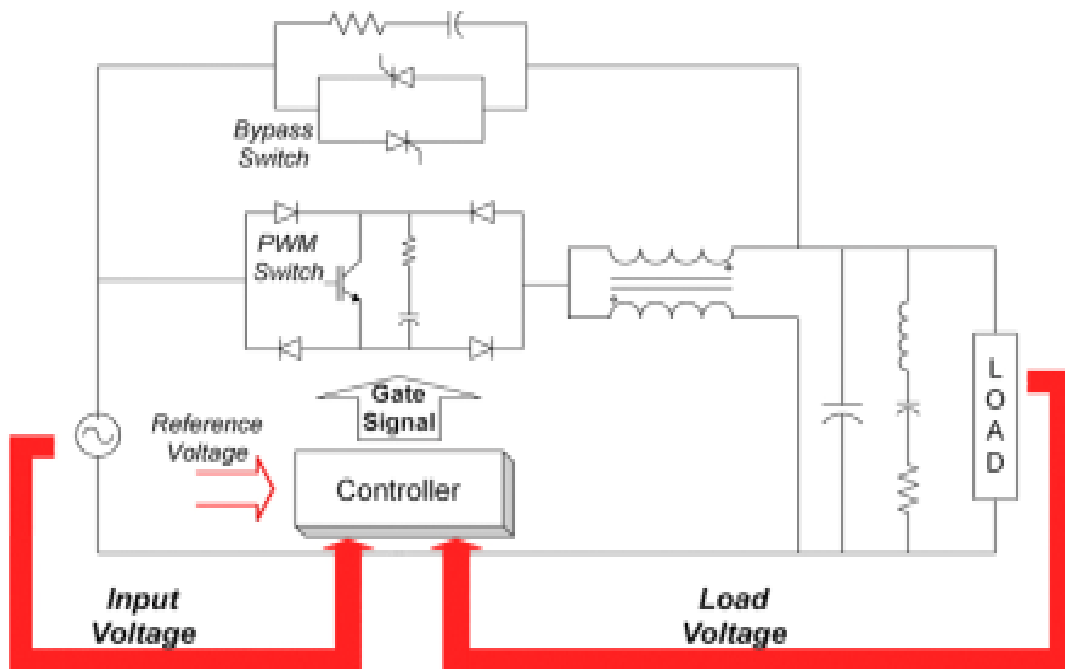


Figure 3.17: Basic configuration of autotransformer

Adapted from (Mehranfar et al., 2011)

This configuration, with an appropriately controlled circuit, maintains a steady RMS voltage. Swell begins when one of the RMS voltages transcends the limit and finishes when every one of the three RMS voltages have recouped beneath the edge (Bollen et al., 2009). In Figure 3.17, an autotransformer is utilised instead of a two-winding transformer. A transformer with $N1:N2 = 1:1$ proportion is utilised to alleviate the voltage swell. The switch is situated on the essential side of the autotransformer. At the point when the swell is determined by the voltage controller, IGBT exchanging began, directed by the heat created of arbitrary hysteresis voltage control with the end goal being that the heap voltage on the auxiliary of the autotransformer becomes RMS voltage.

3.2.4.3 Static Series Compensator (SSC)

Swells and overvoltage can cause overheating, stumbling or the obliteration of engine drives and control transfers. This area explores the likelihood of utilising the Static Series Compensator (SSC) to alleviate voltage swells and overvoltages. On account of voltage swells, dynamic power might be drawn from the matrix into the vitality stockpiling capacitor (ESC) of the SSC, contingent upon the heap current and the SSC impedance. This dynamic power may cheat the ESC. Two conceivable outcomes to overcome this circumstance are investigated in this segment. The first being, that if the DC-voltage of the ESC is lower than a preordained

voltage level, the dynamic power can be utilised to charge the ESC to the required voltage level, and secondly, the overvoltage assurance of the SSC must work.

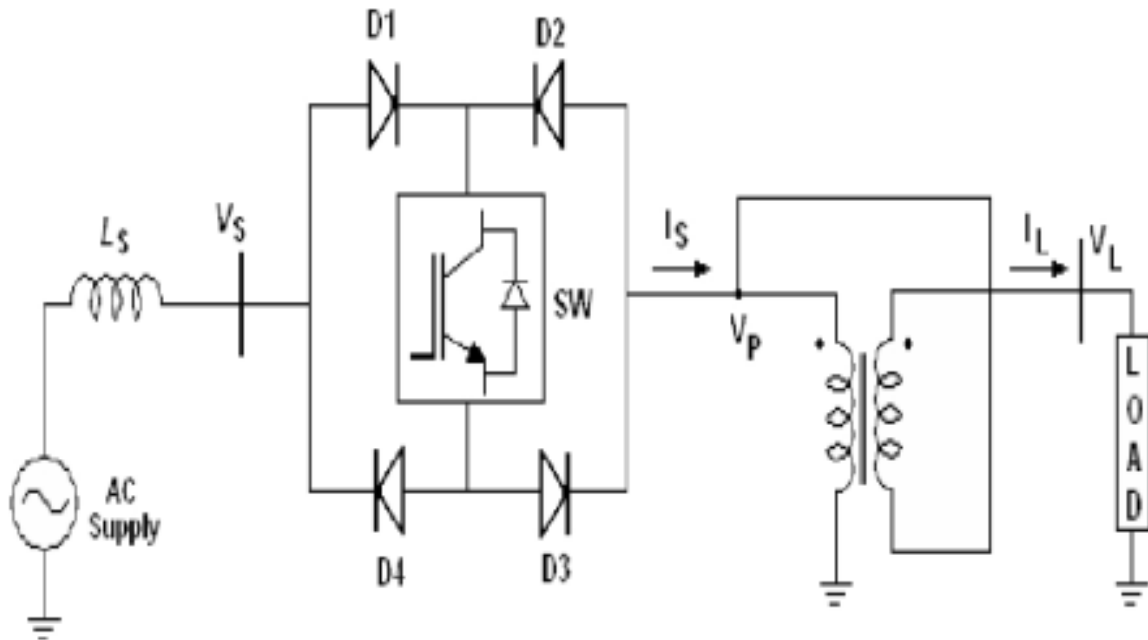


Figure 3.18: Voltage swell mitigation device

Adapted from (Mehranfar et al., 2011)

The fundamental capacity of SSC is to progressively infuse a controlled voltage to keep the heap voltage steady. Model of SSC appears in Figure 3.19.

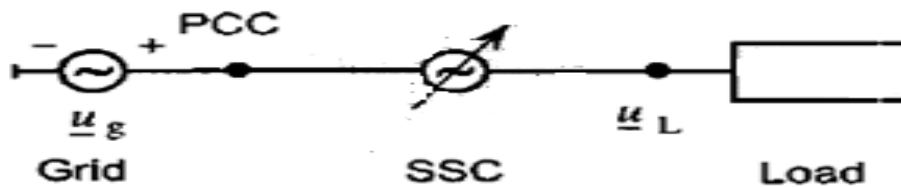


Figure 3.19: Simplified circuit diagram of SSC

Adapted from (Awad & Blaabjerg, 2004)

Figure 3.20 demonstrates a more detailed single stage model of an appropriation feeder with a SSC (Awad & Blaabjerg, 2004), where the network voltage u_g , the SSC voltage, u_{inj} , and the load voltage u_L , are in series.

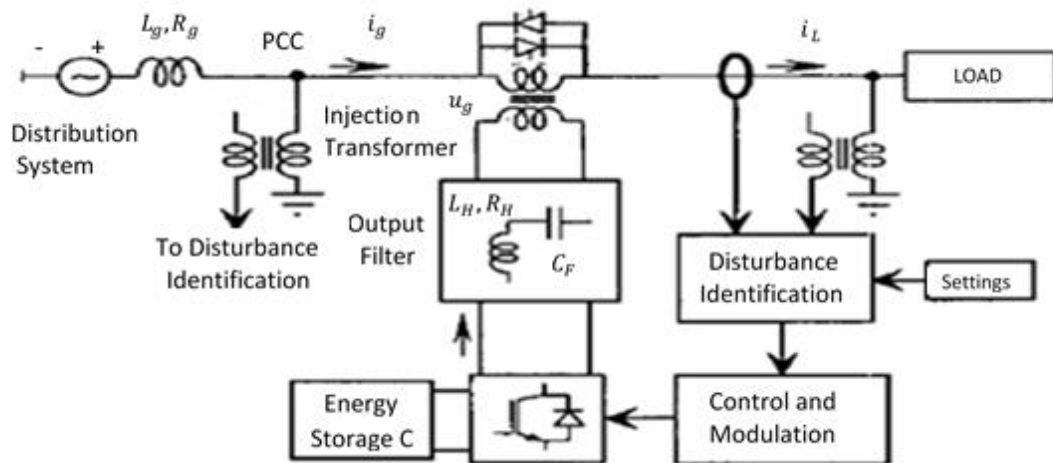


Figure 3.20: Detailed single-phase model of SSC
Adapted from (Awad & Blaabjerg, 2004)

Overvoltage assurance of the SSC can be made or disconnected relying upon the achieved level of the DC voltage. The on-line assurance depends on exchanging a resistor by means of a DC-chopper to disseminate the vitality overabundance in the DC capacitor. The disconnected security is activated if the DC voltage surpasses its cut-off and thus the SSC ought to be skirted.

3.2.5 Voltage fluctuation mitigation

Voltage fluctuation is caused by the frequent starting or stopping of motors. There are various methods to mitigate voltage fluctuation, which are as per the following.

3.2.5.1 Static Synchronous Compensator (STATCOM) Modelling

Voltage fluctuations caused by fast mechanical load changes have been a noteworthy concern for both power organisations and clients with regards to power quality. The quick reaction of the Static Compensator (STATCOM) makes it an effective answer for enhancing the power quality in distribution frameworks. This subsection depicts a model for a PWM-based STATCOM utilised as a part of a distribution system for mitigation of voltage fluctuations created by an Electric Arc Furnace (EAF).

Static and dynamic performance of STATCOM is assessed and voltage fluctuation mitigation moderation are performed and discussed. The voltage fluctuation mitigation is acquired by estimations and as indicated by international standards. It incorporates a 2-level voltage source inverter with a capacitor bank in DC interface. The design of this power system can be seen in Figure 3.21.

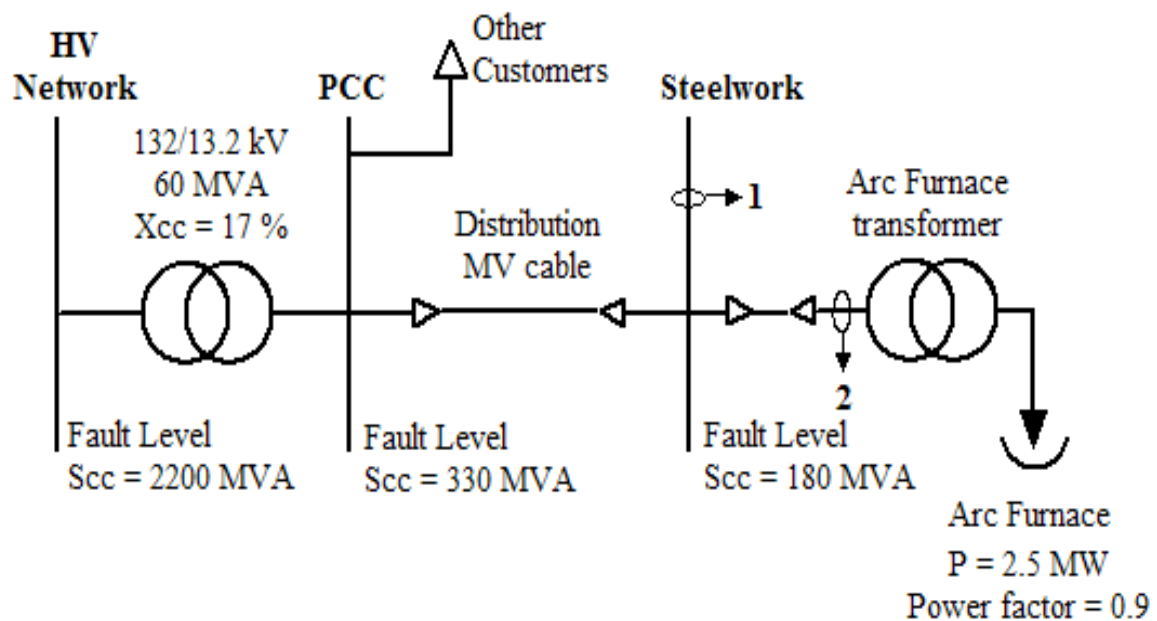


Figure 3.21: Electrical system configuration

Adapted from (Aguero et al., 2006)

The STATCOM is composed in such a way that it can be controlled to mitigate voltage fluctuation (Aguero et al., 2006). The power system at the point of connection to the disturbing load bus bar is described by its non-load voltage, E_s , and its impedance, Z_s . The voltage is denoted by V . The load consumes active power, denoted by P , and reactive power,

represented by Q. The portrayal of the power system with the EAF and the STATCOM is shown in Figure 3.22.

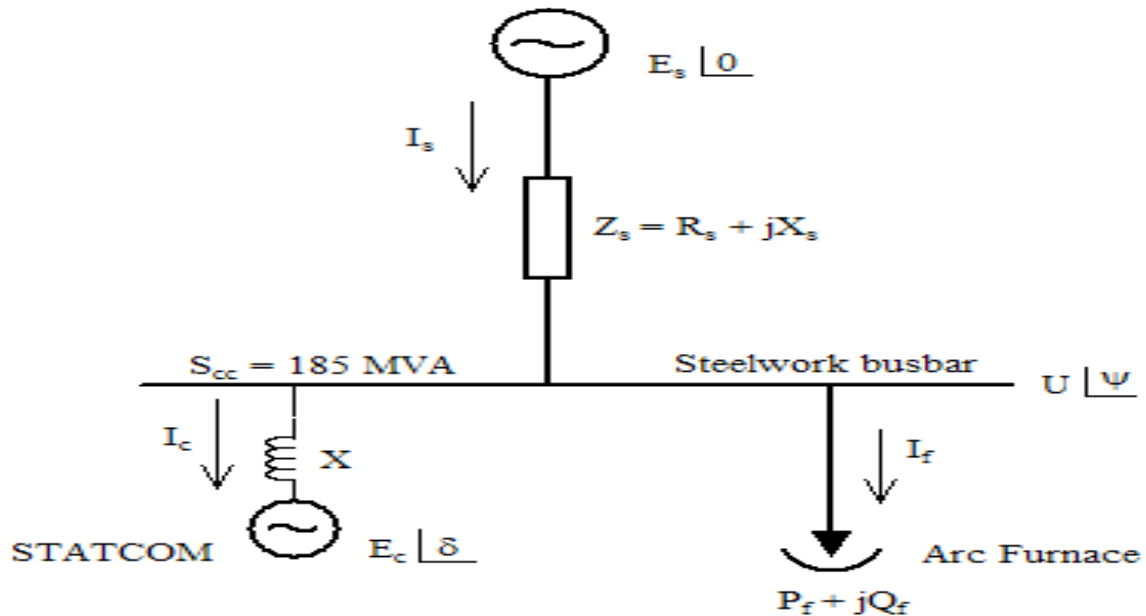


Figure 3.22: Power system single line diagram

Adapted from (Aguero et al., 2006)

The current flowing in the system impedance is the aggregate of the current drawn by the arc furnace and the current infused by the STATCOM.

3.2.5.2 Strategy produced by arc furnace

Voltage flicker has picked up a great deal of attention as of late in light of the multiplication of the non-linear varying loads in modern industrial distribution systems. This section presents a control calculation for DSTATCOM to lessen the flicker level to an adequate range as per IEEE measures.

The control procedure of this stage depends for the most part on re-establishing the voltage by injecting reactive power. The control block is used for the most part concluded from the literature (Hosono et al., 1979). In this control system, the reactive current is specifically identified with the difference in voltage at the point of DSTATCOM establishment (Sensarma et al., 2001).

Electric arc furnace strategy (EAF) is an effective strategy to mitigate voltage fluctuation. Electric arc furnace is designed as a source of current which is controlled by a non-linear resistance. This model which is developed for EAF is applied to DSTATCOM model for voltage fluctuation mitigation. The EAF model is shown in Figure 3.23. It consists of three main parts (a) a current controlled PWM inverter with a DC capacitor (b) a closed loop controller, and (c) the coupling inductors as shown in Figure 3.23 (Anuradha et al., 2008)

The controller with DSTATCOM basically works in reactive power compensation mode. EAF load will produce voltage fluctuations near point of common coupling. The DSTATCOM is connected in shunt with the system in order to mitigate fluctuations.

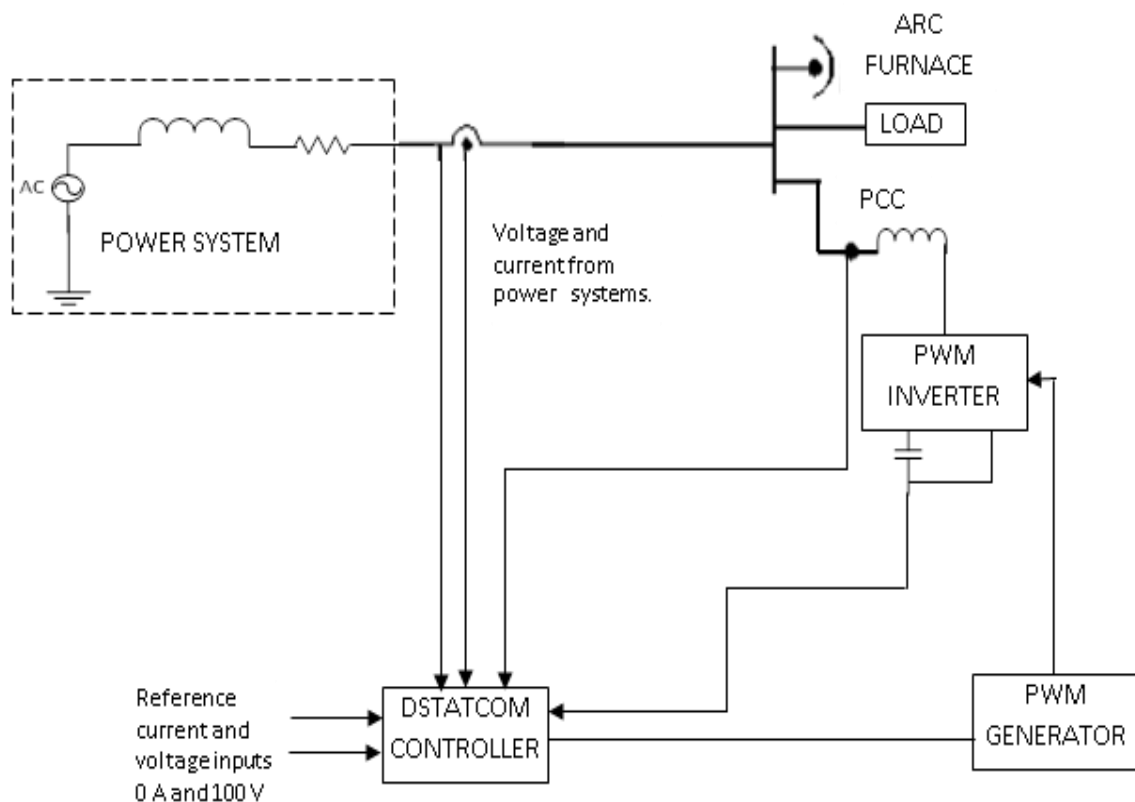


Figure 3.23: Control block diagram for voltage fluctuation compensation

Adapted from (Anuradha et al., 2008)

3.2.5.3 Mitigation of voltage fluctuation in HVDC systems

Switching loss of Modular Multilevel Converter (MMC) may increment drastically in High-voltage Direct Current (HVDC) systems on the grounds that the quantity of the sub-module (SM) is relative to the DC connected voltage. The voltage fluctuation of the capacitor in the SM increases as the switching frequency decreases. The capacitor with large capacitance, which is the primary bit of equipment cost for SM, is required to mitigate the voltage fluctuation. This segment (Lee et al., 2014) presents the second-order harmonic circulating current injection to smoother the voltage fluctuation. Through numerical loss analysis, it is determined that the second-order harmonic current injection does not cause serious extra loss. With this harmonic current injection, the capacitance of the SM capacitor could be decreased by 33% at the cost of just 0.05% effectiveness debasement in the given simulation condition.

Figure 3.24 demonstrates the flowchart of the proposed adjusting calculation that utilises an arranging technique with the virtual capacitor voltage. The real voltage fluctuation of the capacitor in the SM, be that as it may, increases as the switching frequency decreases, on the grounds that the arm current flows through the capacitor of the SM for a longer period under the low switching frequency. The second-order harmonic circulating current is likewise injected to smother the voltage fluctuation due to reduced switching frequency.

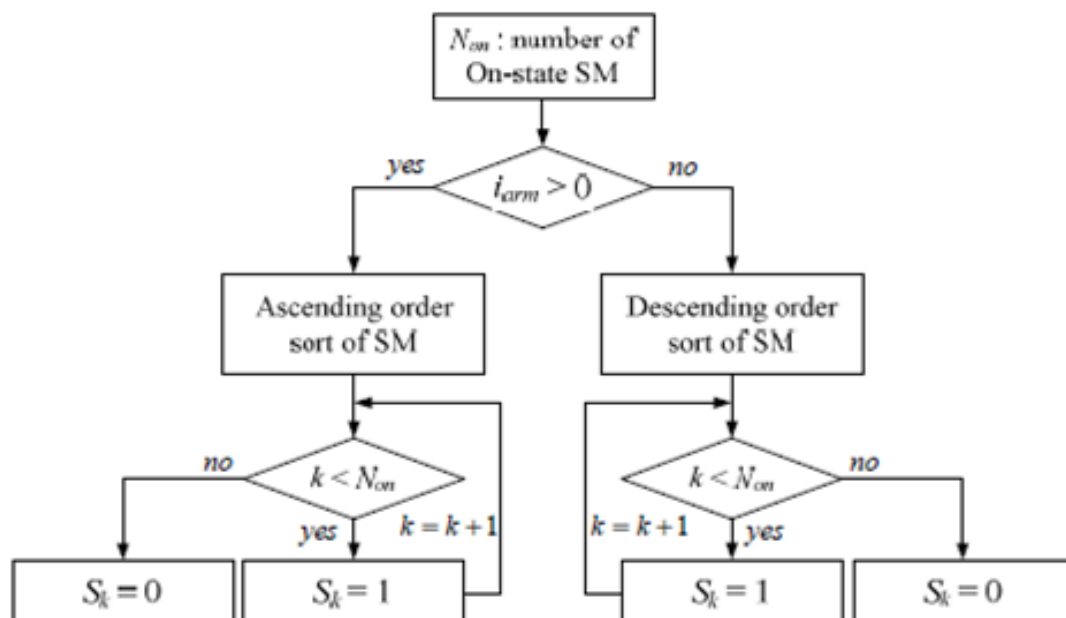


Figure 3.24: Flowchart of the proposed balancing theorem

Adapted from (Lee et al., 2014)

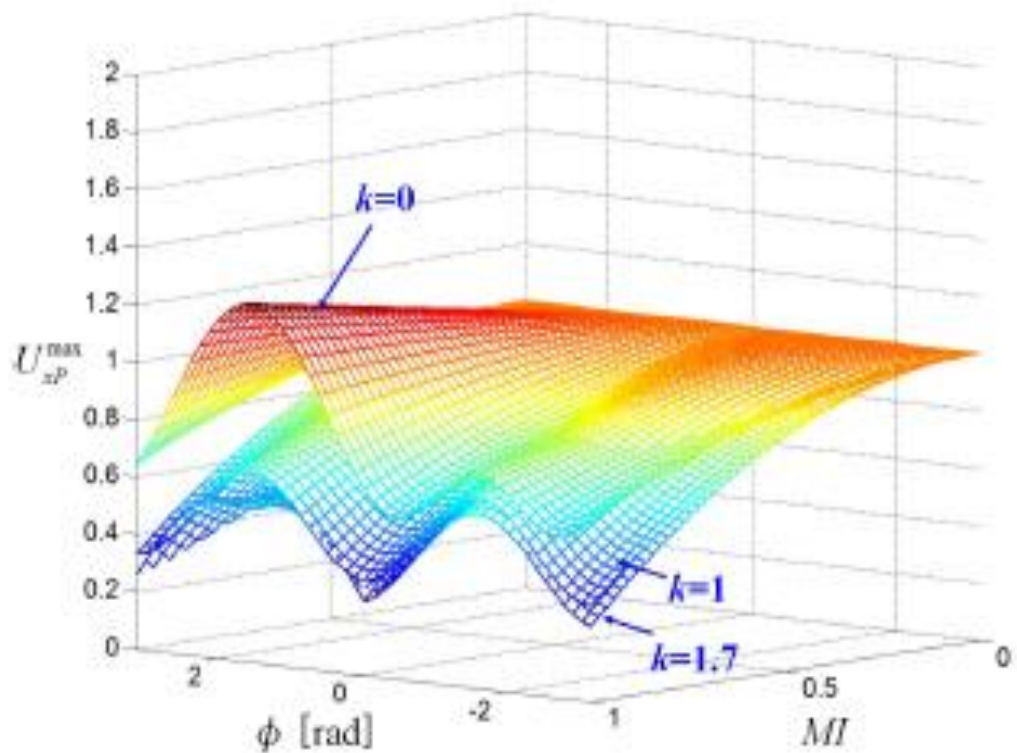


Figure 3.25: Maximum normalised upper arm energy with respect to the weighting factor, k
Adapted from (Lee et al., 2014)

As portrayed in Figure 3.25, the maximum normalised energy, which implies the maximum value of average capacitor voltage, decreases with the injection of the second-order harmonic circulating current.

On the off chance that k is 1.7, the maximum arm energy would be limited. However, the strength of the instance of k equals 1.7 is by all accounts little distinction that of k equals 1 next to the increased circulating current. Subsequently, the greatest k value is constrained to 1.

Table 3.1: Simulation condition

Adapted from (Lee et al., 2014)

Parameters	Values
Grid Voltage	$V_{rms} = 110, f = 60$
DC Voltage	200
Sampling Frequency	10000
Number of SMs/arm	6
SM Normal capacitor voltage	40
SMcapacitor capacitance	4.4 M
Arm inductance	0.002
Rated power	6000
Units: Frequency (Hz), Voltage (V), Inductance (H), Capacitance (F), Power (W).	



Figure 3.26: Prototype MMC model

Adapted from (Lee et al., 2014)

A series of tests was performed to confirm the attainability of the proposed systems. The test conditions are given in Table 3.1. Figure 3.26 demonstrates 7-level MMC model used for the trial setup.

3.2.6 Harmonic Distortion Mitigation

Because of the expansion of non-direct loads drawing non-sinusoidal currents, power quality distortion has turned into a major issue in electrical power systems. Harmonics are caused by non-direct loads, that is, loads that draw a non-sinusoidal current from a sinusoidal voltage source. A few cases of harmonic-producing loads are the electric arc furnace, static VAR compensators, inverters, DC converters, switch-mode control supplies, and AC or DC engine drives. A few strategies to lessen the harmonic distortion are hereby mentioned.

3.2.6.1 Active power filter controller

In this section (El-Mamlouk et al., 2011), a proficient dynamic power filter (APF) scheme is created to appraise and adjust harmonic distortion in an electrical power network. The created APF control scheme depends on a double proportional feedback controller and a single-phase voltage-source and half-wave bridge inverter. This filter utilises a Multi-layer Artificial Neural Network (MLANN) with a move strategy for system harmonic currents and voltages at a designated point. The scheme is tried on a 13-bus industrial distribution system.

The APF scheme utilises two autonomous ML-ANNs with move strategy, or test by test examination, in order to gauge the fundamental voltage and current components for the electrical system. The fundamental frequency voltage and current components are subtracted from the control line voltage and current, individually, to get the harmonic components. At that point, these components are used as reference signals for the multi-loop feedback controller in view of the inductor voltage as indicated in Figure 3.27.

Two proportional controller (TPC) gains are used in the feedback paths of both the inner and outer loops to increase the loop bandwidth. In the external loop, the current signal generated is sustained back and contrasted with its reference. The resulting error signal is multiplied by the first proportional controller gain, and the output is then added to the error signal obtained when comparing the feedback voltage by an inductor and its reference.

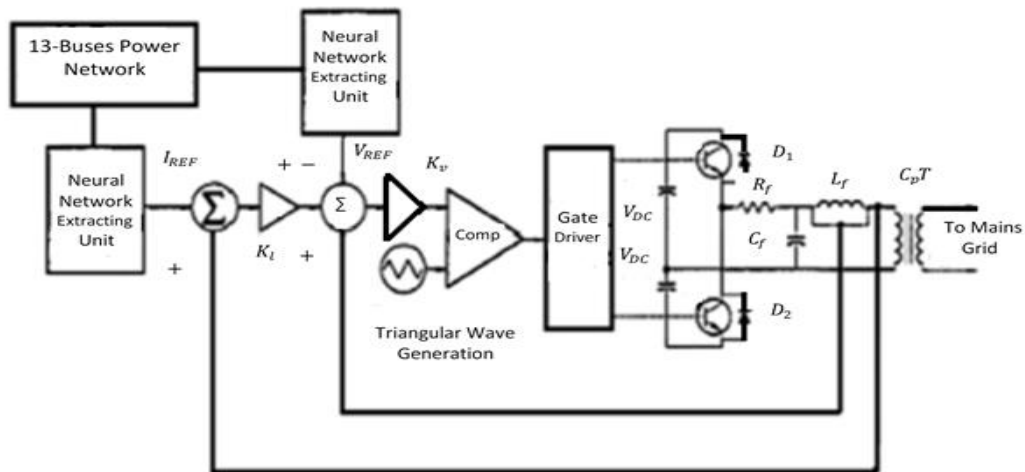


Figure 3.27: Structure of current compensation scheme

Adapted from (El-Mamlouk et al., 2011)

The resulting signal is multiplied by the second corresponding controller gain in the inner control loop and the output is contrasted with the triangular waveform of fixed-switching frequency, which is then passed to the gate drive circuit. The gate drive circuit for the compensation of current will create an ideal exchanged control signals for the Pulse Width Modulated (PWM) and Voltage Source Inverter (VSI) of various CSC modules as shown in Figure 3.27.

Figure 3.28 shows a block diagram for the simulated control circuit of the TPC active power filter representing all the components from Figure 3.27.

The ML-ANN utilised as a part of this investigation. Its accuracy is guaranteed in a past work of the creators. The ML-ANN consists of an information layer with 32 hubs, two shrouded layers, and one-hub yield layer with a testing rate of 960 HZ. The 32 input hubs of the information layer incorporates 16 tests from the present cycle and 16 tests from the past cycle. The ANN plays out an example by examining tests and as such, the most established specimen is discarded and the rest of the examples are uprooted to the neighbouring position which leaves a void position to the new specimen as appeared in Figure 3.29. The tansigmoidal work is utilised as a part of the two shrouded layers, while the yield layer utilises purelin work.

Preparing the weights and inclinations of the system are iteratively changed in accordance with the limit of the system execution work. The ANN parameters in this investigation are as per the following.

- Epochs between refreshing display=200
- Maximum number of cycles to train=40,000

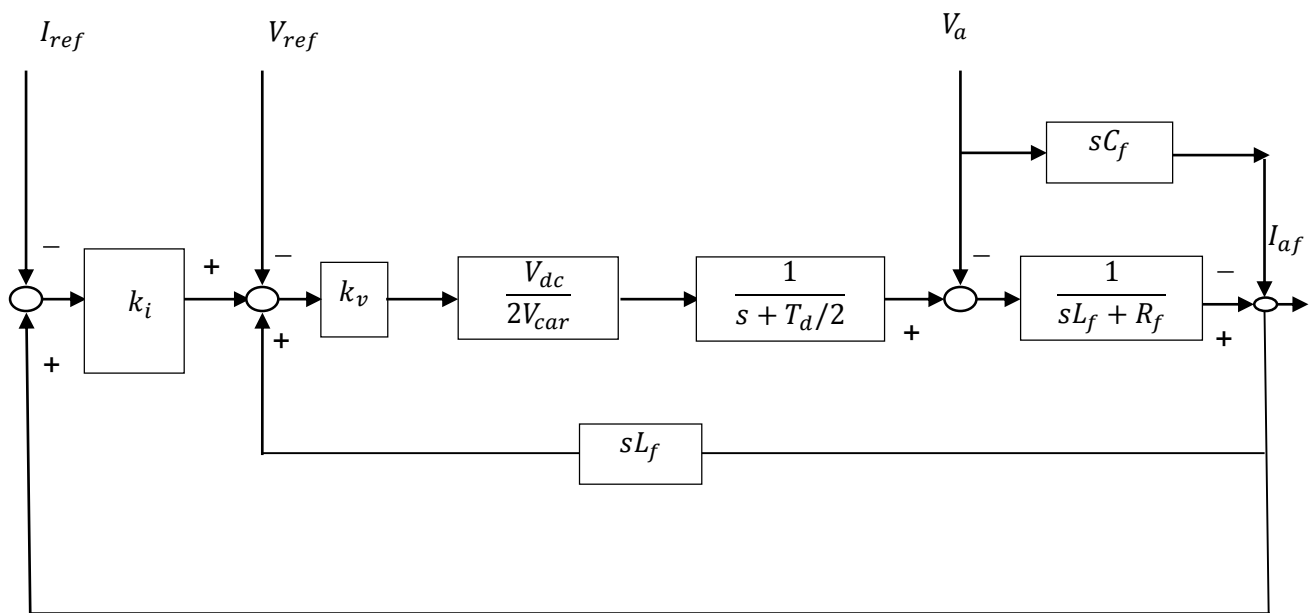


Figure 3.28: Block diagram for the control circuit

Adapted from (EI-Mamlouk et al., 2011)

A similar structure is used for two ML-ANNs to process the signs received from the electrical cable. The main ML-ANN (the present system) assesses the principal recurrence segment of the twisted line current flag, while the second ML-ANN (the voltage arrange) gauges the crucial part of the line voltage flag. The yields of the two ML-ANNs are utilised for developing and adjusting signs of the dynamic synchronous channel.

Operation of the ML-ANN scheme

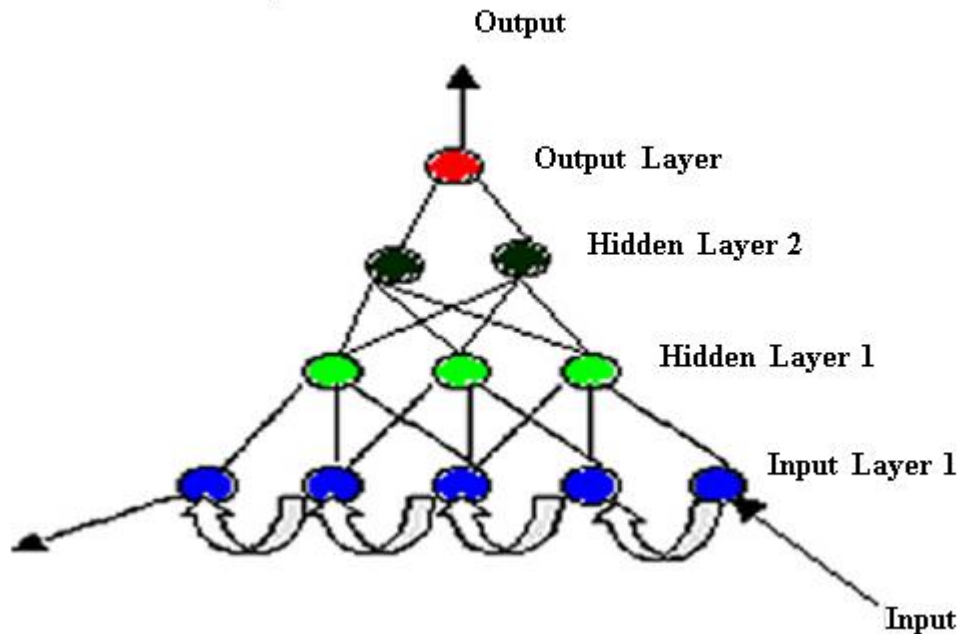


Figure 3.29: ML-ANN Scheme

Adapted from (El-Mamlouk et al., 2011)

3.2.7 Conclusion

In this chapter, several approaches and methods are discussed which enhance the power quality by the mitigating of power quality parameters. The first section studies an AC to AC converter based on a voltage sag supporter which is fed from the line voltage and compensates voltage sag with a jump in phase. This circuit provides the benefit of excluding the use of storage devices while having a high range of compensation. A conditioner which is based on an 8-switch converter is also studied. The 8 switch converter is divided into two units, i.e., the top is termed as the shunt converter, and the bottom is termed as the series converter. The top unit is placed in series of the passive LC-filter which is tuned in the 7th harmonic, providing a good harmonic compensation performance. The switches required by this conditioner is lesser compared to other conditioners mentioned in the literature. The top unit control algorithm is done using feedback which feeds forward compensations. This also controls the DC link voltage. The bottom unit behaves as the traditional DVR, which has voltage sag compensation capabilities.

The ride through functions of ASDs together with the SW-SVC for contactors and PLCs is a cheaper and more suitable option to save processes from voltage sags. The DSTATCOM method provides the following advantages:

- at the nominal load, the compensator injects load currents reactive and harmonic components, resulting in UPF
- near to UPF is kept for a load change
- voltage regulation process is fast during voltage disturbances
- Losses in the VSI and feeder are significantly lesser with increased sag supporting capabilities using the same VSI rating as compared to traditional schemes in the literature.

The approach based on customer trust and protection gave a quantitative comparison between many mitigation approaches. It is important to clearly differentiate between the problem of voltage dips and interruptions, Knowledge of the interruption cost allows for the correct selection of a mitigation device in a particular situation. Even in the condition when the interruption costs are not known clearly, the device selection is easier by looking at previous interruptions and the selected device. This approach also allows the comparison of completely different mitigation approaches easier for both specialists and non-specialists.

The exploratory perceptions on a high-voltage PV exhibit utilising a fast information have proposed that the morning and night start up and shutdown of PV inverters can deliver transient voltage spikes that can possibly diminish the lifespan of the PV framework segments. These spikes can reach the kilovolt range, and give off an impression of being caused by intrusion of the current in parasitic inductances by the DC-side transfer in the inverter. It is not yet quantitatively clear what affect these spikes have on the PV framework's unwavering quality, yet it makes sense that they will abbreviate it by a sum.

Air conditioning PV display has a unimportant parasitic inductance between the inverter and module. The fault type probabilities because of lightning incited overvoltage's in a MV organise ensured by spark gaps was researched. The real combinations of AC and impulse voltages deliver both single and multiphase faults. The extent of lightning-induced overvoltage entering through the transformer to the client side was examined by using a basic high frequency model of the transformer. The under conditions of conceivable MV spark gap, the LV system ought to be ensured by LV surge arresters, whatever the LV organise development (OHC or UGC). This data is featured as some system designers assume that the capacitance of the UGC can dampen the overvoltage. Be that as it may, the overvoltage are still sufficiently high to be

destructive. Introducing a surge arrester at the LV organise starting can secure the LV arrange and keep these overvoltage to reach at the client entrance.

Voltage droop or swell in any one stage in a 3-stage supply may make breakdown sensitive single-stage loads. A zig-zag winding 3-stage transformer associated over the load may overcome the glitch. At the event of the voltage disturbance the influenced period of the supply is detached from the heap and the unbiased purpose of the transformer is unequally associated with supply voltage. Under this single stage condition, the crisscross transformer recovers the open stage voltage and supplies the heap current. The open stage stack current is shared by the sound stages with the expansion of source streams in those two stages. At the point when the voltage aggravation vanishes, the heap obtains energy from the 3-stage supply and the crisscross transformer is segregated. Moderation of voltage sag/swell for a brief term may be achieved by utilising a strong state exchanging gadget. An exchanged autotransformer is more affordable and mitigates the voltage swell in a powerful way. The static arrangement compensator (SSC) has demonstrated the capacity to adjust for voltage swells at the distribution side. The voltage swell attributes and stacking conditions are the elements that decide if the vitality stockpiling capacitor of the SSC will charge or release during a voltage swell. Overvoltage insurance of the SSC can be made on-line or disconnected, relying upon the achieved level of the DC voltage. The on-line assurance depends on exchanging a resistor through a DC-chopper to disperse the vitality abundance in the DC-capacitor. The disconnected security is activated if the dc-voltage surpasses its breaking point and thus the SSC ought to be skirted.

The quick reaction and the adaptable control arrangement of the STATCOM permit a proficient moderation of voltage glimmer caused by electric circular segment heaters. The voltage flicker is lessened from 3% to under 0.8% by using a circular segment heater technique. DSTATCOM with the proposed control calculation set up the reasonability of utilising the introduced relieving gadget to settle the voltage level within the admissible level. The voltage variance of the capacitor in SM, be that as it may, increments as the exchanging recurrence diminishes. Thus, the second flowing current infusion to alleviate the voltage levels is found.

The acquired reproduction comes about because the APF plot guarantees the adequacy of the shunt dynamic power channel to lessen the present THD entering the objective straight load. This must be assured as far as possible by IEEE 519-1992. In control gadgets interface, the association of a capacitor in parallel with the inductor delivers a full channel that can

decrease the present mutilation. The viability of this arrangement relies upon the quality of the inductor.

CHAPTER FOUR

DSTATCOM AND ITS OPERATING PRINCIPLES

4.1 Introduction

Due to the rapid increase in the use of power electronics, appliances for energy distribution and generation is in high demand. Traditional devices provide degraded performance, which paved the path for advanced compensated devices. Distribution Static Synchronous Compensator (DSTATCOM) can be dynamically controlled and helps to improve power quality (PQ) problems. In this chapter, DSTATCOM operating principles, components, and different topologies are discussed. The chapter also discusses the various control methods required to improve dynamic capabilities of DSTATCOM for various applications.

All electronics has the potential to suffer from power quality (PQ) issues when connected to a distribution system. This leads to current distortion and voltage collapse (Bollen, 2000; Hsu, 1998), which can result in power loss or the poor performance of equipment. Due to the rapid growth in the use of power electronics devices for industries and utility grid systems, providers must select a device carefully. Among all controllers, Distribution compensator is the most effective and powerful device to address the issues associated with power quality (Akagi et al., 1984; Varschavsky et al., 2010; Ghosh et al., 2000; Singh et al., 2015; Zaveri et al., 2011; Singh & Solanki, 2009; B. Singh, A. Adya, Mittal, et al., 2008; Jung et al., 2002).

4.2 Organization of the Chapter

The chapter also discusses the various control methods required to improve the dynamic capabilities of DSTATCOM for various applications. Various topologies like 3-phase 3-wire DSTATCOM and 3-phase 4-wire DSTATCOM are discussed. The control strategies like voltage-control, current-control, as well as voltage and current control are mentioned.

4.3 DSTATCOM and its operating principles

The DSTATCOM is a power device that is connected to a shunt. Its components includes a VSI, a DC-link device which is required for energy storage, a filter in output stage, and a coupling transformer as shown in Figure 4.1 (Masdi et al., 2004). A VSI is used to convert the DC voltage stored in energy devices into AC output voltages in three phases. The voltages

which are generated are in-phase with each other due to the coupling transformer and the connection to the utility grid. Control of the active and reactive power flow between the compensator and its grid can be maintained by using a relevant setting of the magnitude and phase across the output of the shunt compensator (Reddy & Reddy, 2012; Hatami et al., 2007; Olimpo Anaya-Lara and E. Acha, 2002).

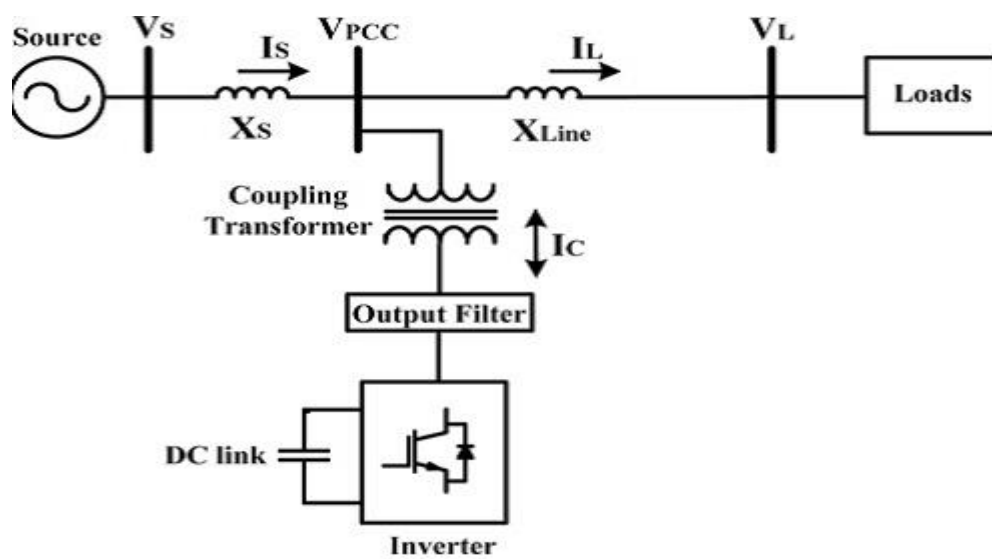


Figure 4.1: DSTATCOM schematic diagram

Adapted from (Masdi et al., 2004)

Figure 4.2 depicts the structure using a single-phase shunt compensator. V_I indicates the inverter output voltage; $V_{Coupling}$ indicates the coupling impedance voltage drop; V_{PCC} reflects the voltage at the point of common coupling (PCC), while V_S is the source of the voltage.

If $V_I = V_{PCC}$, the shunt compensator will not exchange any reactive power with its utility grid. The reactive power is neither absorbed nor generated by the DSTATCOM.

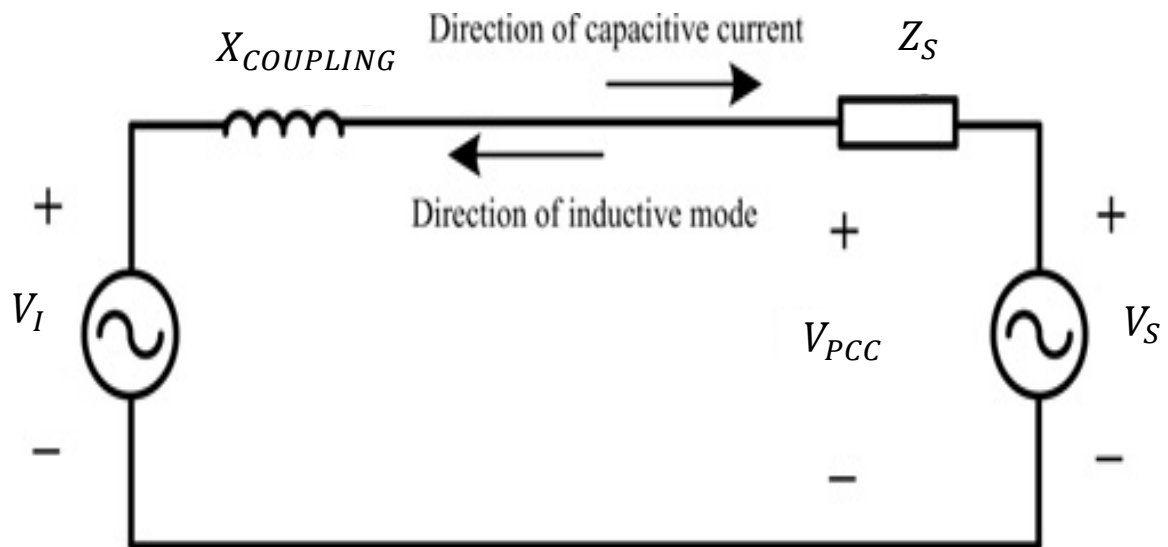


Figure 4.2: A DSTATCOM with a single-phase power system

Adapted from (Masdi et al., 2004)

For $V_I > V_{PCC}$, DSTATCOM behaves as if a reactance which is inductive in nature is connected to its terminal. From the transformer reactance of DSTATCOM, there is a flow of current in the utility grid. The power generated is capacitive.

If $V_I < V_{PCC}$, the DSTATCOM performs as if a reactance which is capacitive in nature is connected to its terminal. In this condition (Masdi et al., 2004; Reddy & Reddy, 2012; Hatami et al., 2007; Olimpo Anaya-Lara and E. Acha, 2002; Lei et al., 2016), the inductive power is absorbed by the device and the direction of current flow is from the grid to the compensator.

In Figure 4.3 (a) and (b), V-I and V-Q characteristics of the shunt compensator are shown, demonstrating the exchange of reactive power between the utility grid and the compensator, where V_{Ref} is the nominal voltage at PCC.

The phase angle between the voltages in the utility grid and the distribution compensator output controls the active power flow, which results in further reduction of inside the inverter. It maintains the DC capacitor charge and adjusts the magnitude of the DSTATCOM output voltage. The Distribution compensator representation of vector at the fundamental frequency

is shown in Figure 4.4. This shows a transition from inductive to capacitive mode and vice versa.

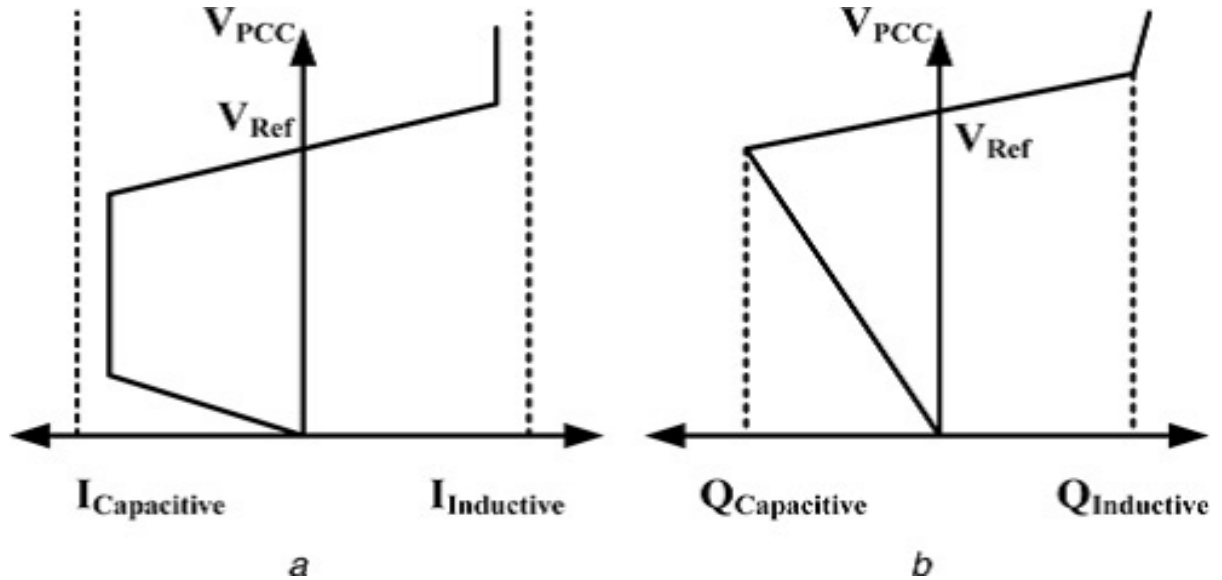


Figure 4.3: Operational characteristics of the shunt compensator (a) V-I (b) V-Q

Adapted from (Masdi et al., 2004; Reddy & Reddy, 2012; Hatami et al., 2007; Olimpo Anaya-Lara and E. Acha, 2002; Lei et al., 2016)

By changing angle $\delta = 0$ to $\delta =$ positive value, switching from an inductive mode to a capacitive mode is achieved. Active power from the utility grid is transferred using a DC capacitor, which also brings about a drop in the DC link. When angle " δ " is changed to a negative value from zero, there is a mode change from an inductive to capacitive. DC link voltage increases when there is a transfer of active power to the capacitor from the utility grid (Acha et al., 2002).

The active power (P) and reactive power (Q) variation between the shunt compensator and its grid can be shown as follows in Equation (4.1) and (4.2).

$$P = \frac{V_{PCC} \times V_1}{X_{Coupling}} \sin\delta \quad (4.1)$$

$$Q = \frac{V_{PCC}^2}{X_{Coupling}} - \frac{V_{PCC} \times V_1}{X_{Coupling}} \cos\delta \quad (4.2)$$

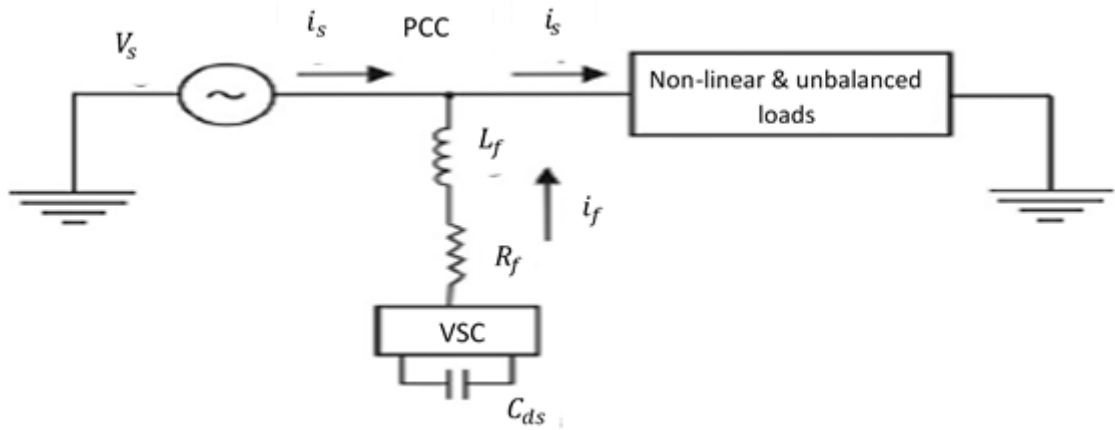


Figure 4.4: Single line diagram of the DSTATCOM

Adapted from (Acha et al., 2002)

The use of VSC allows for bidirectional power flow. VSCs are constructed using devices like insulated gate bipolar transistors (IGBT) and metal oxide field effect transistors (MOSFET) (Freitas et al., 2005). Pulse width modulation (PWM) is used for switching these devices (Freitas et al., 2005; Bahramirad et al., 2013). A DC bus capacitor and an interfacing inductor are some of the components of VSC (Chilipi et al., 2014). The minimum voltage across the DC bus must be greater than twice the peak value of the phase voltage of the system. The DC capacitor value depends upon the instantaneous energy available during transients to the DSTATCOM. The two split sections of the DC bus capacitor can also be used with equal or unequal values (Srikanthan & Mishra, 2010; Ota et al., 2015). The DC bus voltage V_{dc} and capacitor C_{dc} are calculated as shown in Equation (4.3) and (4.4).

$$V_{dc} = \frac{2\sqrt{2} \times V_{LL}}{\sqrt{3}m} \quad (4.3)$$

$$C_{dc} = \frac{6a V \times I \times t}{V_{dc}^2 - V_{dc1}^2} \quad (4.4)$$

Where,

m =modulation index

V_{LL} = AC line voltage

a = overloading factor

V = phase voltage

I = phase current

V_{dc1} = phase voltage

t = time by which the DC bus voltage is to be recovered

4.3.1 Transformer unbalances and non-linear loads

Unbalances in the transformer, as well as non-linear loads in the distribution system, creates the problem of excessive neutral current. Transformers are therefore utilised for neutral current compensation, the effectiveness of which depends on the compensator position and the system impedance (Sreenivasarao et al., 2013; Gupta et al., 2007). The transformers are used in a non-isolated condition for neutral current compensation. It can also be used to provide isolation of the VSC. The most common transformer topologies with DSTATCOM are zig-zag, star-delta, T-connected, and star-hexagon (Sreenivasarao et al., 2012). Figure 4.5 shows the equivalent circuit of DSTATCOM. The lagging and leading operations of DSTATCOM is further illustrated in Figure 4.6.

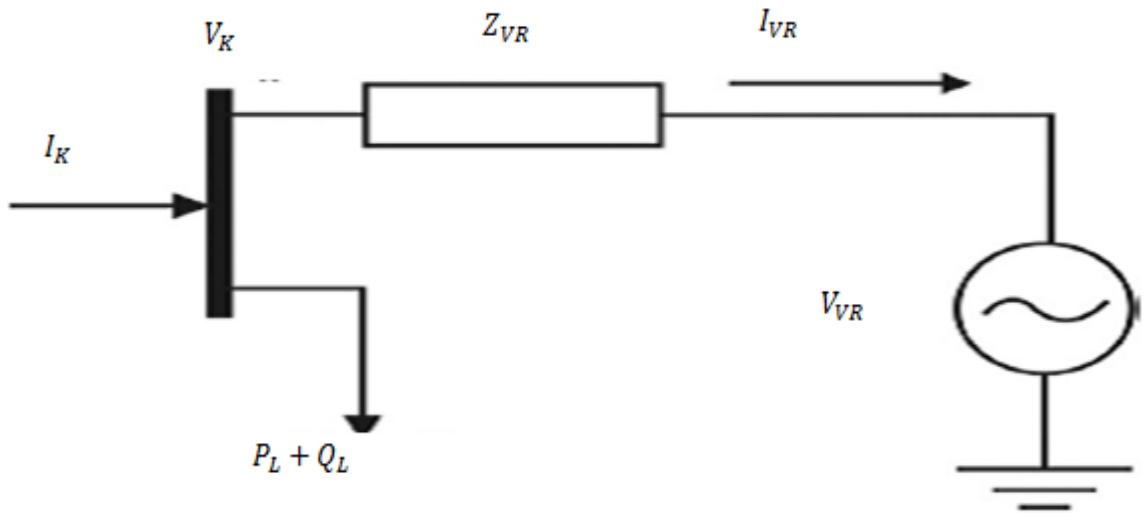


Figure4.5: Equivalent circuit of the DSTATCOM
Adapted from (Sreenivasarao et al., 2012)

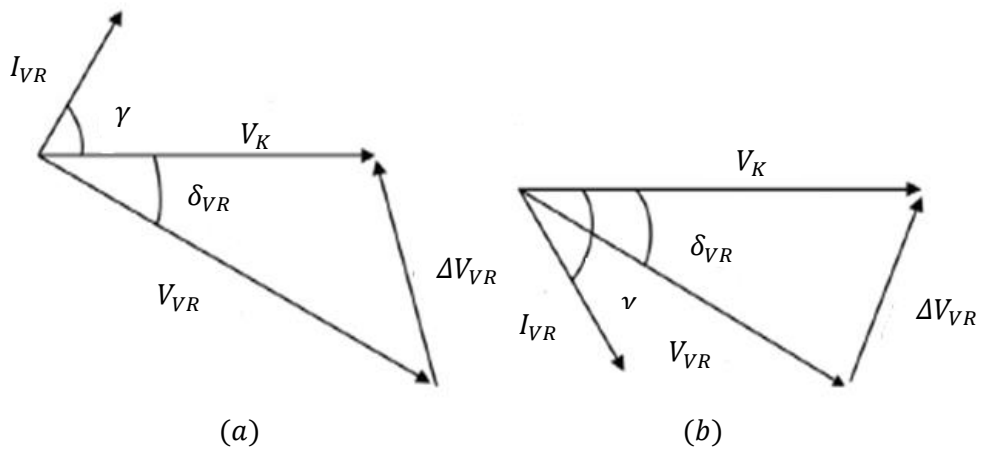


Figure4.6: Phasor diagram (a) lagging operation (b) leading operation
Adapted from (Sreenivasarao et al., 2012)

4.3.2 Ripple filter

A 1st order high pass (HP) filter which is tuned at half the switching frequency is utilised to filter the high frequency noise from the voltage at the PCC (Rohilla & Pal, 2013). A resistor (R_f) in series with the capacitor (C_f) is then used (Arya & Singh, 2013b; Yang et al., 2014). As shown in the equation below, the time constant ($R_f C_f$) of the filter must be smaller than the fundamental time period (T) (Singh, Jayaprakash, Somayajulu, et al., 2009).

$$R_f C_f \ll \left(\frac{T}{10} \right) \quad (4.5)$$

4.3.3 AC inductor

The compensating currents contains ripple. In order to compensate, the tuned values of interfacing inductors are connected at the AC output of the VSC (Singh & Arya, 2014). The AC inductance (L_f) of the VSC depends on the current ripple ($i_{cr,p-p}$); switching frequency (f_s); and DC bus voltage (V_{dc}). Its value is given in Equation 4.6 (Singh et al., 2005).

$$L_f = \frac{\sqrt{3}mV_{dc}}{12af_s i_{cr,p-p}} \quad (4.6)$$

Where,

m = modulation index

a = overloading factor

4.4 DSTATCOM topologies

DSTATCOM topologies are broadly categorised depending on the transformers used for isolation and neutral compensation, as well as the type of switching devices that is used. These DSTATCOMs find their applications to suit the requirements of systems like 3-phase 3-wire and 3-phase 4-wire distribution.

4.5 Three-Phase Three-Wire DSTATCOM

DSTATCOMs with 3-phase 3-wire are used for PQ improvement and the compensation of user loads. The topologies for these DSTATCOMs are categorised as shown in Figure 4.7 (a).

These are first categorised as a DSTATCOM which includes a non-isolated VSC and an isolated VSC (Akagi et al., 1984; Lin & Yang, 2006; Hosseini & Sabahi, 2007; Arya & Singh, 2014; Singh et al., 2007; Gupta & Ghosh, 2006; Fujita & Akagi, 2007; Kedjar & Al-Haddad, 2009; Rahmani et al., 2009; Singh & Arya, 2013; Lin & Yang, 2006; Gupta & Ghosh, 2006; Chung et al., 2004; Singh et al., 2006; Singh et al., 2004; Karimi-Ghartemani & Mokhtari, 2006; Freitas et al., 2005; Shukla et al., 2005; Griffo & Lauria, 2008).

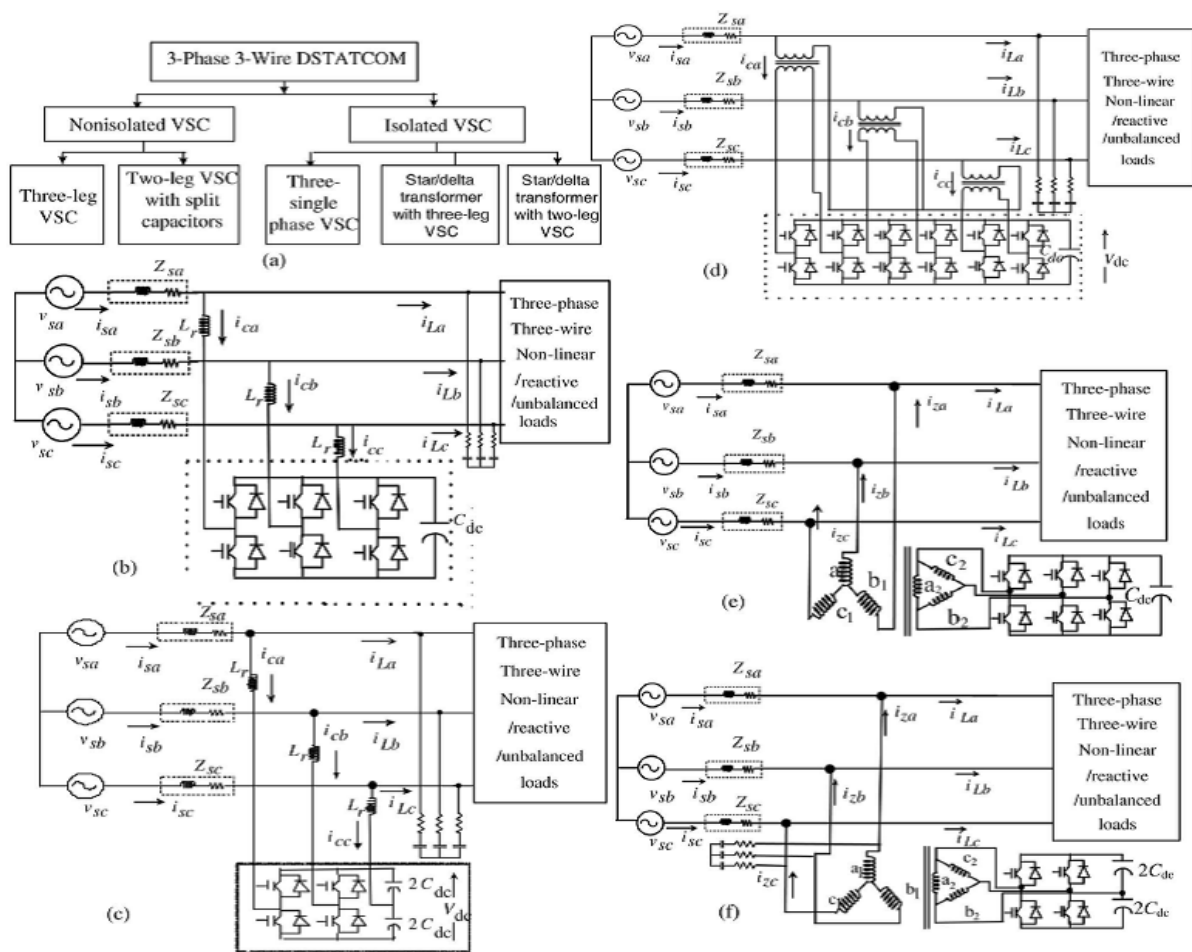


Figure 4.7: (a) Classification of 3-phase 3-wire DSTATCOM, (b) 3-leg topology of the 3-phase three-wire DSTATCOM, (c) 2-leg with split capacitor, (d) 3 single-phase topology, (e) isolated 3-leg VSC, and (f) isolated 2-leg VSC

Adapted from (Singh & Arya, 2013a; Lin & Yang, 2006)

4.5.1 Non-isolated VSC-Based DSTATCOMs

The 3-leg topology based upon VSC is shown in Figure 4.7(b) and is widely portrayed in the literature (Akagi et al., 1984; Chung et al., 2004; Singh et al., 2007). The 2-leg VSC using split capacitors has the advantage of using the least amount of switching devices (Akagi et al., 2007a; Griffo & Lauria, 2008). This is shown in Figure 4.7(c). However, the topology suffers from the requirements of very high DC bus voltage levels as well as the regulation of DC capacitors which need equal DC voltages.

4.5.2 Isolated VSC-Based DSTATCOMs

A 4-phase 3-wire DSTATCOM is proposed in (Akagi et al., 2007a; Hosseini & Sabahi, 2007), which uses three single-phase VSCs. This topology, shown in Figure 4.8(d), suffers from the disadvantage of using more switching devices. Two more isolated topologies of DSTATCOM using star or delta transformers respectively is shown in Figure 4.7(e) and 4.7 (f). A kVA star or delta transformer is used to make the kVA rating equal to the required power for reactive compensation. The transformer here provides isolation from the system, including the flexibility to use an “off-the-shelf” VSC for the desired application.

4.6 Three-Phase Four-Wire DSTATCOM

The 3-phase 4-wire DSTATCOMs are used in the 3-phase 4-wire distribution systems for the improvement of PQ. Different topologies for this kind of DSTATCOM is shown in Figure 4.8.

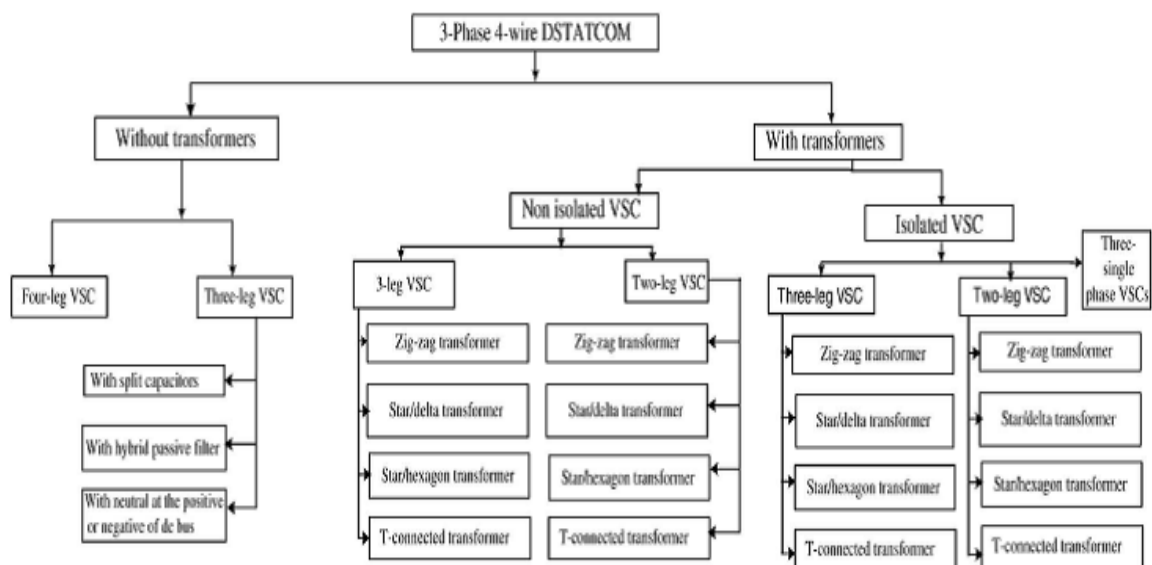


Figure 4.8: Classification of 3-phase 4-wire DSTATCOM

Adapted from (Singh & Arya, 2013a)

These are mainly categorised as two types, namely, DSTATCOMs with transformers or without transformers (Salmerón et al., 2004; Dinavahi et al., 2004; Bina et al., 2005; Benhabib & Saadate, 2005; Singh et al., 2008; Soares & Verdelho, 2006; De Moraes & Barbi, 2006; Barrado et al., 2007; ZHOU et al., 2007; Ucar & Ozdemir, 2008; Montero et al., 2007; Jou et al., 2008; Karanki et al., 2012; Singh et al., 2010; Choi & Jang, 2007; Lohia et al., 2008; Luo et al., 2009; Lavopa et al., 2009; Molinas et al., 2010; Liu & Hsu, 2010; Borisov & Ginn, 2010; Verma et al., 2010; Zhu et al., 2010; Chang et al., 2010; Song & Huang, 2010; Singh et al., 2011)

4.6.1 Non-isolated VSC without Transformers

The DSTATCOM topologies without transformers are classified as 4-leg VSC and 3-leg VSC (ZHOU et al., 2007; Ucar & Ozdemir, 2008; Montero et al., 2007; H.-L. Jou et al., 2008; Karanki et al., 2012; Singh et al., 2010). These are shown in Figure 4.8. Figure 4.9(a) reflects the DSTATCOM 4-leg topology used in the literature (A. Ghosh and G. Ledwich, n.d.; R. C. Dugan, M. F. McGranaghan, 2006; Moreno-Munoz, 2007; Akagi et al., 2007b; Transmission, 2007; Fuchs & Masoum, 2008).

The neutral conductor is connected to the fourth leg of the VSC in order to control the neutral current compensation. DSTATCOM topologies which mitigates PQ compensation in the supply current along with neutral current includes a 3-leg VSC using split capacitors, shown in Figure 4.9(b). Another example is the 3-leg VSC in which the neutral terminal is at the positive or negative of the DC bus, as shown in Figure 4.9(c) (H.-L. Jou et al., 2008). Furthermore, a hybrid topology of DSTATCOM is shown in Figure 4.9(d) (Karanki et al., 2012).

4.6.2 Non-isolated three-Leg VSC with Transformers

DSTATCOM topologies can be broadly categorised as non-isolated VSC and isolated VSC-based DSTATCOMs with transformers. A DSTATCOM of non-isolated topology which uses a 3-leg VSC and a zig-zag transformer is given in Figure 4.10(a). A zig-zag transformer is advantageous as it provides roughness, active or passive compensation, and is less complex compared to techniques given in (Singh et al., 2010; Choi & Jang, 2007; H. L. Jou et al., 2008; Singh, Jayaprakash, Somayajulu, et al., 2009; Singh, Jayaprakash, Kumar, et al., 2011). In Figure, 4.10(b), one more topology which uses 3-leg VSC and star-delta transformer configuration is shown (Bhim Singh, P Jayaprakash, et al., 2008), (Jayaprakash, B. Singh, et al., 2009). Figure 4.10(c) displays a T-connected transformer (Bhim Singh, P. Jayaprakash & Kothari, 2008). Additionally, Figure 4.10(d) shows a star-hexagon transformer (Jayaprakash, Bhim Singh, et al., 2009) which also uses 33-leg VSC as 3-phase 4-wire DSTATCOM.

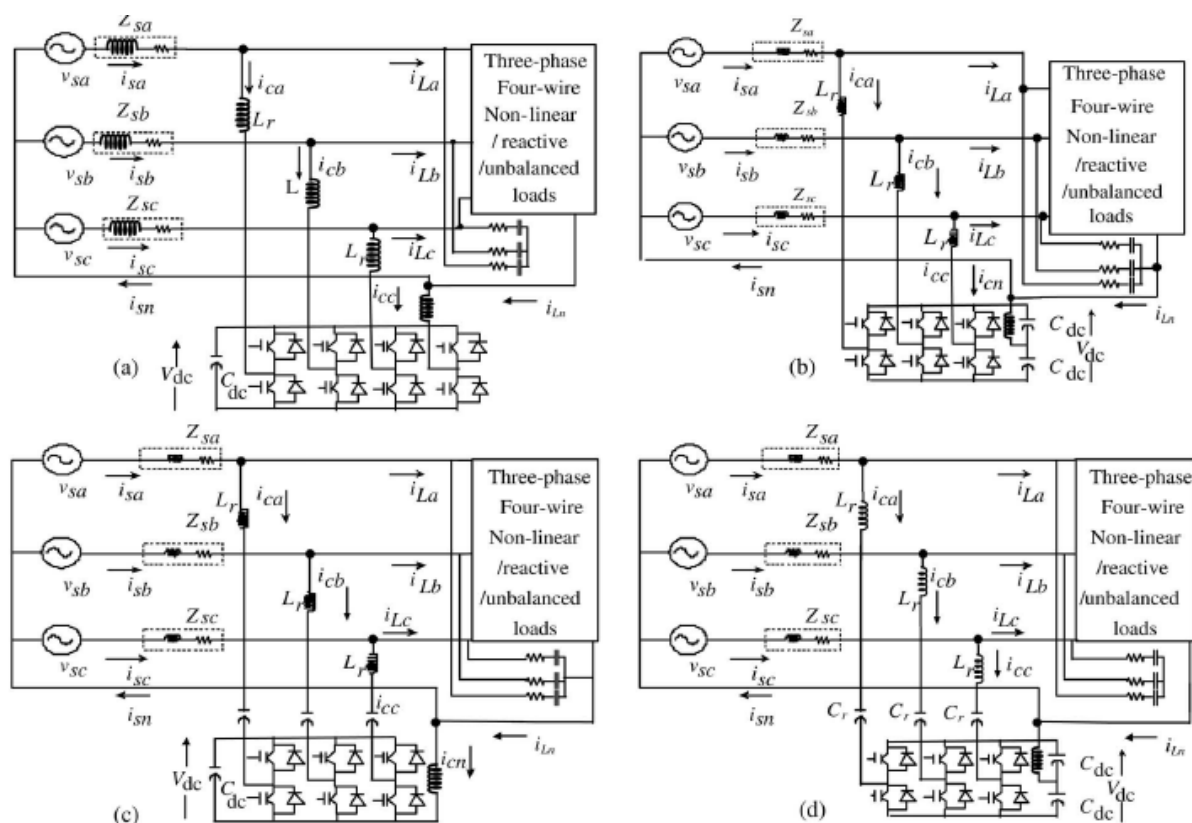


Figure 4.9: D-STATCOM 3-phase and 4-wire configurations (a) 4-leg VSC (b) 3-leg VSC and split capacitors (c) Neutral terminal at the DC bus and 3-leg VSC (d) 3-DC capacitors and 3-leg VSC.

Adapted from (Singh & Arya, 2013a)

4.6.3 Non-isolated Two-Leg VSC With Transformers

In Figure 4.10(e), a 3-phase 4-wire DSTATCOM is made using 2-leg VSC containing split capacitors and a zig-zag transformer (Bhim Singh, P. Jayaprakash, Somayajulu, et al., 2008). In Figure 4.10(f) (B Singh, P Jayaprakash & Kothari, 2008), Figure 4.10(g) (B. Singh, P. Jayaprakash, 2008), and Figure 4.10(h) (Jayaprakash et al., 2008), the two-leg VSC along with different transformers are used as three-phase four-wire DSTATCOMs. These include zig-zag, star/delta, T-connected, and star/hexagon transformers respectively. These require fewer power electronics switches.

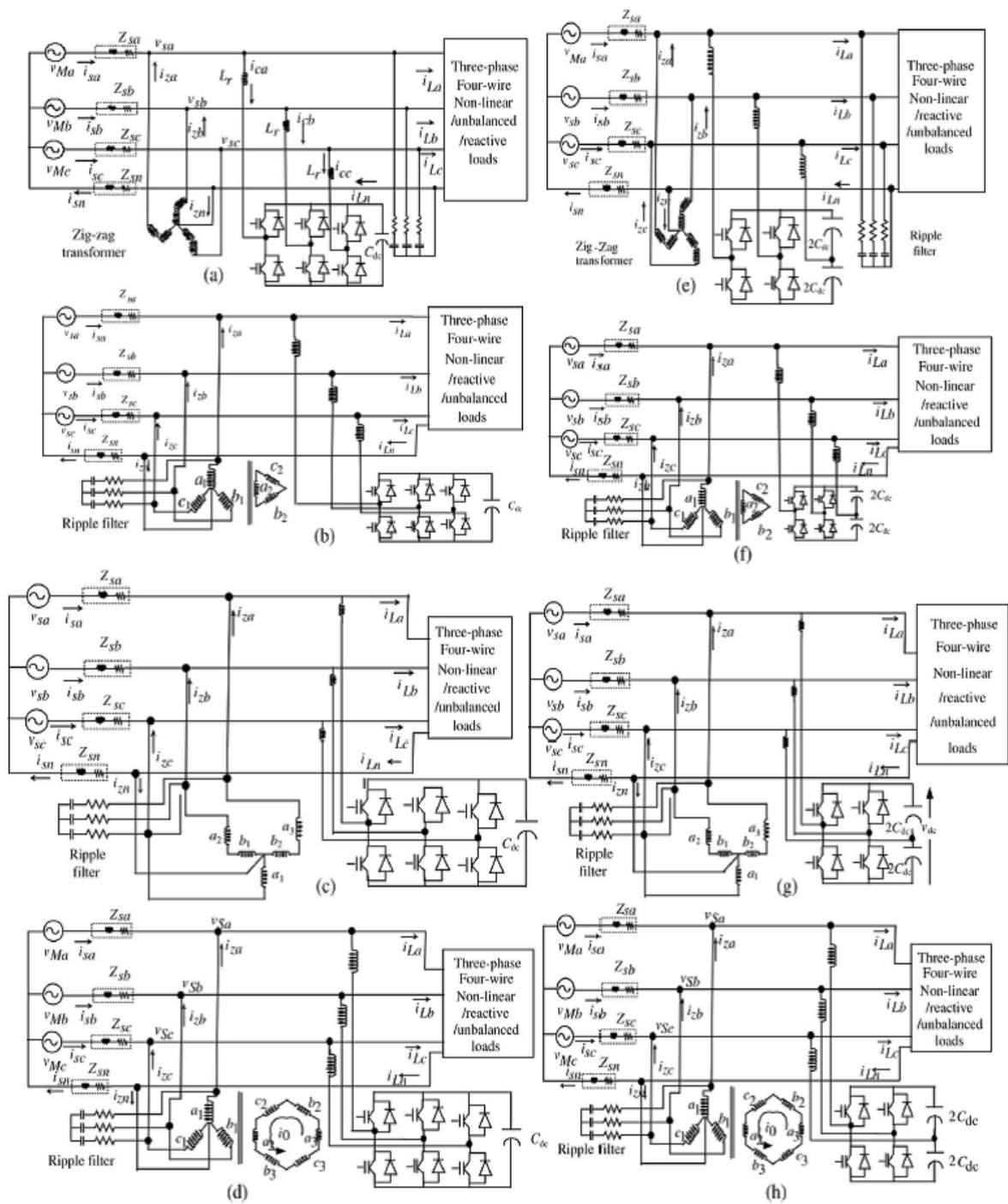


Figure 4.10: D-STATCOM 3-phase and 4-wire configurations including non-isolated VSC utilizing transformers (a) zig-zag transformer and 3-leg VSC (b) star delta transformer and 3-leg VSC (c) T-connected transformer and 3-leg VSC (d) star hexagon transformer and 3-leg VSC (e) zig-zag transformer and 2-leg VSC (f) T-connected transformer and 2-leg VSC (g) star hexagon transformer and 2-leg VSC.

Adapted from (Singh & Arya, 2013a)

4.6.4 Isolated Three Single-Phase VSCs

The papers in (Akagi et al., 2007a) and (Singh, Jayaprakash & Kothari, 2009b) uses three single-phase VSCs as 3-phase 4-wire DSTATCOM. The configuration uses 3-leg VSC with zig-zag transformers as shown in Figure 4.11 (a). The three H-bridge VSCs which are supported by a common DC storage capacitor constitutes a DSTATCOM. Each of these VSCs are connected to a single-phase transformer that provides isolation between these transformers as well as inductance between VSCs and the PCC.

4.6.5 Isolated Three-Leg VSC with Transformers:

Another DSTATCOM configuration which uses 3-leg VSC connected to a star-delta transformer is shown in Figure 4.11(b) (Jayaprakash et al., 2011). The circuit is rebuilt by using a T-connected transformer, a star-hexagon transformer, and an isolated 3-leg VSC as 3-phase 4-wire DSTATCOM. This is shown in Figure 4.11(c), 4.11(d), and 4.11(e) respectively. (Singh, Jayaprakash & Kothari, 2009a; Jayaprakash et al., 2008; Jayaprakash, Bhim Singh, et al., 2009.)

4.6.6 Isolated Two-Leg VSC with Transformers

An isolated H-bridge VSC containing split capacitors is utilized including a transformer as a 3-phase 4-wire DSTATCOM. This configuration uses less semiconductor devices to build a VSC. An H-bridge VSC connected to the secondary of a zig-zag transformer is used as 3-phase 4-wire DSTATCOM which is shown in Figure 4.11(e) (P. Jayaprakash, B. Singh, n.d.). The star-delta transformer (Bhim Singh, Jayaprakash, et al., 2014), T-connected, and star-hexagon transformer (Bhim Singh, Jayaprakash, et al., 2014) are also utilized including the 2-leg VSC as 3-phase 4-wire DSTATCOM and are shown respectively in Figure 4.11(g), (h), and (i). The transformer gives segregation from the framework and furthermore gives the adaptability to utilize an "off-the-shelf" VSC in numerous applications.

4.7 Modes of control of DSTATCOM

A Distribution compensator is the power device which is implemented in shunt configuration to improve problems related to power quality. It provides stability in the voltage by controlling reactive power, suppressing flicker noise, and ensuring compensation is done. The DSTATCOM can operate in two modes namely: *voltage* and *current*. The control algorithm which is used for voltage source inverter (VSI) switching (Akagi et al., 1984) decides the effect

of the compensation. The DSTATCOM's performance largely depends on the control algorithms which are used to generate source current. An overview of recent control techniques which are available in the literature for DSTATCOM is described in this section.

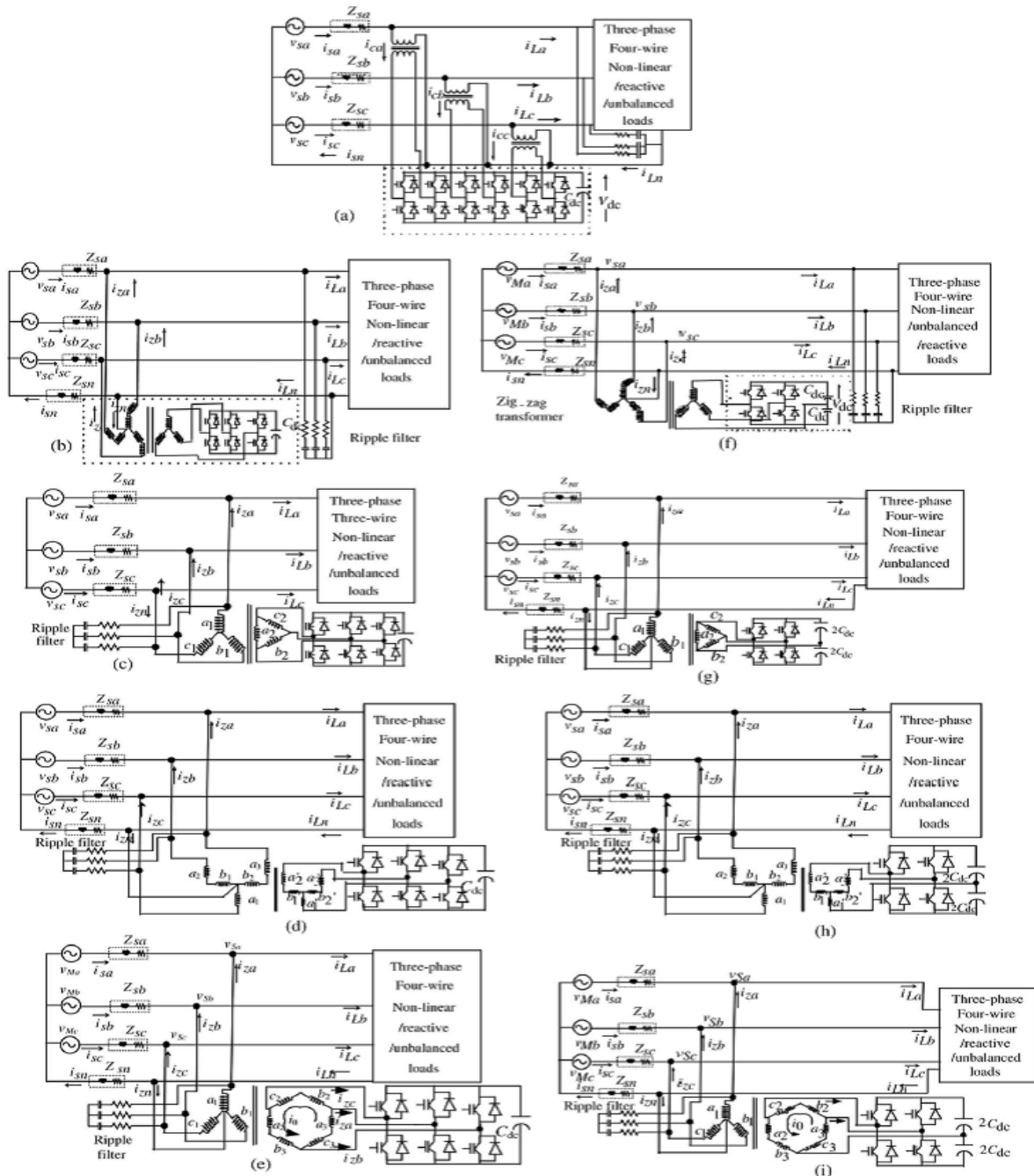


Figure 4.11: D-STATCOM 3-phase and 4-wire configurations including isolated VSC utilizing transformers (a) zig-zag transformer and 3-leg VSC (b) star delta transformer and 3-leg VSC (c) T-connected transformer and 3-leg VSC (d) star hexagon transformer and 3-leg VSC (e) zig-zag transformer and 2-leg VSC (f) star delta transformer and 2-leg VSC (g) T-connected transformer and 2-leg VSC (h) star hexagon transformer and 2-leg VSC (i) hexagon transformer and 2-leg VSC

Adapted from (Singh & Arya, 2013a)

4.8 Classification according to Mitigated PQ problems

The DSTATCOM is mainly used to compensate PQ problems which include voltage and current quality, harmonics distortion, and load unbalance problems such as reactive current component or unbalance and neutral current at the PCC. The DSTATCOM can be made to function in two modes: single and dual. In this section, two modes of operation are discussed. The single mode provides compensation to either current or voltage while the dual mode provides compensation for both current and voltage.

4.8.1 Voltage control strategies

A voltage control strategy which uses multiple DSTATCOMs can be applied to a low voltage (LV) network in order to anticipate voltage support. Multiple DSTATCOMs shared the required reactive power, thus, the approach is promising as it requires minimum reactive power (Mokhtari et al., 2013).

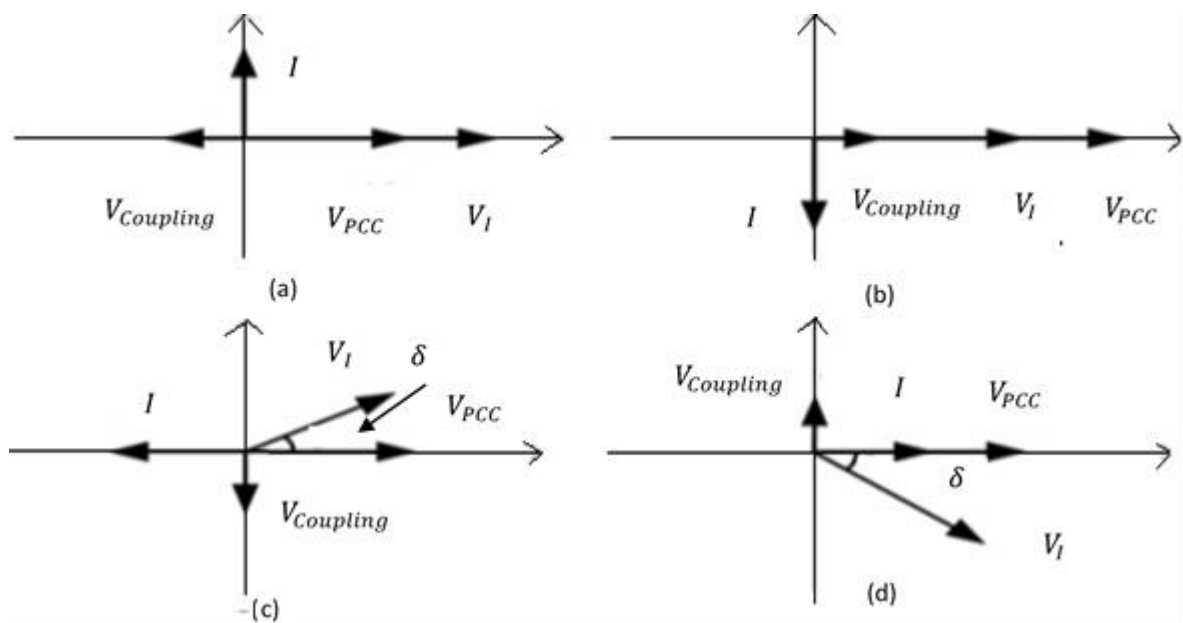


Figure 4.12: Vectors of different DSTATCOM modes (a) Capacitive mode (b) Inductive mode (c) Active power release (d) Active power absorption

Adapted from (Kumar & Mishra, 2014a)

A voltage controlled hybrid DSTATCOM of reduced rating, multiple features and with the ability of a single shunt compensator to alleviate several PQ problems are investigated in (Kumar & Mishra (2013)). There is a connection of an external inductor between the source and the load. This reduces the current requirement for mitigation of voltage sag and enhances the DSTATCOM voltage regulation bandwidth. An algorithm is proposed which is multi-functional and has indirect control of the source currents while operating normally in order to mitigate PQ problems that arise due to current and load terminal voltage. It is constant at the instances of voltage disturbances.

A stiff source connected load using a DSTATCOM is likely to have voltage disturbances. This is done by joining the source, an external inductance, and the load of a suitable value in series. Different modes of DSTATCOM vector diagrams is shown in Figure 4.12(a-d). A multiple feature DSTATCOM with stiff source can operate in voltage control mode. Also, it provides fast regulation of voltage at the time when disturbances in voltage appears across load terminals as defined in Kumar & Mishra (2014a). It protects critical loads and during normal operating conditions, source currents can also be controlled via generated reference load voltages. In order to achieve source power factor to unity, DSTATCOM also provides reactive current load and harmonic components. The resulting outcomes are able to address PQ issues related to voltage and current.

A resilient voltage support strategy which uses multiple DSTATCOMs based on distributed coordination is given in (Mokhtari et al.,(2013)). It is applied to low voltage (LV) networks accompanied by Photo Voltaic source which acts as the renewable source for consumers. These DSTATCOMs share the required reactive power, taking into account their effectiveness on voltage support, and also uses its state information to match its operation with the neighbouring DSTATCOM. The resilient voltage support strategy requires less reactive power compared to other voltage support strategies.

For application in low-voltage distribution grids, a voltage regulator using DSTATCOM is proposed(Hock et al., 2014).The low pass filter (second order) is used to connect the DSTATCOM. Its control structure provides active damping with the help of the two DC bus loops and the three output voltage loops. The DSTATCOM is forced to operate with minimum power due to the introduction of a new idea to bring no compensation in certain conditions, also known as Minimum Power Point Tracking (MPPT). These three output voltage loop

reduces apparent power processed by the converter to nearly 32% and has a light load of 95%.

In order to produce DSTATCOM reference voltage in the voltage control mode operating condition, a new control scheme is proposed in (Kumar & Mishra (2014b)). There are several advantages of this scheme over existing DSTATCOM, which is voltage controlled, DSTATCOM for which 1.0 p.u is taken randomly as the reference voltage. Due to the injection of lower currents in the compensator and at the load terminal, unity power factor (UPF) under normal condition can be achieved. This later leads to reduced losses of the feeder and VSI. An uphold in the DSTATCOM rating is achieved, which results in the increase of its ability to mitigate voltage sag. The scheme has advantages of providing correction in power factor, elimination of harmonics, balancing loads, and regulating voltage proportional to the load requirement.

A three-phase DSTATCOM which is based on modular multilevel converters (MMC), uses voltage control strategy, and is described in Xu et al. (2015). The method that can be used to solve the unknown modulation index and circulation current of the electrical quantities is also illustrated in this section. The sets of phase messages are used as compared to output current across each voltage control loop which leads in the reduction of data communication resources and current sensors. It is advantageous as the number of MMCs module increases in the actual engineering application.

An adaptive control system is developed (Xu et al., 2015) for a standalone power generation system (distributed) fed by an induction generator (self-excited). This is applied to regulate voltage. A four-leg shunt compensator is connected to the AC bus used to perform the voltage regulation. The proposed adaptive controller provides voltage regulation with respect to parameter variations such as the connecting and disconnecting of load, and variation of the induction generator's parameters.

Scherer et al. (2015) proposes a control system which brings voltage regulation using an induction generator (self-excited) in generation systems which are standalone. It is a hybrid technology of four wires which contains capacitor banks that are switchable. Switchable capacitor banks supply the reactive power required for voltage regulation. The reactive power that remains is accumulated from the control of DSTATCOM to bring balance of IG currents

and also to compensate harmonics which are present in load currents. The proportional resonant derivative (PRD) controller, when liked with proportional integral controller, is used to compensate currents control and is done by the shunt compensator. The generator voltages and currents are in sinusoidal form with less distortion in harmonics, which is desirable for generator safety. This allows the use of the voltage source converter (VSC) for low power rate.

Mokhtari et al. (2013) uses multiple DSTATCOMs to share the reactive power and control voltage. Multiple-feature DSTATCOMs(Kumar & Mishra, 2014a; Kumar & Mishra, 2013) which provides both voltage and current source control in order to mitigate PQ problems is proposed, as well as voltage control for three phase using a single DSTATCOM to generate reference of a voltage controlled source (Kumar & Mishra, 2014b). The voltage regulation that is generated (Mokhtari et al., 2013; Hock et al., 2014) is applied to a low voltage grid. The voltage regulation of stand-alone generation systems is provided in Mokhtari et al. (2013) and Hock et al. (2014).

4.8.2 Current Control Strategies

An *id-iq* based control algorithm is proposed (Bajaj et al., 2016) for the active and reactive power control in a time varying environment. The load fluctuations are compensated by DSTATCOM. This scheme of control algorithm enhances steady-state performance and ensures the useful elimination of PQ disturbances. In order to regulate time varying active and reactive power control, an extra current control loop system is used under the fluctuations of load.

A DSTATCOM (3-phase 4-wire) configuration in current control mode containing an inverter and three-level clamped neutral points is proposed in order to compensate load and to enhance the PQ (Pande et al., 2014). A synchronous detection method is used to analyze the shunt compensator characteristics. This scheme provides complete sinusoidal source currents in the presence of distorted conditions. All three different approaches are analyzed for both unbalanced and non-linear load conditions with equal power, equal current, and modified equal current. This modified equal current approach is better compared to other approaches as it is effective even in the presence of highly distorted and unbalanced source voltages.

4.8.3 Inverter Technologies for DSTATCOM

There are different inverter topologies under non-linear load conditions for a high voltage distribution system as shown in Figure 4.13. The high voltage and low voltage distribution system using a single DC capacitor is not capable of providing full compensation with a 3-phase and 3-leg VSI shown in Figure 4.14. This drawback can be overcome by using neutrally clamped DC capacitor topology. However, it still suffers from an unbalanced capacitor, which brings the requirement of an extra circuit for balancing and thus affects the overall cost of the compensator. This is given in Figure 4.15. An alternative solution to the problem is by using an independent three-single phase inverter along with single DC capacitor which is given in Figure 4.14. The requirements here include the need for more switches, resulting in increased cost once again. The load neutral current is compensated using a 3-phase 4-leg VSC with the requirements of coordination between the third leg and fourth leg as shown in Figure 4.17.

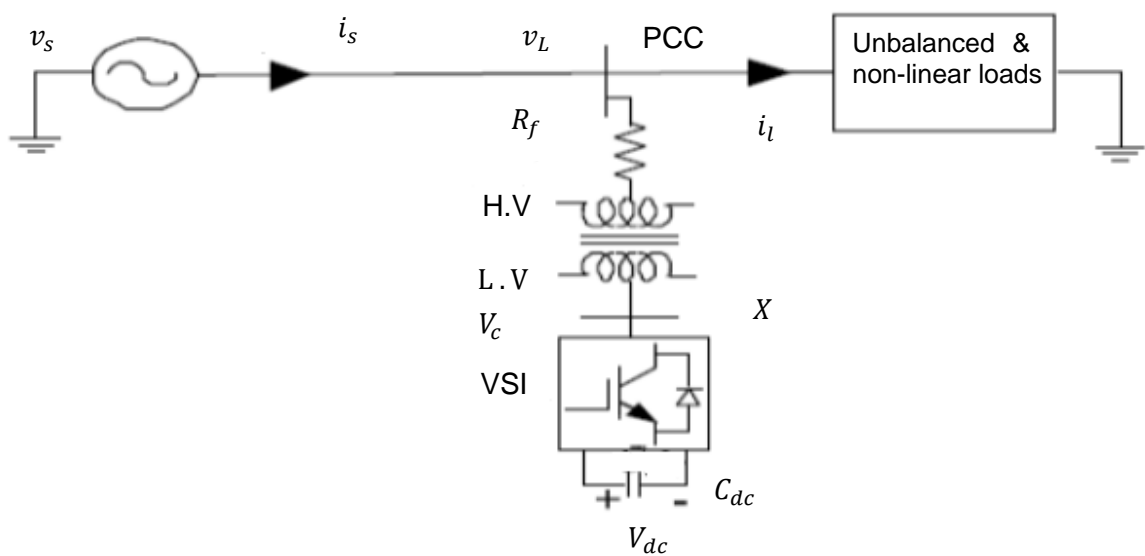


Figure 4.13: DSTATCOM structure for HV distribution system

Adapted from Henini et al. (2015)

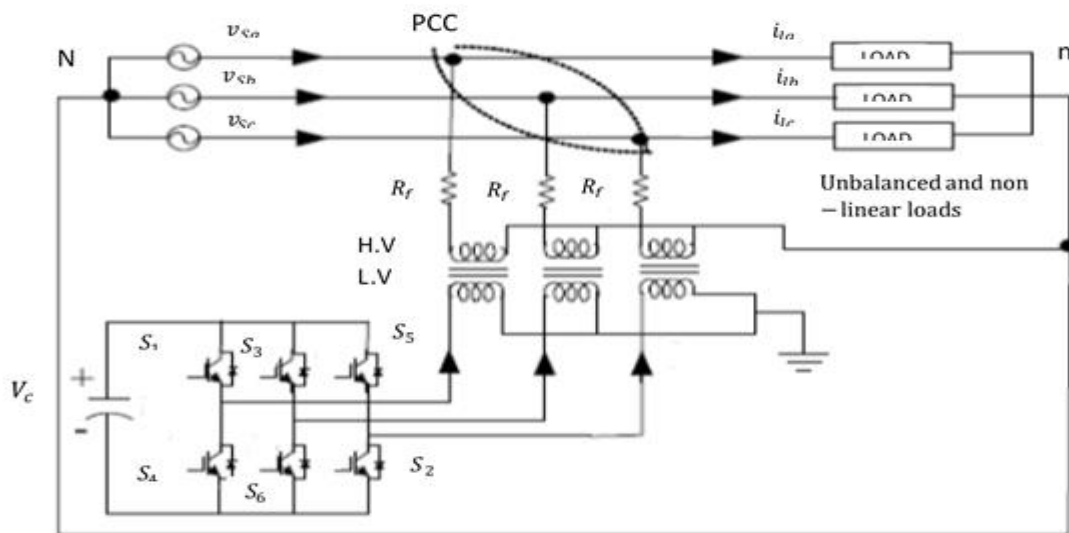


Figure 4.14: DSTATCOM (3-phase 3-leg inverter with a single DC capacitor)

Adapted from Henini et al. (2015)

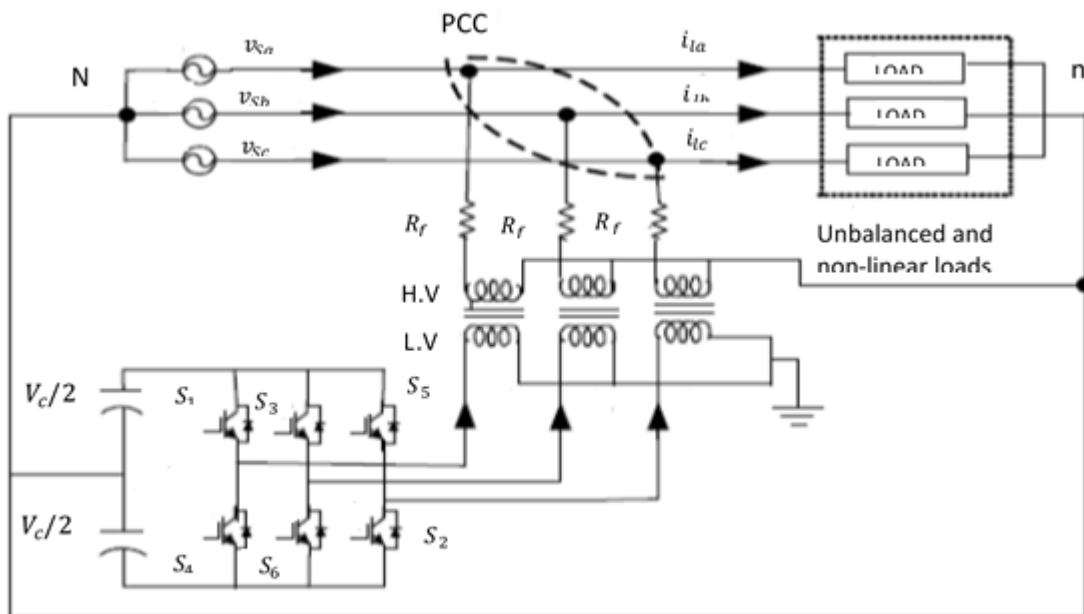


Figure 4.15: Split capacitor based DSTATCOM

Adapted from Henini et al. (2015)

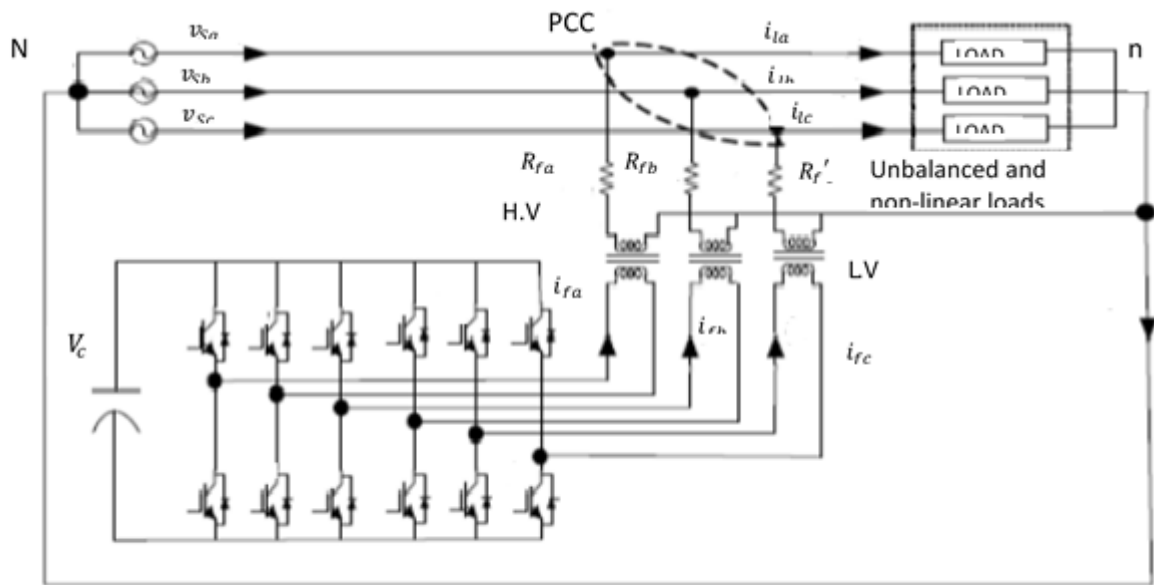


Figure 4.16: Independent single phase inverter with single DC capacitor based DSTATCOM

Adapted from Henini et al. (2015)

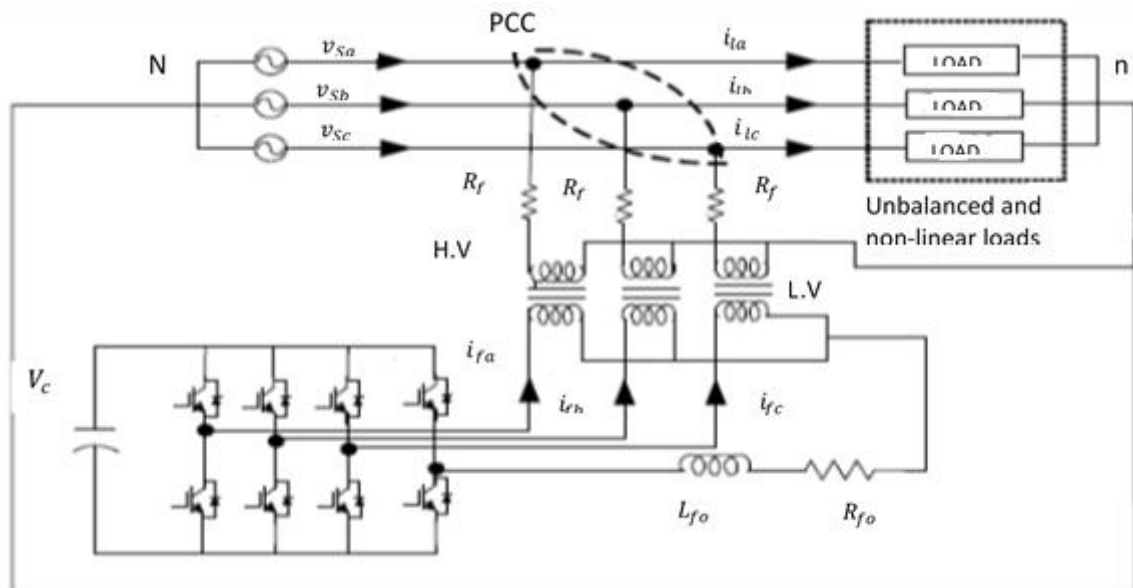


Figure 4.17: 3-phase 4-leg inverter based DSTATCOM

Adapted from Pande et al., 2014)

The DSTATCOM five level inverter configuration uses a fuzzy logic controller that improves the PQ as done in Henini et al. (2015). The inverter with five level switching signals is generated using the space vector modulation (SVM) method. The fuzzy controller uses the operator's knowledge, a feature that is different from conventional controllers that use mathematical equations, significantly increasing the stability of the power system.

4.8.4 Voltage and Current Control Strategies

The linear sinusoidal tracer (ILST) control algorithm is improved in Singh & Arya (2013) to achieve reactive compensation of power for linear and non-linear loads. The compensation of parameters like elimination of harmonics, correction of power factor, and regulation of voltage, which uses adaptive theory for hardware implementation of three phases DSTATCOM, is thereby achieved. The digital signal processor is used to compare performance analysis of the DSTATCOM model. The DSTATCOM with both PCC and DC bus voltages are regulated while using unbalanced loads.

For power conditioning applications, an efficient control algorithm is used to implement three phase DSTATCOM. This proves to be an effective way for suppressing harmonics and balancing loads. This scheme makes use of a double toned filter, a zig-zag transformer, rectifiers, and DSTATCOM with VSC. In the presence of voltage distortion, this derives the fundamental component of current.

4.8.5 Artificial Neural Networks

An excellent hybrid control approach (Penthia et al., 2016) which uses an artificial neural network (ANN) with a zig-zag transformer and hysteresis current controllers (HCC) for a DSTATCOM is proposed in literature. The power factor and reduction in line current harmonics of the network can be reduced using a hybrid controller. The controller is used in the network to push the source current into a sinusoidal one while trying to be in-phase with line voltage. It provides two controls, which include the estimation of the weighting factor of three phase load current and the hysteresis switching algorithm for driving the VSC of DSTATCOM. The compensator is optimised using an ANN with a suitable learning rate.

The adaptive neuro-fuzzy inference system which is least-mean-square based (ANFIS-LMS) is proposed in Badoni et al., 2016. This algorithm is used to implement a three phase DSTATCOM in order to compensate PQ problems related to current. This algorithm addresses many problems like harmonics compensation, correction of power factor, balancing of loads, and regulation of voltage. In order to estimate supply currents using the proposed algorithm, active and reactive power components are extracted from non-sinusoidal load currents. Voltage regulation modes under varying load conditions are also achieved.

A 3MVA DSTATCOM controller based on fuzzy logic is used for the improvement of PQ and to stabilise the distribution power system. The grey wolf optimization (GWO) algorithm is used to tune the scaling factors of the fuzzy logic controllers. When the voltage sag and load variations at grid end occurs, the DSTATCOM controllers are evaluated. This improves dynamic response and hence improves PQ.

Fuzzy logic controller (FLC) based on DSTATCOM is proposed which is used for elimination of harmonics, correction of power factor, balancing of loads, and voltage regulation. The need for a mathematical model is eliminated as this controller uses linguistic variables. A voltage source converter which is current controlled (CC-VSC) and is 3-phase insulated gate bipolar transistors (IGBTs) based can be used in place of DSTATCOM. The control algorithm uses two FLCs. The DSTATCOM DC link and phase voltages amplitudes are the FLC's input signals. The TS-FLC is made using only two functions of membership which results in less complexity. This algorithm addresses and performs as a good harmonic eliminator, a voltage regulator, and a load balancer. It brings much-needed dynamic voltage control in the DSTATCOM. A fuzzy logic approach is used in order to improve PQ and the stability of the distribution power system. The Genetic Algorithms (GA) is used to optimise the scaling factors of the FLC (Shi et al., 2014).

4.9 Conclusion

This chapter is a comprehensive review on the DSTATCOMs in order to improve PQ problems. DSTATCOM offers many advantages and addresses many issues. The review of DSTATCOM papers in the literature are valuable to reduce both current and voltage generated PQ problems. The voltage and control strategies are both reviewed, along with ANN-based control strategies. To mitigate various PQ problems using DSTATCOMs, further research can focus on the evolution of effective control strategies with regard to multiple-function compensation. Research on DSTATCOMs can solve the problems in grids and industrial units in order to

supply electricity with better quality and reliability. New control strategies, switching methods, as well as simultaneous compensation of flicker and harmonics on DSTATCOMs would be beneficial in the future.

CHAPTER FIVE

GRID-CONNECTED ALTERNATIVE SYSTEMS AND REACTIVE POWER COMPENSATION USING STATCOM

5.1 Introduction

In the modern world there is a rapid increase in demand for electric energy due to the growth in population, industrialization, and commercialisation. Therefore, more electricity generating units are required to fulfil the increased electric energy demand. Recent data shows that world net electricity generation was 21.6 trillion kilowatt-hours (kWh) in 2012 and is expected to increase to 25.8 trillion kWh by 2040. This is a total increase of 69% in electricity generation by 2040 (U.S. Energy Information Administration, 2016). Wind accounts for one-third of the increase in renewable generation as shown in Figure 5.1.

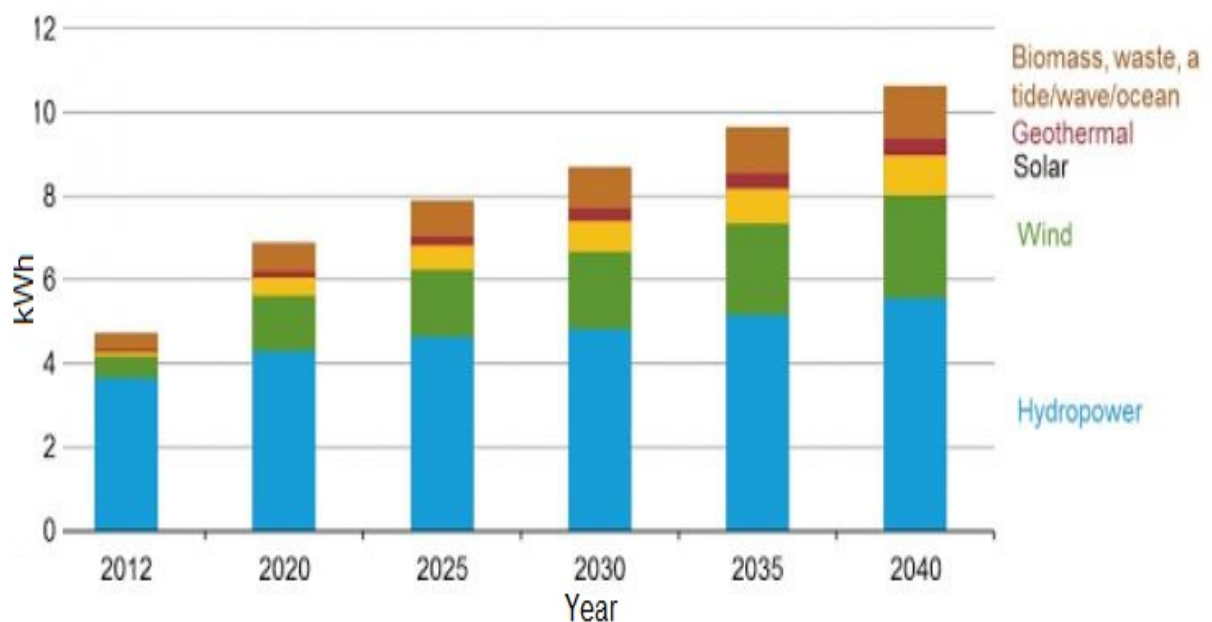


Figure 5.1: World's net electricity generation from renewable energy

Adapted from (U.S. Energy Information Administration, 2016)

Electricity generation is commonly achieved through the use of coal-fired power plants due to its cheap prices. However, due to the resulting emission of CO₂ in the environment, issues like global warming is brought to the fore. For instance, coal emits close to 1.4 to 3.6 pounds of CO₂ equivalent per kWh. The coal and natural gas plants create pollution in air and water as

well, which is not only a threat to human health, but to all life forms as well. Some consequences of pollution include breathing problems, heart attacks, cancer and skin diseases. With the increase demand in electricity, fossil fuels are getting diminished and there is a large fluctuation in oil prices which rise due to the high demand yet low supply.

In order to fix the issue and to save the environment, electricity should be generated from renewable sources such as the sun or wind. Electricity generated from these sources has a minimum effect on the environment. Compared to the CO₂ emission in when using coal, electricity generated using wind emits only 0.02 to 0.04 pounds of CO₂ Emission/kWh, and 0.07 to 0.2 pounds of CO₂ Emission/kWh while using the solar method. Geothermal and hydroelectric power generation also emits less Carbon-Dioxide per Kilowatt-Hour(U.S. Energy Information Administration, 2016).

5.2 Organization of the chapter

In this chapter, sources of renewable energy and their advantages are discussed. The advantages and disadvantages of wind energy are discussed and then classification of wind turbines is mentioned. This chapter looks at the working principle and how STATCOM is used as an effective device in improving power quality and regulation in distribution systems.

The work done in this chapter is on power quality disturbances such as suppression of the overvoltage and fluctuation caused by the small wind turbines injected, which leads to serious problems in household electrical appliances. When energy generated by wind farms is integrated with existing energy in distribution lines, there is a reactive power. A STATCOM is an effective devise to compensate that reactive power. The voltages at different feeders are compared with the feeder where STATCOM is connected. Also, the STATCOM reactive power compensation variance is compared when connected in parallel and series.

5.3 Renewable Energy Systems Connected to Grid

Before connecting home energy systems to the grid, research regarding equipment and terms of agreement with the service provider is required. Renewable energy systems can provide power to houses and businesses without any physical connection to the distribution grid. Due to this, people prefer the grid connection.

These grid connected systems provide power to the users home or business as long as the source of energy is available on a daily basis or during in a particular season. For e.g. when sun is shining, solar energy is available, hydro power depends on water flow, and the wind energy when wind is blowing. If the electricity generated is more than required it is fed back into the distribution grid. In absence of sources of these energies, the distribution grid provides the electricity to the user. This makes the user get rid of the requirement of electric storing devices like batteries and leads to saving of money from user's perspective. In some countries, public electricity utilities have an arrangement in which the extra electricity generated by grid-connected renewable energy system reduces the meter bill. The users then pay only the difference of electricity used.

The things which a user needs to consider and resolve before placing a renewable home energy system in conjugation with a distribution grid connection includes:

- The equipment that will connect the renewable home energy system to the distribution grid.
- The power company requirements for connecting the renewable energy systems.
- Community codes and State requirements in terms of the effect on the environment.

5.4 Equipment Required for Grid-Connected Systems

Besides buying the renewable energy set-up, additional equipment is required for the safe transmission of electricity to the home or business. These must also comply with the power utility company requirements. These are as follows:

- Power conditioning equipment
- Safety equipment
- Meters and instrumentation

5.5 Types of Grid-tied Systems

5.5.1 Solar PV Systems

Solar panels are easily installable and are the most common type of renewable energy used in residential homes or small businesses. Grid-tied solar power systems can be operated from the roof. Alternatively, they can be mounted to the ground which is often the case in community solar cells and companies. These systems do not include a battery bank in which to store energy produced by a solar array, therefore will not operate when the main power grid is down whether due to storms or power outages (M. Maehlum and M. Mæhlum, 2017). A grid-tied

solar kit layout is depicted in Figure 5.2. Grid-tied electric systems combine a solar panel array with a grid-tie inverter and various electrical system components in order to create electricity that is then fed to the main electrical grid. A typical system includes the following components:

- Solar Panels
- Inverter
- Midnite Solar Surge Protector
- Midnite Solar Combiner Box
- Delta Lighting Arrestors
- Wiring & Cables
- Fuses & Breakers
- Mounting System (Roof or Ground)

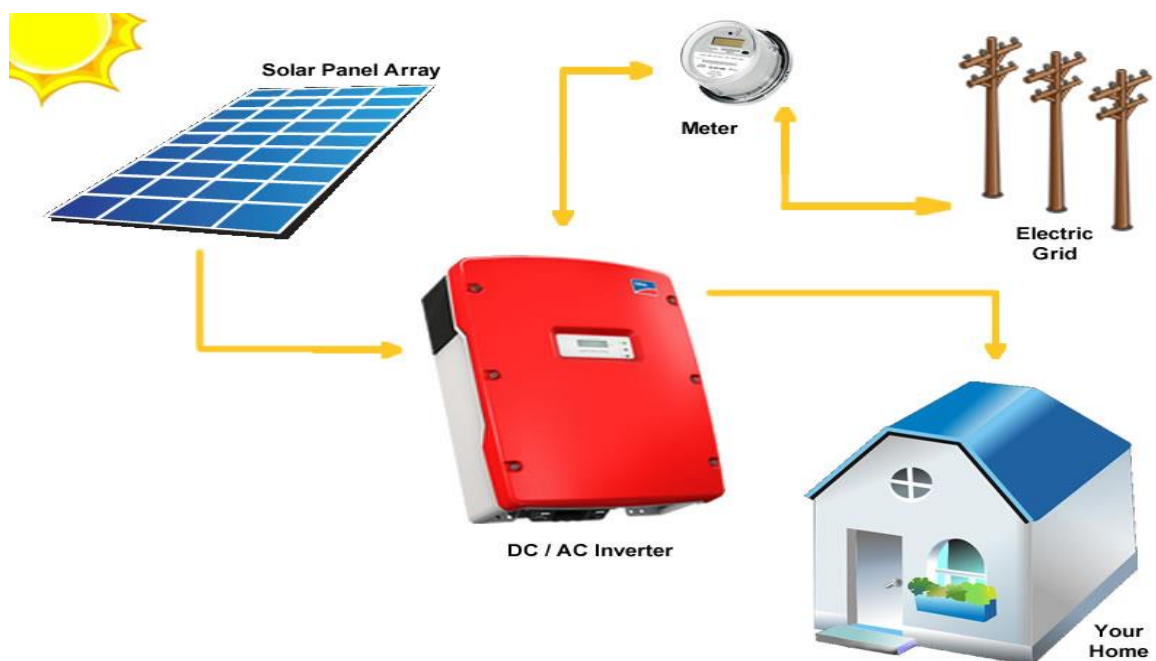


Figure 5.2: Grid-tied solar kit layout and components

Adapted from (M. Mæhlum and M. Mæhlum, 2017)

5.5.2 Wind Turbines

Wind turbines are generally used to provide energy to a larger area, and likewise, requires a large area for installation. The grid-tie inverter feeds the power grid by using power generated

by the wind turbine which converts the mechanical energy into 3-phase AC voltage. The voltage and frequency of the AC produced by the wind are variable and rely upon the wind speed. The grid tied-inverter converts the power to the frequency and voltage level of the grid before it is exported.

At the point of coupling, when wind turbines are connected in parallel with the power grid, the alternating current produced by the inverter is fed into the domestic distribution grid, which is also connected to the public distribution power grid. The wind generator system would thus be able to specifically nourish all the connected subscribers loads, for example, lighting, PC, and other household appliances.(Sharma & Singh, 2014). Figure 5.3 shows the grid-tied wind generation system.

At the point when the wind turbine isn't creating adequate energy, the power required to guarantee legitimate operation of connected subscriber loads is taken from public power distribution grid. Moreover, if the energy generated by the wind turbine is more than the required, It will be able to provide energy to more number of electrical subscribers.

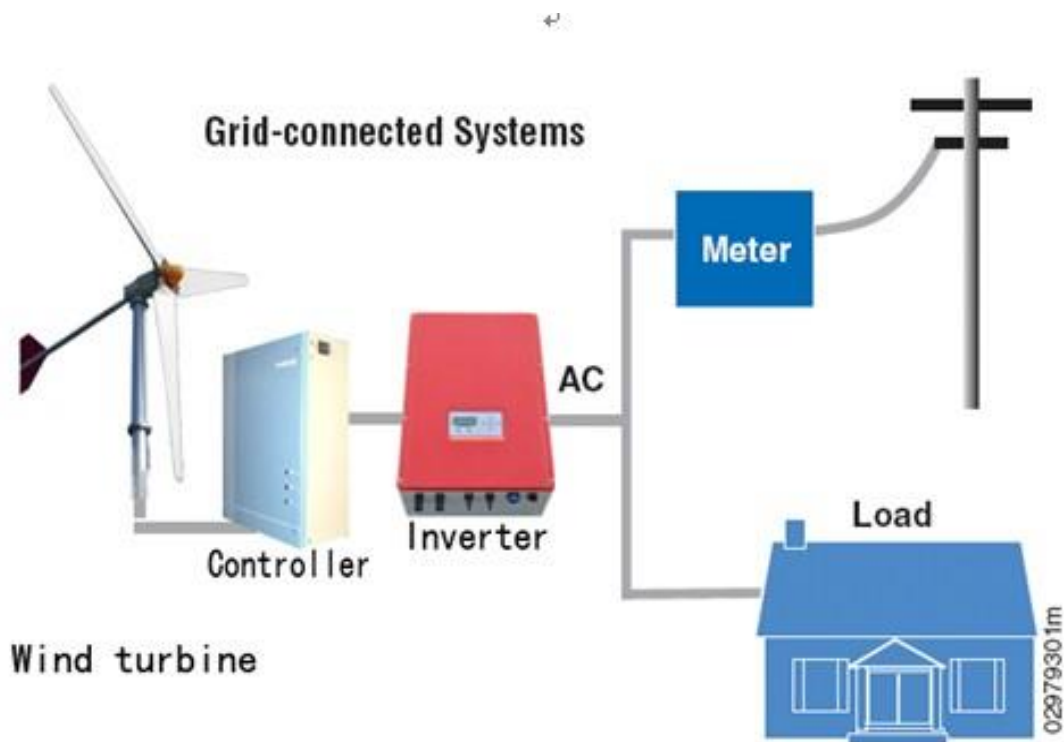


Figure 5.3: Grid-tied wind generation system

Adapted from (Sharma & Singh, 2014)

5.6 Advantages of grid-tied systems

Grid-tied systems has many advantages, which are as follows:

- Save more money with net metering
- No requirement of purchasing batteries and other equipment for storage.
- Solar panels usually generate more electricity than required by the user. With the net metering concept, almost 10 years of the installation of solar panel is free.
- Most utility companies usually purchases electricity from the user at the same rate they charge.
- Wind turbines require a large installation area and provides electricity to a large area. Therefore, they usually run like a business.

5.7 Wind as a source of energy

The global climate is severely affected due to the burning of fossil fuels. Every country in the world is accepting and taking steps to reduce the use of fossil fuels. In order to effectively reduce severity in climate change, some steps must be taken to reduce greenhouse gas emissions.

Effective mitigation of environmental change will require profound decreases in greenhouse harming substance outflows, with UK evaluations of a 60– 80% cut being essential by 2050 (Treasury, 2007). Compared to other sectors of the economy such as rail, road transport, air transport, water transport and domestic heating; electricity distribution systems are considered as the sector where low-carbon emitting sources can be replaced with existing ones.

Therefore, in addition to meeting demands, a cost-effective and reliable electricity generation which emits low carbon contents is required. This is a major objective in the energy policy of many countries (GWEC, 2016). Since the last decade, wind energy generation has shown faster growth compared to any other form of renewable energy source. Its development is braced by energy diversity, security, safety and climate change for national policy makers.

Figure 5.4 shows the global cumulative wind power capacity worldwide (GWEC, 2016). According to this report, wind power which can generate clean renewable 54GW power was installed in 2016 across the globe. This consists of 90 countries, with 9 having installed more than 10,000 MW. 29 countries installed more than the 1000 MW mark.

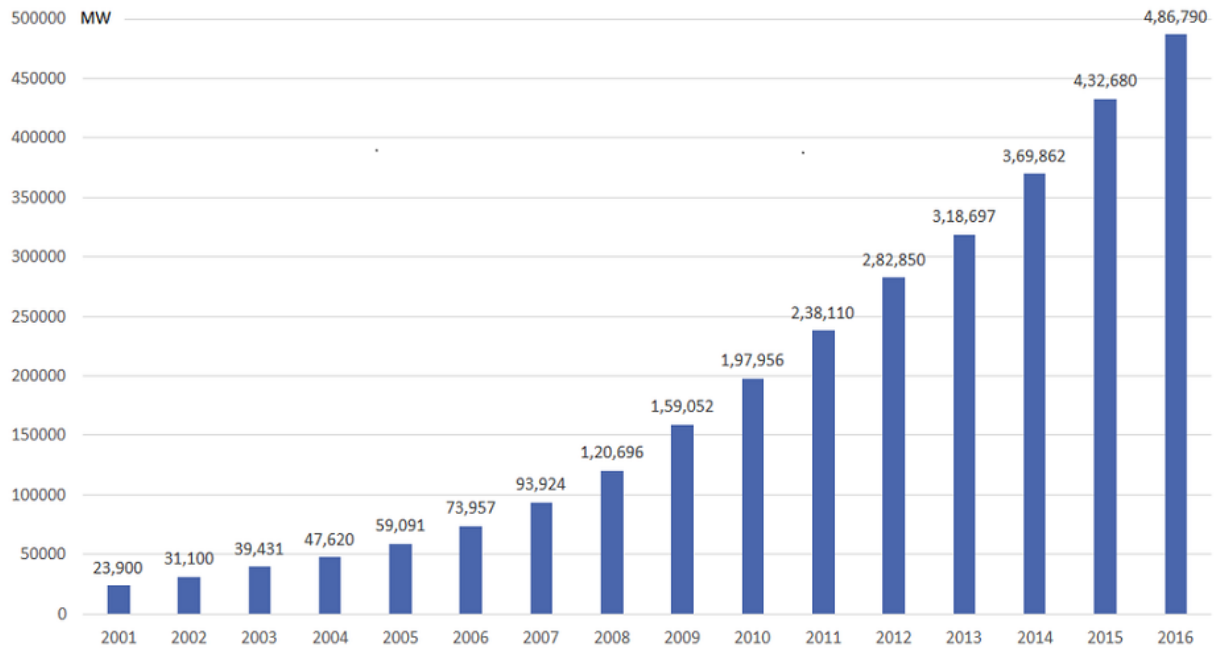


Figure 5.4: Global cumulative wind power capacity

Adapted from (GWEC, 2016)

Wind is a natural and indirect form of energy which results due to a horizontal movement of the air covering the earth's surface. It originates due to the pressure difference between two regions of the earth solar irradiation. This pressure difference then exerts a force which results in the movement of air from the high pressure area to a region of low pressure (Hau, 2013; Chiras, 2010). The earth receives an estimated 1.8×10^{11} MW of the total solar power. Out of this total power, energy converted to wind energy is 3.6×10^9 MW, which is around 2%. The remaining wind energy which is converted to another form is approximately 1.26×10^9 MW. This is twenty times the rate of the actual world-energy usage.

Wind energy can fulfil the world's energy requirements (Tong, 2010). The use of wind as a source of energy dates back many centuries and was used to sail ships in the Nile some 5000 years ago (Patel, 2008). In Asia, the first system using wind power appeared 3000 years ago and was used for irrigation systems. History reveals that wind power had also been used in 7th-century Afghanistan for grain milling.

In Europe, windmills became prominent from the 12th century, particularly in the Netherlands for land drainage. Later, it was used for milling grain and sawing wood. In North America, the windmills were used in the 19th century for water pumping (Volker Quaschnig, 2010; Hau, 2013).

The use of wind as a primary energy source for electrical energy generation started in the United States of America where the first wind power plants were built in New York in 1882 with a power output of about 500 kW. Thereafter they appeared in Berlin in 1884. The first three phase wind turbine was introduced in 1891 (Hau, 2013). However, during this period, the use of wind power was not significant and was mostly used to charge batteries in the areas which did not have access to power lines. It was replaced once the access of electricity from the grid became available (Burton et al., 2011).

The interest in wind power re-emerged in 1973 with the energy crisis when the countries that were members of Organisation of Petroleum Exporting Countries (OPEC) declared an oil embargo. At that time, oil and coal were the primary energy sources for electrical energy generation. This situation encouraged many countries that wanted to be independent of these energy sources to initiate research into the development of wind turbines and other alternative energy systems (Ghosh & Prelas, 2011).

5.8 Wind Farms

Wind farms are built around the world with both offshore and onshore improvements. In Europe, both the types are developed, whereas North America focus primarily on large onshore developments. These sites are usually selected before installation, using information provided by a wind atlas related to wind availability and speeds, which is further confirmed via local measurements. Local wind resources is monitored for a year or more before obtaining approval to install wind turbines.

However, the installation of onshore turbine is frequently carried out in upland terrain in order to exploit the higher wind speeds available. Onshore wind farms are difficult as high wind-speed location are usually of high visual amenity value. Furthermore, they are sensitive to the environment. The offshore wind farms are particularly larger and are developed in an area at least 5 km away from developed areas in order to reduce impact on humans and environment.

An advantage of this is reduced visual intrusion and impact of acoustic noise generated due to currents. This will also reduce wind turbulence in the presence of higher than average wind speeds. Table 5.1 shows the applications of the wind turbines.

Table 5.1: Applications of wind turbine
Adapted from (Elliott, 2002)

Small Rating ≤10 kW	Intermediate Rating =10-500 kW	Large Rating =500 kW-5 MW
Homes (grid-connected)	Village power	Wind power plants
Wind Farms	Hybrid systems	Distributed Power
For remote autonomous applications e.g. water pumping	Distributed power	Offshore and Onshore wind generations

Offshore wind turbines suffer from a disadvantage of higher installation and running cost, as well as having to consider the safety of longer cables that connect wind turbines to the distribution power grid. In practice, the areas with good wind energy are located away from built-up areas and new transmission circuits are laid down to connect distribution power grids to the wind farms. For example, in Germany it is estimated that additional high voltage and extra high voltage lines, which are approximately 1400 km in length will be used to connect wind farms in next 10 years (Bartels et al., 2006).

Smaller wind turbines generate electricity in rural areas and may be used as standalone power systems for homes, hospitals and community centres. (Elliott, 2002).

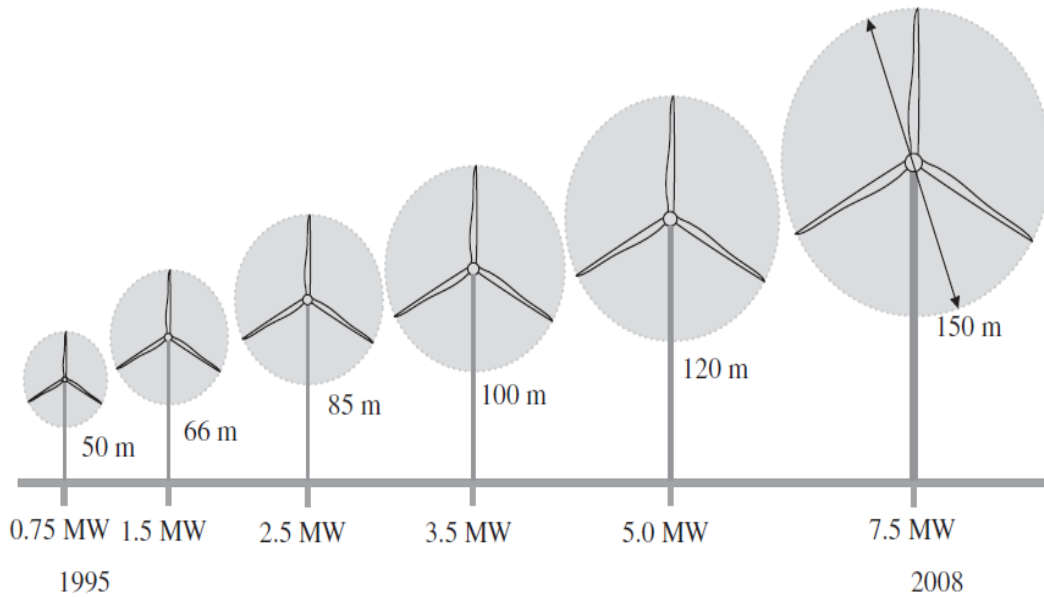


Figure 5.5: Wind Turbine Dimensions Evolution

Adapted from (Anaya-Lara et al., 2011)

5.9 Wind Energy-generating Systems

Figure 5.5 indicates the rapid evolution of wind technology in the last three decades. The rotor diameter is increased and advanced power electronics allows operation variation in rotor speed.

5.9.1 Power in Wind Turbines

Wind turbines generate electricity by using wind power to drive an electrical generator. The wind moves across the turbine blades which generate lift and exerts a turning force or torque. The shaft turns inside the nacelle due to the rotating blades, which then goes into the gearbox. The gearbox in turn increases the rotational speed to a level which is suitable for the generator, which then converts rotational energy into electrical energy using the magnetic fields. The output power goes to a transformer which converts the electricity from the generator at around 700V to the suitable voltage for the system collecting the power collection approximately 33 kV. As shown in Figure 5.6, the wind turbine takes out the kinetic energy from the swept area of the blades. The power in the airflow is given by Equation 5.1 (Manwell et al., 2009; Burton et al., 2001)

$$P_{air} = \frac{1}{2} \rho A v^3 \quad (5.1)$$

Where,

ρ = air density (approx. 1.225 Kg/m³)

A = swept area, m²

v = upwind free wind, m/s

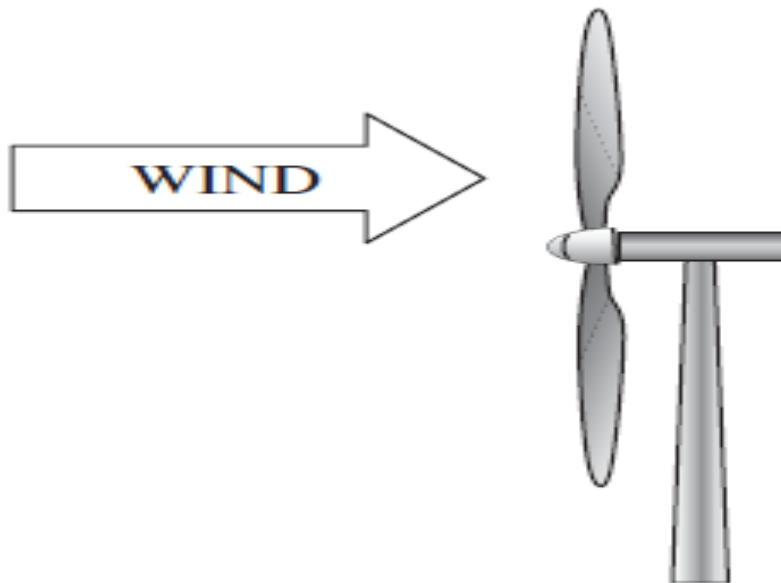


Figure 5.6: Wind turbine of horizontal axis

Adapted from (Anaya-Lara et al., 2011)

The available power in the wind can be calculated using Equation 5.3. The power which is actually transferred to the turbine rotor is reduced by the power coefficient as mentioned in Equation 5.2:

$$C_p = \frac{P_{windturbine}}{P_{air}} \quad (5.2)$$

$$P_{windturbine} = P_{air} C_p = C_p \frac{1}{2} \rho A v^3 \quad (5.3)$$

The Betz limit defines the maximum value of C_p , according to which the maximum percentage of power that the turbine can extract from air stream is 59.3%. In actual fact, a turbine rotor can have $25 \leq C_p \leq 45$ in percentage. The tip speed ratio is also defined in Equation 5.4 and is denoted by λ .

$$\lambda = \frac{\omega R}{v} \quad (5.4)$$

Where,

ω =rotational speed of rotor

v = free upwind speed m/s

R = radius to tip of rotor

The power coefficient (C_p) and tip speed ratio (λ) are dimensionless quantities and can therefore be used to describe the performance of wind turbines of any size. In Figure 5.7, the tip speed ratio effect on the power coefficient is portrayed. Therefore, the power curve conventionally explains the variation in the output power of the wind turbine at variable speed of rotation. The power curve provides the electrical power output in steady-state at hub height and varies with wind speed. It is measured by taking the average of data for 10 minutes. The power is explained with the help of an example of a power curve as shown in Figure 5.8.

On the velocity scale the power curve has three key points:

- **Cut-in Wind Speed** – This is the minimum wind speed required by the machine in order to provide useful power. It is usually 7-9 mph.
- **Rated Wind Speed** – At evaluated wind speed, the turbine can create power at its most extreme. It is for the most part in the range of 25-35 mph.
- **Cut-out Wind Speed** – The maximum wind speed at which the turbine can provide suitable power or the maximum speed above which the turbine cannot operate. It is not very well defined for all turbines.

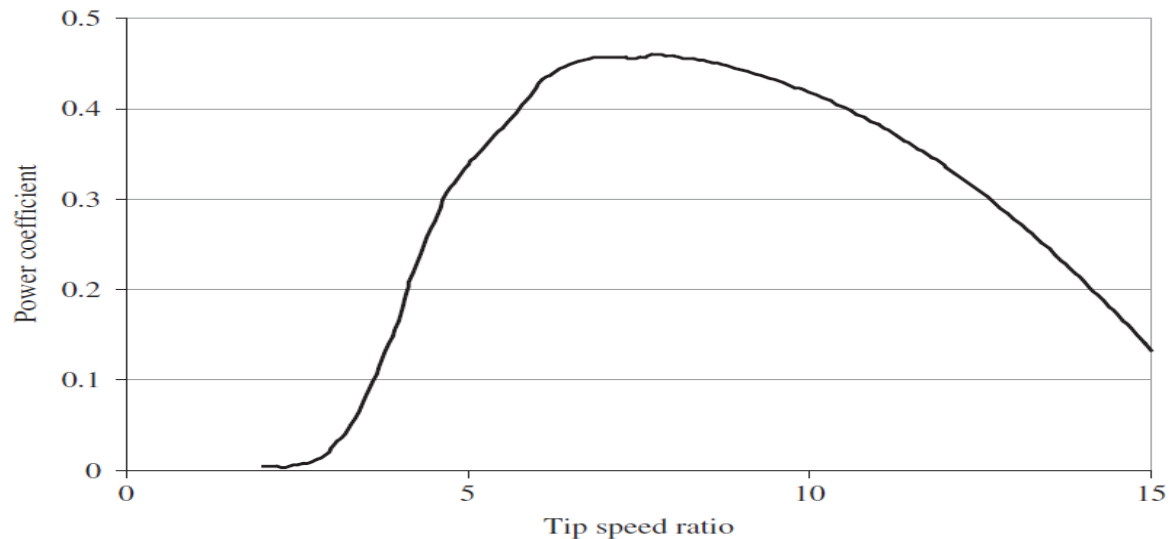


Figure 5.7: Illustration of power coefficient/tip-speed ratio curve, C_p/λ
Adapted from (Anaya-Lara et al., 2011)

If the cut-in speed is less than 5 m/s, the wind speed is too low for successful operation therefore electricity cannot be produced. When a wind turbine starts operating, the output power increases proportional to the cube of wind speed (v^3) till rated speed is achieved. When the wind speed increases beyond rated wind speed, the rotor is adapted in order to limit the mechanical power taken from the wind and in effect minimise the mechanical loads on the drivers. The turbines are shut down at high speed for safety reasons.

Figure 5.8 shows that for an annual site, wind speed, $V_m = 8m/s$. Typical values of cut-in wind speed will be 5m/s which is 60% of V_m , rated wind speed is 12 to 14m/s which is $1.5V_m - 1.75V_m$, and cut-out wind speed is 25m/s which is $3V_m$ (Fox et al., 2007).

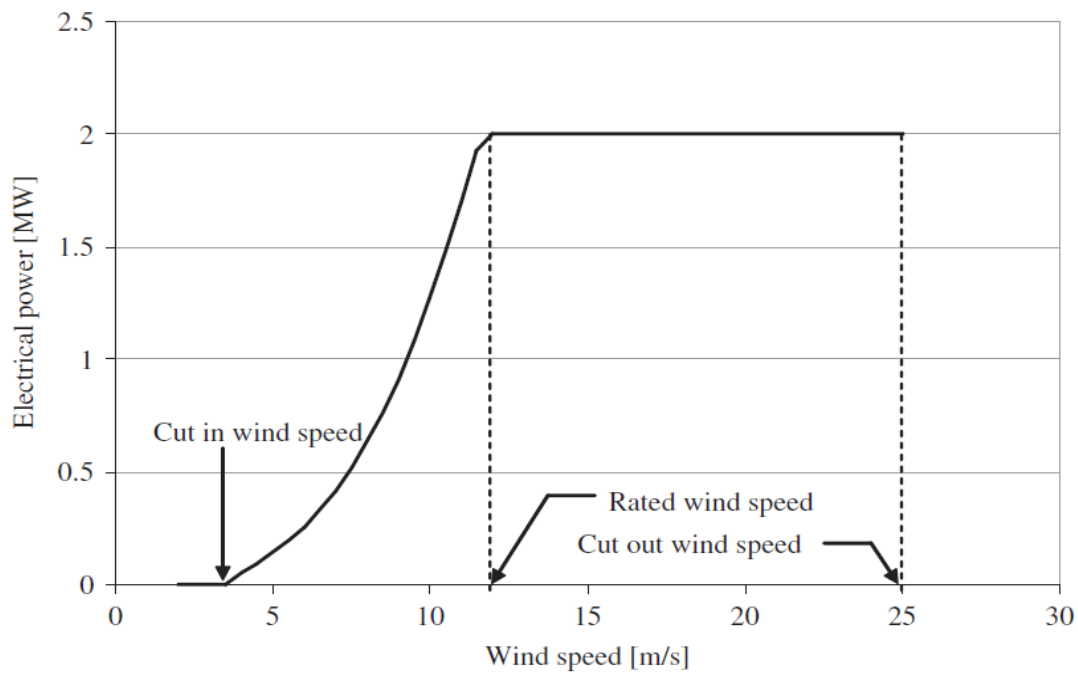


Figure 5.8: Power curve for a 2MW wind turbine

Adapted from (Anaya-Lara et al., 2011)

The power curves for existing machines is normally held by wind turbine manufacturing companies. An anemometer is used to find them by field measurements.

5.10 Advantages and disadvantages of wind power

5.10.1 Wind power advantages

The major advantages of wind power systems can be summarised as follows:

- The use of wind power reduces expenditure and amount of utility bills. The subscriber faces no power shortages or failures as experienced by subscribers who use distribution electrical grids.
- It is environmentally friendly and provides electrical energy at a cheaper cost, particularly in regions where electrical distribution grids do not provide services, such as in remote or hilly areas.
- The installation of wind turbines never effects the value of the installation site. The installation is easy to remove and does not leave negative effects on the land.
- The maintenance of the turbine is not frequent, thus, no maintenance or operational costs are incurred.

- The technology essentially offers home-made electrical energy and off-grid living, which is not readily possible with other technologies.

5.10.2 Wind power disadvantages

According to (Chiras, 2010) the main disadvantages of wind power are:

- The variable nature of wind and wind energy.
- Risk of flying birds.
- Wind noise.
- It is more dependent on location than solar electricity.
- Ice forming and falling from turbines after storms and interference with radio and televisions signals.
- Wind turbine installation cost depends on site selection, tower height, and output power rating.

5.11 Classification of wind turbines

Wind turbines use the kinetic energy of the wind to generate electricity. According to (Tong, 2010) and (Hau, 2013) wind turbines are classified according to the following aspects:

- Power generating capacity.
- Driving condition in the wind generator system.
- Constructional design.
- Location of the installation.
- Power supply mode.

5.11.1 Wind Turbines power capacities

Wind turbines are extensively arranged into small scale, micro scale, medium scale, large and ultra large wind turbines relying upon their energy generating capacities (Tong, 2010). Micro wind turbines are mainly used for water pumping, street lighting, and remote residences in areas where the electrical grid are not available. Micro wind turbines have a power rate of less than several kilowatts (Tong, 2010).

Small wind turbines with an electrical power output below 100kW are used mostly for telecommunication dishes, remote residential homes, and irrigation water pumping application in remote areas (Anaya-Lara et al., 2011).

Medium wind turbines have a power rate ranging from 100kW to 1MW. They are the most commonly used and are suitable for grid connected or off-grid systems for wind power plants, hybrid systems, distributed systems, and village power(Tong, 2010).

The wind turbines that have a power rate ranging from a few MW up to 10MW are classified as large wind turbines. Presently, most wind farms around the world are using this category of wind turbines, especially in offshore areas(Tong, 2010).

Research into ultra wind turbines are still under development. This category of wind turbines has a power output rate more than 10MW (Tong, 2010).

5.11.2 Geared drive and direct drive wind turbines

Considering the driving condition in wind generator systems, wind turbines can be classified in direct drive and geared drive types. In direct drive types, the generator shaft is directly connected to the blade rotor and the system offers more reliability, energy efficiency and design simplicity (Tong, 2010).

5.11.3 Grid-connected and off-grid wind turbines

Most large and medium wind turbines are connected to the grid whereas small wind turbines are used in remote areas and are considered off-grid turbines. The main advantage of grid-connected wind turbines is that there is no need for storage systems. Off-grid wind turbine generation systems always need a battery in storage because of the unpredictable power output due to the intermittence of wind (Tong, 2010).

5.12 Wind energy and power quality concerns

The two main effects of wind energy on PQ are voltage flicker and harmonic distortion. In the wind turbines with constant speed, the fluctuations of the wind are directly converted into fluctuations in output power due to the absence of a buffer for energy storage between mechanical input energy and the output of electrical energy.

Depending upon the quality of the distribution grid connection, the subsequent power fluctuations may bring about voltage fluctuations on the grid which might lead to changes in the brightness of an electric bulb. These fluctuations are termed as 'flicker'. This kind of flicker never arises in wind turbines with variable speed due to the fact that fluctuations in wind speed

are not converted into fluctuations in output power in this particular type of system. However, harmonic distortion usually arises in wind turbines with variable speed since they use power electronic converters, which gives rise to high frequency harmonic currents. This concern is increasing in large offshore wind farms, where extensive cable networks or wind turbine converters can lead to harmonic resonances. Here, high harmonic currents caused by existing harmonic voltages are already present on the power system.

Power quality is a major concern affecting the distribution systems in the present era. WTs connected to the grid are affecting PQ, such as fluctuations and overvoltage problems (Lund, 2005). Torque fluctuations caused by tower shadow and wind shear produces periodic fluctuations in the wind energy conversions systems (Vilar et al., 2006), resulting in a compromise of quality service in wind farm areas.

The wind turbine system remains one of the most useful and promising technology in renewable energy. WTs consist of three parts, namely, the blades, transformer and the generator which steps up the voltage when connected to the distribution networks. Research is being carried out with the aim of achieving uninterrupted operation and high performance during faults in grids. In (Mascarella, Li, et al., 2015), a reactive power dispatcher is proposed, which decreases the flicker problem and limits the maximum wind power injected into the grid. A reactive power controller is developed for voltage regulation and mitigation of flicker in the wind farm. This scheme is tested for certain ranges of wind speeds and has a satisfactory performance (Mascarella, Venne, et al., 2015).

Wind power as a renewable energy creates minimum pollution or environmental threats. However, the main drawback associated with WTs is the killing of birds or insects upon impacting fans. Wind power is variable in its nature due to the variable speed of wind. Therefore, the power generated from it requires regulation.

5.13 STATCOM and power quality improvement

A STATCOM can be implemented on a small wind farm equipped with Wind Turbines (WT) in such a way that it helps to improve PQ faults. This device absorbs or generates reactive power to or from the grid. Three WTs in a wind farm can all be operated at the same time or with an introduced delay. The low, moderate and high-generation mode is defined as one, two, or three generating turbines. The low, moderate, and high generation mode is defined as one, two or three turbines are generating.

A MATLAB/Simulink-based model is used for simulation. It shows that a STATCOM, when connected in shunt, gives better voltage control than if it was connected in series to the end of the feeder.

A STATCOM significantly enhances the performance of the wind turbines. It is also an effective device used to reduce the fluctuations caused by the voltage, also known as flicker, which arises due to the variation in the wind speed compared to the other devices, like Static Var Compensator (SVC)-thyristor based, STATCOM provides faster dynamic voltage control. Due to its fast and continuous response characteristics, STATCOM is generally used to enhance and improve power quality in the distribution systems (Hingorani & Gyugyi, 2000; Vilar et al., 2006).

In literature (Wang & Truong, 2013), STATCOM, when combined to power oscillation damping controller, can improve damping characteristics of the studied distribution system. Sivaranjani (2016) shows a simulation being carried out with and without STATCOM. The results reveal that the device helps in compensating negative sequence voltage and increases the life span of the wind turbines in wind farms

5.14 Reactive Power Compensation

Wind farms initially used Fixed Speed Induction Generators (FSIGs), which were consuming more reactive power. Therefore, the real power control was not effective (Holdsworth et al., 2003). Technical requirements are imposed for a grid connection like a fault ride through the power control ability of active and reactive power. New systems like Doubly Fed Induction Generator (DFIGs) and Fully Rated Converters (FRCs) are developed by wind generation manufacturers. Along with these, wind farms use compensation devices for reactive power like SVCs or STATCOMs (Hingorani & Gyugyi, 2000; Acha et al., 2002). These devices react to AC voltage changes within fewer frequency cycles which eliminates the requirement of capacitor banks, fast switching, or a change in transformer tapping. This SVC/STATCOM also keeps the voltage drop at minimum during remote AC system faults at the site of wind farms, which improves the fault-ride.

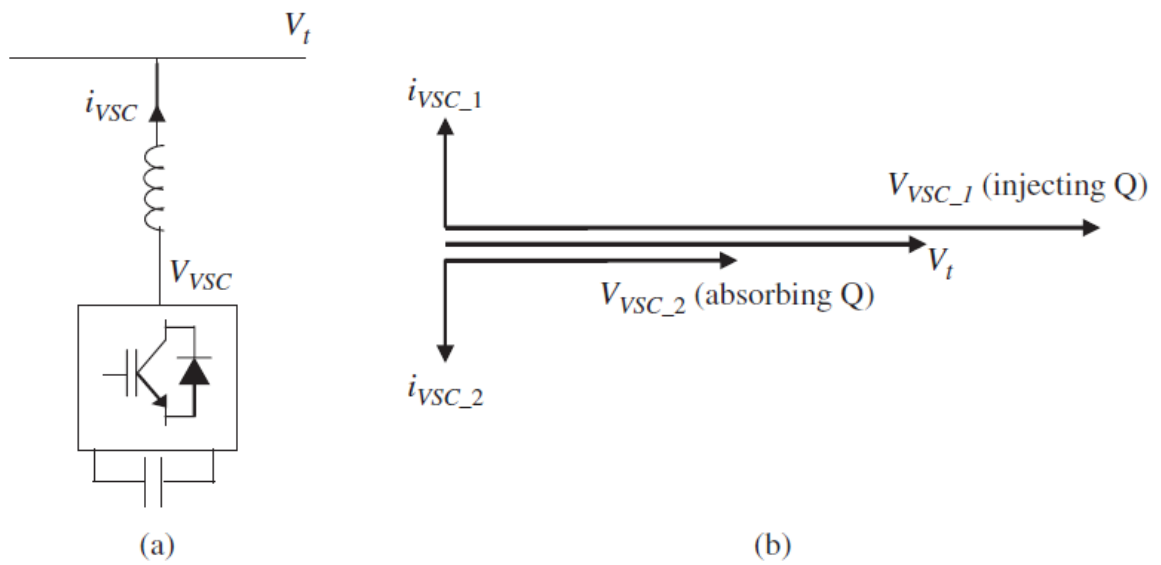


Figure 5.9: STATCOM arrangement. (a) STATCOM connection; (b) vector diagram

Adapted from (Anaya-Lara et al., 2009)

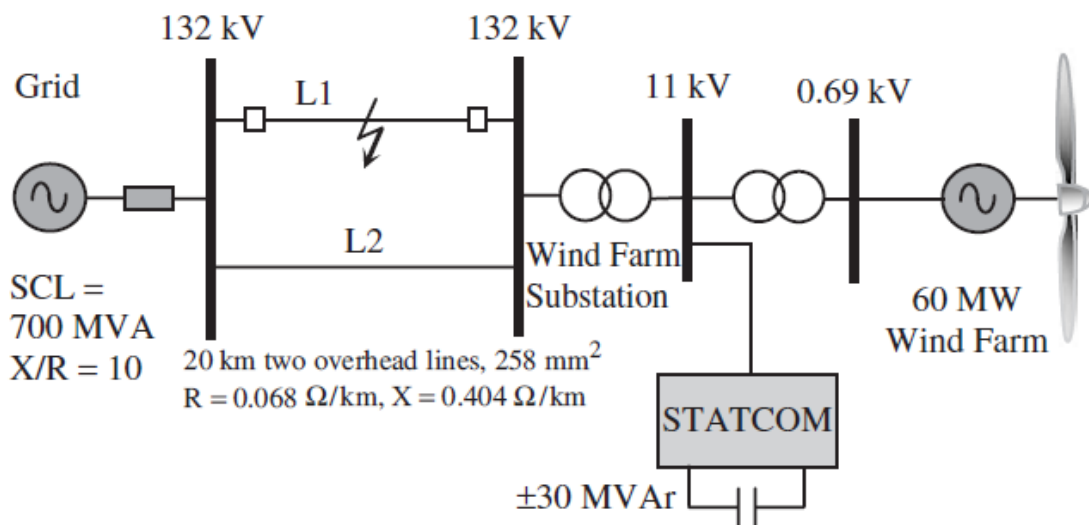


Figure 5.10: A large FSIG-based wind farm connected to the system with a STATCOM

Adapted from (Anaya-Lara et al., 2009)

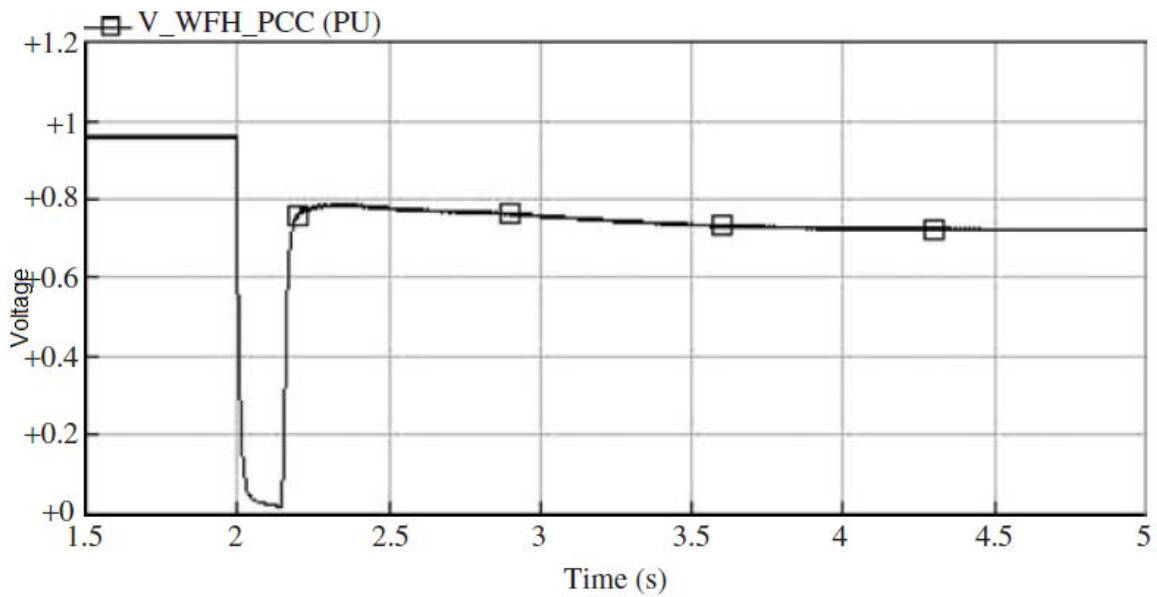


Figure 5.11: System voltage without STATCOM

Adapted from (Cartwright et al., 2004)

5.15 STATCOM and FSIG Stability

A STATCOM is a voltage source converter (VSC) based device in which the voltage source is behind the reactor as shown in Figure 5.9. The DC capacitor is used to create voltage. Due to this, STATCOM has very small real power capability. A way of enhancing the real power capability is by connecting an energy storage device across the DC capacitor. The voltage source amplitude decides the reactive power at the terminals of the STATCOM. For example, if the AC voltage at the point of connection is lower than the terminal voltage of the VSC, the STATCOM will generate reactive current while it absorbs reactive power, when the amplitude of the AC voltage is higher.

The STATCOM response time is lower compared to the response time of a SVC. This is mainly due to the IGBTs of the VSC which provides faster switching times.

A simple model of a fixed speed wind farm which provides fault ride through solution and voltage control is provided by STATCOM (Wu et al., 2003). The arrangement and case study using STATCOM are shown in Figure 5.10. The wind farm model has $30 \times 2MW$ FSIG, and stall regulated wind turbines. At the point of connection to the wind farm, the short circuit ratio

is 10. The simulations are carried out by inducing three phase faults of 150 ms duration at 2s along one of the parallel circuits for a 132kV network.

When the circuit is operated without the STATCOM, the circuit never regains the voltage level at the point of connection on which it was operating before the fault appeared. This is shown in Figure 5.11. When the STATCOM is included in the circuit, the wind farm easily rides through the fault as shown by the responses in Figure 5.12 (a). In the presence of the fault, due to the voltage drop, the reactive power supplied by the STATCOM reduces as in Figure 5.12 (b). During the circuit's recovery, the reactive power supplied by the STATCOM to the wind farm helps to ride through the fault.

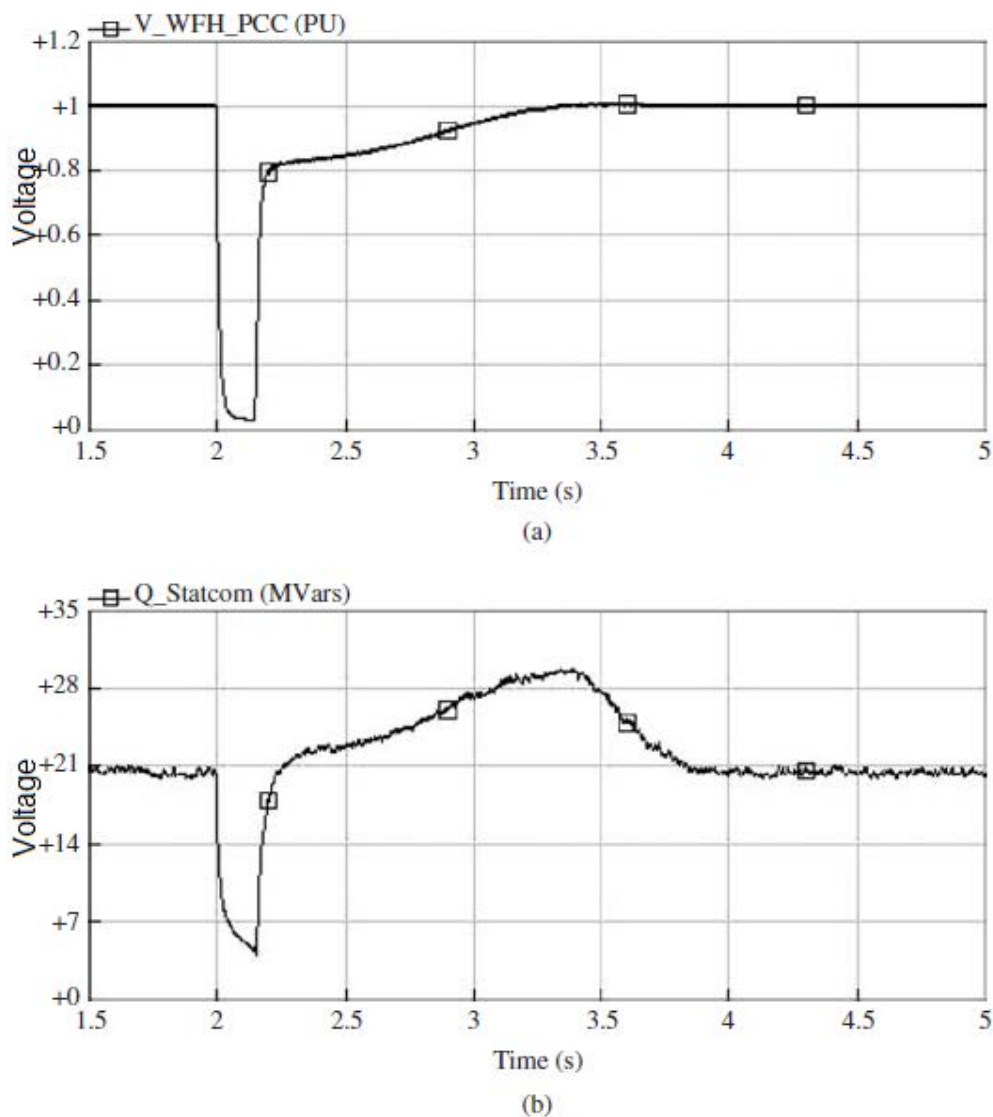


Figure 5.12: With STATCOM: (a) RMS voltage at point of connection (b) supplied reactive power
Adapted from (Cartwright et al., 2004)

5.16 Transmission Cost of Wind Farm

The transmission cost is the cost required to deliver a unit (kWh) of energy from the wind farm to the onshore grid. The energy conveyed from the wind farm is calculated using the following formula as mentioned in Equation 5.5.

$$E_D = E_P \times (1 - L) \times (1 - U) \quad (5.5)$$

Where,

E_D = energy delivered (MWh)

E_P = energy produced (MWh)

L = losses (%)

U = unavailability (%)

The analysis assumes that a loan would be required to pay for the initial investment. With this in mind, the annual instalments for this loan could be calculated using Equation 5.6.

$$R = \textit{Investment} \times \frac{r(1+r)^N}{(1+r)^N - 1} \quad (5.6)$$

Where,

R = annual loan instalments (£m)

Investment = initial investment in the system (£m)

r = loan interest rate (%), assumed to be 3%

N = windfarm lifetime (years), assumed to be 30 years

From this calculation, the cost of energy transmission can then be calculated using the formula mentioned in Equation 5.7.

$$\textit{Cost}_{trans} = \frac{R}{E_D} \times \frac{1}{1-p} \quad (5.7)$$

Where,

$Cost_{trans}$ = cost of energy transmission $\text{£}(kWh)^{-1}$

p = transmission system owner's profit (%), assumed to be 3%

5.17 Distribution grids variations with injection of wind energy

Wind energy is injected to the distribution grid and the effect of flicker, voltage, and power on the wind turbines is noted. The calculation of the power compensation in the distribution grid is discussed. Simulation results are carried out for two conditions, namely, when the STATCOM is connected in series or in parallel.

With the increase in capacity of wind energy injected, the PQ of the distribution grid (DG) is severely affected and power control is required. Otherwise, losses, faults, and wastage of energy will affect the efficiency, reliability and safety of the DG. This may result in faults or permanent damage of electrical household appliances. The electricity injected by wind power is highly variable in terms of hours, day to day basis, and seasons also. Due to this, instantaneous and variable electrical generation and its consumption needs balance in order to maintain grid stability.

The intermittency factor and the non-dispatchable nature of wind power generation can significantly raise costs for regulations, increase running service, as well as the points of high injection. Things brings about the requirement of managing energy demands, storage, and load shedding solutions. For the points of low-level wind power, fluctuations of loads with requirement of reserve capacity can compensate the variable low injection of wind generation (Vlad et al., 2009; Piwko et al., 2005; Weisser & Garcia, 2005; Breu et al., 2008). The Simulink distribution grid model is shown in Figure 5.13.

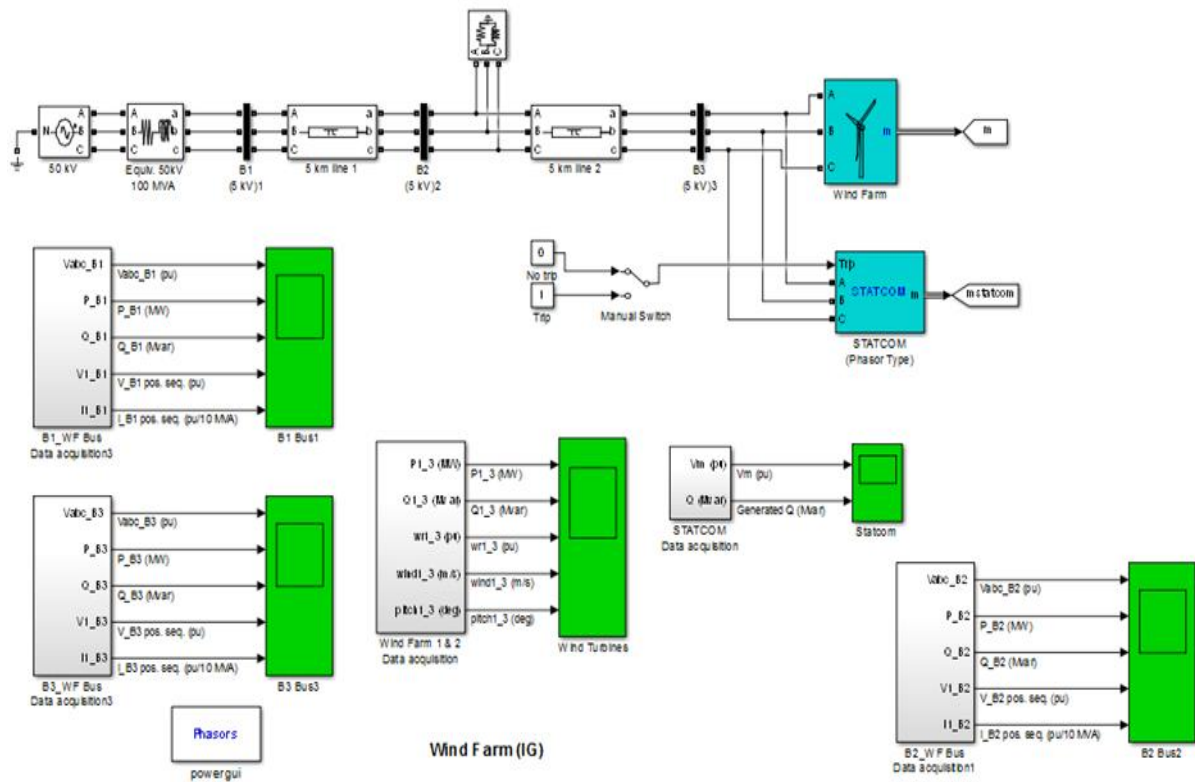


Figure 5.13: Simulink distribution grid model

Adapted from (G. Gupta, 2017)

5.17.1 Effect of voltage flicker or fluctuations

The variations in wind power leads to voltage fluctuations in DGs which are known as flickers. These rapid fluctuations in voltage can damage electrical appliances. A single wind turbine can produce significant flickers in a weak grid (G. Gupta, 2017).

5.17.2 Voltage above limits

The flow of electricity in traditional DGs is unidirectional. The feeder voltage drops with distance in the direction of flow. The injection of small wind power makes the flow complex and voltages at some nodes may even rises above the limits.

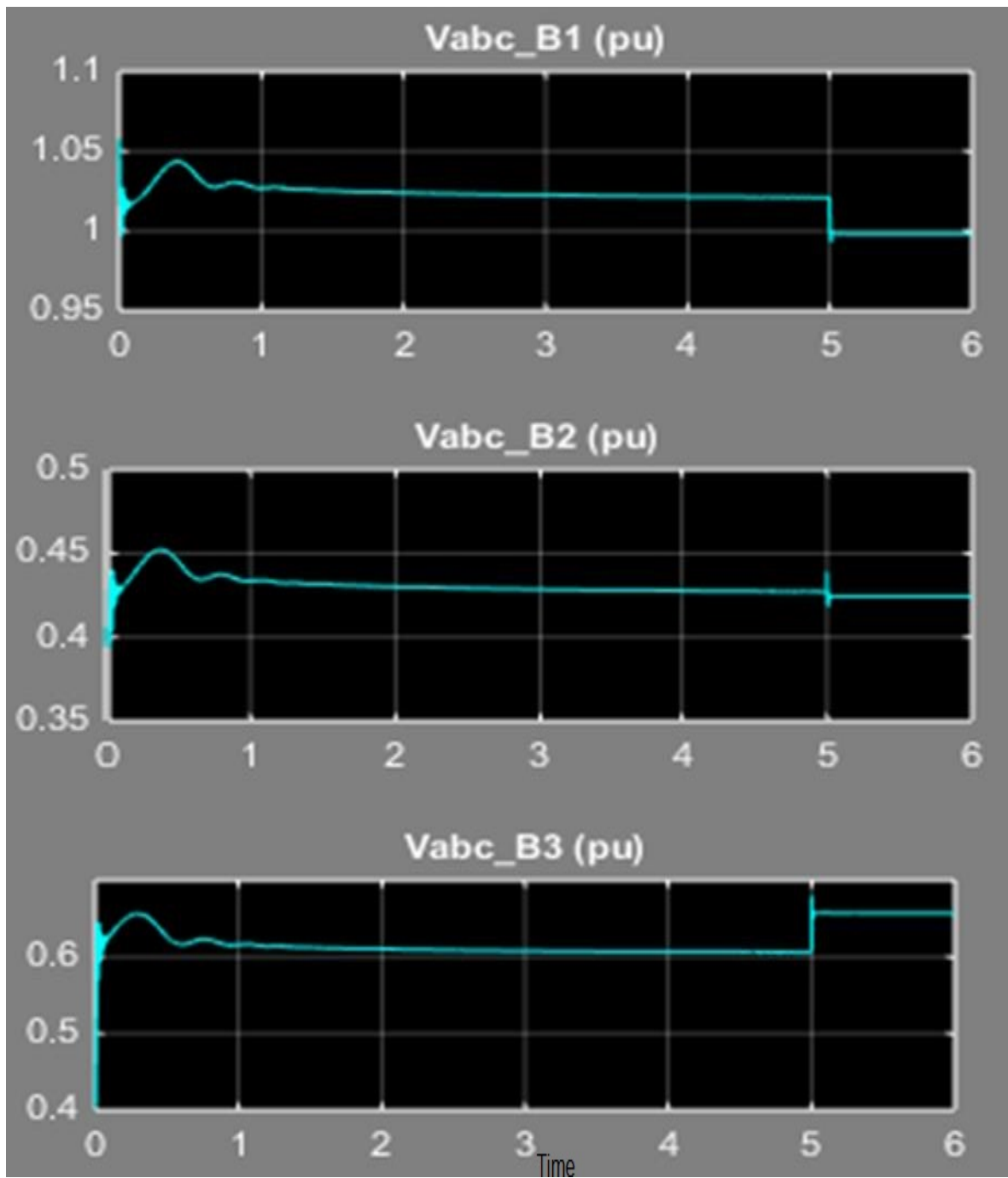


Figure 5.14: Voltages at buses B1, B2 and B3 for series and parallel connection of STATCOM

Adapted from (G. Gupta, 2017)

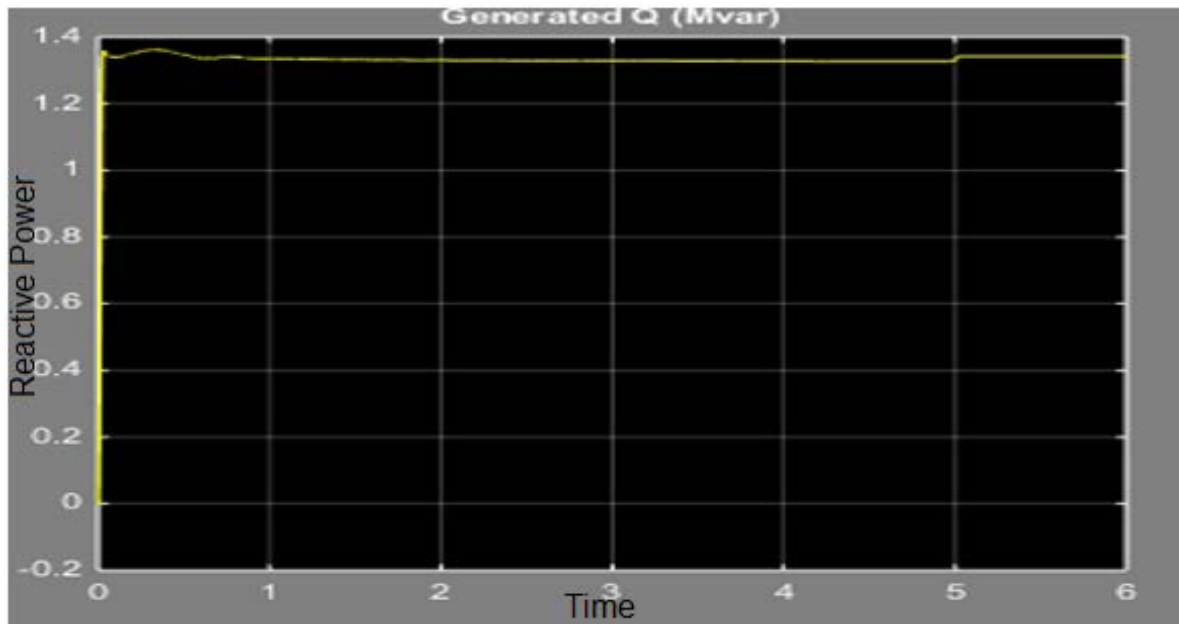
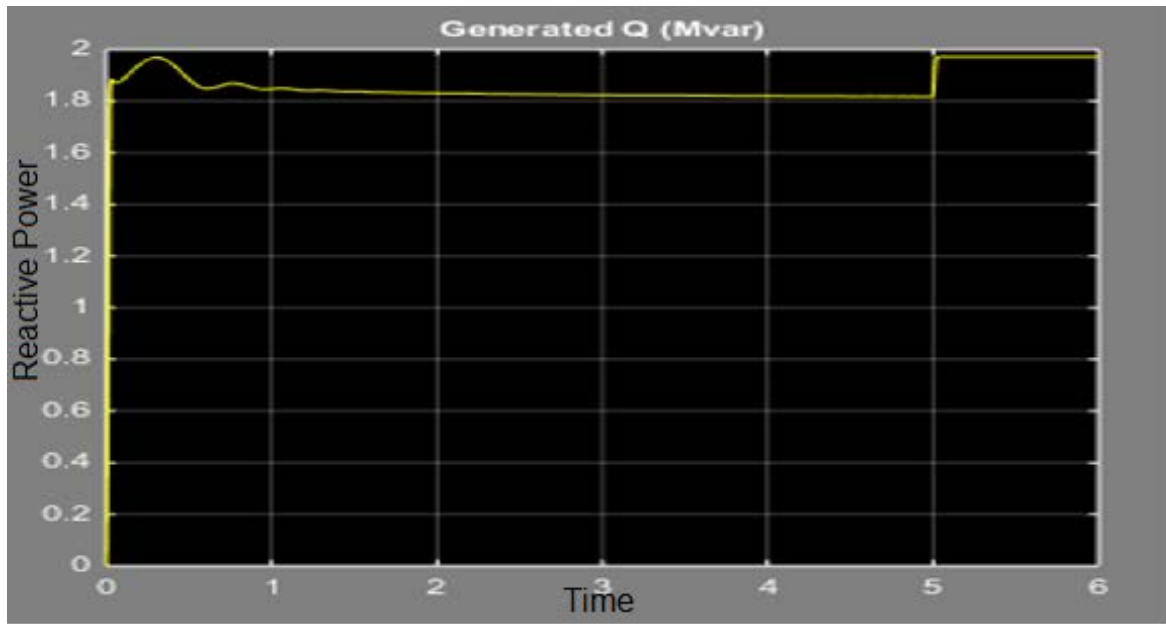


Figure 5.15: Reactive power generated by STATCOM (a) series connection and (b) parallel connection

Adapted from (G. Gupta, 2017)

5.17.3 Power loss

The transmission system has a higher reactance and resistance ratio compared to DGs. The injection of real power from wind farms into the feeder leads to a voltage drop therefore affecting the original loss of power. The loss increases or decreases are dependent on the amount of injected power.

5.18 Distribution grid power compensation

In the DG, the two power grids A and B are connected to each other through a lossless transmission line and reactance X_L . The phasor voltages of the power grids are $V_A \angle \theta_A$ and $V_B \angle \theta_B$, where θ_A , and θ_B , represents their phase angles. The angle between the phase voltages is therefore $\theta = \theta_A - \theta_B$. The current magnitude (I_L) of transmission line is then given by:

$$I_L = \frac{V_L}{X_L} = \frac{|V_A \angle \theta_A - V_B \angle \theta_B|}{X_L} \quad (5.8)$$

The flow of active and reactive power at bus A is:

$$P_A = \frac{V_A V_B \sin \theta}{X_L}$$

and

$$Q_A = \frac{V_A(V_A - V_B \cos \theta)}{X_L} \quad (5.9)$$

and bus B is

$$P_B = \frac{V_A V_B \sin \theta}{X_L}$$

and

$$Q_B = \frac{V_B(V_B - V_A \cos \theta)}{X_L} \quad (5.10)$$

5.18.1 STATCOM operating principle

The STATCOM consists of semiconductor switches which are used to rapidly control the phase and voltages of three phase balanced voltage generated. It also has a voltage source inverter (VSI), coupling transformer, capacitor (DC), and control circuit. If the voltage of any power grid is V_A , the VSC produces V_B voltage. In steady-state, V_A and V_B are in phase and the only reactive power is present. For $V_A > V_B$, the flow of reactive power is from the power grid to the VSC. In this case, STATCOM is absorbing extra power on the grid. For $V_A < V_B$, the flow of reactive power is from the VSC to the power grid, therefore STATCOM is generating reactive power for the grid. For $V_A = V_B$, there is no flow of reactive power.

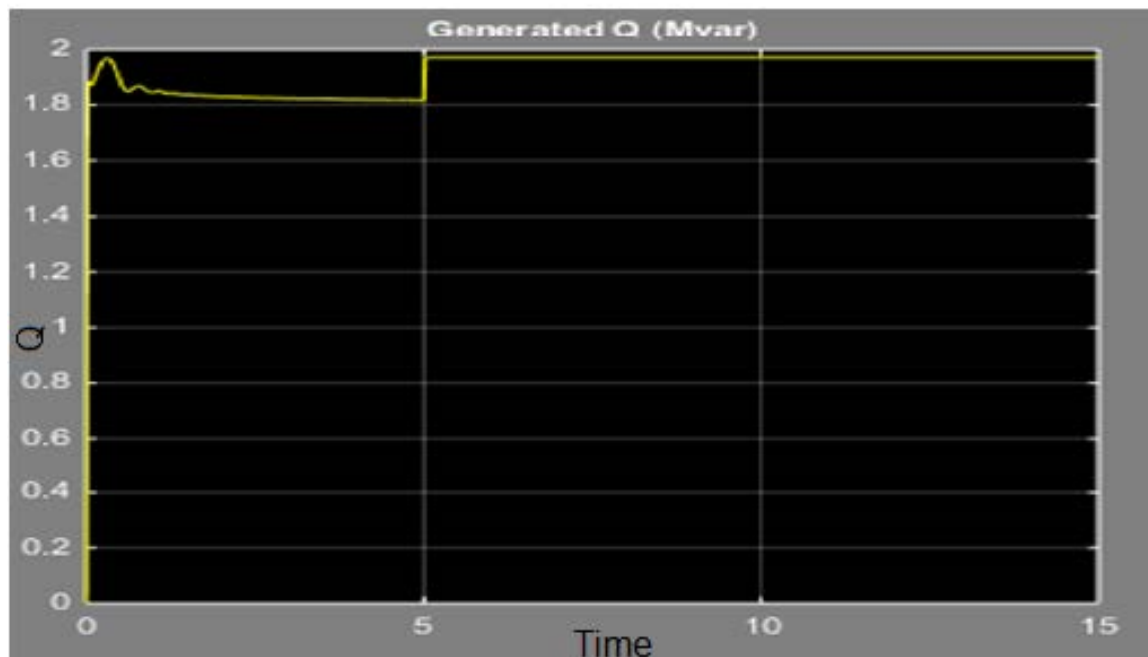
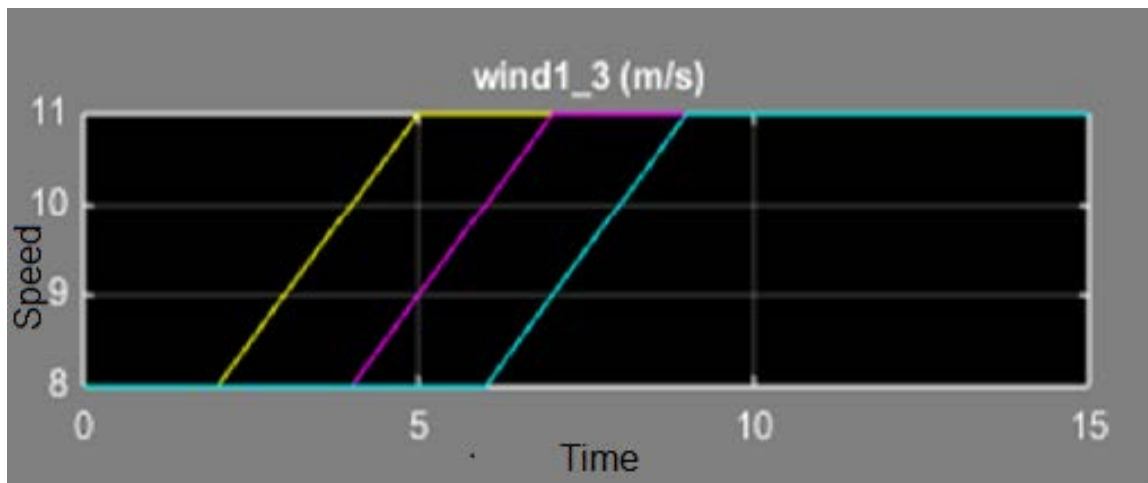


Figure 5.16: Series connection of STATCOM for 15 seconds simulation (a) wind speed (b) reactive power generated by STATCOM

Adapted from (Gupta et al., 2017)

5.18.2 Use of STATCOM

Wind power injected into DGs require regulation of voltages. One solution to this problem is to use inductors and capacitors at feeders for compensation, as well as switching wind turbines frequently. Due to voltage dips, the use of a parallel capacitor and inductance has no significance. Considering the good performance a STATCOM provides, it is used for compensation in DGs with injected wind power. In this chapter, the DG with or without STATCOM is compared and also the STATCOM installation in series and parallel is compared.

5.18.3 Distribution grid, STATCOM, and wind turbines model

The wind farm in the network uses three 3MW wind turbines, using squirrel cage induction generators (SCIG). It is connected to a 5 kV DG which uses this power to supply it to a 50kV grid through two 5 km lines and two 5 kV feeders(Gagnon et al., 2012) in Appendix A, Figure D. The work is extended by adding an extra load in parallel. The MATLAB code is in Appendix B.

A load that equals $500 + j242$ is also connected between line 2 and 3. The DG is directly connected to the stator windings. The 9MW wind farm is simulated at the frequency of 60 Hz for grid. A variable pitch WT is used to drive. The generator output power is restricted to nominal value by restraining the pitch angle for wind speeds greater than 9m/s. To generate output power, the synchronous speed should be lesser than the IG speed. The WT are equipped with a preventive system which monitors current, voltage, and the speed of the machine.

The reactive power which SCIGS absorbs is somewhat compensated by capacitor banks connected to the low voltage bus of the WT. The remaining reactive power in order to maintain 50kV voltage on B4 bus close to 1pu comes from 3Mvar STATCOM equipped with a setting of 3% droop. The WT mechanical power is converted as a function of WT speed (v_t) It is given with speeds of wind ranging from $4 \leq v_t \leq 10$ m/s. The 9m/s speed results in 3 MW power.

The speeds which are considered is applied to the turbines block wind 1, wind 2 and wind 3 of wind farm. The initial speed of wind is set to 8 m/s. From $t=2s$ to 5s, for WT1, the speed of wind rises to 11m/s. In a similar way, the wind speed is varied for WT2 and WT3 with an introduced delay of 2s and 4s.

5.19 Simulation results

5.19.1 STATCOM in series

For this mode, the STATCOM is connected in series at one end of the circuit as shown in Figure 5.13. The voltages at B1, B2 and B3 are measured. Figure 5.14 (a), (b) and (c) shows the voltages at these nodes for both series and parallel connection (G. Gupta, 2017).

Reactive power generated by the STATCOM is shown in Figure 5.15 (a), where upto 5 seconds of the reactive power varies as the WTs run with low speeds. Once they attain maximum speed at $t=6s$, the reactive power demand is stabilised at 2×3 Mvar as shown in Figure 5.16, where simulation running time is 15s (G. Gupta, 2017).

5.19.2 STATCOM in parallel

For this mode, the STATCOM is connected in a parallel line after bus B2. The voltages at B1, B2, and B3 are measured for parallel connection. Figure 5.14 (a), (b), and (c) shows the voltages at these nodes for parallel connection which are the same as in series connection. Reactive power generated by STATCOM is shown in Figure 5.14 (b), where the reactive power variations for parallel connection stabilises at 1.37×3 Mvar, and the reactive power demand is stabilised at 2×3 Mvar (G. Gupta, 2017).

5.20 Conclusion

The STATCOM provides compensation dynamically in the presence of wind power injection on DG. The simulations verify that presence of STATCOM compensates the reactive power component of DG efficiently at both parallel and series connection. The voltage variation at feeder B3 is minimum due to presence of STATCOM. The reactive power for the parallel connection of STATCOM stabilises earlier compared to series connection; also their value stabilises at 1.37×3 Mvar and 2×3 Mvar respectively. The variation due to speed of wind is handled efficiently for DGs used for domestic use. In the future, work can be done to trip or introduce the fault in one of the WTs or integration of solar energy also.

CHAPTER SIX

MODELLING AND SIMULATION

6.1 Introduction

Power grids are one of the most important requirements for developing an infrastructure in today's era. All the countries of the world whether developed or developing require a secure and stable grid in order to supply energy to families, industry and other role players. To accomplish this goal, we introduced faults, induced loads and provided DER's which leads to abnormal conditions in distribution grid. The distribution grid employs DSTATCOM and STATCOM to recover from these variations.

In this chapter, D-STATCOM and STATCOM both are used to provide reactive power compensation in presence of faults and extra loads appeared on the grid. The work done in this chapter also compensates other PQ problems like voltage flicker along with the reactive power.

The average model of D-STATCOM does not constitute harmonics but it conserves the dynamics which arises due to the interaction of the control system and power systems is used for smaller time frames. With the average model of D-STATCOM, an insulated-gate bipolar transistor (IGBT), voltage source converters (VSC) are represented by equivalent voltage sources generating the AC voltage taken for one cycle on average of the switching frequency. The average model permits much larger time steps, around 40-50 μ s, which allows simulations during an interval of several seconds. The phasor model of STATCOM is used for simulations with larger time frames.

The organization of the chapter is as follows. In section 6.2, the DSTATCOM is connected at the same point of coupling where faults are introduced which is not covered in literature. In section 6.3, the DSTATCOM connected in parallel is again used to provide reactive power to a distribution network with a three phase breaker before the load and the results are compared with the model in which three phase breaker is not used. In section 6.4, a STATCOM phasor and static VAR compensator (SVC) models are compared in presence of faults. In section 6.5, voltage fluctuations on a distribution grid are tested with different DSTATCOM point of coupling.

6.2 Description of Average Model

In this section, a Distribution Static Synchronous Compensator (D-STATCOM) is utilized to regulate voltage on a 25kV distribution network as shown in Figure 6.1 by modifying model given in (Qaraca Ođlu & Mehemed Ođlu, 2011) in Appendix A, Figure A. The average model and data acquisition is shown in Appendix A Figure A. The model is used in presence of three phase faults, the work which is not covered in the literature. In order to transmit power to loads connected at buses B2 and B3, two feeders (21 km and 2 km) are employed. For power factor correction at bus B2, a shunt capacitor is employed. A 25kV/600V transformer is used to connect with the 600V load at bus B3. This model is an equivalent to an industrial power plant which absorbs changing currents continuously and produces voltage flicker like an arc furnace. The current magnitude of the variable load is modulated at a frequency of 5 Hz thereby making its apparent power variation approximately between 1 MVA and 5.2 MVA while maintaining a 0.9 lagging power factor. A three-phase fault circuit is introduced in this section which creates fault in all of the three, any of the two or in a one-phase respectively.

The D-STATCOM consists of the following components:

- A coupling transformer of 25kV/1.25kV which ensures proper coupling between the distribution network and the PWM inverter.
- A voltage sourced PWM inverter. On the AC side, the PWM inverter is replaced with 3 voltage sources providing equivalent voltage with average taken over one cycle of the switching frequency. The inverter is modeled by a DC capacitor charged by a current source on the DC side. The DC current denoted by I_{dc} is computed so that the instantaneous power at the AC input of the inverter remains equal to the instantaneous power at the DC output. The phases are denoted by a, b and c in the following equation: $V_a I_a + V_b I_b + V_c I_c = V_{dc} I_{dc}$.
- LC damped filters are connected at the inverter output. A quality factor of 40 to 60 Hz is provided by connecting resistances in series with capacitors.
- A DC voltage source provided by using a $10^4 \mu F$ capacitor for the inverter.
- A voltage regulator is employed for controlling voltage at bus B3.
- Anti-aliasing filters are used for the acquisition of voltage and current.

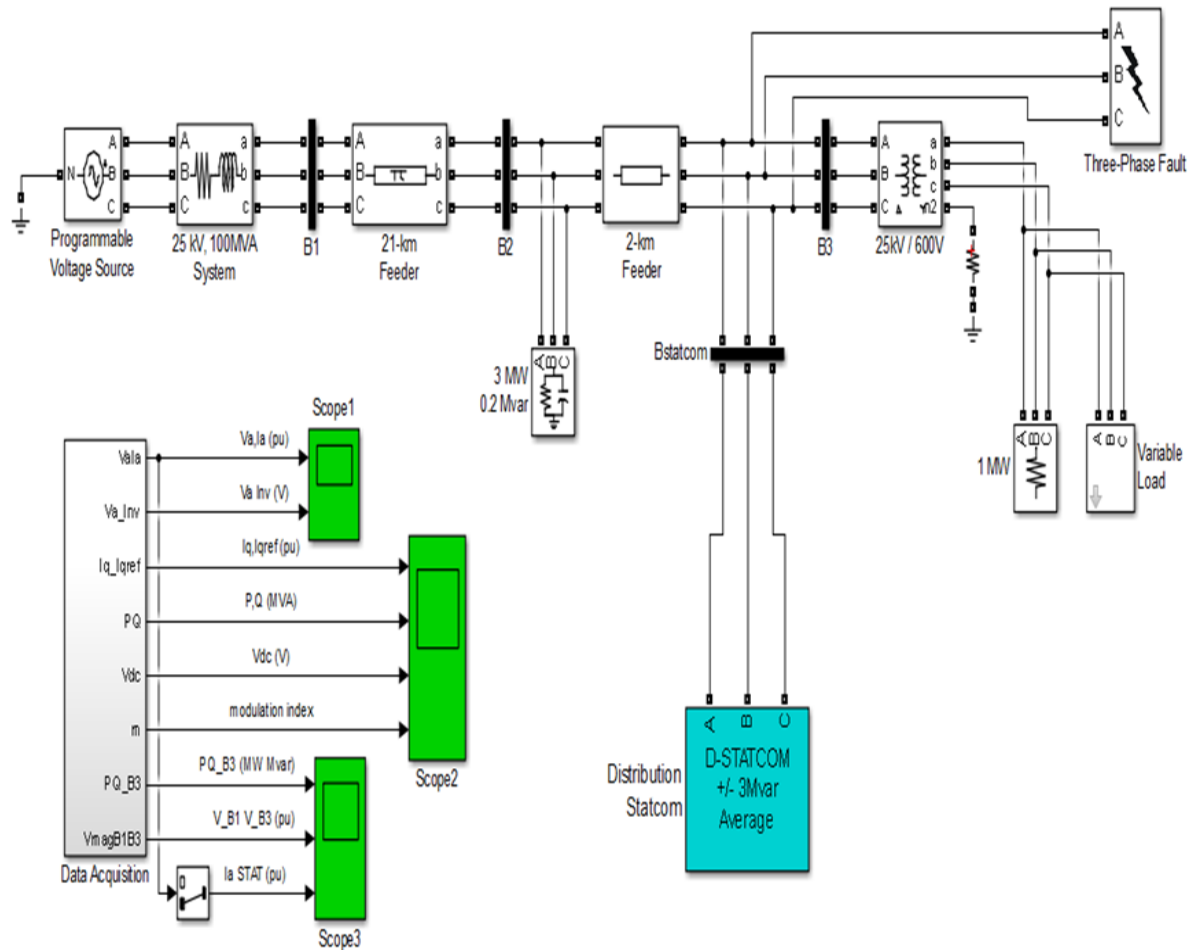


Figure 6.1: DSTATCOM average model
Adapted from (Gupta, G., Fritz, W., 2017)

The functional blocks of the D-STATCOM controller are:

- **A Phase Locked Loop (PLL):** The PLL is synchronized to the fundamental of the transformer primary voltages.
- **Measurement Systems:** Two blocks are used with V_{meas} and I_{meas} blocks which computes the d and q-axis components of the voltages and currents by executing an abc-dq transformation in the synchronous reference determined by $\sin(\omega t)$ and $\cos(\omega t)$ provided by the PLL.
- **An inner current regulation loop:** This loop has two proportional integral (PI) controllers that control the d-axis and q-axis currents. The PWM inverter generates the controller's outputs voltages and is denoted by V_d and V_q . The phase voltages V_a, V_b, V_c are generated by V_d and V_q . PWM voltages are synthesized by the phase voltages. The

reference current, I_q , comes from the outer voltage regulation loop while the reference current, I_d , comes from the DC link voltage regulator.

- **An outer voltage regulation loop:** In automatic mode regulated voltage, a PI controller maintains the primary voltage equal to the reference value defined in the control system dialog box.
- **A DC voltage controller:** It is used which keeps the DC link voltage constant to its nominal value ($V_{dc} = 2.4 \text{ kV}$).

The electrical circuit is discretized by using a sample time of $T_s = 40\mu\text{s}$ while the controller uses a larger sample time of $4 * T_s = 160\mu\text{s}$.

The D-STATCOM here regulates voltage at bus B3 by generating or absorbing the reactive power. This reactive power transfer is accomplished through the leakage reactance of the coupling transformer by generating a secondary voltage in the same phase with the primary voltage. The PWM inverter, which is voltage sourced, provides this voltage. The D-STATCOM works like an inductance when voltage at the bus is higher than the secondary voltage and absorbs reactive power. When the bus voltage is higher than the secondary voltage, the D-STATCOM works as a capacitor and generates reactive power.

6.2.1 Simulation

6.2.1.1 DSTATCOM dynamic response

In the simulation, the variable load is kept constant and the dynamic response of a D-STATCOM is observed to step changes in source voltage. The Programmable Voltage Source block modulates the 25kV equivalent of the internal voltage. The voltage is programmed as [1 1.06 0.94 1] p.u at time [0 0.2 0.3 0.4]s which increases the source voltage by 6% at time 0.2s and decreases by 6% at the time 0.3s and then increases back by 0.6% at time 0.3s.

6.2.1.1.1 Simulations with Q regulation

The simulations are carried out by setting the D-STATCOM controller to Q i.e. reactive power compensation. The faults are introduced close to bus B3 at the time [1/60 5/60]s. The faults are introduced in all the phases, in phase A and B, or phase A only. The results of the simulation are compared for D-STATCOM current and reactive power, voltage and reactive power at bus B3.

6.2.1.1.1.1 DSTATCOM current and reactive power

The faults are introduced at [1/60 5/60]s. The D-STATCOM generates and absorbs reactive power to compensate the effect of the faults. In Figure 6.2, the D-STATCOM current denoted as $I_{STATCOM}$ increases and decreases when faults are introduced. This is in order to generate reactive power and compensate reactive power as shown in Figure 6.3.

When the faults are introduced in one or two phases, the compensation required is less compared to when phases are with faults. Initially, the voltage source does not vary, which makes D-STATCOM inactive. At time $t=0.2s$, source voltage increases while at time $t=0.3s$, the source voltage decreases, which D-STATCOM compensates by absorbing and generating reactive power respectively.

In Figure 6.2, the D-STATCOM current denoted as $I_{STATCOM}$ increases and decreases when faults are introduced in order to generate reactive power and compensate reactive power as shown in Figure 6.3. When the faults are introduced in phase one or two, the compensation required is less compared to the condition in which phases are with faults.

Therefore, the current in the D-SATATCOM is less. In Figure 6.3, the reactive power is absorbed or generated by the D-STATCOM, and with no fault it appears to stabilize faster. When faults are introduced in all the three phases, the D-STATCOM generates (-10 Mvar) or absorbs (+5 Mvar) maximum reactive power.

6.2.1.1.1.2 Voltage and reactive power at bus B3

Faults are introduced at [1/60 5/60]s. When the faults are introduced, the voltage and reactive power at B3 varies. The D-STATCOM generates or absorbs reactive power to compensate the effect of the faults. In Figure 6.4, the faults are introduced at $t=0.016 s$ and $t=0.8 s$. It can be concluded that the reactive power compensation required by the circuit with faults in all phases is maximum, and therefore is minimum for the circuit with no faults.

The reason for this reactive power compensation for the circuit with faults is clearly evident from the voltage at B3, shown in Figure 6.5. The voltage at B3 lowers close to '0' for the circuit with faults in all phases. For the circuit with a fault in phase A and B, the voltage is close to

'0.8pu' while for the circuit with the fault in phase A, it is close to '1.5 pu'. In the case of an absence of faults, the voltage varies around '2 pu' for the duration of the faults.

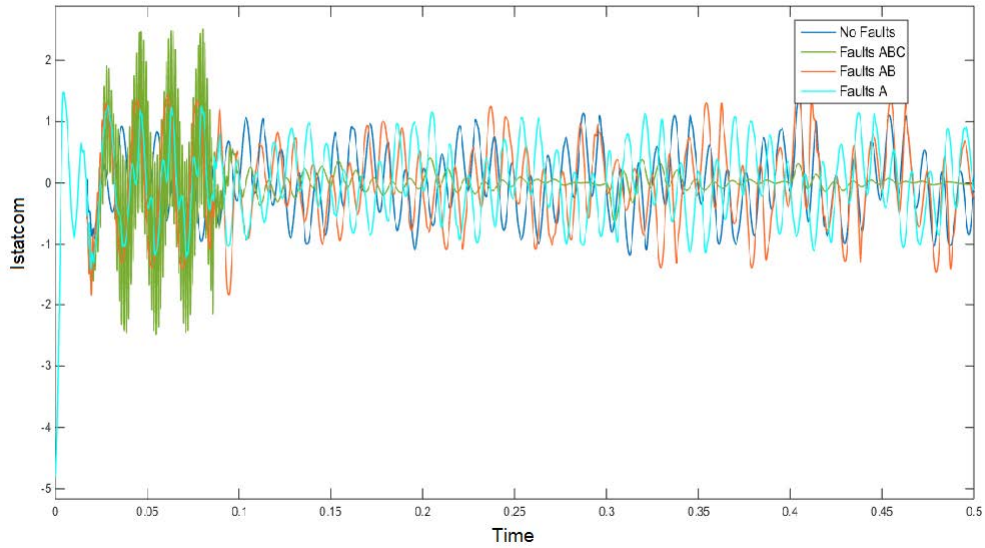


Figure 6.2: DSTATCOM current with controller set to Q regulation

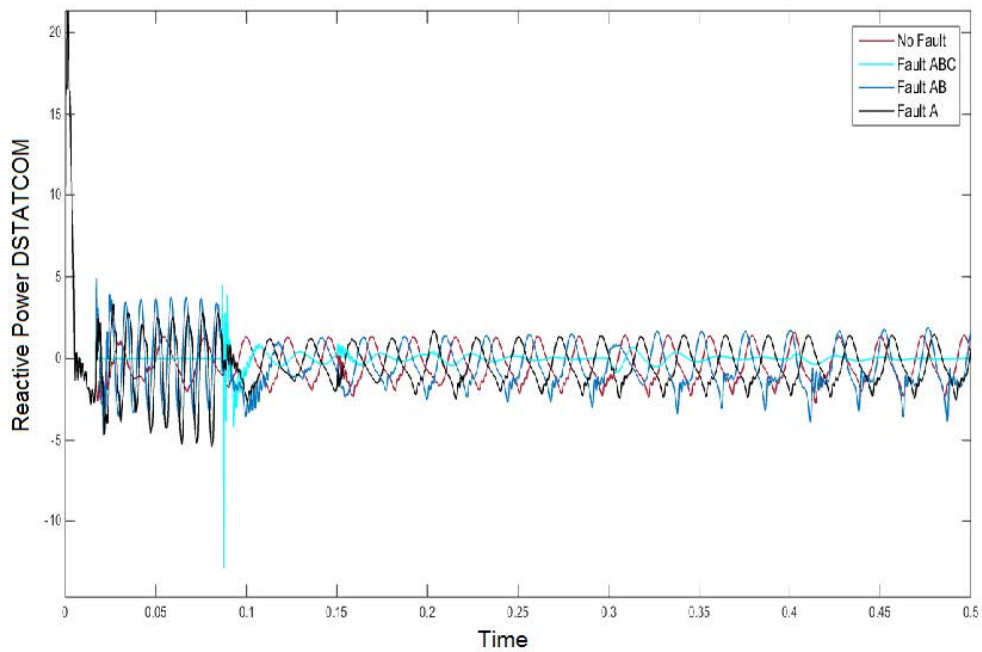


Figure 6.3: Reactive power of DSTATCOM controller set to Q regulation

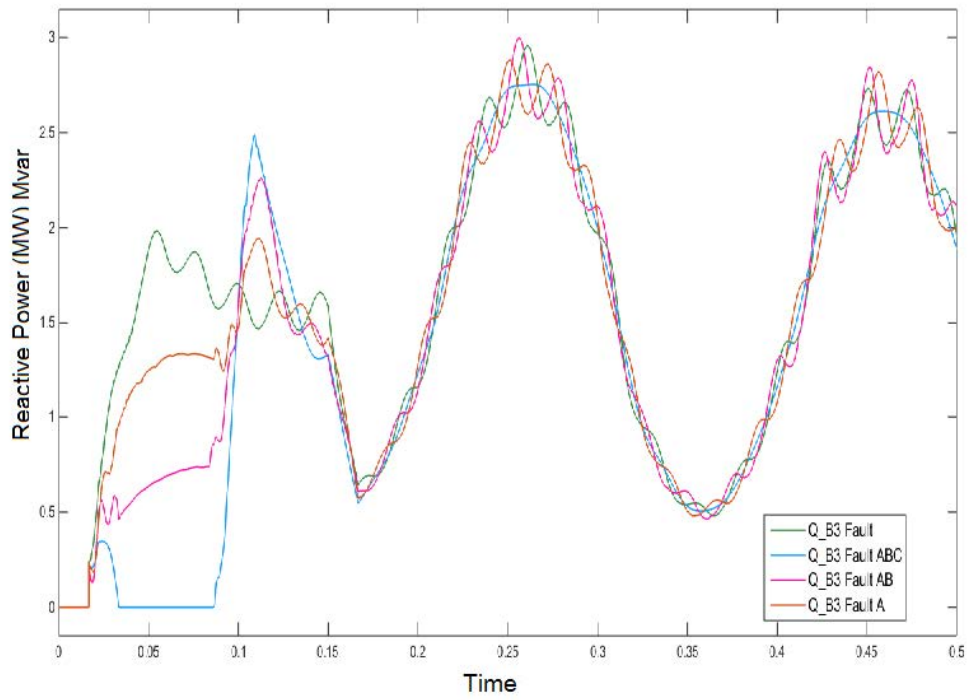


Figure 6.4: Reactive power at bus B3 with DSTATCOM controller set to Q regulation

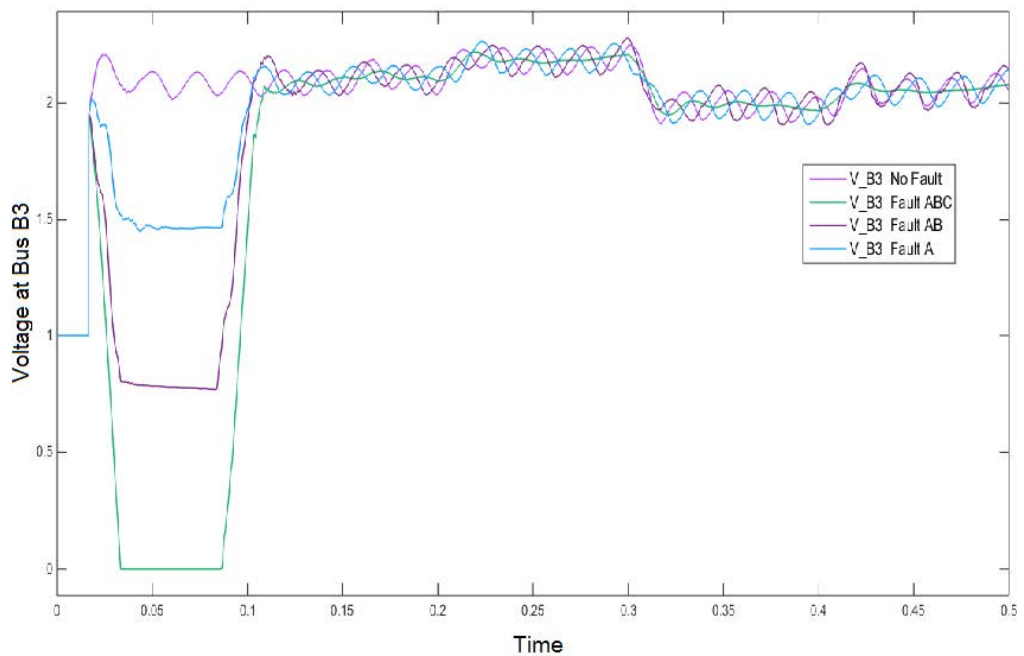


Figure 6.5: Voltage at bus B3 with DSTATCOM controller set to Q regulation

6.3 DSTATCOM with a three phase breaker

In this section the D-STATCOM connected to distribution network in parallel is again simulated. A 25 kV distribution network with DSTATCOM connected in parallel and variable load as shown in Figure 6.6. A variable load is used with the current amplitude *RMS* value at 3000 and the power factor at 0.9 which is modulated with an amplitude *RMS* value of 2000 at 5Hz frequency with modulation time $T_{on} = 0.15$ and $T_{off} = 1$.

The results of Figure 6.6 are then compared to the distribution network connected to load 3MW and 0.2 Mvar with a three phase breaker circuit switching at 1/60 and 5/60 seconds as shown in Figure 6.7.

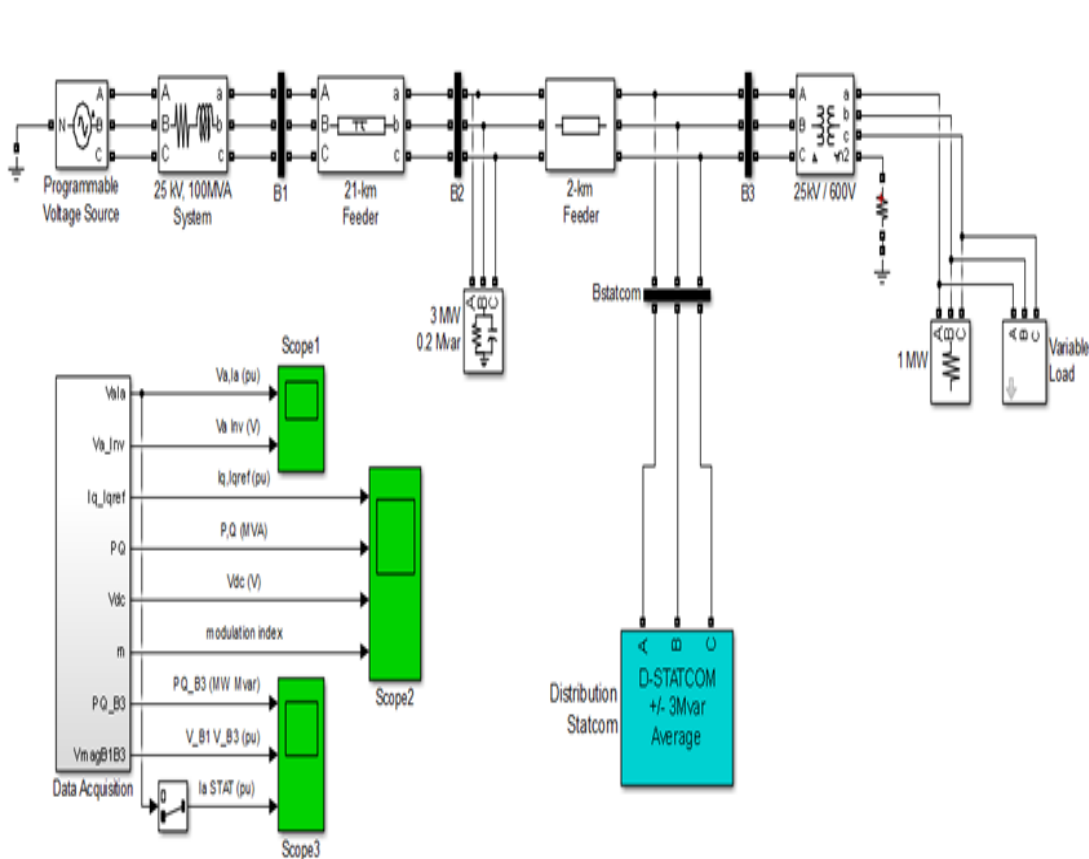
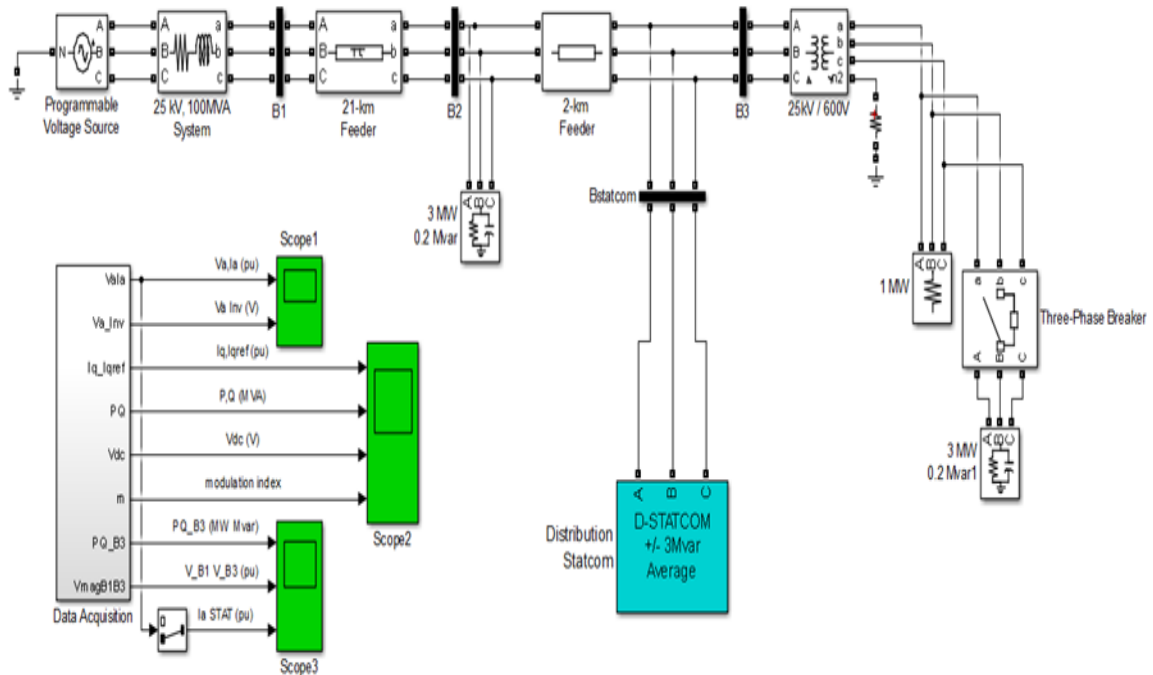


Figure 6.6: A 25kV distribution network with D-STATCOM connected in parallel with variable load

Adapted from (Qaraca Oğlu & Mehmed Oğlu, 2011)



**Figure 6.7: A 25kV distribution network with D-SATCOM connected in parallel with a three phase breaker circuit before load
Adapted from (G.Gupta, 2017)**

The simulated output of these circuits are compared in Figure 6.8 to Figure 6.12. Initially, the D-STATCOM is inactive and its current, denoted by $I_{STATCOM}$ in Figure 6.8, is almost constant for both networks before increasing after $t=0.2s$. The D-STATCOM current for the circuit in Figure 6.9 appears higher for most of the time as the higher load of 3MW and 0.2Mvar switches due to the breaker circuit. This is due to the fact that the D-STATCOM absorbs and provides reactive power to the network. The voltage at bus B1 is compared in Figure 6.9. The voltage for both the networks follow the same pattern, however in Figure 6.9, the network is slightly higher for the time values of $t=0.2s$ and $t=0.34s$. The load is connected at bus B3 introduces active and reactive power variations which are compensated by DSTATCOM connected at bus B3 in parallel. The comparison of voltage, active power (P), and reactive power (Q) at bus B3 for both the distribution network are shown in Figure 6.10, Figure 6.11 and Figure 6.12 respectively. For the distribution network in which variable load presence lasts for a small duration, the circuit has the capacity to compensate due to the presence of the D-STATCOM. However, for the distribution network with a three phase breaker, the compensation provided by D-STATCOM is not enough to compensate the active and the reactive power.

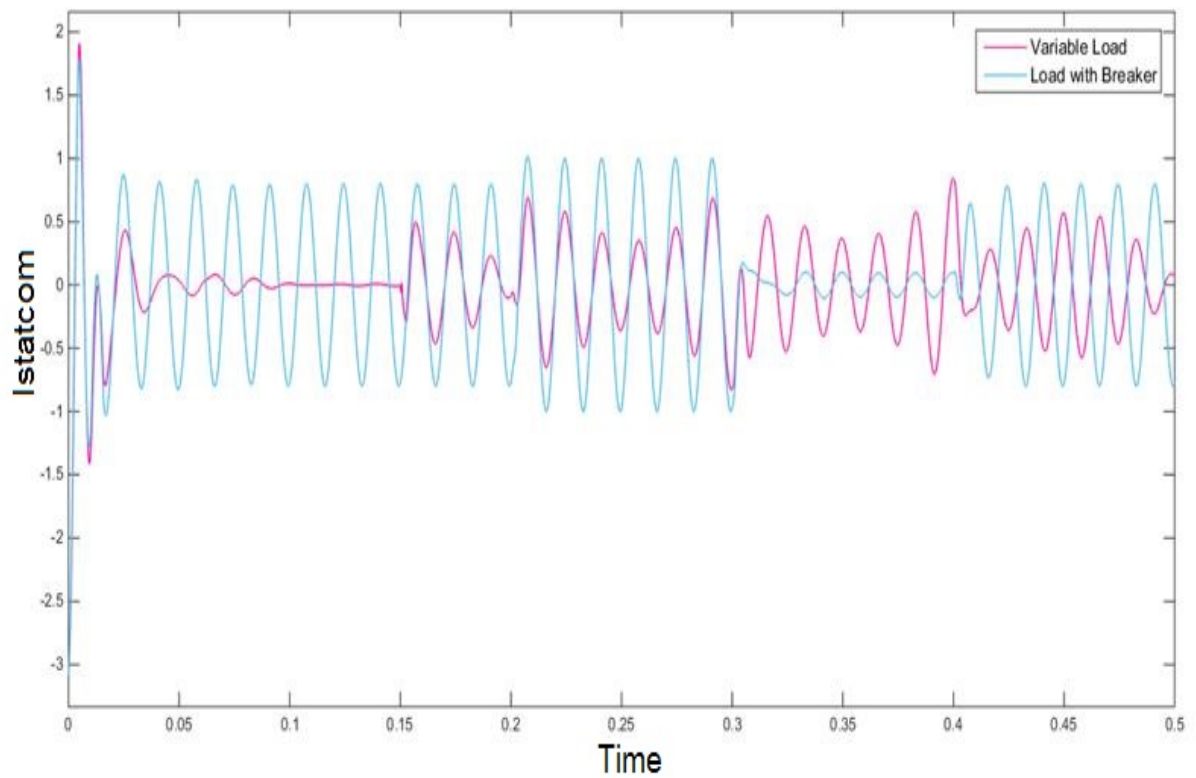


Figure 6.8: DSTATCOM current in circuit with variable load at bus B3 and an extra load with three phase breaker

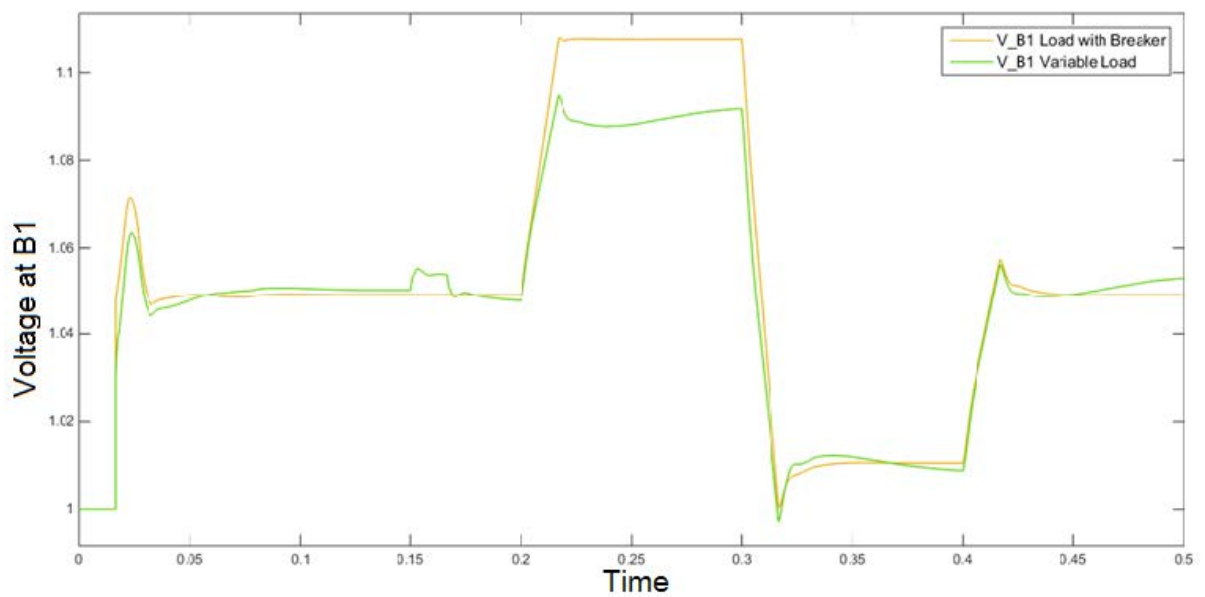


Figure 6.9: Voltage at bus B1 in circuit with variable load at bus B3 and an extra load with three phase breaker

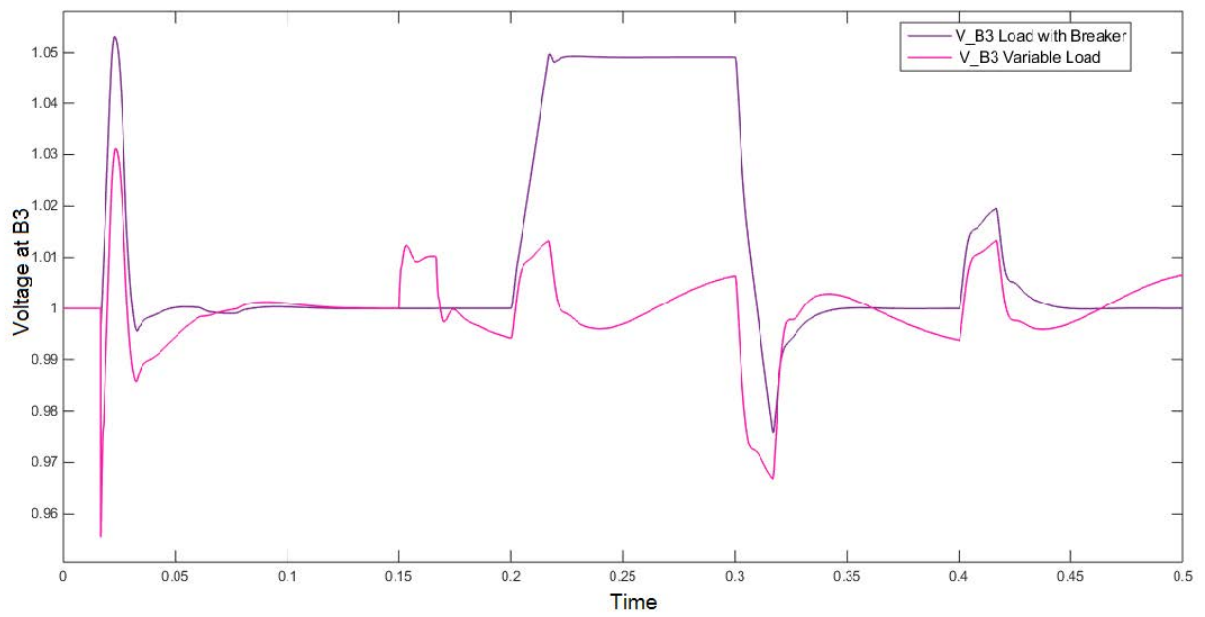


Figure 6.10: Voltage at bus B1 in circuit with variable load at bus B3 and an extra load with three phase breaker

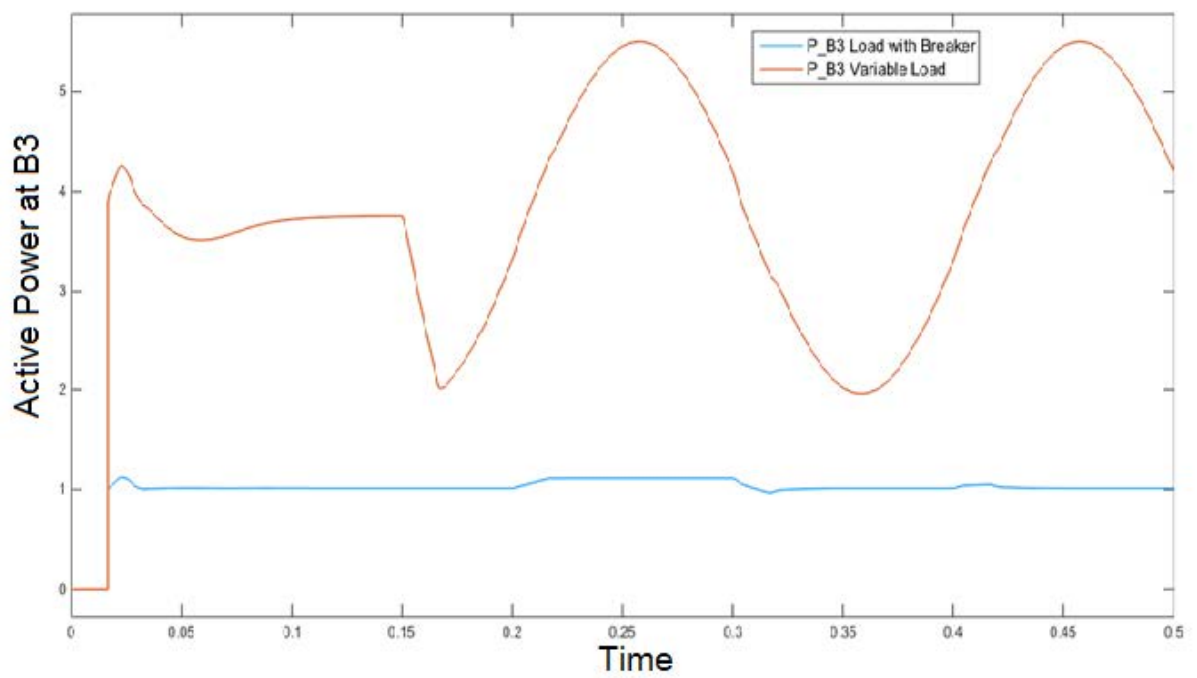


Figure 6.11: Active power in circuit with variable load at bus B3 and an extra load with three phase breaker

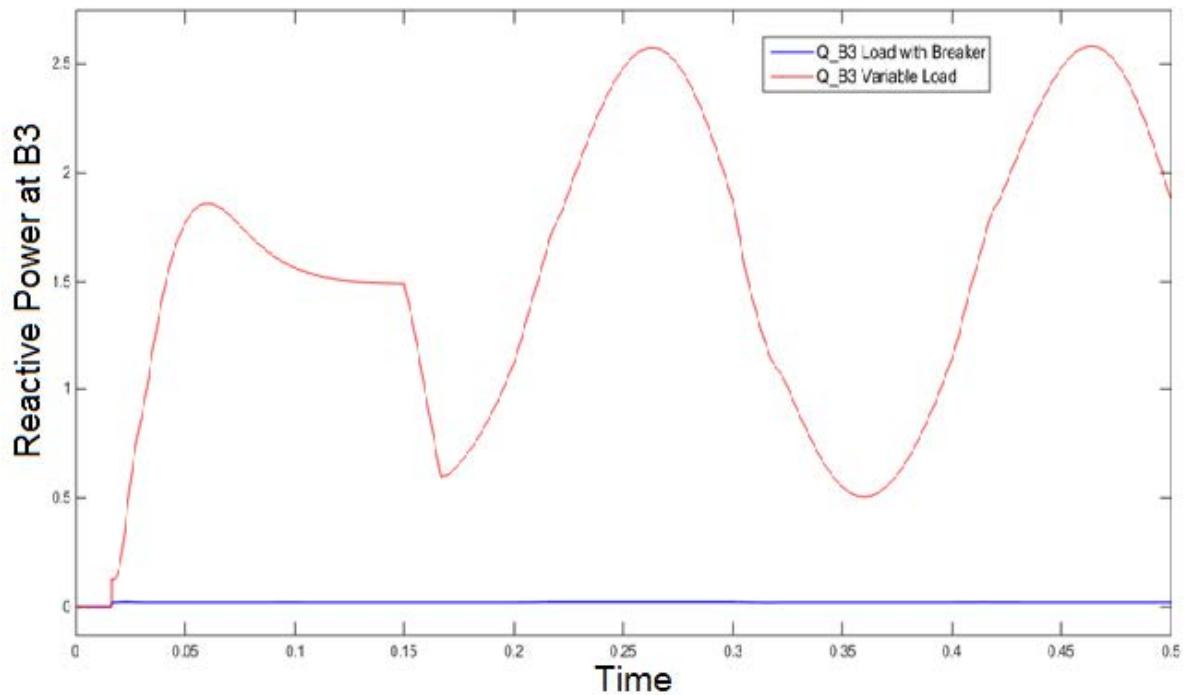


Figure 6.12: Reactive power in circuit with variable load at bus B3 and an extra load with three phase breaker

6.4 STATCOM Phasor model

In this section, a three level PWM STATCOM phasor model dynamic response is verified and STATCOM performance is compared with an SVC in the presence of faults. The power grid shown in Figure 6.13 consists of 3000 MVA and 2500 MVA i.e. two 500kV equivalents connected by a 600 km transmission line. In the absence of the STATCOM device, 930MW of power flows from bus B1 to B3. The STATCOM scope and signals are shown in Appendix A Figure E.

The STATCOM with a ± 100 MVA rating is placed closed to the bus B2. A three-level PWM STATCOM phasor model is used for the simulations. The STATCOM has a 40 kV DC link nominal voltage and an equivalent capacitance of 375 μF . For the AC, the total equivalent impedance of STATCOM is 0.22 per unit (p.u) on 100 MVA.

6.4.1 Dynamic response

In this subsection, the dynamic response is compared with the disabled fault breaker which is shown in Figure 6.13. The STATCOM controller is set to voltage regulation. Reference voltage is controlled externally and is denoted as V_{ref} .

The droop parameter of the STATCOM is set to 0.03. The V_{ac} regulator shows a proportional gain of $K_p = 5$ and an integral gain of $K_i = 1000$. A step function block is used to provide step input to reference voltage of STATCOM V_{ref} . This block brings variation in V_{ref} with respect to time starting from $V_{ref} = 1$ p.u.; at $t = 0.2$ s it reduces to 0.97 p.u.; at $t = 0.4$ s it increases to 1.03 p.u., and at $t = 0.6$ s, it attains its initial value of 1 p.u.

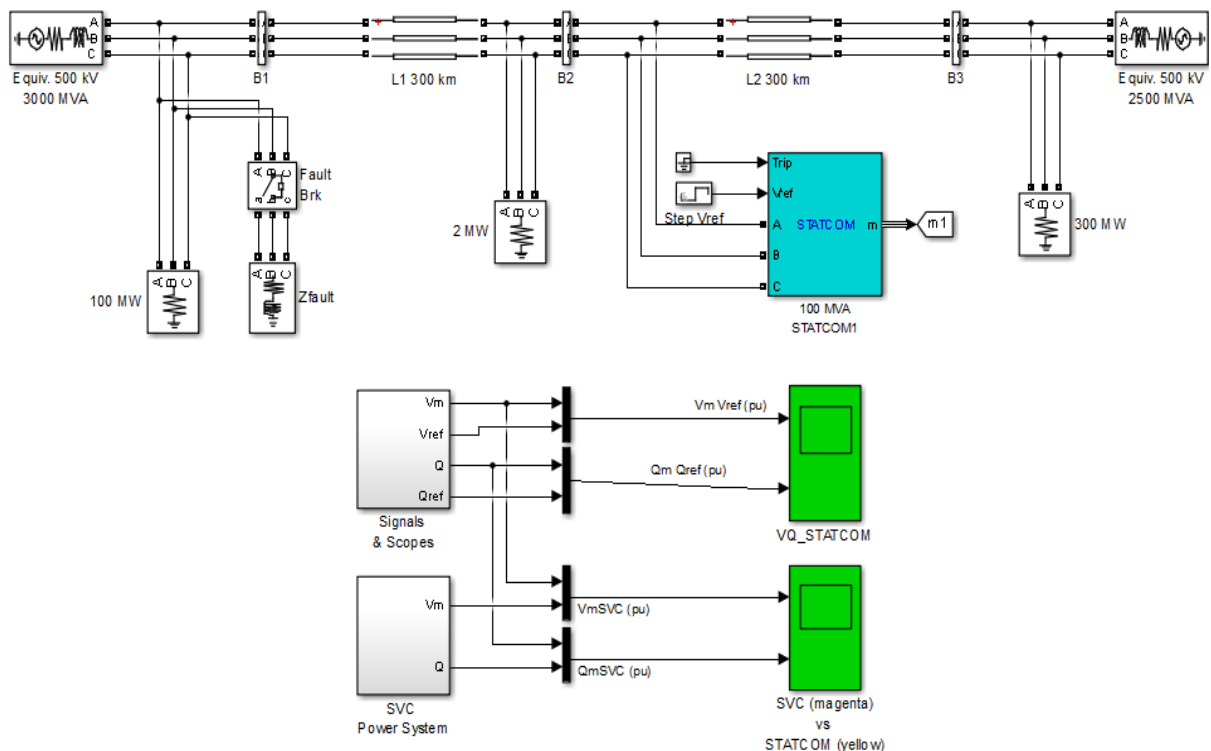


Figure 6.13: Power grid for STATCOM phasor model

Adapted from (Hannan et al., 2008)

The graph in Figure 6.14 shows the variation of measured voltage denoted by V_{meas} with respect to V_{ref} . From this, it can be easily concluded that the STATCOM is not a perfect voltage regulator. V_{meas} does not smoothly follow V_{ref} which is mainly due to the regulator drop of 0.03 pu. The regulator droop is used for regulating the slope. This droop extends the linear operating range of the STATCOM with respect to a maximum allowable capacitive or inductive range. It also ensures automatic load-sharing with other voltage compensators present in the grid.

If the simulation is rerun with the droop parameter set to 0, the V_{meas} will exactly follow V_{ref} . The graph in Figure 6.15 shows the variation of the measured reactive power denoted by Q_{meas} with respect to V_{ref} . Q_{ref} is constant with respect to time and Q_{meas} shows the variation of reactive power with respect to time.

6.4.2 Fault condition and performance comparison of STATCOM with SVC

In this subsection, the STATCOM model with a fault breaker circuit enabled as shown in Figure 6.13 is compared with an SVC model of the rating $\pm 100\text{MVA}$, connected to the same power grid shown in Figure 6.16.

A fault is introduced in both the systems remotely by using a fault breaker with impedance in series. The value of fault impedance is selected so that it introduces a 30% voltage sag. The step function which provides the step input is disabled. The faults are introduced to operate at $t=0.2\text{s}$ and remain for 10 cycles.

The measured voltage and reactive power generated or absorbed by a STATCOM and SVC are compared in Figure 6.17 and Figure 6.18. It can be concluded that the maximum capacitive power generated by an SVC is proportional to the square of the system voltage (constant susceptance) while the maximum capacitive power generated by a STATCOM decreases linearly with voltage decrease (constant current).

This ability to provide more capacitive power during a fault is one important advantage of a STATCOM over the SVC. In addition, the STATCOM will normally exhibit a faster response than the SVC because with the voltage-sourced converter, the STATCOM has no delay associated with the thyristor firing.

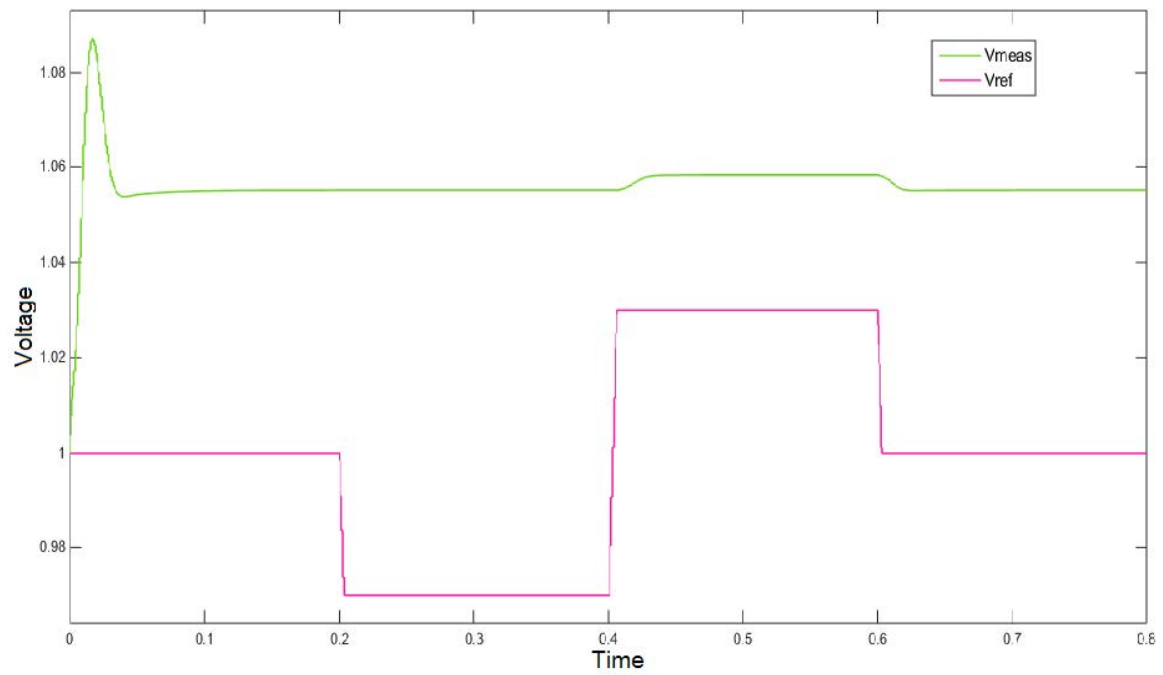


Figure 6.14: Dynamic response measured voltage and reference voltage

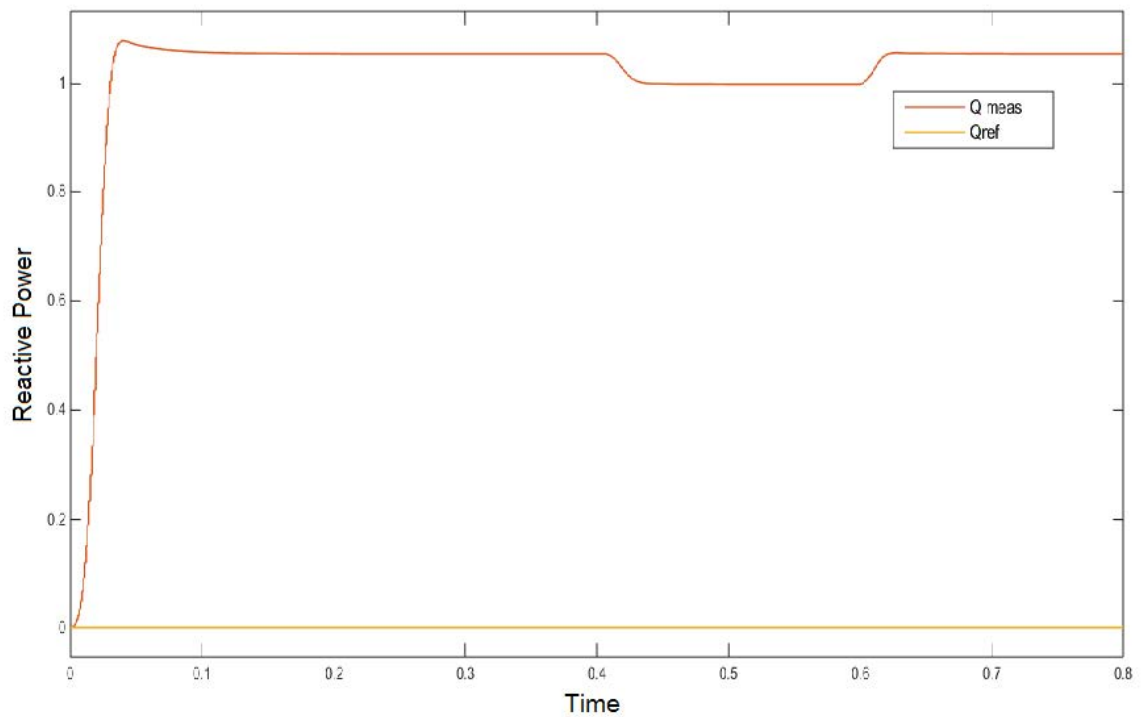


Figure 6.15: Dynamic response: measured reactive power and reference power

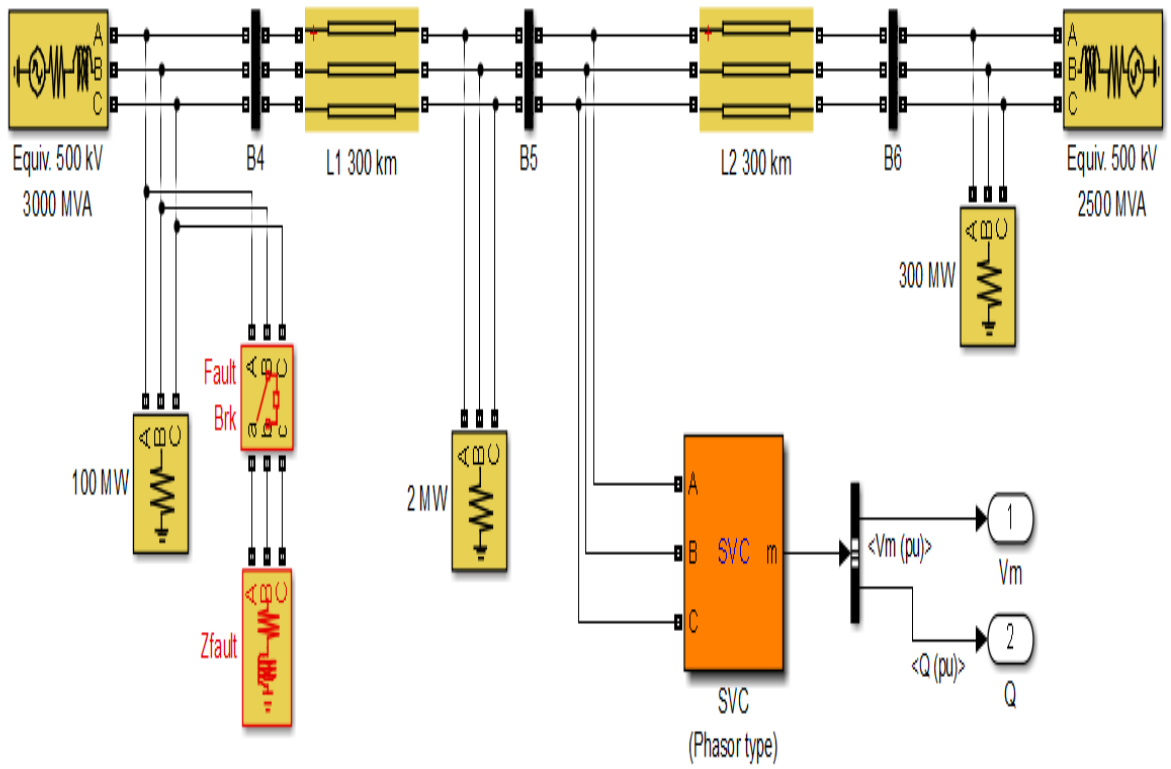


Figure 6.16: SVC Power System with Faults

Adapted from (Hannan et al., 2008)

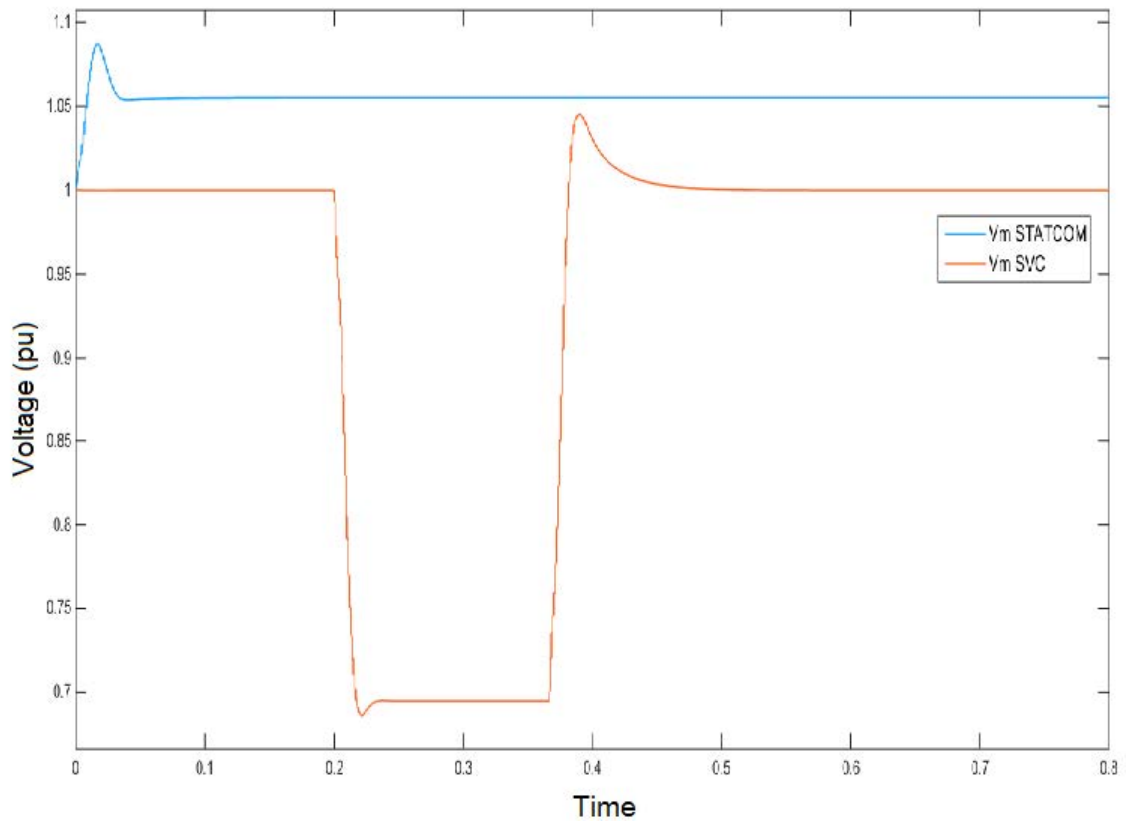


Figure 6.17: Measured voltage v_m on a STATCOM and SVC fault

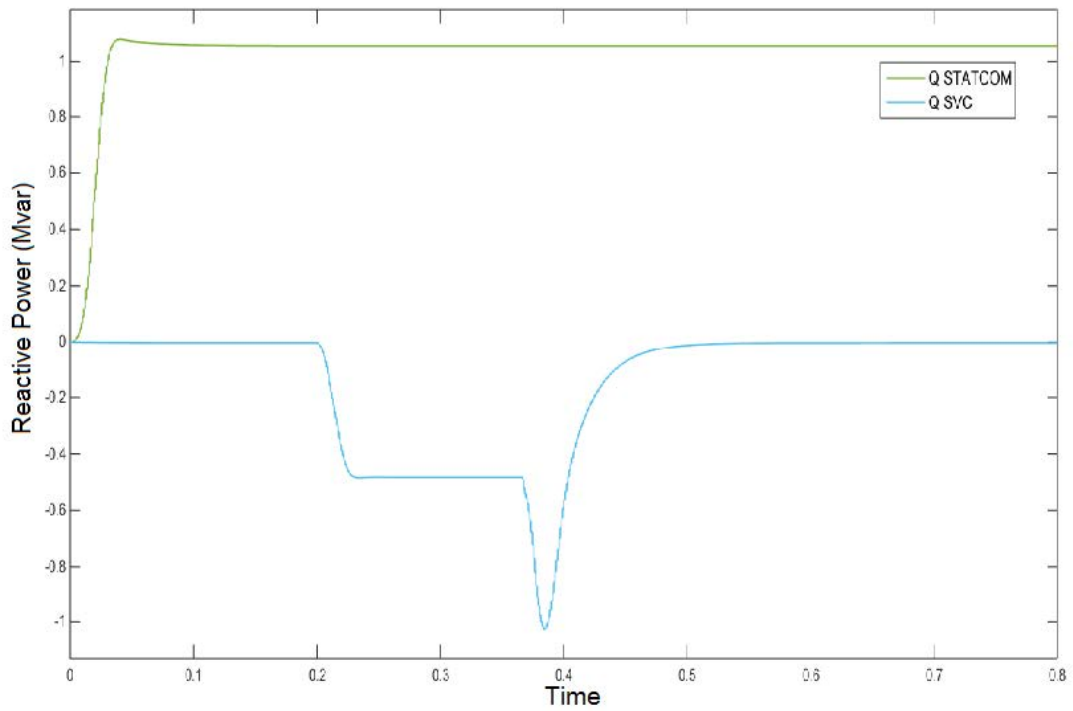


Figure 6.18: Measured reactive power on a STATCOM and SVC fault

6.5 Power grid simulation model description

In this section, the reasons and procedure of voltage fluctuation are analysed with the help of a distribution grid. The main model of the power grid simulated power system has a single feeder and four distribution points (DPs) namely DP2, DP3, DP4, and DP5 located at equal distances along the grid. Furthermore, one more DP is also located close to feeder DP1 and is termed as the point of common coupling (PCC). The sixth distribution point, DP6, is used as an option for the future and is located at the end of the line. The single line diagram of the simulated model is shown in Figure 6.19.

The STATCOM used for voltage control can be connected close to PCC at the beginning of the line or in series at the end of the line. A STATCOM can be connected in parallel also, between DPs, which was already analysed in previous sections. The main function of a STATCOM is to control voltage of the DP where it is connected. The STATCOM when connected to PCC, controls the voltage there at PCC i.e. DP2. When connected in series at the end of the line, it controls voltage of DP5, also known as the local voltage.

DP2 is the distribution point which is connected to heavy loads and represents an industrial steel plant with huge hammers and motors. The load in DP1 is considered to be variable as half of it is always connected and another half switches on and off. This is also equipped with power factor correction and filtering in harmonics.

The simulated model is compared for three distribution transformer ratings: 100, 200 and 315 kVA shown in Figure 6.19. The inductance(L) and resistance(R) for these ratings are $L_{100kVA} = 250 \mu H$ and $R_{100kVA} = 16m\Omega$, $L_{200kVA} = 125 \mu H$ and $R_{200kVA} = 8m\Omega$, $L_{315kVA} = 80 \mu H$ and $R_{315kVA} = 5.1m\Omega$.

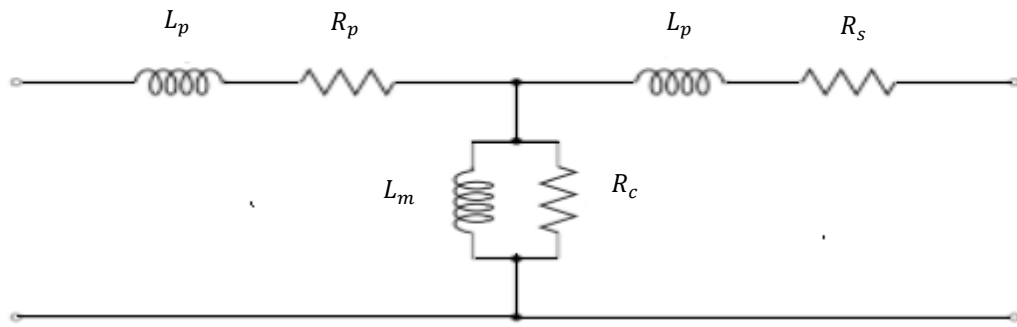


Figure 6.19: Inductance and resistance on distribution line

Adapted from (Hingorani, N.G. & Gyugyi, L. 2000.)

All the DPs in the simulated model has three switched loads, which switches independently, and are inductive, capacitive, or a combination of both. The line impedance between DPs is considered by increasing impedance value. The impedance is based on (Vahedy, 2006) $R = 0.43m\Omega/m$ and $L = 0.414 \mu H/m$.

Initially, the STATCOM is not used for voltage control and the gain of the controller for AC voltage is assumed to be around 3, which is equivalent to 1mH of supply reactance. The controller time constant $\tau = 0.05s$ is considered for the simulated model.

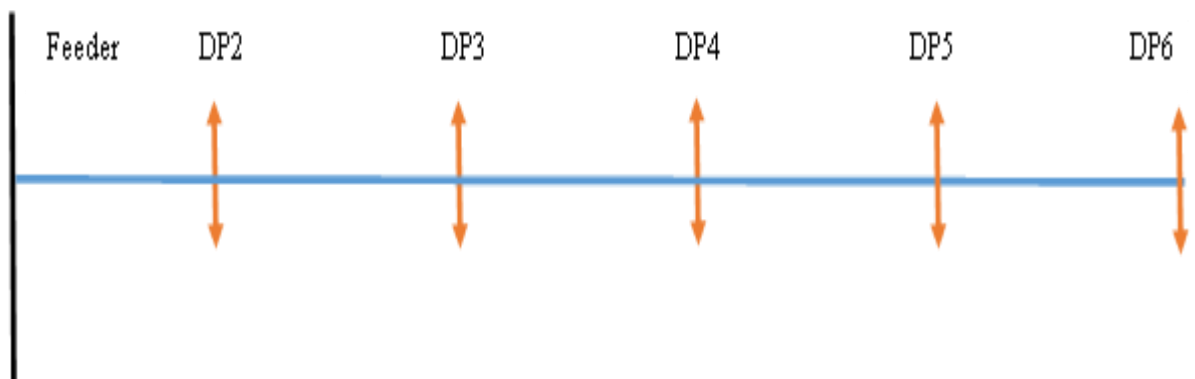


Figure 6.20: Simulated power distribution grid

6.5.1 Single source system

The simulations are initially done for a linear system with single source. The aim of these simulations is to check and demonstrate the accuracy of the proposed control strategy and to find out the correct sizing of a STATCOM with respect to the rating of the power grid. A single STATCOM is used for voltage regulation connected at a fixed position along the line with droop control. The simulations are also done by placing a STATCOM at different places along the line, such as at the PCC or at the end of the line.

Table 6.1: Maximum load of the system associated with each distribution point for 100, 200 and 315 systems in kVA

100 kVA		
Distribution Point	Active Power (kW)	Reactive Power (kVar)
1	23.6	11.4
2	14.2	6.85
3	14.2	6.85
4	14.2	6.85
5	14.2	6.85
Total	80.4	38.8
200 kVA		
Distribution Point	Active Power (kW)	Reactive Power (kVar)
1	47.2	22.8
2	28.4	13.7
3	28.4	13.7
4	28.4	13.7
5	28.4	13.7
Total	160.8	77.6
315 kVA		
Distribution Point	Active Power (kW)	Reactive Power (kVar)
1	74	35.2
2	44	20.5
3	44	20.5
4	44	20.5
5	44	20.5
Total	255	117.2

6.5.2 STATCOM fixed-positions

A STATCOM is placed at PCC first and then connected in DP5 for comparing the performance. The active power and reactive power of 100 kVA, 200 kVA and 315 kVA system is given Table 6.1. The load values are taken in a way to keep the power factor (Φ) of each DP equal to 0.9, while keeping the total apparent power equal to 90% with respect to the power system rating.

In Figure 6.21, the voltage is measured along the line from PCC in a step of 10m and maximum distance 90m, for 100, 200 and 315 kVA systems without a STATCOM, with a STATCOM at PCC, and with a STATCOM at the last DP. While doing these simulations, STATCOM current controllers used are without any limits. As a result, the STATCOM is always working as a voltage regulator. It is clearly evident from the output that with the use of a STATCOM for voltage support, the overall voltage is not affected. Instead, the system voltage increases regardless of the STATCOMs position along the line.

In Figure 6.22, the reactive current required at DP1 is compared with the reactive current at DP5 to regulate the voltage for a 100 kVA system. It is evident that more reactive power is required at DP5 for voltage regulation as compared to the voltage at DP1. The reactive current required is almost equal to 1p.u. The required reactive current at DP1 is around 0.7 p.u for the case of 200 and 315 kVA systems. However, the required reactive current at DP5 is more than the system rated current.

The results in Figure 6.23 shows the reactance, estimated and calculated with the ideal values for 100, 200 and 315 kVA systems. The calculated reactance is close to the ideal values in a band of frequencies.

The reactive current injected by the STATCOM for 100, 200 and 315 kVA systems are shown in Figure 6.24, Figure 6.25, and Figure 6.26 respectively. The STATCOM controller is tuned and untuned. The plots show that the settling time of an untuned system varies considerably with the increase in rating. In the case of a tuned controller, the settling time becomes consistent early.

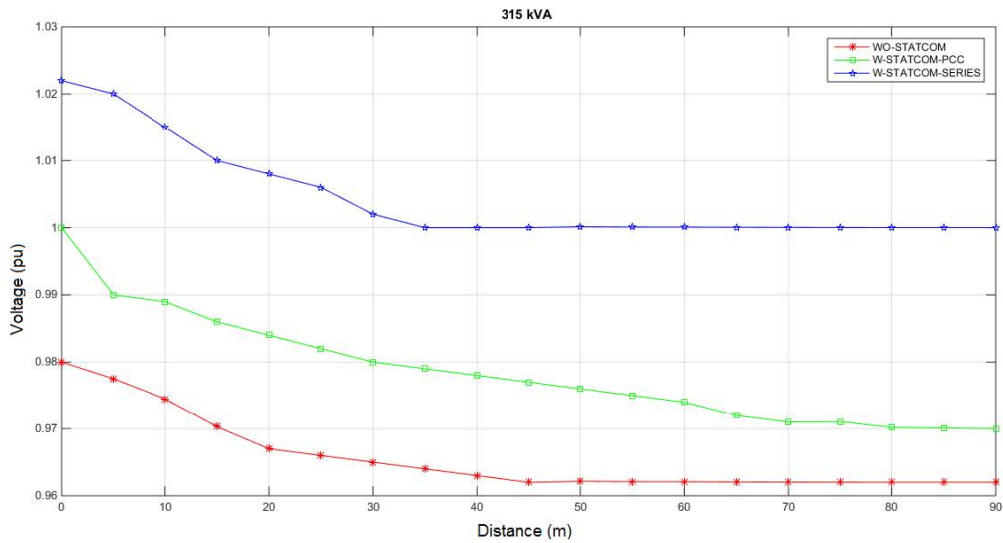
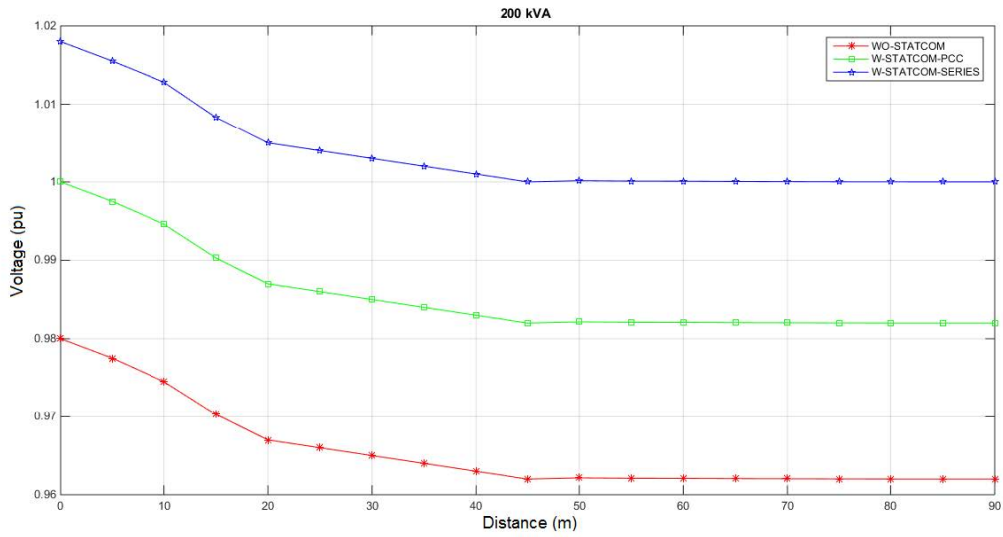
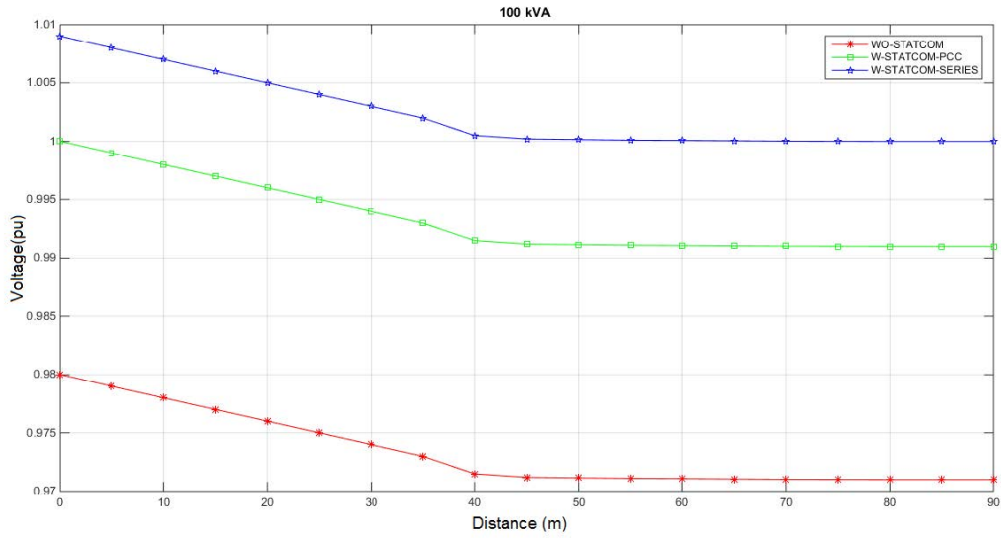


Figure 6.21: Voltage in steps of 10m from the PCC along the distribution line for 100, 200 and 315 kVA systems without a STATCOM, with a STATCOM at PCC, and with a STATCOM at final DP

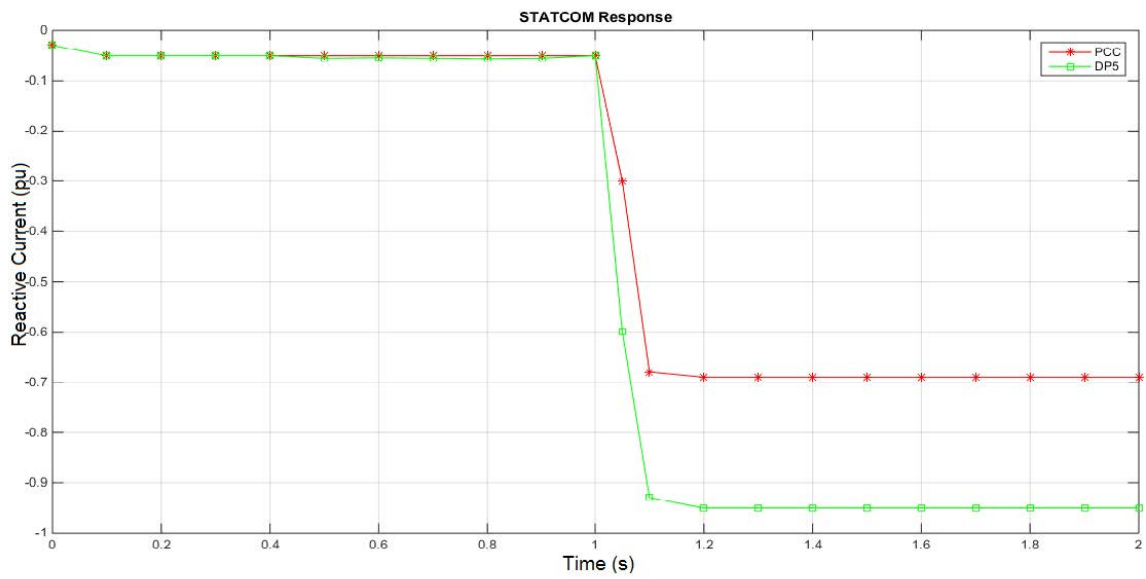


Figure 6.22: A STATCOM response for load change from no load to full load at PCC (DP1) and DP5

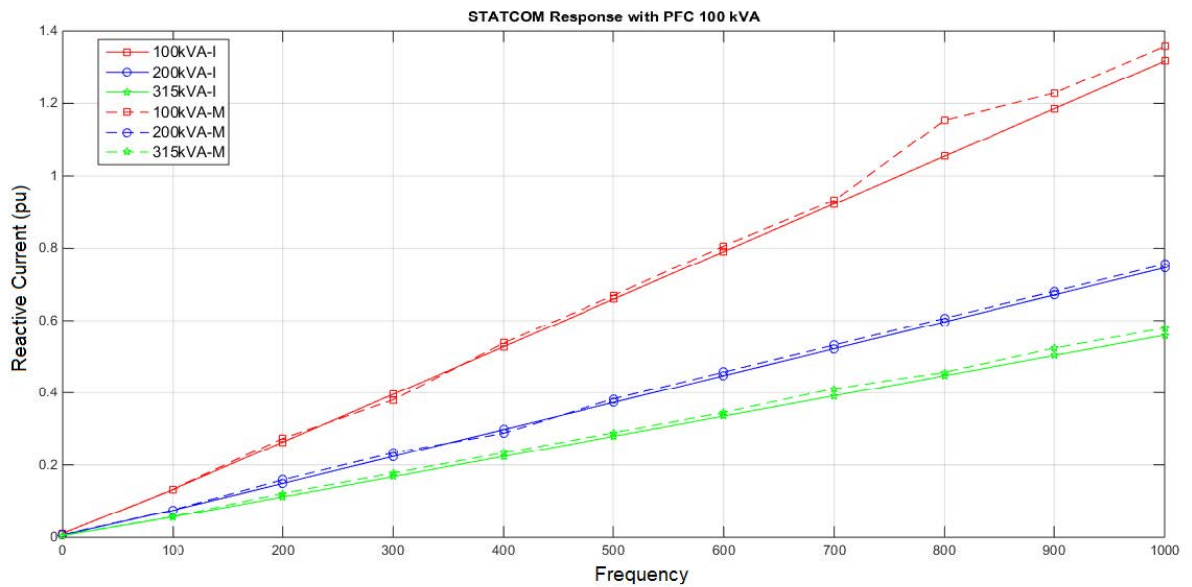


Figure 6.23: Estimated reactance measured for 100, 200 and 315 kVA systems for different frequencies or band of frequencies.

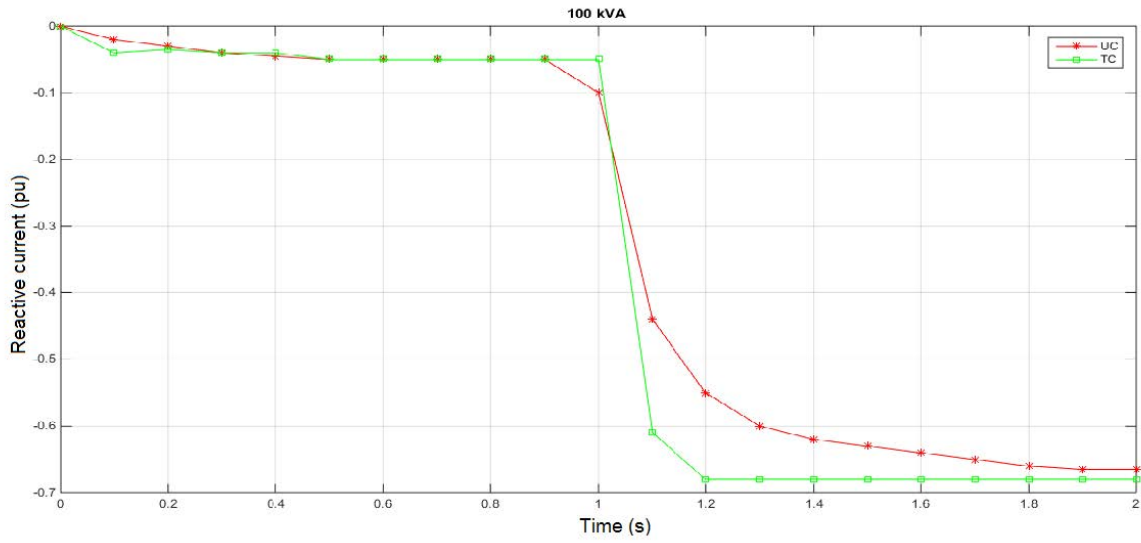


Figure 6.24: Reactive current injected response for both states of a STATCOM controller tuned and untuned for a 100 kVA system

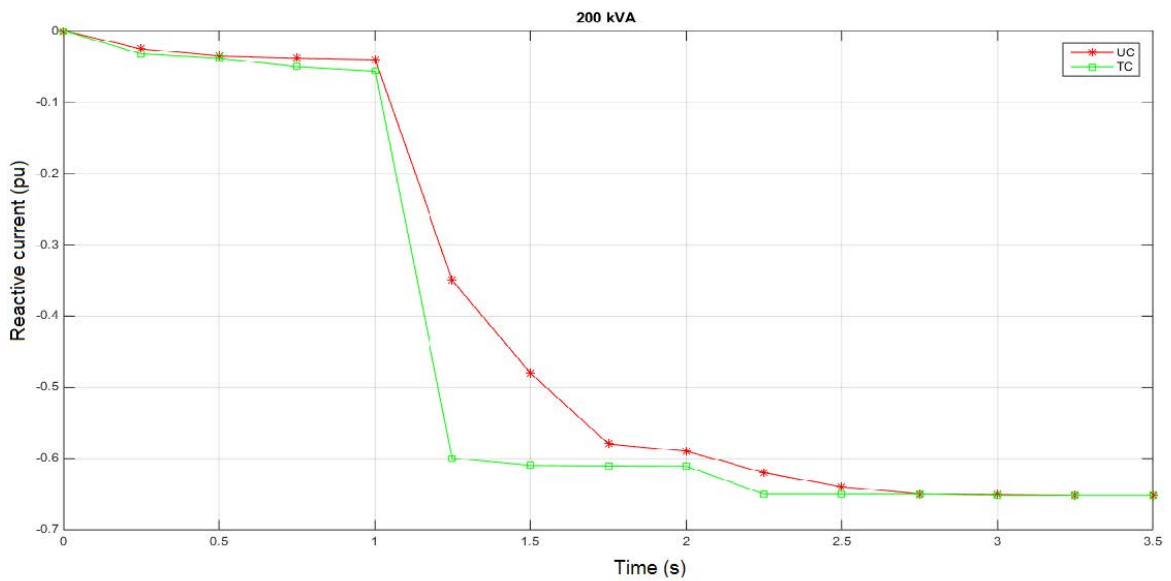


Figure 6.25: Reactive current injected response for both states of a STATCOM controller (tuned and untuned) for a 200 kVA system

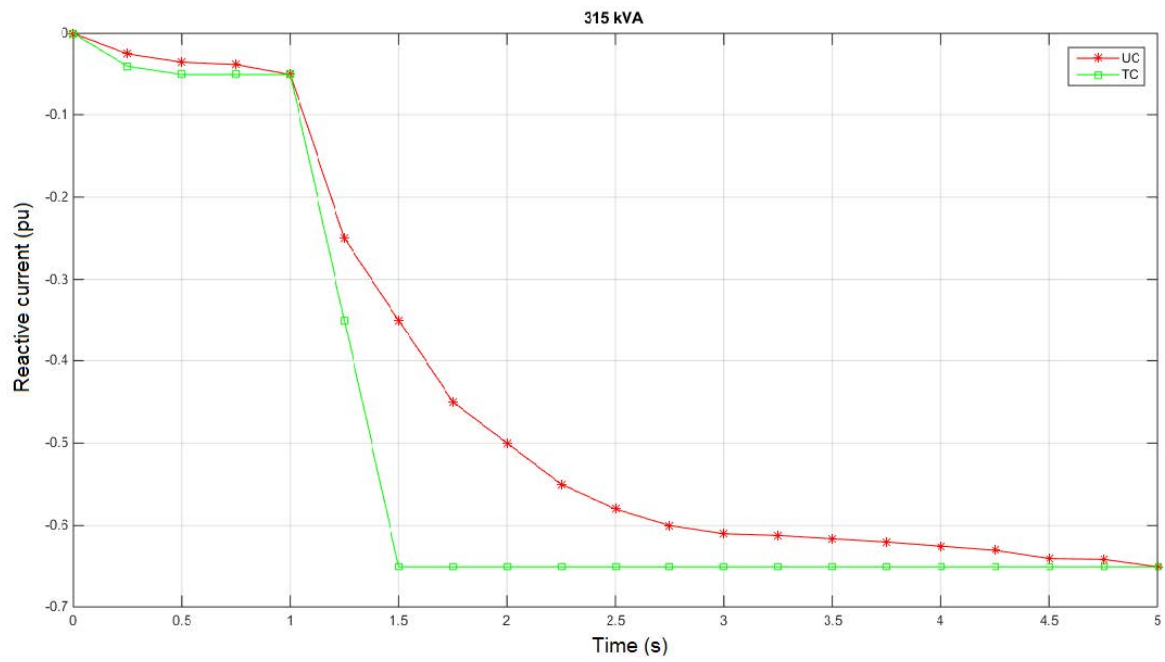


Figure 6.26: Reactive current injected response for both states of a STATCOM controller (tuned and untuned) for a 315 kVA system

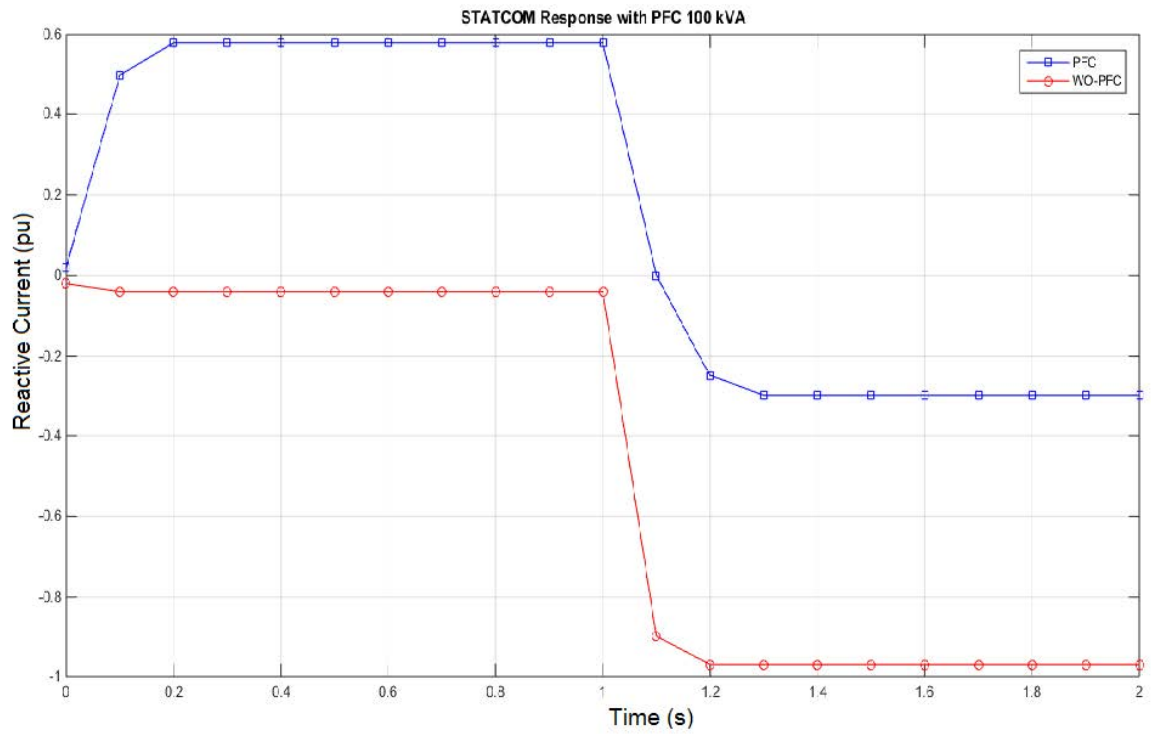


Figure 6.27: Reactive current injected response for both states with power factor correction capacitors (PFC) and without PFCs for a 100kVA system

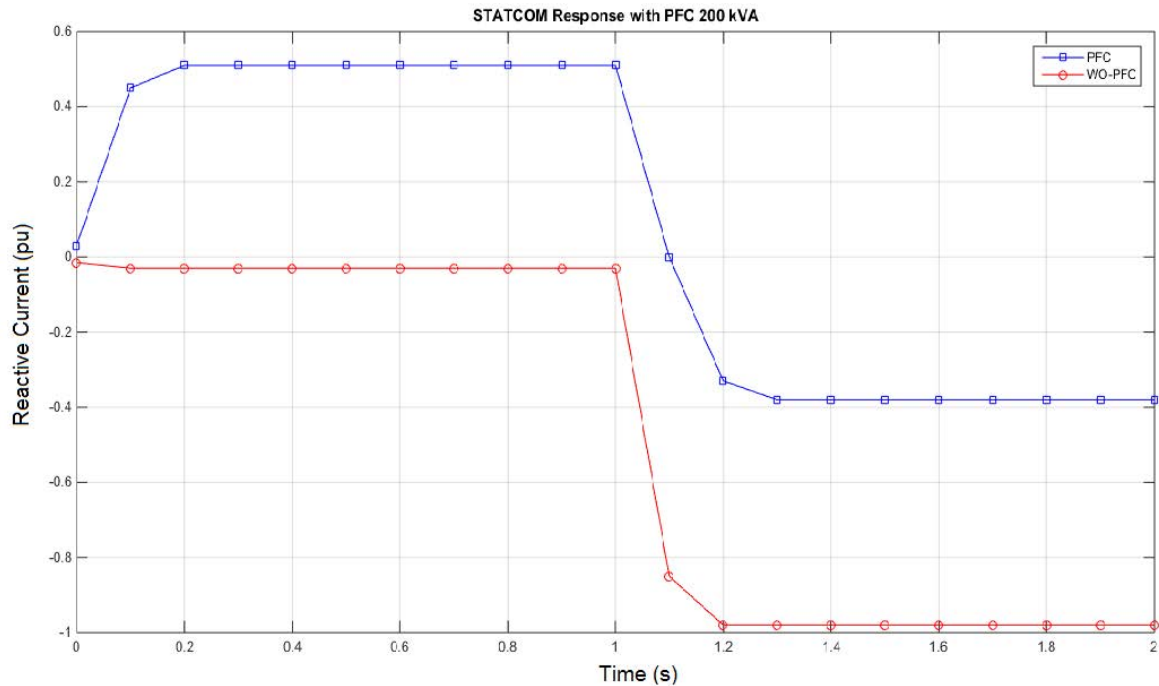


Figure 6.28: Reactive current injected response for both states with power factor correction capacitors (PFC) and without PFCs for a 200 kVA system

It takes 0.2 s for the system to return to steady state when tuned controllers are used; the steady state value being a voltage of 1p.u. This is expected as the time constant of the controller is $\tau = 0.05s$. The DP1 is mostly capacitive for these simulations in order to reduce the required reactive power demand by 75 %.

Simulations are also done with the inclusion of capacitive load at DP1. The power factor (Φ) in each distribution point is adjusted to 0.8 while the apparent power of each distribution point is the same.

The capacitors used in 100, 200, and 315 kVA system are 815 μF , 1620 μF and 2500 μF respectively. The capacitors acts as a reactive power source which leads to the increase in voltage at DP1 and the subsequent reduction on a STATCOM load. The inclusion of power factor correction capacitors (PFCs) leads to varied reactive power demand which is compared in Figure 6.27-6.29. The figures compare the influence of PFC on 100, 200 and 315 kVA systems.

It is evident that a STATCOM induces reactive power for light loads which lowers the voltage, and for high loads it must provide negative reactive or absorb the reactive power.

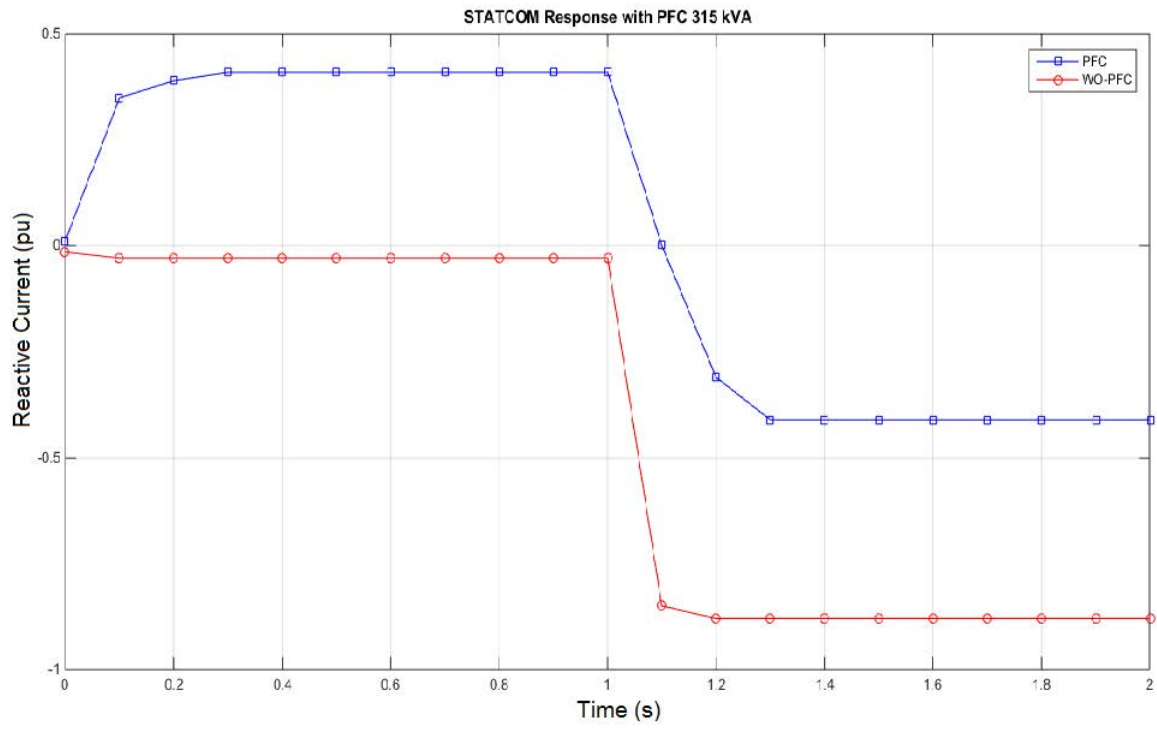


Figure 6.29: Reactive current injected response for both states with power factor correction capacitors (PFC) and without PFCs for a 315 kVA system

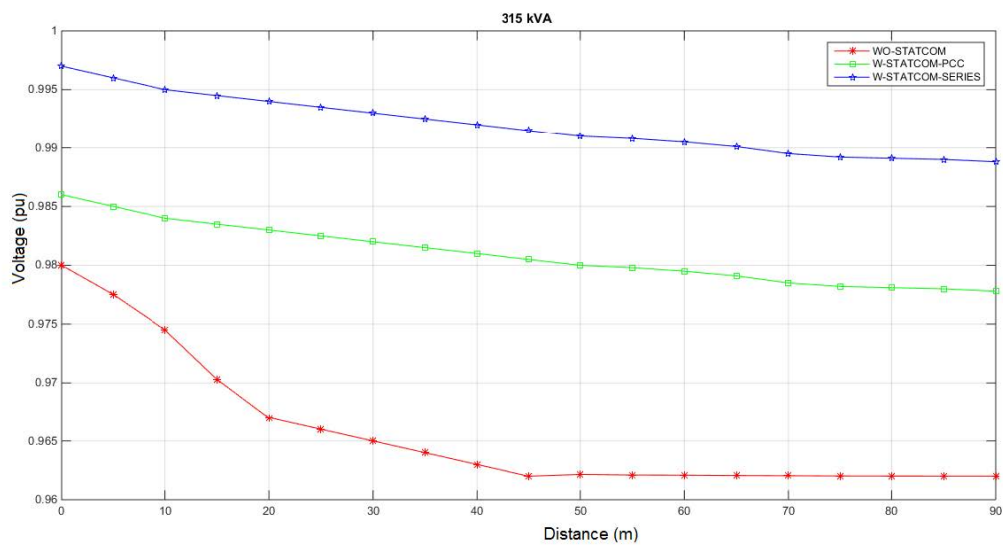
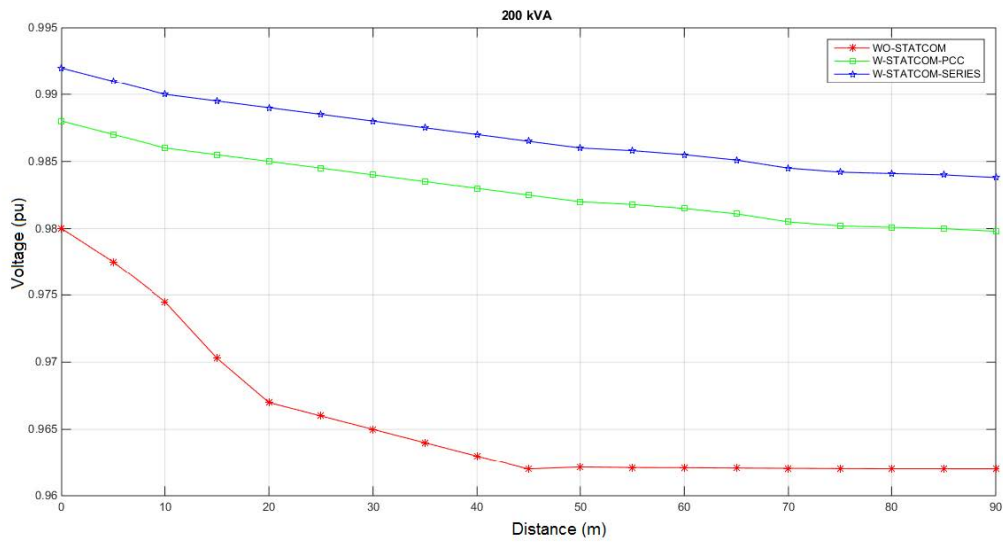
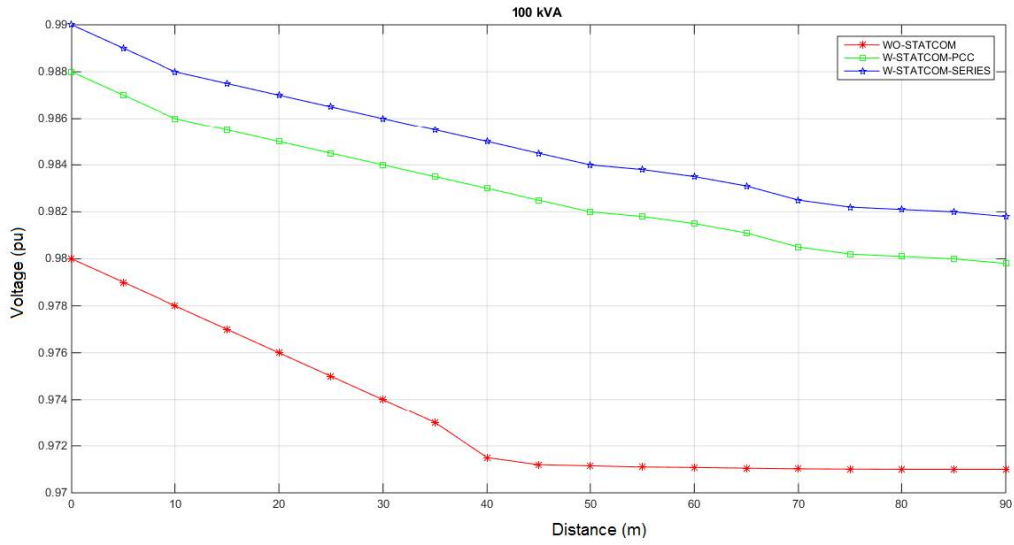


Figure 6.30: Voltage in steps of 10m from the PCC along the distribution line for 100, 200 and 315 kVA systems without a STATCOM, with a STATCOM at PCC and with a STATCOM at the last DP with droop control

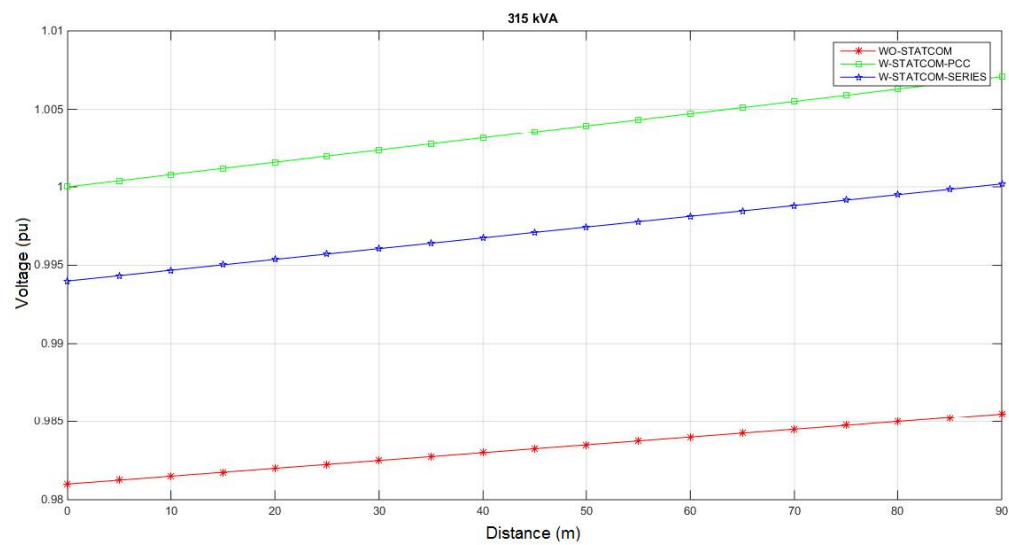
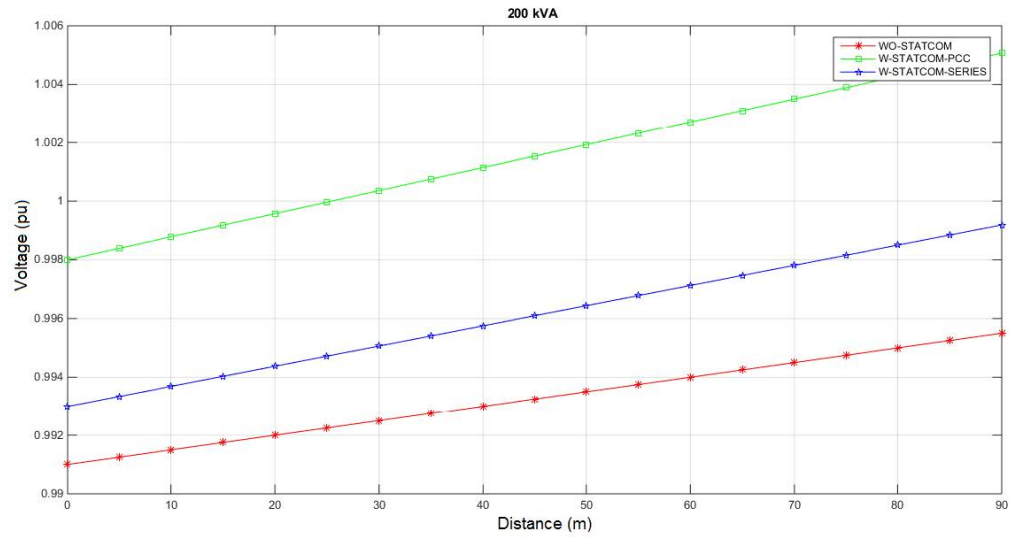
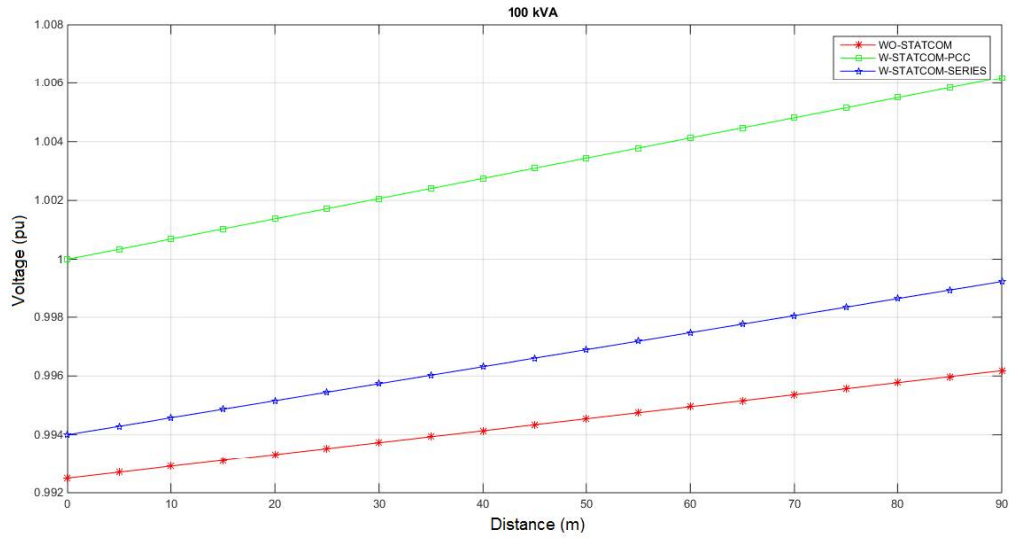


Figure 6.31: Voltage in steps of 10m from the PCC along the distribution line for 100, 200 and 315 kVA systems without a STATCOM, with a STATCOM at PCC and with a STATCOM at the last DP with light loads and a distributed energy source of voltage source type connected at the DP5

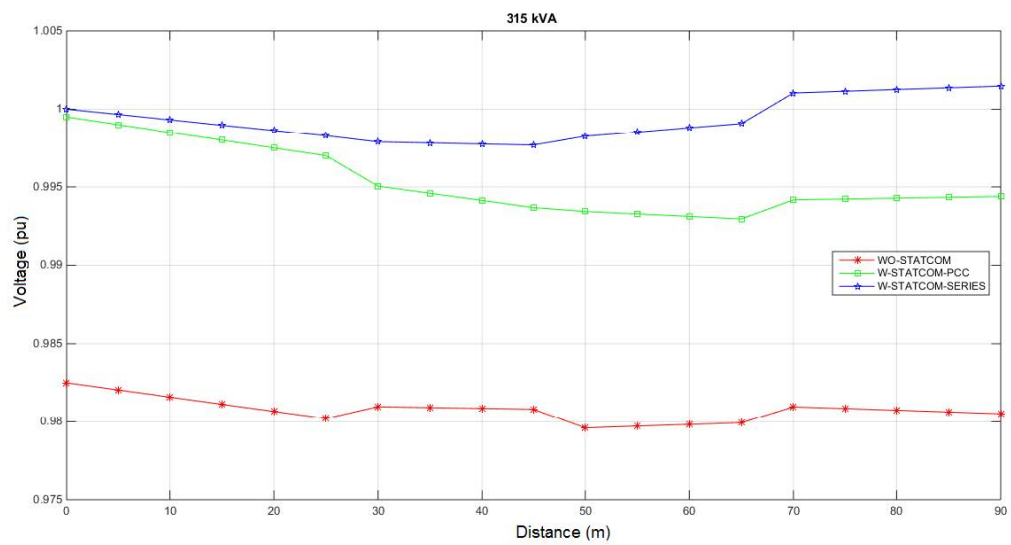
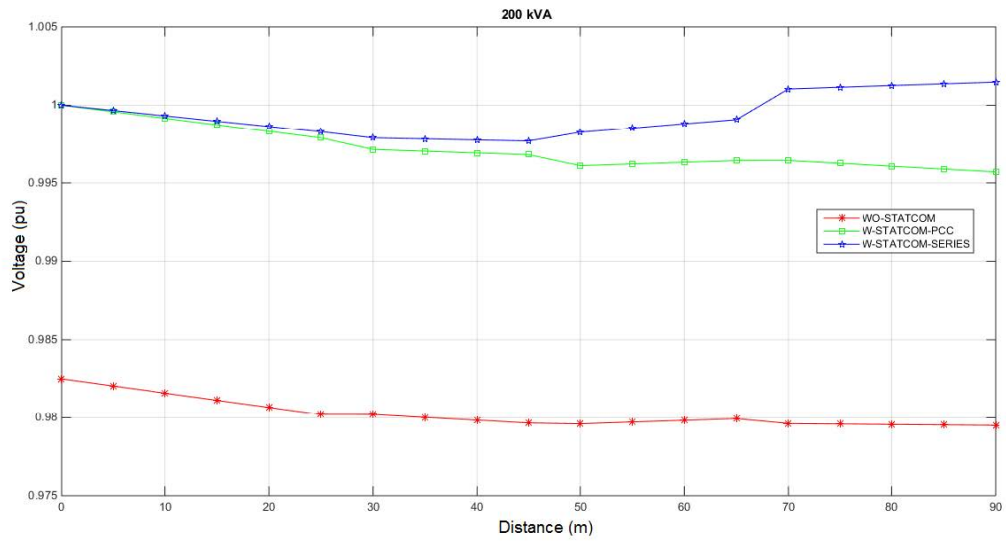
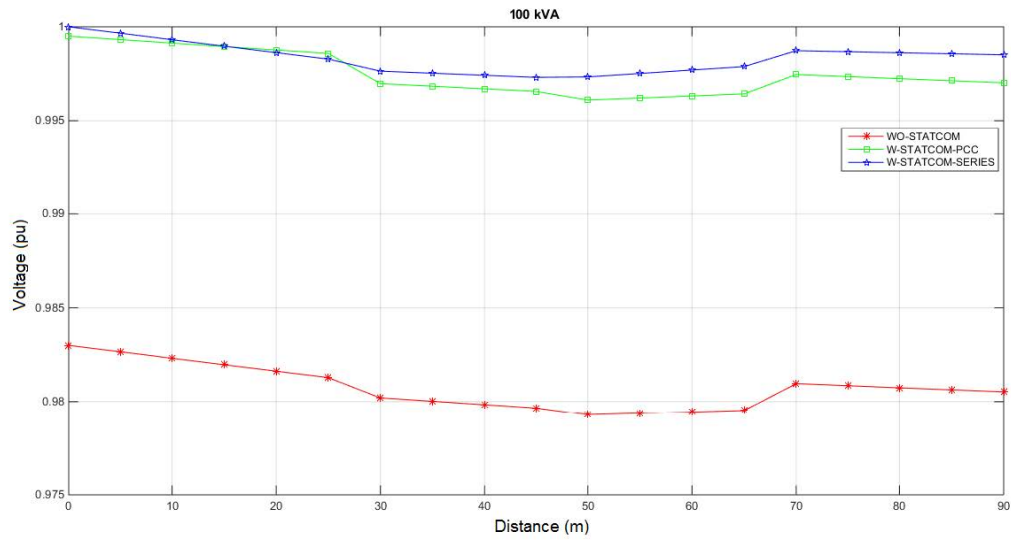


Figure 6.32: Voltage in steps of 10m from the PCC along the distribution line for 100, 200 and 315 kVA systems without a STATCOM, with a STATCOM at PCC, with a STATCOM at the last DP, and a distributed energy source of voltage type for heavy loads

6.5.3 STATCOM droop control

In this section, the same simulations are performed again with the same kVA rating systems. The difference is that the rating of a STATCOM which is 50% of the system rating and droop percentage is set to 5%. The model is simulated for 100, 200, and 315 kVA rating systems with a STATCOM connected at DP1 or DP5.

The voltage in steps of 10m from the PCC along the distribution line for 100, 200 and 315 kVA systems without a STATCOM, with a STATCOM at PCC, and with a STATCOM at the last DP with droop control is shown in Figure 6.30. Although, the STATCOM has a 5% droop control which is not a constant value at all times, the system voltage is within limits and thus the STATCOM injects lesser reactive current compared to when the controller was without droop control. This revealed the advantage of using a STATCOM of reduced rating without affecting power quality (PQ). It also lowers load response time when a step change is applied without affecting controller gains. The STATCOM with droop control takes only 0.1s to reach a steady state of voltage while the controller without droop took 0.2s to reach steady-state.

The STATCOM placed at DP5, when used without droop control, exceeds the reactive current demand higher than the system rating. On the other hand, a STATCOM equipped with droop control reduces the reactive current requirement considerably. The main advantage of this is that the reduced rating leads to reduction in size and cost.

6.5.4 System with distributed energy resources

In this section, the impact of the distributed energy resources (DERs) on the performance of the impedance algorithm and the STATCOM is illustrated. The two DERs used are voltage source and current source which are modelled using two different methods. A voltage source DER is modelled by placing a voltage source in series with inductive filter in output stage. The current source DER is placed in parallel with a LC filter. The voltage or current source are varied for both DERs in such a way that it supplies constant current to the system, which is in phase with the voltage of the grid at the point of connection.

The model is simulated for 100, 200, and 315 kVA systems without a STATCOM, with a STATCOM at DP1 and DP5, and with a DER connected at DP5. The STATCOM regulates the system voltage to a fixed voltage i.e. no droop control is utilized. In Figure 6.31, the loads are light whereas in Figure 6.32, heavy load distribution points are considered for comparison purposes.

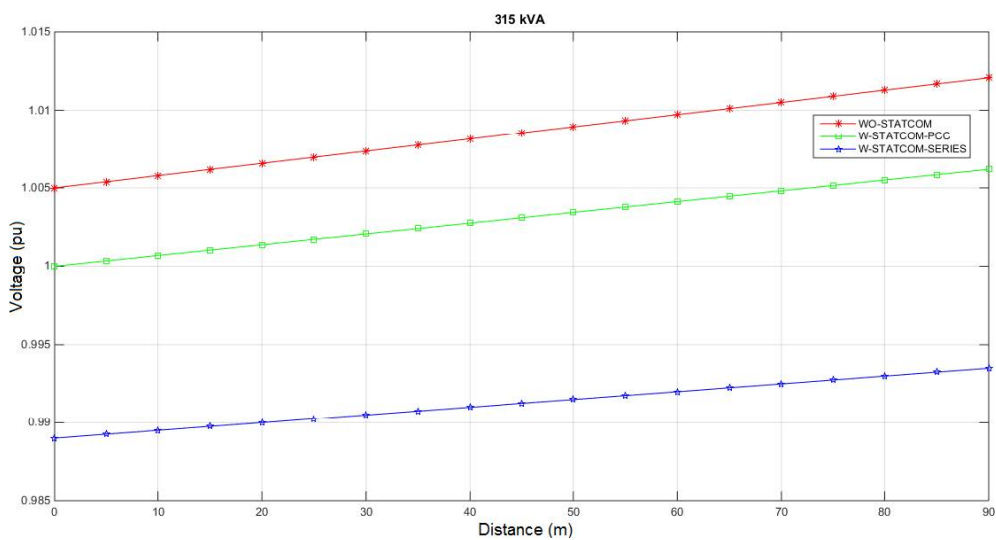
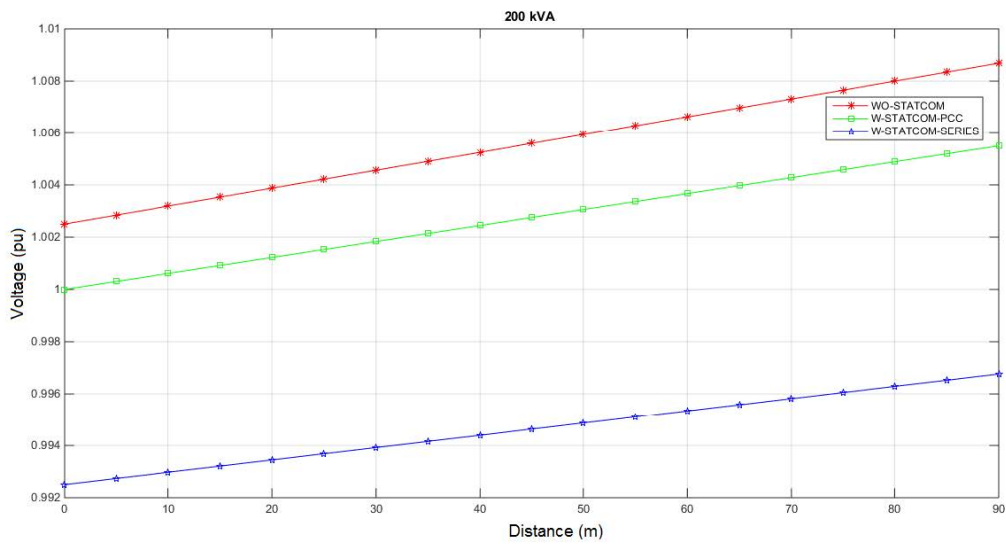
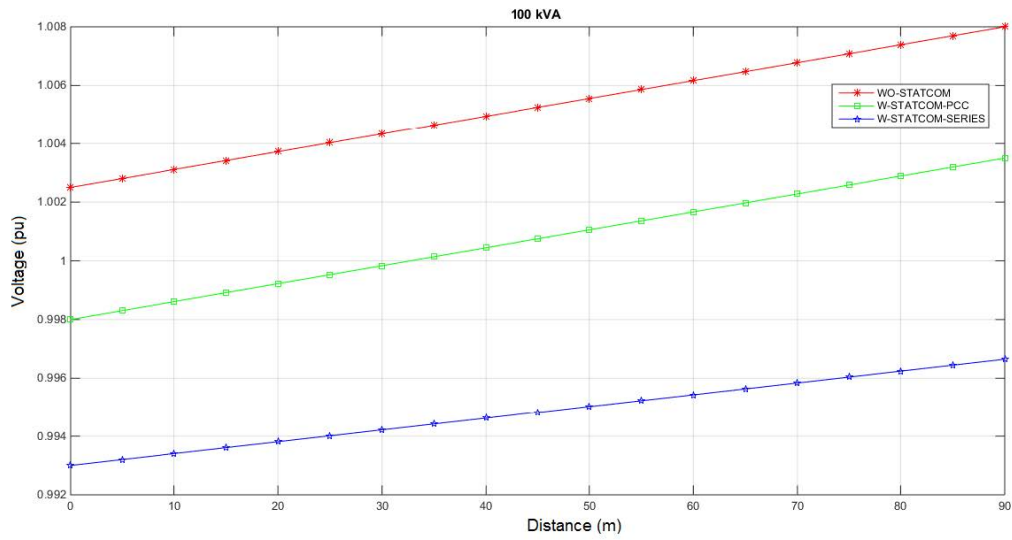


Figure 6.33: Voltage in steps of 10m from the PCC along the distribution line for 100, 200, and 315 kVA systems without a STATCOM, with a STATCOM at PCC, and with a STATCOM at the last DP and a distributed energy source of current type for light loads

The STATCOM reduces the overall system voltages for the 200 and 315 kVA lightly-loaded systems. For the lightly loaded 200 kVA and 315 kVA systems, the STATCOM must reduce the system voltage. The voltage measured in each DP drops initially due to the increase in distance from DP1 when system loading increases. The voltage then increases due to the decrease in distance from DER, making the overall voltage plots almost constant. It can be concluded from this that the advantage of using DER is that the system reactance can be calculated accurately.

The accuracy however in a real environment depends upon the DER capacity and type. In the case of heavy loads shown in Figure 6.32, the voltage variation is very small. The system voltage variation for current source DERs in case of light and heavy loads shown in Figure 6.33 and Figure 6.34 are similar to the results of voltage source. This is due to the steady-state supply of power to the grid by both a voltage and current source DER with different filter types.

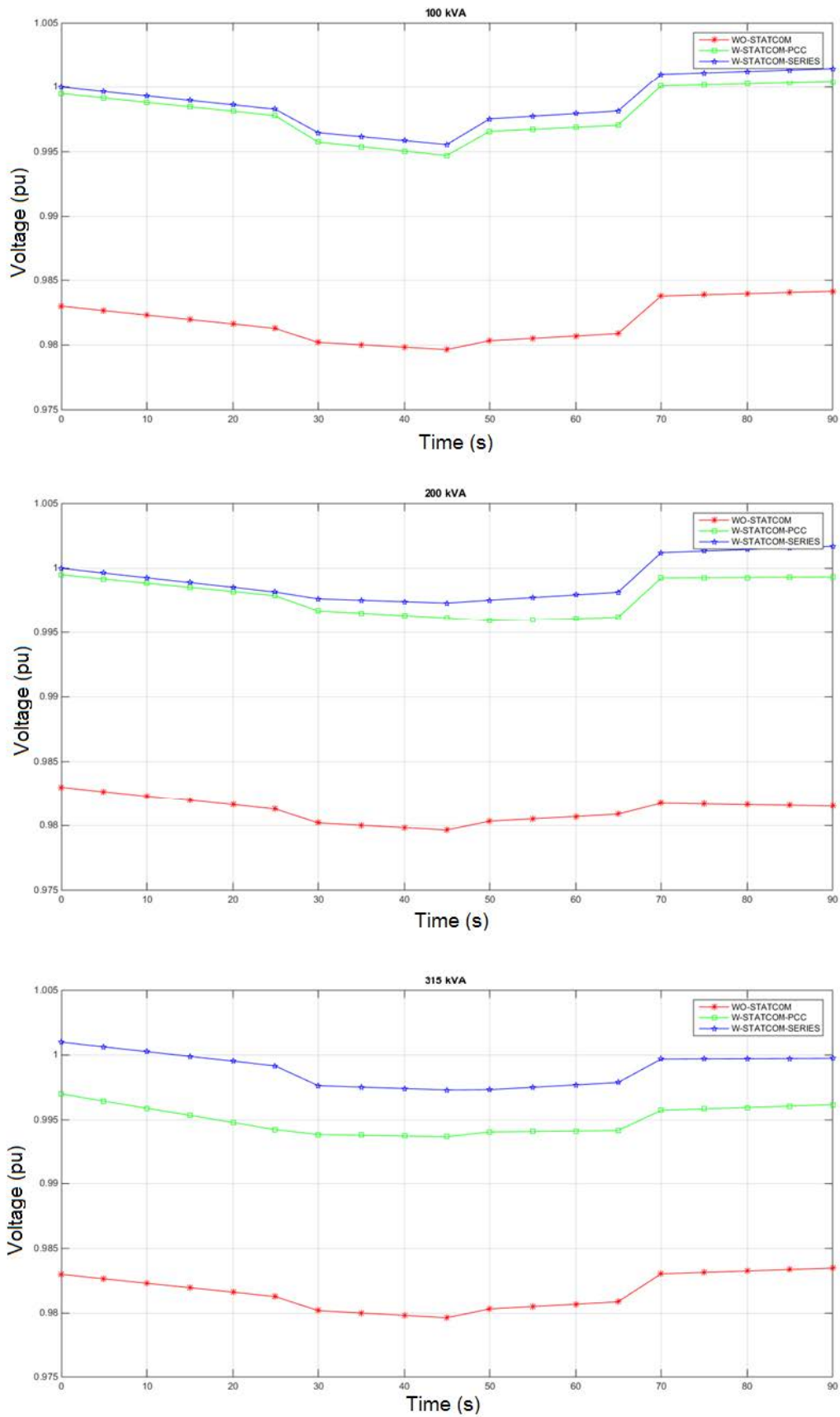


Figure 6.34: Voltage in steps of 10m from the PCC along the distribution line for 100, 200 and 315 kVA systems without a STATCOM, with a STATCOM, with a STATCOM at PCC, and with a STATCOM at the last DP and a distributed energy source of current type for heavy loads

6.6 Conclusion

The chapter uses D-STATCOM and STATCOM regulation of reactive power on distribution lines. The D-STATCOM is utilized both in series and in parallel. The D-STATCOM is used for both voltage and reactive power compensation, and dynamic response behaviour is checked in the presence of faults. The D-STATCOM provides reactive power compensation by absorbing or supplying reactive power at the point of connection which thereby reduces the effect on the power quality of the line.

The D-STATCOM is used for compensation in the presence of a breaker circuit before the load. The use of D-STATCOM compensates the effect of breaker circuit and the circuit then returns back to its steady state with reduced effect on power quality.

A series of simulations is done to analyse the behaviour of a STATCOM placed in parallel and series. The STATCOM phasor model is used and compared with Static Var compensation (SVC), which proves the dominance of a STATCOM over SVC, as a STATCOM provides linear variations in power with respect to system voltage while SVC provides variations which is square of the system voltage. Also, the response of a STATCOM is faster as compared to SVC, which reduces influence on power quality of the line.

The simulation on line is conducted with the STATCOM placed closed to PCC and at the end of the line for a 100, 200, and 315 kVA system. The controller is used without droop and with droop, the STATCOM with droop requires half time to reach the steady state. The STATCOM without droop requires very high reactive power. The STATCOM used with droop-control leads to considerable reduction in rating and size.

PFC is used at the PCC for consistent controller dynamics irrespective of the system's impedance. Additional simulations are carried out to inspect the effect of both types of DERs, namely voltage and current source. This proves that the system voltage regulating ability of STATCOM is unaffected in the presence or absence of voltage or current supplies and impedances.

The utilization of STATCOM and D-STATCOM provides stability in grid especially in terms of reactive power. These devices help grid to recover fast from the appeared faults, presence of

extra load at their point of connection. In future, more number of devices can be used to provide better compensation at other feeders or distribution points.

CHAPTER SEVEN

CONCLUSIONS AND FUTURE WORK

This thesis has presented the use of DSTATCOM and STATCOM for the regulation of reactive power on distribution lines.

The STATCOM is used for compensation when wind energy is injected on the distribution line. A STATCOM is capable of providing compensation dynamically in the presence of wind power injection on the distribution grid. A STATCOM, when connected in series and in parallel, compensates the reactive power component of the distribution grid in the presence of wind power. An efficient scheme is proposed to handle variation due to the speed of wind.

Another device, DSTATCOM, is also used in series and parallel to compensate both voltage and reactive power. The dynamic response behaviour is measured in the presence of faults. The compensation of reactive power is done at the Point of Common Coupling by absorbing or supplying the reactive power. It is also utilised for compensation in the presence of a circuit-breaker before the load. The circuit returns to its steady state very fast with minimal effects on the power quality.

In this chapter, a conclusion is made for the work done, with particular reference to the goals expressed in Chapter 1 and how they have been accomplished. Furthermore, impediments are distinguished and the scope for future research is specified.

7.1 Objective-Specific Conclusions

In chapter 1, the four objectives of this work were stated. They were:

- 1) To have better knowledge on power quality problems affecting distribution grids, power quality measurement devices and instruments, as well as various methods to mitigate power quality problems.
- 2) To have a better understanding of the voltage and control methods of the efficient power electronic device, DSTATCOM, for compensating reactive power.

- 3) To develop a model with a STATCOM injected on a distribution grid in the presence of wind power for regulating reactive power and to demonstrate the method using MATLAB/Simulink environment.
- 4) To develop an AC voltage control strategy for DSTATCOM and STATCOMs installed on distribution networks to compensate reactive power, as well as demonstrating the method using a MATLAB/Simulink environment.

How each of these objectives has been addressed and key findings will now be considered.

7.1.1 Objective 1

The first objective has been addressed in Chapter 1, 2, and 3. In the first chapter, the main emphasis is on the power quality problems in grid-tied alternative systems at the distribution end. The power quality standards are mentioned. Applying standards and specifications brings compatibility between the manufacturer and customer. Monitoring and evaluation procedures are the primary criterion to resolve any problem encountered at the distribution side. Various power quality problems such as transients, long and short duration voltage variations, voltage unbalance, and waveform distortion has a high impact on the performance of the system. At any cost, these problems must be reduced to meet the desired performance. Electrical devices may fail or lead to complete shutoff if these problems are not resolved. FACTS and custom power devices are discussed. Custom power devices are mainly used to avoid conditions like memory loss, glitches, and tripping at the distribution end. The literature survey reflects various proposed algorithms to mitigate these power quality problems. LMF adaptive filtering algorithm, ANFIS-LMS-based control algorithm, and PLL-less control algorithm are the most efficient algorithms to compensate reactive power and to mitigate other power quality problems.

In Chapter 2, power quality measurement devices like multimeters, oscilloscopes, disturbance analysers, spectrum analysers, harmonic analysers, flicker meters, and energy monitors are described briefly. Circuit problems such as overloading, undervoltage, and overvoltage can be detected easily by utilising multimeters. The oscilloscope shows the variation of current and voltage waveforms of the instrument that is checked. Disturbance analysers and monitors belong to the category of equipment which are developed especially for measuring a vast variety of disturbances like short and long duration transients, undervoltage, and overvoltage. Spectrum and harmonic analysers display harmonic waveforms on a screen. These devices

are advantageous and due to their reliability, they have various applications in industrial power quality monitoring and system maintenance.

Chapter 3 surveys various mitigation techniques like direct AC-AC converter, eight-switch power conditioner, and the SW-SVC method. These are useful for voltage sag mitigation. Micro-interruptions and long-interruptions are mitigated by using a customer-based approach and probabilistic life cycle method. One method to reduce voltage spikes is to reduce the parasitic inductance via AC photovoltaic models. The MV spark gap operation model is presented in literature to evaluate single-phase, dual-phase and three-phase spark gap breakdown possibilities in cases of lightning induced overvoltage. The most efficient method to reduce voltage swell is the zig-zag transformer method and the autotransformer with random hysteresis voltage control. Other methods are surveyed to mitigate voltage fluctuation and harmonic distortion. Faults in the power system can cause interruptions that ultimately affect cost and production. Therefore, these devices are helpful to mitigate these faults for the sake of improved efficiency.

7.1.2 Objective 2

Chapter 4 deals with the second objective. Research is done on a DSTATCOM with the aim of improving power quality. Traditional devices are found to provide degraded performance. As a result, the DSTATCOM is developed and is dynamically controlled when connected to the distribution systems. The schematic diagram and operating principle is discussed in Chapter 4, as well as various voltage and current control strategies. Continued research on DSTATCOM devices could lead to the solution for problems that occur in grids and industrial units. Some of the strategies provide better compensation at the cost of other important PQ parameters. The control strategy needs to be used for addressing a specific parameter.

7.1.3 Objective 3

The third objective has been discussed in Chapter 5. This chapter focuses on wind energy, which is considered the most widely used source of renewable energy in the present era. Wind turbines are used in grid-tied wind generation systems. The main advantage of this method is the fact that it is cost-effective due to net metering concept. Furthermore, there is no need to purchase batteries. This chapter classifies wind turbines and their power capacities. A STATCOM is established in a small wind farm equipped with wind turbines in such a way that it helps to improve PQ faults. A simple model of a fixed-speed wind farm is provided by the STATCOM, which provides fault ride through voltage control. The wind farm model has 30 x 2

MW FSIG as well as stall regulated wind turbines. The simulations shows that in the presence of injected wind energy, the reactive power of the distribution grid is efficiently compensated by a STATCOM.

7.1.4 Objective 4

The fourth objective has been discussed in Chapter 6. In this chapter, D-STATOM and STATCOM are both used for addressing the problem in a specific model. D-STATCOM is used for the compensation of reactive power in the presence of faults. The faults are introduced in either all or a combination of phases. The D-STATCOM thereby provides fast recovery and reactive power compensation. D-STATCOM is then used in a model with the circuit-breaker before the extra load. This condition is variable in nature, similar to conditions in which there is an increase in the load on the distribution line due to users who are not paying for the services. The D-STATCOM absorbs and injects reactive power for reactive power compensation at the point of connection.

The STATCOM is used on a distribution line with distribution points. It is connected at DP1, known as the point of common coupling, as well as at the end of the distribution line for compensation. Different scenarios are then considered: fixed position of the STATCOM, STATCOM placed along the line with power factor correction capacitors, STATCOM with droop control, injected DERs for three transformer ratings 100 kVA, 200 kVA, and 315 kVA. The STATCOM provides reactive power compensation for all three aforementioned ratings.

A STATCOM phasor model is specifically utilized in the thesis for wind farms and distribution lines with different loads, DERs and proved out to be an ideal device to compensate reactive power and voltage compensation too. The D-STATCOM is used for distribution lines with three phase breaker circuit and in presence of faults. The breaker circuit and induced faults both affects the distribution line reactive power considerably, the use of D-STATCOM is able to settle it quickly.

Some of the other outcome achieved including above are :

- MATLAB is the software used for verification of both DSTATCOM and STATCOM.
- Utility distribution lines, industrial loads and critical home appliances suffers from many unwanted outages and interruptions whose frequent appearances and existence will result in significant financial losses. All these PQ problems are addressed by employing

STATCOM and DSTATCOM which reduces complexity and cost of the lines, as one device will address all these PQ problems.

- In this thesis, the kVA rating used by STATCOM and DSTATCOM is 50% which is fairly lower than other compensating device like SVC.
- In actual most of the loads have a non-linear behaviour due to which they inject harmonics, the use of STATCOM and DSTATCOM eliminates the injected harmonics and maintains constant terminal voltage.
- The existence of an unbalanced voltage at the PCC results in a negative succession current segment that decays the control execution. The STATCOM and DSTATCOM regulates the PCC voltage in lines which might get affected by grid disturbances. They provide independent control of both positive and negative sequences.

7.2 Statistical Conclusion

The work in this thesis is basically to provide reactive power compensation which is an important power quality parameter. We have considered several practical scenarios, where reactive power is varied and is compensated with the help of single STATCOM or D-STATCOM.

CASE 1: In ideal distribution line, no faults occurs. However, in real life the faults can appear on any distribution line due to both internal and external disturbances. The fault can appear in any phase or any combination of phases. The faults considered by us here are in phase A, AB and ABC. When faults are introduced in model of Figure 6.1 at time $[1/60, 5/60]$, the D-STATCOM connected in parallel at bus B3 absorbs or injects current with amplitude in the range $\pm 2.5pu, \pm 1.5pu$, and $\pm 1.5pu$, the reactive power of D-STATCOM is in the range $\pm 5pu, \pm 4pu$, and $\pm 3.8pu$, respectively for faults in phase , AB and A as compared to no fault condition where absorbed or injected current and reactive power of D-STATCOM is in range 0.8pu and 2 pu respectively.

CASE 2: Another case is when the load suddenly appears and disappears from the distribution line. We have used a Simulink breaker circuit which controls absence or presence of an extra load at bus B3 in Figure 6.7, the results are compared with case when a variable nature load is present all the time Figure 6.6. The single D-STATCOM is used to provide reactive power compensation. The single D-STATCOM easily compensates the reactive power for Figure 6.6 model by absorbing or injecting $\pm 0.5pu$ of current, the single D-STATCOM try to provide

reactive power compensation by absorbing or injecting a current of $\pm 0.75pu$, but fails to provide compensation due to limitation in single D-STATCOM.

CASE 3: When STATCOM is placed at fixed positions without any limits on current controllers. The system voltage is 0.98pu without any STATCOM. When STATCOM is placed at PCC i.e in parallel it's closed to 1pu and decreases up to 0.99pu. While when STATCOM is placed at closed to final DP i.e in series, the system voltage starts from 1.005 pu and decreases to 1 pu from PCC to DP5. The STATCOM in this conditions is always regulating voltage, even though the reactive current required is higher than the rated current of the system. The absence or presence of STATCOM is not affecting voltage of the system, but increases the system voltage even in presence of STATCOM.

CASE 4: When we change the load from no load to full load, the voltage at DP5 or end of the line require more reactive power as compare to PCC for 100 kVA system and the difference in reactive current is $|0.25| pu$. The performance follows the same pattern for 200 and 315 kVA systems. For all distribution points the voltage in each zone is within +5%/ -10%.

CASE 5: After that we used the STATCOM controller in both tuned and untuned conditions. The reactive current injected by STATCOM for 100, 200 and 315 kVA systems is more when controller is tuned. The difference in reactive current injected is 0.04 pu to 0.1 pu after the settling time. The settling time here is close to 1sec.

CASE 6: Then we have used power factor correction (PFC) capacitors to reduce the STATCOM load. The PFC capacitors provides reactive power which leads to increase in voltage at PCC. The STATCOM has to absorb reactive power initially instead of supplying it. The reactive current absorbs is close to 0.6 pu. After 1 sec, the injected current by STATCOM is very less as compared to case when PFCs are not utilized. The difference is 0.6 pu.

LIMITATIONS: These systems suffered from limitations. The controller allows only single STATCOM and when power demands exceeds the rated current system. In order to address these limitation, we have used STATCOM with droop control. The droop control not only address these issues but also decreases the STATCOM size. The droop control STATCOM reduces the system voltage close to 0.99pu for series and 0.9825pu for parallel case, which 0.1% less as compared to the case when STATCOM is used without droop control. The droop

control STATCOM takes 0.1s to return to steady state. This substantially reduces current demand and provides reactive power compensation.

The distributed energy resources (DERs) are also placed at the end of the line to increase the voltage at the end of line and DPs close to it. The STATCOM used here is also with droop control capability. For the lightly loaded with voltage source DER, for the 200 and 315 kVA systems, the STATCOM reduces the system voltage as the system voltage is greater than 1pu. The tuned controllers returned to voltage 1pu after 0.2s. For heavily loaded system with voltage source and current source DER at the end of the line, the system voltage initially decreases with distance and then increases as the distance from DER reduces. The STATCOM here reduces the system voltage for reactive power compensation.

7.3 Future Work

In this work, the work is more focused on reactive power compensation is done using only one compensating device at a time. Better compensation can be achieved by using two or more devices placed at different positions along the distribution line.

Since the use of two or more devices can affect the overall budget, this study can be extended to find the operating costs as placement of STATCOM or D-STATCOM effect on overall budget.

REFERENCES

- A. Ghosh and G. Ledwich. *Power Quality Enhancement Using Custom Power Devices*. Norwell, MA, USA. <http://www.springer.com/gp/book/9781402071805>.
- Acha, E., Agelidis, V.G., Anaya-Lara, O. & Miller, T.J.E. 2002. *Power Electronic Control in Electrical Systems*. <http://www.sciencedirect.com/science/article/pii/B9780750651264500080>.
- Agarwal, R.K., Hussain, I. & Singh, B. 2016. Implementation of LLMF Control Algorithm for Three-Phase Grid Tied SPV-DSTATCOM System. *IEEE Transactions on Industrial Electronics*, 7(4): 1–1. <http://ieeexplore.ieee.org/document/7748533/>.
- Aguero, J.L., Issouribehere, F. & Battaiotto, P.E. 2006. STATCOM modeling for mitigation of voltage fluctuations caused by electric arc furnaces. *2006 IEEE Power Engineering Society General Meeting*, (1900): 1900.
- Ahmad, M.T., Kumar, N. & Singh, B. 2016. A discrete derivative control technique for DC link voltage in shunt compensator. *12th IEEE International Conference Electronics, Energy, Environment, Communication, Computer, Control: (E3-C3), INDICON 2015*: 1–5.
- Akagi, H., Kanazawa, Y. & Nabae, A. 1984. Instantaneous Reactive Power Compensators Comprising Switching Devices without Energy Storage Components. *IEEE Transactions on Industry Applications*, IA-20(3): 625–630.
- Akagi, H., Watanabe, E.H. & Aredes, M. 2007a. *Instantaneous Power Theory and Applications to Power Conditioning*. <http://dx.doi.org/10.1002/9780470118931.ch3>.
- Akagi, H., Watanabe, E.H. & Aredes, M. 2007b. The Instantaneous Power Theory. *Instantaneous Power Theory and Applications to Power Conditioning*: 41–107. <http://dx.doi.org/10.1002/9780470118931.ch3>.
- Anaya-Lara, O., Jenkins, N., Ekanayake, J., Cartwright, P. & Hughes, M. 2011. *Wind energy generation: modelling and control*. <http://strathprints.strath.ac.uk/14944/>.
- Anaya-Lara, O., Jenkins, N., Ekanayake, J., Cartwright, P. & Hughes, M. 2009. *Wind Energy Generation: Modelling and Control*. <http://books.google.com/books?hl=en&lr=&id=R4yUPKB8dgkC&oi=fnd&pg=PP8&dq=Wind+Energy+Generation:+Modelling+and+Control&ots=6tTjB2b9jc&sig=HXJXUW5sV2hVhbODUz9-LTadawQ>.
- Anuradha, K., Muni, B.P. & Kumar, A.D.R. 2008. Electric arc furnace modeling and voltage flicker mitigation by DSTATCOM. *IEEE Region 10 Colloquium and 3rd International Conference on Industrial and Information Systems, ICIS 2008*: 8–13.
- Arya, S.R., Niwas, R., Bhalla, K.K., Singh, B., Chandra, A. & Al-Haddad, K. 2015. Power quality improvement in isolated distributed power generating system using DSTATCOM. *IEEE Transactions on Industry Applications*, 51(6): 4766–4774.
- Arya, S.R. & Singh, B. 2012. CTF control algorithm of DSTATCOM for Power factor correction and zero voltage regulation. *2012 IEEE Third International Conference on Sustainable Energy Technologies (ICSET)*: 157–162.
- Arya, S.R. & Singh, B. 2013a. Kurtosis driven variable learning adaptive filter for suppression of power quality problems. *2013 Annual IEEE India Conference, INDICON 2013*.
- Arya, S.R. & Singh, B. 2014. Neural network based conductance estimation control algorithm for shunt compensation. *IEEE Transactions on Industrial Informatics*, 10(1): 569–577.

- Arya, S.R. & Singh, B. 2013b. Performance of DSTATCOM using leaky LMS control algorithm. *IEEE Journal of Emerging and Selected Topics in Power Electronics*, 1(2): 104–113.
- Arya, S.R., Singh, B., Chandra, A. & Al-Haddad, K. 2014. Learning-based anti-hebbian algorithm for control of distribution static compensator. *IEEE Transactions on Industrial Electronics*, 61(11): 6004–6012.
- Arya, S.R., Singh, B. & Jain, C. 2014. Simple peak detection control algorithm of distribution static compensator for power quality improvement. *IET Power Electronics*, 7(7): 1736–1746. <http://digital-library.theiet.org/content/journals/10.1049/iet-pel.2013.0494>.
- Awad, H. & Blaabjerg, F. 2004. Mitigation of voltage swells by static series compensator. *PESC Record - IEEE Annual Power Electronics Specialists Conference*, 5: 3505–3511.
- B. Singh, P. Jayaprakash, and D.P.K. 2008. H-Bridge VSC with a T-connected transformer based three-phase four-wire DSTATCOM for power quality improvement. In *NSC'08*. roorkee, India: 1–6.
- Badoni, M., Singh, A. & Singh, B. 2016a. Adaptive Neurofuzzy Inference System Least-Mean-Square-Based Control Algorithm for DSTATCOM. *IEEE Transactions on Industrial Informatics*, 12(2): 483–492.
- Badoni, M., Singh, A. & Singh, B. 2016b. Real time recurrent learning based algorithm for control of DSTATCOM. *12th IEEE International Conference Electronics, Energy, Environment, Communication, Computer, Control: (E3-C3), INDICON 2015*: 1–6.
- BADONI, M., Singh, A. & Singh, B. 2016. Comparative Performance of Wiener Filter and Adaptive Least Mean Square based Control for Power Quality Improvement. *IEEE Transactions on Industrial Electronics*, 46(c): 1–1.
- Bahramirad, S., McClanahan, J. & Khodaei, A. 2013. Application of real-time monitoring in efficient operation of distributed static compensators. In *IEEE Power and Energy Society General Meeting*.
- Bajaj, M., Pushkarna, M., Rana, A.S. & Khan, M.T. 2016. A modified algorithm for time varying reactive power control and harmonics compensation by D-STATCOM. In *12th IEEE International Conference Electronics, Energy, Environment, Communication, Computer, Control: (E3-C3), INDICON 2015*.
- Barrado, J.A., Griñó, R. & Valderrama, H. 2007. Standalone self-excited induction generator with a three-phase four-wire active filter and energy storage system. In *IEEE International Symposium on Industrial Electronics*.
- Bartels, M., Gatzen, C., Peek, M., Schulz, W., Wissen, R., Jansen, A., Molly, J.P., Neddermann, B., Gerch, H.-P., Grebe, E., Saßnick, Y. & Winter, W. 2006. Planning of the grid integration of wind energy in Germany onshore and offshore up to the year 2020. *Int. J. Glob. Energy Issues*, 25(3): 257–275.
- Basu, K.P. & Hafidz, S.A. 2008. Mitigation of single-phase voltage sag and swell with zigzag transformer. *3rd International Conference on Deregulation and Restructuring and Power Technologies, DRPT 2008, (April)*: 2369–2373.
- Benhabib, M.C. & Saadate, S. 2005. New control approach for four-wire active power filter based on the use of synchronous reference frame. *Electric Power Systems Research*, 73(3): 353–362. <http://www.sciencedirect.com/science/article/pii/S0378779604002020>.
- Bina, M.T., Eskandari, M.D. & Panahlou, M. 2005. Design and installation of a ??250 kVAr D-STATCOM for a distribution substation. *Electric Power Systems Research*, 73(3): 383–391.

- Bingham, R.P. 2008. Measurement Instruments for Power Quality Monitoring. , 4019: 1–3.
- Bollen, M., Gu, I., Santoso, S., Mcgranaghan, M., Crossley, P., Ribeiro, M. & Ribeiro, P. 2009. Bridging the gap between signal and power. *IEEE Signal Processing Magazine*, 26(4): 12–31. <http://ieeexplore.ieee.org/lpdocs/epic03/wrapper.htm?arnumber=5174495>.
- Bollen, M.H. 2000. Understanding Power Quality Problems: Voltage Sags and Interruptions. *IEEE Press, New York*. http://books.google.ps/books/about/Understanding_Power_Quality_Problems.html?id=Je0eAQAAIAAJ&pgis=1%5Cnhttp://scholar.google.com/scholar?hl=en&btnG=Search&q=intitle:UNDERSTANDING+POWER+QUALITY+PROBLEMS+Voltage+Sags+and+Interruptions+Math#1%5Cnhttp://schol.
- Borisov, K. & Ginn, H.L. 2010. Multifunctional VSC based on a novel fortescue reference signal generator. *IEEE Transactions on Industrial Electronics*, 57(3): 1002–1007.
- Breu, F., Guggenbichler, S. & Wollmann, J. 2008. 20% Wind Energy by 2030 Increasing Wind Energy's Contribution to U.S. electricity Supply. Vasa, U.S. Depar: 248. <http://medcontent.metapress.com/index/A65RM03P4874243N.pdf>.
- Burton, T., Jenkins, N., Sharpe, D. & Bossanyi, E. 2011. *Aerodynamics of Horizontal Axis Wind Turbines*. <http://doi.wiley.com/10.1002/9781119992714.ch3>.
- Burton, T., Sharpe, D., Jenkind, N. & Bossanyi, E. 2001. *Wind Energy Handbook*.
- Cartwright, P., Anaya-Lara, O., Wu, X., Xu, L. & Jenkins, N. 2004. Grid compliant offshore wind power connections provided by {FACTS} and {HVDC} solutions. In *European Wind Energy Conference*.
- Cavalcanti, M.C., Limongi, L.R., Gomes, M.D.B., Azevedo, G.M.S. & Genu, L.G.B. 2015. Eight-Switch Power Conditioner for Current Harmonic Compensation and Voltage Sag Mitigation. *IEEE Transactions on Industrial Electronics*, 62(8): 4655–4664.
- Chang, G.W., Chen, C.I. & Teng, Y.F. 2010. Radial-basis-function-based neural network for harmonic detection. *IEEE Transactions on Industrial Electronics*, 57(6): 2171–2179.
- Chilipi, R.R., Singh, B. & Murthy, S.S. 2014. Performance of a self-excited induction generator with dstatcom-dtc drive-based voltage and frequency controller. *IEEE Transactions on Energy Conversion*, 29(3): 545–557.
- Chiras, D. 2010. *Wind Power Basics: A Green Energy Guide*. http://books.google.com/books?hl=en&lr=&id=kY1-cilQd9UC&oi=fnd&pg=PP1&dq=Wind+Power+Basics:+A+Green+Energy+Guide&ots=0hbODTcNqP&sig=40g_5llmXDj5f19vlmodIPvGQ0w.
- Choi, S. & Jang, M. 2007. Analysis and control of a single-phase-inverter-zigzag-transformer hybrid neutral-current suppressor in three-phase four-wire systems. *IEEE Transactions on Industrial Electronics*, 54(4): 2201–2208.
- Chung, L.W., Siam, M.F.M., Ismail, A.B. & Hussein, Z.F. 2004. Modeling and simulation of sodium sulfur battery for battery-energy storage system and custom power devices. *PECon 2004. Proceedings. National Power and Energy Conference, 2004.*: 205–210.
- Cupertino, F., Lavopa, E., Zanchetta, P., Sumner, M. & Salvatore, L. 2011. Running DFT-based PLL algorithm for frequency, phase, and amplitude tracking in aircraft electrical systems. *IEEE Transactions on Industrial Electronics*, 58(3): 1027–1035.
- Dinavahi, V.R., Iravani, M.R. & Bonert, R. 2004. Real-time digital simulation and experimental verification of a D-STATCOM interfaced with a digital controller. *International Journal of Electrical Power & Energy Systems*, 26(9): 703–713.

<http://www.sciencedirect.com/science/article/pii/S0142061504000729>
<http://linkinghub.elsevier.com/retrieve/pii/S0142061504000729>.

- Dube, S.K., Singh, B. & Arya, S.R. 2014. Hyperbolic tangent function-based least mean-square control algorithm for distribution static compensator. *IET Generation, Transmission & Distribution*, 8(12): 2102–2113. <http://digital-library.theiet.org/content/journals/10.1049/iet-gtd.2014.0172>.
- El-Mamlouk, W.M., Mostafa, H.E. & El-Sharkawy, M.A. 2011. Active power filter controller for harmonic suppression in industrial distribution system. *Ain Shams Engineering Journal*, 2(3–4): 161–172. <http://dx.doi.org/10.1016/j.asej.2011.09.004>.
- Elliott, D. 2002. Assessing the world's wind resources. *IEEE Power Engineering Review*, 22(9): 4–9.
- Fox, B., Ebooks Corporation. & Ebook Library. 2007. *Wind Power Integration : Connection and System Operational Aspects*. http://0-www.newcastle.eblib.com.library.newcastle.edu.au/EBLWeb/patron?target=patron&extendedid=P_407993_0&%5Chttp://library.newcastle.edu.au/screens/EBL-instructions.html.
- Freitas, W., Morelato, A., Xu, W. & Sato, F. 2005. Impacts of AC generators and DSTATCOM devices on the dynamic performance of distribution systems. *IEEE Transactions on Power Delivery*, 20(2 II): 1493–1501.
- Fuchs, E. & Masoum, M. 2008. *Power Quality in Power Systems and Electrical Machines*.
- Fujita, H. & Akagi, H. 2007. Voltage-regulation performance of a shunt active filter intended for installation on a power distribution system. *IEEE Transactions on Power Electronics*, 22(3): 1046–1053.
- G. Gupta, W.F. and M.T.E.K. 2017. Power Quality and Power Control of a Wind Turbine Utilizing a STATCOM. In *25th Southern African Universities Power Engineering Conference SAUPEC 2017*.
- G.Gupta, W.F. and M. Kahn. 2017. Improvement of Distribution line reactive power with breaker circuit. In *ICICIT*. in press.
- Gagnon, R., Fecteau, M., Prud'Homme, P., Lemieux, E., Turmel, G., Paré, D. & Duong, F. 2012. Hydro-Québec strategy to evaluate electrical transients following wind power plant integration in the Gaspésie transmission system. *IEEE Transactions on Sustainable Energy*, 3(4): 880–889.
- Ghosh, A., Joshi, A. & Mishra, M.K. 2000. A new algorithm for active shunt filters using instantaneous reactive power theory. *IEEE Power Engineering Review*, 20(12): 56–58. <http://ieeexplore.ieee.org/lpdocs/epic03/wrapper.htm?arnumber=890380>.
- Ghosh, T.K. & Prelas, M.A. 2011. *Solar Energy*.
- Girbau-Llistuella, F., Sumper, A., Díaz-González, F., Sudrià-Andreu, A. & Gallart-Fernández, R. 2017. Local performance of the smart rural grid through the local energy management system. *Proceedings - 2017 International Conference on Modern Power Systems, MPS 2017*, (Mps).
- Golkar, M. a. 2004. Electric power quality: types and measurements. *2004 IEEE International Conference on Electric Utility Deregulation, Restructuring and Power Technologies. Proceedings*, 1(April): 1–8.
- Griffo, A. & Lauria, D. 2008. Two-leg three-phase inverter control for STATCOM and SSSC applications. *IEEE Transactions on Power Delivery*, 23(1): 361–370.

- Gupta, G., Fritz, W., M.T.E.K. 2017. Enhancement in Distribution Power Quality Using D-STATCOM with Phase Faults. *International Journal of Applied Engineering Research*, 12(21): 11441–11446.
- Gupta, G., Fritz, W. & Kahn, M.T.E. 2017. A comprehensive review of DSTATCOM: Control and compensation strategies. *International Journal of Applied Engineering Research*, 12(12): 3387–3393.
- Gupta, R. & Ghosh, A. 2006. Frequency-domain characterization of sliding mode control of an inverter used in DSTATCOM application. *IEEE Transactions on Circuits and Systems I: Regular Papers*, 53(3): 662–676.
- Gupta, R., Ghosh, A. & Joshi, A. 2007. Control of cascaded transformer multilevel inverter based DSTATCOM. *Electric Power Systems Research*, 77(8): 989–999.
- GWEC. 2016. Global Wind Report 2015 | Gwec. *Wind energy technology*. 75. <http://www.gwec.net/global-figures/wind-energy-global-status/>.
- Hannan, M.A., Mohamed, A. & Hussain, A. 2008. Modeling and power quality analysis of STATCOM using phasor dynamics. In *2008 IEEE International Conference on Sustainable Energy Technologies, ICSET 2008*. 1013–1018.
- Hatami, H., Shahnia, F., Pashaei, A. & Hosseini, S.H. 2007. Investigation on D-STATCOM and DVR operation for voltage control in distribution networks with a new control strategy. *2007 IEEE Lausanne POWERTECH, Proceedings*: 2207–2212.
- Hau, E. 2013. *Wind turbines: Fundamentals, technologies, application, economics*.
- Henini, N., Benzerafa, F. & Tlemcani, A. 2015. Design and simulation of five-level inverter based DSTATCOM using fuzzy logic. In *2015 6th International Renewable Energy Congress, IREC 2015*.
- Van Hertem, D., Didden, M., Driesen, J. & Belmans, R. 2007. Choosing the correct mitigation method against voltage dips and interruptions: A customer-based approach. *IEEE Transactions on Power Delivery*, 22(1): 331–339.
- Hingorani, N.G. & Gyugyi, L. 2000. Understanding FACTS: concepts and technology of flexible AC transmission systems. *Order A Journal On The Theory Of Ordered Sets And Its Applications*: 432. <http://books.google.co.jp/books?id=2-ceAQAIAAJ>.
- Hock, R.T., De Novaes, Y.R. & Batschauer, A.L. 2014. A voltage regulator based in a voltage-controlled DSTATCOM with minimum power point tracker. In *2014 IEEE Energy Conversion Congress and Exposition, ECCE 2014*. 3694–3701.
- Holdsworth, L., Wu, X.G., Ekanayake, J.B. & Jenkins, N. 2003. Comparison of fixed speed and doubly-fed induction wind turbines during power system disturbances. *IEE Proceedings - Generation, Transmission and Distribution*, 150(3): 343. http://digital-library.theiet.org/content/journals/10.1049/ip-gtd_20030251.
- Hosono, I., Yano, M., Corporation, M.E., Yuya, S. & Sueda, S. 1979. type[2][3]. , (6): 2276–2284.
- Hosseini, S.H. & Sabahi, M. 2007. Three-phase active filter using a single-phase STATCOM structure with asymmetrical dead-band control. In *Conference Proceedings - IPEMC 2006: CES/IEEE 5th International Power Electronics and Motion Control Conference*. 754–759.
- Hsu, J.S. 1998. Instantaneous phasor method for obtaining instantaneous balanced fundamental components for power quality control and continuous diagnostics. *IEEE Transactions on Power Delivery*, 13(4): 1494–1500.

- Kant, K., Arya, S.R., Singh, B. & Ieee, F. 2014. Voltage Sensorless Control Algorithm for Power Quality Improvement in Distribution Network. : 3–8.
- Kant, K., Singh, B. & Sekhar, V.C. 2016. DSTATCOM supported induction generator for improving power quality. *IET Renewable Power Generation*, 10(4): 495–503. <http://digital-library.theiet.org/content/journals/10.1049/iet-rpg.2015.0200>.
- Karanki, S.B., Geddada, N., Mishra, M.K. & Kumar, B.K. 2012. A DSTATCOM topology with reduced DC-link voltage rating for load compensation with nonstiff source. *IEEE Transactions on Power Electronics*, 27(3): 1201–1211.
- Karimi-Ghartemani, M. & Mokhtari, H. 2006. Extraction of harmonics and reactive current for power quality enhancement. In *IEEE International Symposium on Industrial Electronics*. 1673–1678.
- Kedjar, B. & Al-Haddad, K. 2009. DSP-based implementation of an LQR with integral action for a three-phase three-wire shunt active power filter. *IEEE Transactions on Industrial Electronics*, 56(8): 2821–2828.
- Kumar, C. & Mishra, M.K. 2013. A multi-functional DSTATCOM operating in voltage control mode. In *2013 IEEE 8th International Conference on Industrial and Information Systems, ICIS 2013 - Conference Proceedings*. 271–276.
- Kumar, C. & Mishra, M.K. 2014a. A multifunctional DSTATCOM operating under stiff source. *IEEE Transactions on Industrial Electronics*, 61(7): 3131–3136.
- Kumar, C. & Mishra, M.K. 2014b. A voltage-controlled DSTATCOM for power-quality improvement. *IEEE Transactions on Power Delivery*, 29(3): 1499–1507.
- Kumar, R., Singh, B., Shahani, D.T. & Jain, C. 2017. Dual-Tree Complex Wavelet Transform Based Control Algorithm for Power Quality Improvement in a Distribution System. *IEEE Transactions on Industrial Electronics*, 64(1): 764–772. http://www.ieee.org/publications_standards/publications/rights/index.html.
- Lavopa, E., Zanchetta, P., Sumner, M. & Cupertino, F. 2009. Real-time estimation of fundamental frequency and harmonics for active shunt power filters in aircraft electrical systems. *IEEE Transactions on Industrial Electronics*, 56(8): 2875–2884.
- Lee, H.J., Jung, J.J. & Sul, S.K. 2014. A switching frequency reduction and a mitigation of voltage fluctuation of Modular Multilevel Converter for HVDC. *2014 IEEE Energy Conversion Congress and Exposition, ECCE 2014*: 483–490.
- Lei, E., Yin, X., Chen, Y., Dai, J. & Yin, X. 2016. DSTATCOM connected to the system through center-tapped distribution transformer for reactive power compensation. In *IEEE Power and Energy Society General Meeting*.
- Lin, B.-R. & Yang, T.-Y. 2006. Analysis and implementation of three-phase power quality compensator under the balanced and unbalanced load conditions. *Electric Power Systems Research*, 76(5): 271–282. <http://www.sciencedirect.com/science/article/pii/S0378779605001987>.
- Liu, C.H. & Hsu, Y.Y. 2010. Design of a self-tuning pi controller for a STATCOM using particle swarm optimization. In *IEEE Transactions on Industrial Electronics*. 702–715.
- Lohia, P., Mishra, M.K., Karthikeyan, K. & Vasudevan, K. 2008. A minimally switched control algorithm for three-phase four-leg VSI topology to compensate unbalanced and non-linear load. *IEEE Transactions on Power Electronics*, 23(4): 1935–1944.
- Lund, H. 2005. Large-scale integration of wind power into different energy systems. *Energy*, 30(13): 2402–2412.

- Luo, A.L.A., Shuai, Z.S.Z., Zhu, W.Z.W. & Shen, Z.J. 2009. Combined System for Harmonic Suppression and Reactive Power Compensation. *IEEE Transactions on Industrial Electronics*, 56(2): 418–428.
- M. Maehlum and M. Mæhllum. 2017. Grid-Tied, Off-Grid and Hybrid Solar Systems - Energy Informative. <http://energyinformative.org/grid-tied-off-grid-and-hybrid-solar-systems/>.
- Manwell, J.F., McGowan, J.G. & Rogers, A.L. 2009. *Wind energy explained: theory, design and application*.
- Mascarella, D., Li, S., Joos, G. & Venne, P. 2015. Reactive power coordination in DFIG based wind farms for voltage regulation & flicker mitigation. In *IEEE Power and Energy Society General Meeting*.
- Mascarella, D., Venne, P., Guerette, D. & Joos, G. 2015. Flicker Mitigation via Dynamic Volt/VAR Control of Power-Electronic Interfaced WTGs. *IEEE Transactions on Power Delivery*, 30(6): 2451–2459.
- Masdi, H., Mariun, N., Mahmud, S., Mohamed, A. & Yusuf, S. 2004. Design of a prototype D-STATCOM for voltage sag mitigation. In *National Power and Energy Conference, PECon 2004 - Proceedings*. 61–66.
- McGranaghan, M. 2001. Trends in power quality monitoring. *IEEE Power Engineering Review*, 21(10).
- McGranaghan, M.F. & Santoso, S. 2007. Challenges and trends in analyses of electric power quality measurement data. *Eurasip Journal on Advances in Signal Processing*, 2007.
- Mehranfar, H., Baghrmian, A. & Rafieinia, F. 2011. Mitigation of voltage swell by switched autotransformer with random hysteresis voltage control. *Asia-Pacific Power and Energy Engineering Conference, APPEEC*: 2–5.
- Meyer, J., Schegner, P., Domagk, M., Kuntner, R. & Hillenbrand, F. 2009. Automated test system for accuracy verification of power quality measurement instruments. *IET Conference Publications*: 677–677. <http://digital-library.theiet.org/content/conferences/10.1049/cp.2009.0913>.
- Mishra, M.K., Ghosh, A. & Joshi, A. 2003. Operation of a DSTATCOM in voltage control mode. *IEEE Transactions on Power Delivery*, 18(1): 258–264.
- Mokhtari, G., Nourbakhsh, G., Zare, F. & Ghosh, A. 2013. A new distributed control strategy to coordinate multiple dstatcoms in LV network. In *2013 4th IEEE International Symposium on Power Electronics for Distributed Generation Systems, PEDG 2013 - Conference Proceedings*.
- Molinas, M., Suul, J.A. & Undeland, T. 2010. Extending the life of gear box in wind generators by smoothing transient torque with STATCOM. In *IEEE Transactions on Industrial Electronics*. 476–484.
- Montero, M.I.M., Cadaval, E.R. & Gonzalez, F.B. 2007. Comparison of Control Strategies for Shunt Active Power Filters in Three-Phase Four-Wire Systems. *IEEE Transactions on Power Electronics*, 22(1): 229–236. <http://ieeexplore.ieee.org/document/4052426/>.
- De Morais, A.S. & Barbi, I. 2006. Power redistributor applied to distribution transformers. In *IECON Proceedings (Industrial Electronics Conference)*. 1787–1791.
- Moreno-Munoz, A. 2007. *Power Quality: Mitigation Technologies in a Distributed Environment*. <http://www.springer.com/in/book/9781846287718>.
- Olimpo Anaya-Lara and E. Acha. 2002. Modeling and Analysis of Custom Power Systems-

- IEEE. *IEEE Transactions on Power Delivery*, 17(1): 266–272.
- Ota, J.I.Y., Shibano, Y., Niimura, N. & Akagi, H. 2015. A phase-shifted-PWM D-STATCOM using a modular multilevel cascade converter (SSBC) - Part I: Modeling, analysis, and design of current control. In *IEEE Transactions on Industry Applications*. 279–288.
- P. Jayaprakash, B. Singh, D.P.K. Integrated H-bridge VSC with a zig-zag transformer based three-phase four-wire DSTATCOM.
- Pande, N.S., Gawande, S.P. & Ramteke, M.R. 2014. Control of D-STATCOM under unbalanced and distorted voltages using Synchronous Detection method for load compensation. In *International Conference on Recent Advances and Innovations in Engineering, ICRAIE 2014*.
- Parle, J.A., Madrigal, M. & Acha, E. 2001. Phase domain transmission line modeling for harmonic analysis. *IEEE Power Engineering Review*, 21(10): 46–48.
- Patel, M.R. 2008. *Wind and Solar Power Systems: Design, Analysis, and Operation*.
- Pathak, G., Singh, B. & Panigrahi, B.K. 2014. Back propagation algorithm based controller for autonomous wind-DG microgrid. *Proceedings of 6th IEEE Power India International Conference, PIICON 2014*: 2–6.
- Pathak, G., Singh, B. & Panigrahi, B.K. 2015. Isolated microgrid employing PMBLDCG for wind power generation and synchronous reluctance generator for DG system. *India International Conference on Power Electronics, IICPE, 2015–May*: 1–6.
- Penthia, T., Panda, A.K., Sarangi, S.K. & Mangaraj, M. 2016. ANN controlled 4-leg VSC based DSTATCOM for power quality enhancement. In *12th IEEE International Conference Electronics, Energy, Environment, Communication, Computer, Control: (E3-C3), INDICON 2015*.
- Philip, J., Singh, B. & Mishra, S. 2015. Analysis and control of an isolated SPV-DG-BESS hybrid system. *India International Conference on Power Electronics, IICPE, 2015–May*.
- Pires, I.A., Silva, S.M. & Cardoso Filho, B.D.J. 2015. Increasing Ride-Through Capability of Control Panels Using Square-Wave Series Voltage Compensator. *IEEE Transactions on Industry Applications*, 51(2): 1309–1316.
- Piwko, R., Osborn, D., Gramlich, R., Jordan, G., Hawkins, D. & Porter, K. 2005. Wind energy delivery issues [transmission planning and competitive electricity market operation]. *IEEE Power and Energy Magazine*, 3(6): 47–56.
- Qaraca Oğlu, E.E. & Mehemmed Oğlu, M.H. 2011. Modeling and simulation of a distribution STATCOM using Simulink's power system blockset. In *2011 5th International Conference on Application of Information and Communication Technologies, AICT 2011*.
- Qdo, R.V.W., Ri, V.L. V, Hylfhv, X., Dqg, I.R.U., Hohfwurphkdqldo, W., Kdyh, S., Zlgho, E., Prphqwdv, V., Ru, L. & Lqwhuuxswlrqv, O. 2009. 3Uredelolwlf /Lih & \Foh & Rvw \$Qdo\lv Ri & Xwvrp 3Rzhu 'Hylfhv Iru 9Rowdjh 6Djv Dqg ,Qwhuuxswlrqv 0Lwljdwlrq. : 6–9.
- R. C. Dugan, M. F. McGranaghan, and H.W.B. 2006. *Electric Power Systems Quality*. 2nd ed. New York, NY: USA: McGraw Hill.
- Rahmani, S., Hamadi, A., Mendalek, N. & Al-Haddad, K. 2009. A New Control Technique for Three-Phase Shunt Hybrid Power Filter. *IEEE Transactions on Industrial Electronics*, 56(8): 2904–2915. <http://www.scopus.com/inward/record.url?eid=2-s2.0-68449100492&partnerID=40&md5=f1f1b6a6d0b3de32b7325b533f3c419a>.

- Reddy, J.G.P. & Reddy, K.R. 2012. Design and simulation of Cascaded H-bridge multilevel inverter based DSTATCOM for compensation of reactive power and harmonics. In *Recent Advances in Information Technology (RAIT), 2012 1st International Conference on*. 737–743.
- Rezkallah, M., Sharma, S., Chandra, A. & Singh, B. 2015. Hybrid standalone power generation system using hydro-PV-battery for residential green buildings. *IECON 2015 - 41st Annual Conference of the IEEE Industrial Electronics Society*. 3708–3713.
- Rohilla, Y. & Pal, Y. 2013. T-connected transformer integrated three-leg VSC based 3P4W DSTATCOM for power quality improvement. In *2013 Nirma University International Conference on Engineering, NUICONE 2013*.
- Sabiha, N.A. & Lehtonen, M. 2010. Overvoltage spikes transmitted through distribution transformers due to MV spark-gap operation. *PQ2010: 7th International Conference - 2010 Electric Power Quality and Supply Reliability, Conference Proceedings*, (Lv): 207–212.
- Saggu, T.S. 2015. Comparative Analysis of Custom Power Devices for Power Quality Improvement in Non-linear Loads. , (December).
- Salmerón, P., Montano, J.C., Vázquez, J.R., Prieto, J. & Pérez, A. 2004. Compensation in nonsinusoidal, unbalanced three-phase four-wire systems with active power-line conditioner. *IEEE Transactions on Power Delivery*, 19(4): 1968–1974.
- Scherer, L.G., Tischer, C.B. & De Camargo, R.F. 2015. Voltage regulation of stand-alone micro-generation SEIG based system under nonlinear and unbalanced load. In *IEEE International Symposium on Industrial Electronics*. 428–433.
- Sedinin, V.I. & Rogulin, L.Y. 2012. Measurement of electric power quality index for uninterruptible power supply devices. *2012 IEEE 11th International Conference on Actual Problems of Electronics Instrument Engineering (APEIE)*: 108–111. <http://ieeexplore.ieee.org/lpdocs/epic03/wrapper.htm?arnumber=6628968>.
- Sensarma, P.S., Padiyar, K.R. & Ramanarayanan, V. 2001. Analysis and performance evaluation of a distribution STATCOM for compensating voltage fluctuations. *IEEE Transactions on Power Delivery*, 16(2): 259–264.
- Sharma, S. & Singh, B. 2014. Asynchronous generator with battery storage for standalone wind energy conversion system. *IEEE Transactions on Industry Applications*, 50(4): 2760–2767.
- Shawon, M.H., Barcentewicz, S. & Kowalski, J. 2016. Identification of asymmetry in power system: Different case studies. *10th International Conference - 2016 Electric Power Quality and Supply Reliability, PQ 2016, Proceedings*: 37–40.
- Shea, J.J. 2004. Electric power substations engineering [Book Review]. *IEEE Electrical Insulation Magazine*, 20(6): chapter 6. http://128.104.77.228/documnts/fplrn/fpl_rn304.pdf.
- Shi, J., Kalam, A., Noshadi, A. & Shi, P. 2014. Genetic algorithm optimised fuzzy control of DSTATCOM for improving power quality. In *2014 Australasian Universities Power Engineering Conference, AUPEC 2014 - Proceedings*.
- Shukla, A., Ghosh, A. & Joshi, A. 2005. Static shunt and series compensations of an SMIB system using flying capacitor multilevel inverter. *IEEE Transactions on Power Delivery*, 20(4): 2613–2622.
- Singh, B., Adya, A., Mittal, A.P. & Gupta, J.R.P. 2008. Modeling, Design and Analysis of Different Controllers for DSTATCOM. *2008 Joint International Conference on Power*

- Singh, B. & Arya, S.R. 2013a. Adaptive theory-based improved linear sinusoidal tracer control algorithm for DSTATCOM. *IEEE Transactions on Power Electronics*, 28(8): 3768–3778.
- Singh, B. & Arya, S.R. 2014. Back-propagation control algorithm for power quality improvement using DSTATCOM. *IEEE Transactions on Industrial Electronics*, 61(3): 1204–1212.
- Singh, B. & Arya, S.R. 2013b. Implementation of single-phase enhanced phase-locked loop-based control algorithm for three-phase DSTATCOM. *IEEE Transactions on Power Delivery*, 28(3): 1516–1524.
- Singh, B. & Arya, S.R. 2012. Software PLL based control algorithm for power quality improvement in distribution system. *2012 IEEE 5th India International Conference on Power Electronics (IICPE)*: 1–6. <http://ieeexplore.ieee.org/lpdocs/epic03/wrapper.htm?arnumber=6450451>.
- Singh, B., Arya, S.R., Chandra, A. & Al-Haddad, K. 2013. Variable step learning control algorithm for VSC based shunt compensator. *2013 4th IEEE International Symposium on Power Electronics for Distributed Generation Systems, PEDG 2013 - Conference Proceedings*.
- Singh, B., Arya, S.R., Maurya, R. & Patel, S.K. 2016. Interior point algorithm for optimal control of distribution static compensator under distorted supply voltage conditions. *IET Generation, Transmission & Distribution*, 10(8): 1778–1791. <http://digital-library.theiet.org/content/journals/10.1049/iet-gtd.2015.0646>.
- Singh, B., Badoni, M. & Singh, A. 2016. Adaptive recursive inverse-based control algorithm for shunt active power filter. *IET Power Electronics*, 9(5): 1053–1064. <http://digital-library.theiet.org/content/journals/10.1049/iet-pel.2015.0170>.
- Singh, B., Dube, S.K. & Arya, S.R. 2015. An improved control algorithm of DSTATCOM for power quality improvement. *International Journal of Electrical Power & Energy Systems*, 64: 493–504. <http://linkinghub.elsevier.com/retrieve/pii/S0142061514004906>.
- Singh, B. & Jain, C. 2015. Single-phase single-stage multifunctional grid interfaced solar photo-voltaic system under abnormal grid conditions. *IET Generation, Transmission & Distribution*, 9(10): 886–894. <http://digital-library.theiet.org/content/journals/10.1049/iet-gtd.2014.0533>.
- Singh, B., Jain, C. & Goel, S. 2014. ILST control algorithm of single-stage dual purpose grid connected solar PV system. *IEEE Transactions on Power Electronics*, 29(10): 5347–5357.
- Singh, B., Jayaprakash, P. & Kothari, D.D. 2008. A T-connected transformer and three-leg VSC based DSTATCOM for power quality improvement. *IEEE Transactions on Power Electronics*, 23(6): 2710–2718.
- Singh, B., Jayaprakash, P. & Kothari, D.P. 2010. Magnetics for neutral current compensation in three-phase four-wire distribution system. In *2010 Joint International Conference on Power Electronics, Drives and Energy Systems, PEDES 2010 and 2010 Power India*.
- Singh, B., Jayaprakash, P. & Kothari, D.P. 2011. New control approach for capacitor supported DSTATCOM in three-phase four wire distribution system under non-ideal supply voltage conditions based on synchronous reference frame theory. *International Journal of Electrical Power and Energy Systems*, 33(5): 1109–1115.
- Singh, B., Jayaprakash, P. & Kothari, D.P. 2009a. Three-leg voltage source converter integrated with t-connected transformer as three-phase four-wire distribution static

- compensator for power quality improvement. *Electric Power Components and Systems*, 37(8): 817–831.
- Singh, B., Jayaprakash, P. & Kothari, D.P. 2008. Three-Leg VSC and a transformer based three-phase four-wire DSTATCOM for distribution systems. *Proc. NPSC'08*, (December): 602–607.
- Singh, B., Jayaprakash, P. & Kothari, D.P. 2008. Three-Phase Four-Wire DSTATCOM with H-Bridge VSC and Star/Delta Transformer for Power Quality Improvement. *Proceedings of the Indicon 2008 Ieee Conference & Exhibition on Control, Communications and Automation, Vol II*: 412–417.
- Singh, B., Jayaprakash, P. & Kothari, D.P. 2009b. Three single-phase voltage source converter based three-phase four wire DSTATCOM. In *2009 International Conference on Power Systems, ICPS '09*.
- Singh, B., Jayaprakash, P., Kothari, D.P., Chandra, A. & Haddad, K. Al. 2014. Comprehensive study of dstatcom configurations. *IEEE Transactions on Industrial Informatics*, 10(2): 854–870.
- Singh, B., Jayaprakash, P., Kumar, S. & Kothari, D.P. 2011. Implementation of neural-network-controlled three-leg VSC and a transformer as three-phase four-wire dstatcom. *IEEE Transactions on Industry Applications*, 47(4): 1892–1901.
- Singh, B., Jayaprakash, P., Somayajulu, T.R. & Kothari, D.P. 2008. DSTATCOM with reduced switches using two-leg VSC and a zig-zag transformer for power quality improvement in three-phase four-wire distribution system. In *IEEE Region 10 Annual International Conference, Proceedings/TENCON*.
- Singh, B., Jayaprakash, P., Somayajulu, T.R. & Kothari, D.P. 2009. Reduced rating VSC with a zig-zag transformer for current compensation in a three-phase four-wire distribution system. *IEEE Transactions on Power Delivery*, 24(1): 249–259.
- Singh, B., Murthy, S.S. & Gupta, S. 2004. Analysis and design of STATCOM-based voltage regulator for self-excited induction generators. *IEEE Transactions on Energy Conversion*, 19(4): 783–790.
<http://bibliotecavirtual.ups.edu.ec:2065/ielx5/60/29826/01359958.pdf?tp=&arnumber=1359958&isnumber=29826%5Cnhttp://bibliotecavirtual.ups.edu.ec:2065/xpl/articleDetails.jsp?tp=&arnumber=1359958&refinements%3D4291944246%26queryText%3DSTATCOM>.
- Singh, B. & Niwas, K. 2014. Power quality improvement of PMSG based DG set feeding 3-phase 3-wire load. *2014 IEEE International Conference on Power Electronics, Drives and Energy Systems, PEDES 2014*.
- Singh, B. & Niwas, R. 2016. Power quality improvement of PMSG-based DG set feeding three-phase loads. *IEEE Transactions on Industry Applications*, 52(1): 466–471.
- Singh, B. & Niwas, R. 2012. Power quality improvements in diesel engine driven induction generator system using SRF theory. *2012 IEEE 5th Power India Conference, PICONF 2012*: 3–7.
- Singh, B., Niwas, R. & Dube, S. 2014. Load Leveling and Voltage Control of Permanent Magnet Synchronous Generator Based DG Set for Standalone Supply System. *IEEE Transactions on Industrial Informatics*, 3203(4): 1–1.
<http://ieeexplore.ieee.org/lpdocs/epic03/wrapper.htm?arnumber=6862883>.
- Singh, B. & Raj Arya, S. 2013. Composite observer-based control algorithm for distribution static compensator in four-wire supply system. *IET Power Electronics*, 6(2): 251–260.

<http://digital-library.theiet.org/content/journals/10.1049/iet-pel.2012.0412>.

- Singh, B., Shahani, D.T. & Verma, A.K. 2013. IRPT based control of a 50 kw grid interfaced solar photovoltaic power generating system with power quality improvement. *2013 4th IEEE International Symposium on Power Electronics for Distributed Generation Systems, PEDG 2013 - Conference Proceedings*: 1–8.
- Singh, B., Shahani, D.T. & Verma, a K. 2014. Neural network controlled grid interfaced solar photovoltaic power generation. *IET Power Electronics*, 7(3): 614–626.
- Singh, B. & Solanki, J. 2009. A Comparison of Control Algorithms for DSTATCOM. *IEEE Transactions on Industrial Electronics*, 56(7): 2738–2745.
- Singh, B., Solanki, J., Chandra, A. & Al-Haddad, K. 2006. A solid state compensator with energy storage for isolated diesel generator set. In *IEEE International Symposium on Industrial Electronics*. 1774–1778.
- Singh, B., Solanki, J. & Verma, V. 2005. Neural network based control of reduced rating DSTATCOM. In *Proceedings of INDICON 2005: An International Conference of IEEE India Council*. 516–520.
- Singh, B., Verma, V. & Solanki, J. 2007. Neural network-based selective compensation of current quality problems in distribution system. *IEEE Transactions on Industrial Electronics*, 54(1): 53–60.
- Sivaranjani, R. 2016. StatCom control at wind farms with fixed-speed induction generators under asymmetrical grid faults. In *International Conference on Electrical, Electronics, and Optimization Techniques, ICEEOT 2016*. 3442–3447.
- Soares, V. & Verdelho, P. 2006. Digital implementation of a DC bus voltage controller for four-wire active filters. In *IECON Proceedings (Industrial Electronics Conference)*. 2763–2768.
- Song, W. & Huang, A.Q. 2010. Fault-tolerant design and control strategy for cascaded H-bridge multilevel converter-based STATCOM. *IEEE Transactions on Industrial Electronics*, 57(8): 2700–2708.
- Sreenivasarao, D., Agarwal, P. & Das, B. 2012. Neutral current compensation in three-phase, four-wire systems: A review. *Electric Power Systems Research*, 86: 170–180.
- Sreenivasarao, D., Agarwal, P. & Das, B. 2013. Performance enhancement of a reduced rating hybrid D-STATCOM for three-phase, four-wire system. *Electric Power Systems Research*, 97: 158–171.
- Srikanthan, S. & Mishra, M.K. 2010. DC capacitor voltage equalization in neutral clamped inverters for DSTATCOM application. *IEEE Transactions on Industrial Electronics*, 57(8): 2768–2775.
- Srinivas, M., Hussain, I. & Singh, B. 2016. Combined LMS – LMF-Based Control Algorithm of DSTATCOM for Power Quality Enhancement in Distribution System. , 63(7): 4160–4168.
- Tong, W. 2010. *Wind Power Generation and Wind Turbine Design*. 1st ed. U. W. TONG, Kollmorgen Corporation, ed. Southampton; Boston: WIT Press / Computational Mechanics. <https://www.witpress.com/books/978-1-84564-205-1>.
- Transmission, I.N.P. 2007. *Facts Controllers in Power Transmission*.
- Treasury, H.M. 2007. Stern review on the economics of climate change. *London: HM Treasury*, 30. <http://link.springer.com/10.1007/s11166-007-9007-8>.
- U.S. Energy Information Administration. 2016. *International Energy Outlook 2016*.

[www.eia.gov/forecasts/ieo/pdf/0484\(2016\).pdf](http://www.eia.gov/forecasts/ieo/pdf/0484(2016).pdf).

- Ucar, M. & Ozdemir, E. 2008. Control of a 3-phase 4-leg active power filter under non-ideal mains voltage condition. *Electric Power Systems Research*, 78(1): 58–73.
- Vahedy, V. 2006. Polymer insulated high voltage cables. *IEEE Electrical Insulation Magazine*, 22(3): 13–18.
- Vangala, P., Ropp, M., Haggerty, K., Lynn, K. & Wilson, W. 2008. Observed voltage spikes on fielded photovoltaic arrays caused by startup and shutdown switching of inverters. *Conference Record of the IEEE Photovoltaic Specialists Conference*: 2–5.
- Varschavsky, A., Dixon, J., Rotella, M. & Moran, L. 2010. Cascaded nine-level inverter for hybrid-series active power filter, using industrial controller. *IEEE Transactions on Industrial Electronics*, 57(8): 2761–2767.
- Verma, A., Singh, B. & Shahani, D. 2014. Modified EPLL based control to eliminate DC component in a grid interfaced solar PV system. *Proceedings of 6th IEEE Power India International Conference, PIICON 2014*.
- Verma, A.K., Singh, B., Shahani, D.T., Chandra, A. & Al-Haddad, K. 2014. Combined operation of a VSC based grid interfaced solar photovoltaic power generation system with night time application. *IEEE Power and Energy Society General Meeting, 2014–October*(October): 1–5.
- Verma, V., Singh, B., Chandra, A. & Al-Haddad, K. 2010. Power conditioner for variable-frequency drives in offshore oil fields. *IEEE Transactions on Industry Applications*, 46(2): 731–739.
- Vilar, C., Amarís, H. & Usaola, J. 2006. Assessment of flicker limits compliance for wind energy conversion system in the frequency domain. *Renewable Energy*, 31(8): 1089–1106.
- Vlad, C., Munteanu, I., Bratcu, A.I. & Ceanga, E. 2009. Anticipative Control of Low-Power Wind Energy Conversion Systems for Optimal Power Regime. *Control Engineering and Applied Informatics*, 11(4): 26–35.
- Volker Quaschnig. 2010. *Understanding Renewable Energy Systems*. <http://www.informaworld.com/openurl?genre=article&doi=10.1080/00207230600720431&magic=crossref%7C%7CD404A21C5BB053405B1A640AFFD44AE3>.
- Wang, L. & Truong, D.N. 2013. Stability enhancement of DFIG-based offshore wind farm fed to a multi-machine system using a STATCOM. *IEEE Transactions on Power Systems*, 28(3): 2882–2889.
- Weisser, D. & Garcia, R.S. 2005. Instantaneous wind energy penetration in isolated electricity grids: Concepts and review. *Renewable Energy*, 30(8): 1299–1308.
- Wu, X., Arulampalam, A., Zhan, C. & Jenkins, N. 2003. Application of a Static Reactive Power Compensator (STATCOM) and a Dynamic Braking Resistor (DBR) for the stability enhancement of a large wind farm. *Wind Engineering*, 27(2): 93–106. <http://www.scopus.com/inward/record.url?eid=2-s2.0-0038208158&partnerID=40&md5=0f5f816f6758a0f4d9e44f1e631c3cac>.
- Xu, C., Dai, K., Kang, Y., Liu, C. & Ieee. 2015. Characteristic Analysis and Experimental Verification of a Novel Capacitor Voltage Control Strategy for Three-Phase MMC-DSTATCOM. *2015 Thirtieth Annual IEEE Applied Power Electronics Conference and Exposition*, 1(c): 1528–1533.
- Yang, K., Wang, Y., Yang, H., Tao, H. & Chen, G. 2014. Design of H-bridge based converter module used in cascaded DSTATCOM. In *Conference Proceedings - IEEE Applied Power*

Electronics Conference and Exposition - APEC. 209–213.

- Zaveri, T., Bhavesh, B. & Zaveri, N. 2011. Control techniques for power quality improvement in delta connected load using DSTATCOM. *2011 IEEE International Electric Machines & Drives Conference (IEMDC)*: 1397–1402.
- ZHOU, J., WU, X. jie, GENG, Y. wen & DAI, P. 2007. Simulation Research on a SVPWM Control Algorithm for a Four-Leg Active Power Filter. *Journal of China University of Mining and Technology*, 17(4): 590–594.
- Zhu, X., Li, X., Shen, G. & Xu, D. 2010. Design of the dynamic power compensation for PEMFC distributed power system. *IEEE Transactions on Industrial Electronics*, 57(6): 1935–1944.

APPENDIX A

D-STATCOM 25kV, +/- 3Mvar Average Model

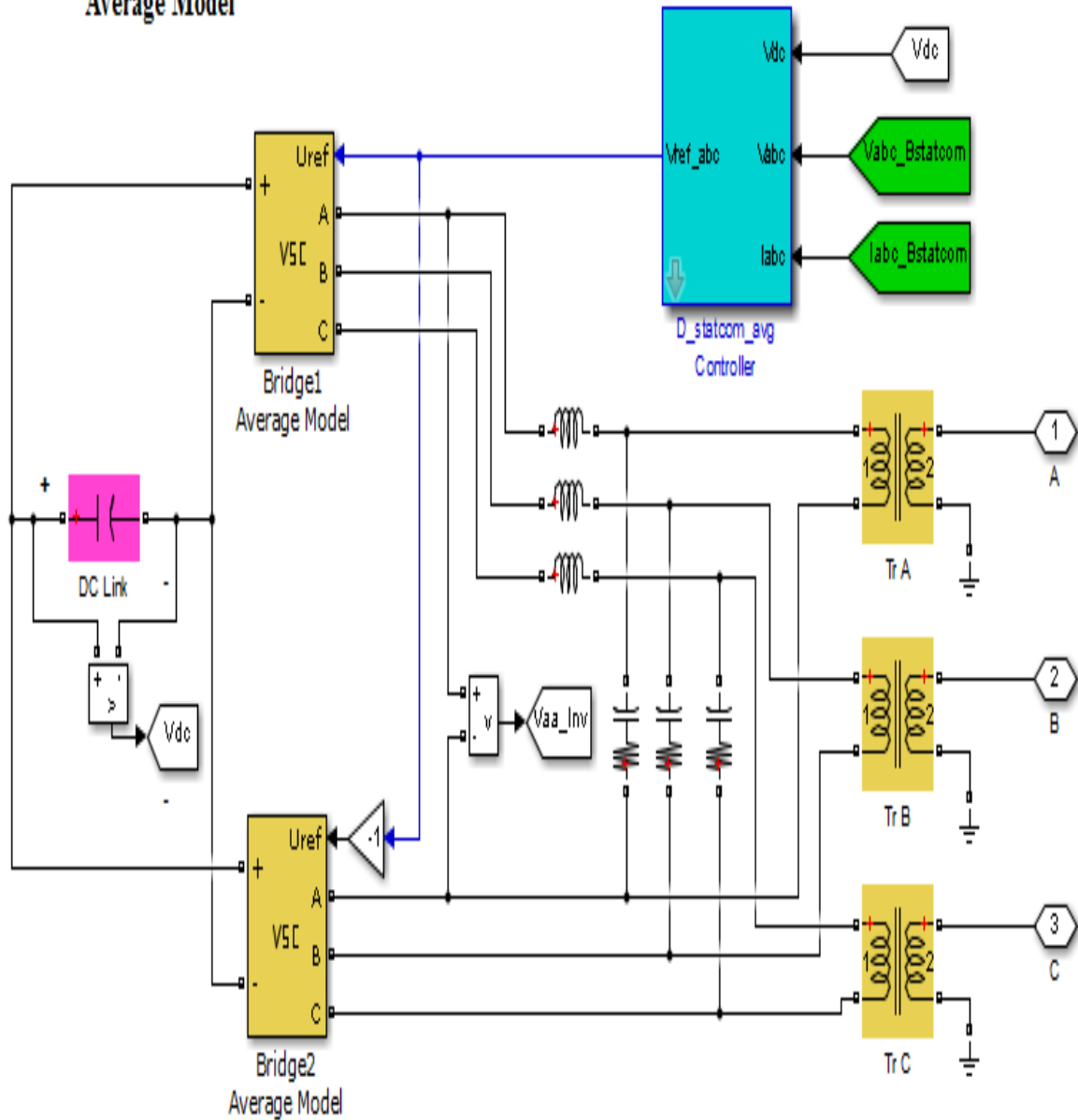


Figure A: DSTATCOM Average model

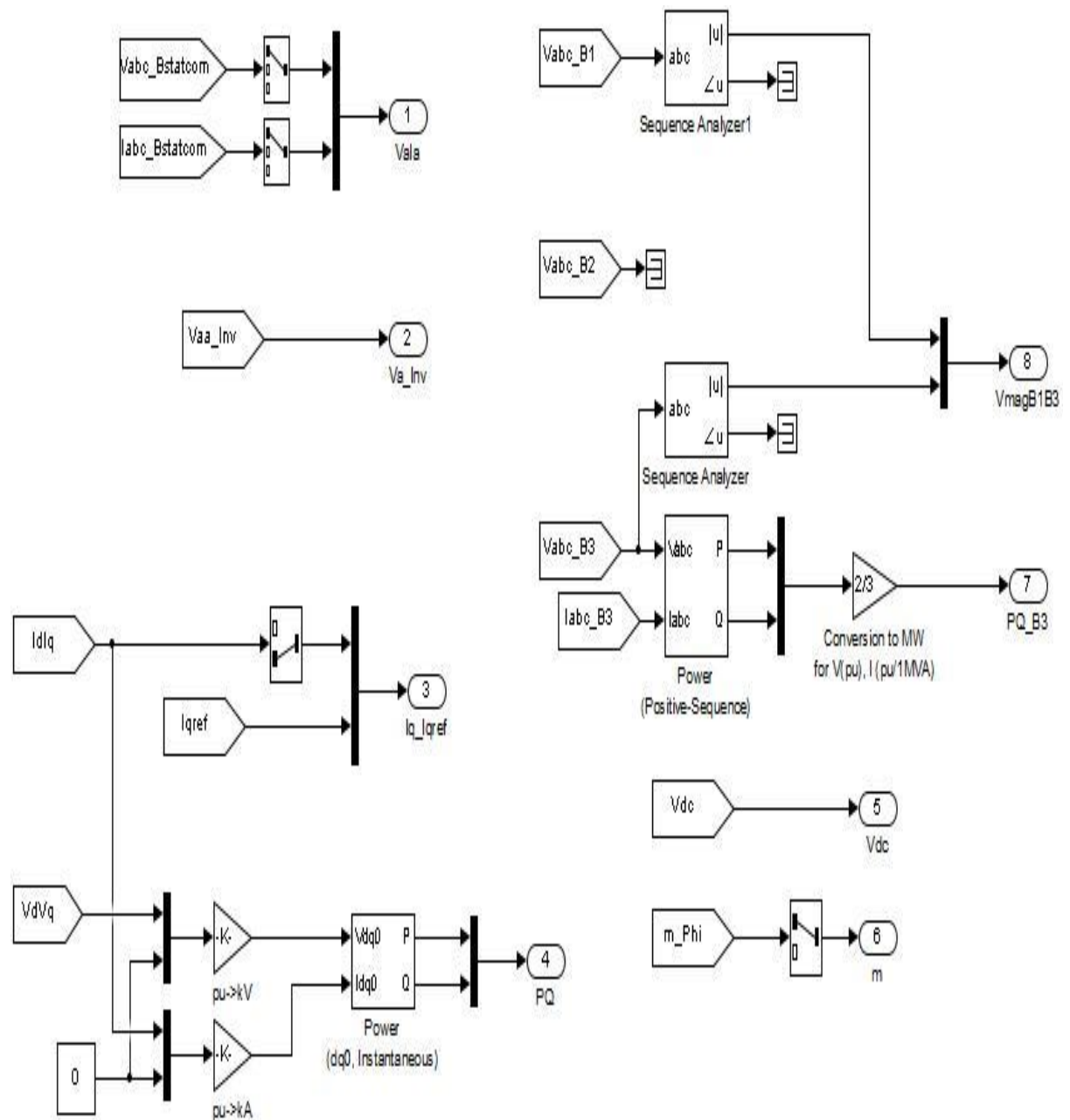


Figure B: Data acquisition

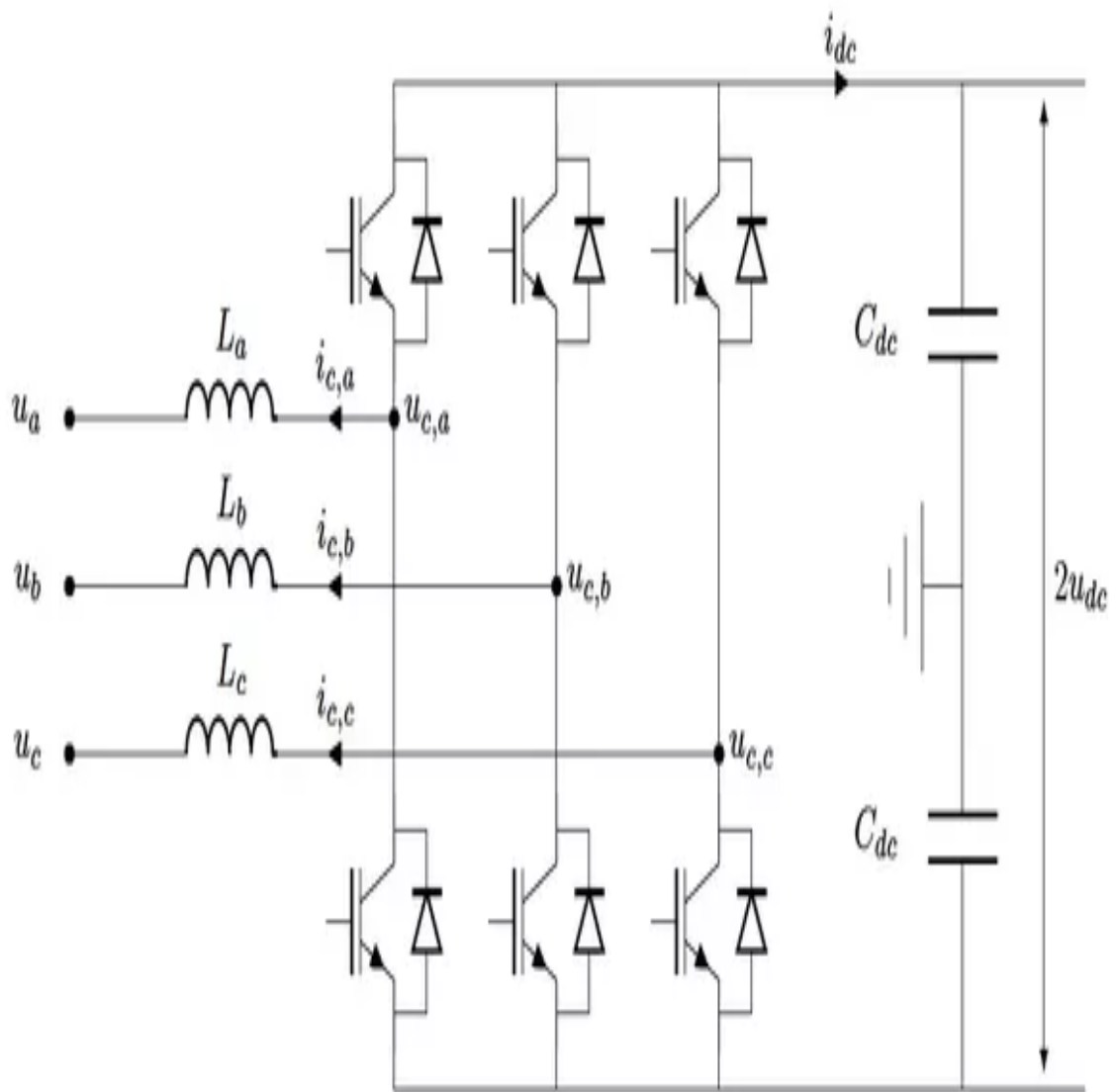


Figure C: Voltage source converter using integrated gate bipolar transistor (IGBT)

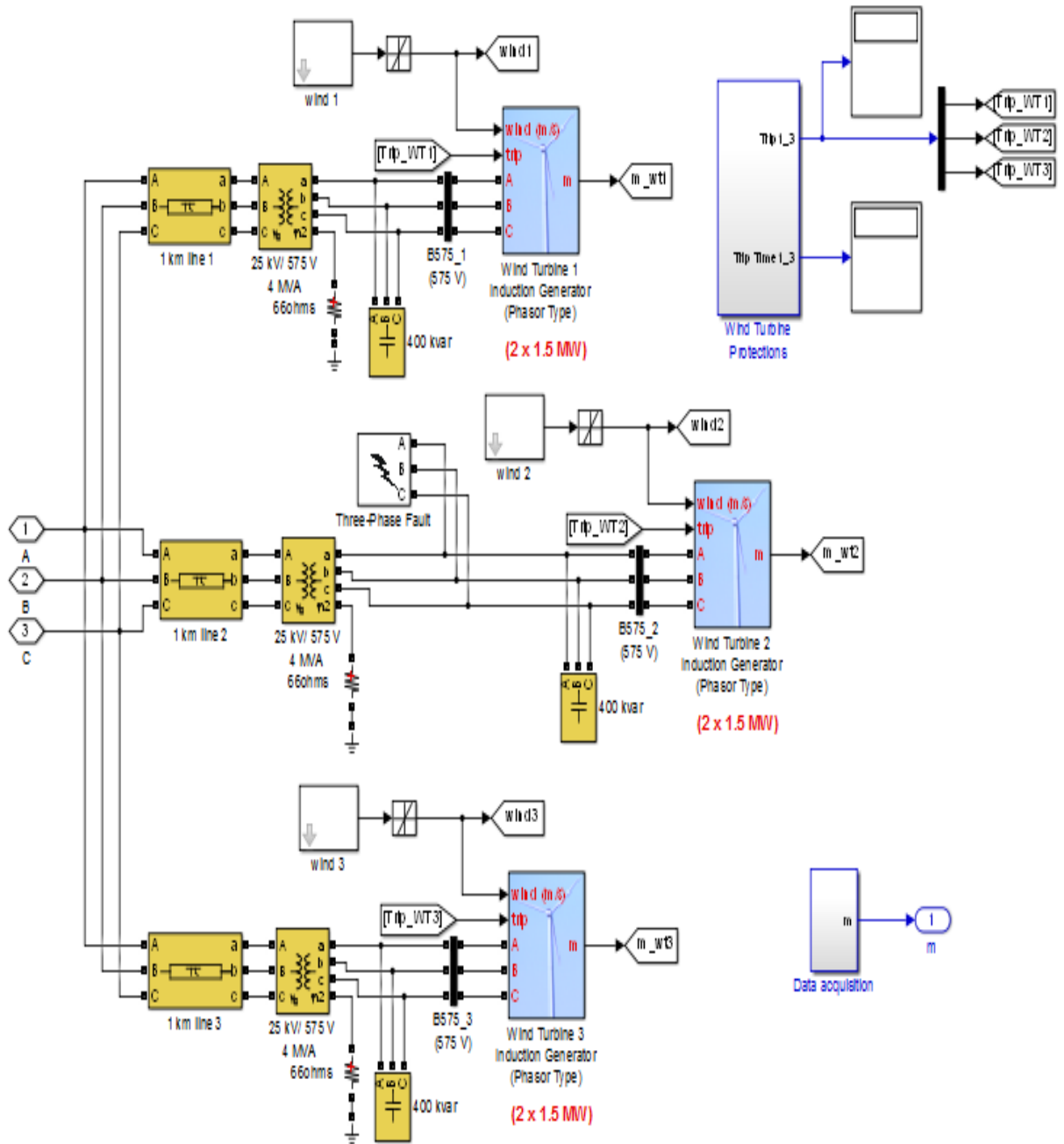


Figure D: Wind Turbine Internal components

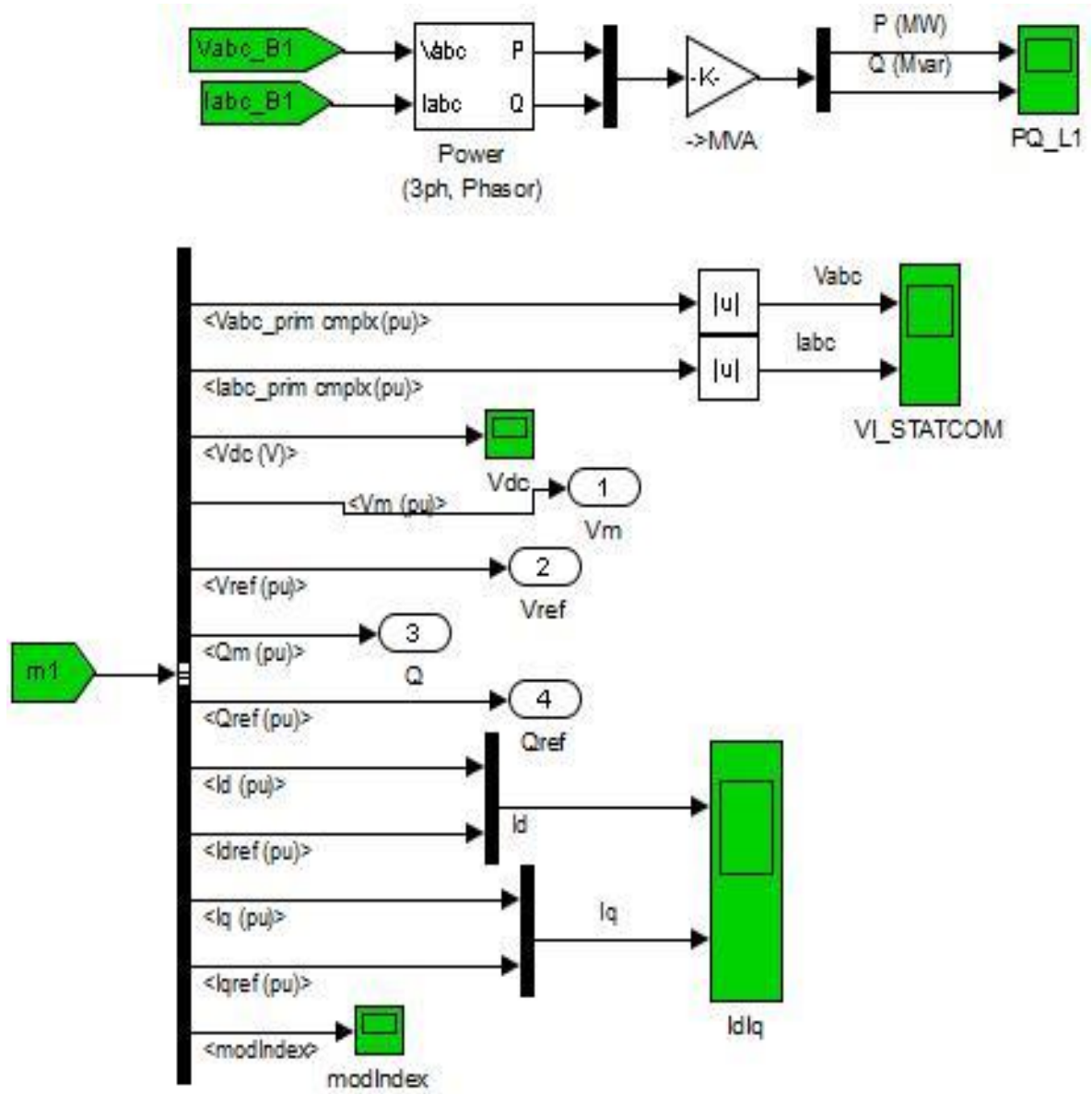


Figure E: STATCOM scopes and signals

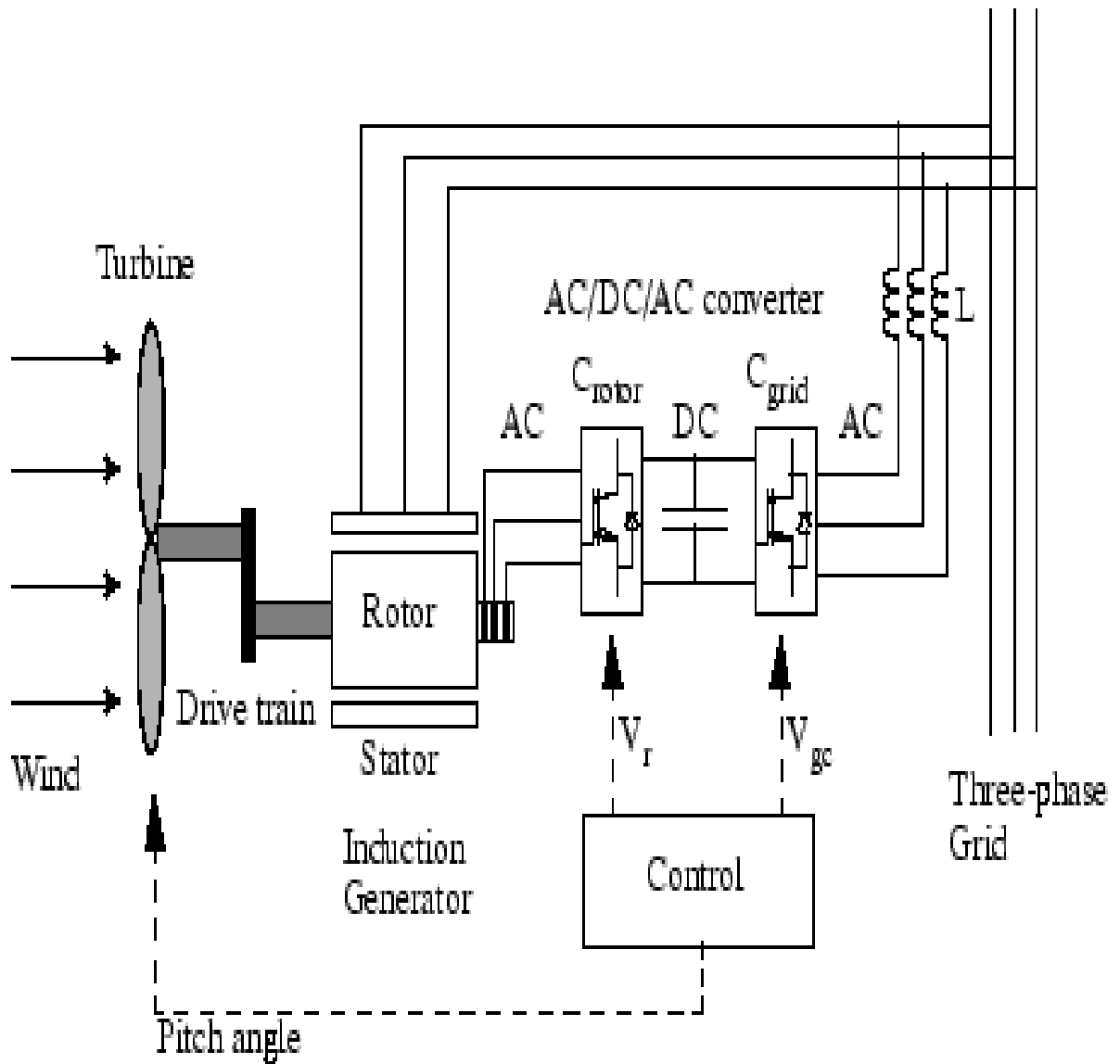
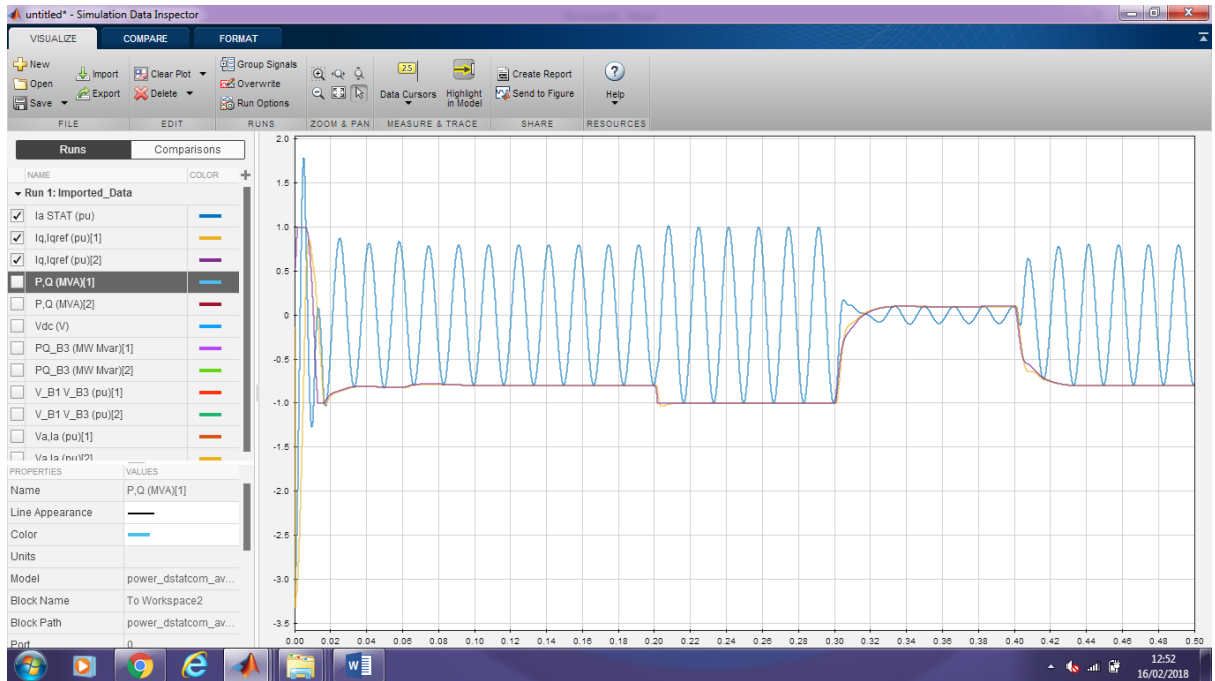
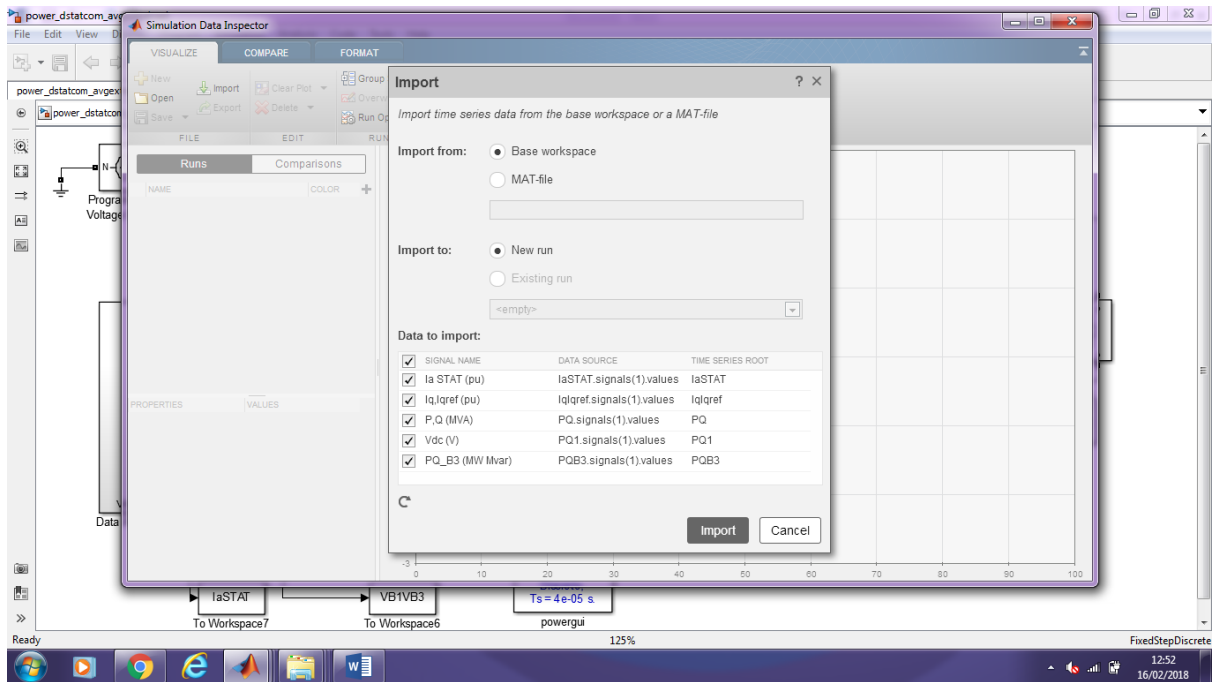
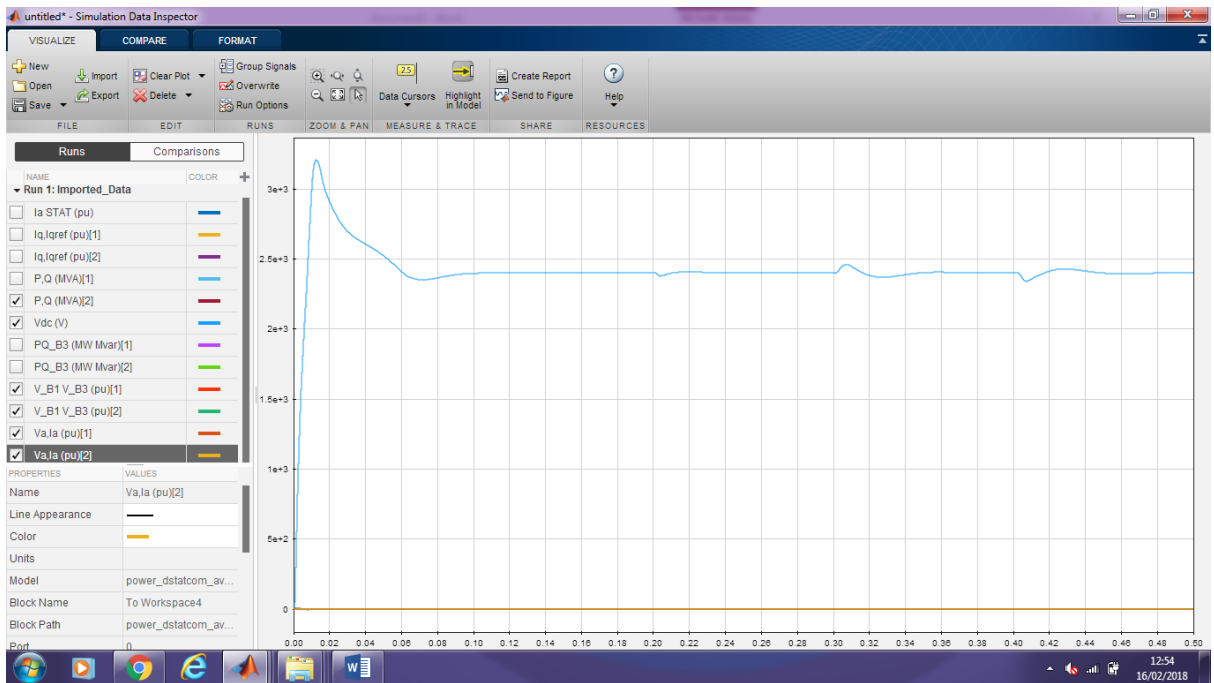
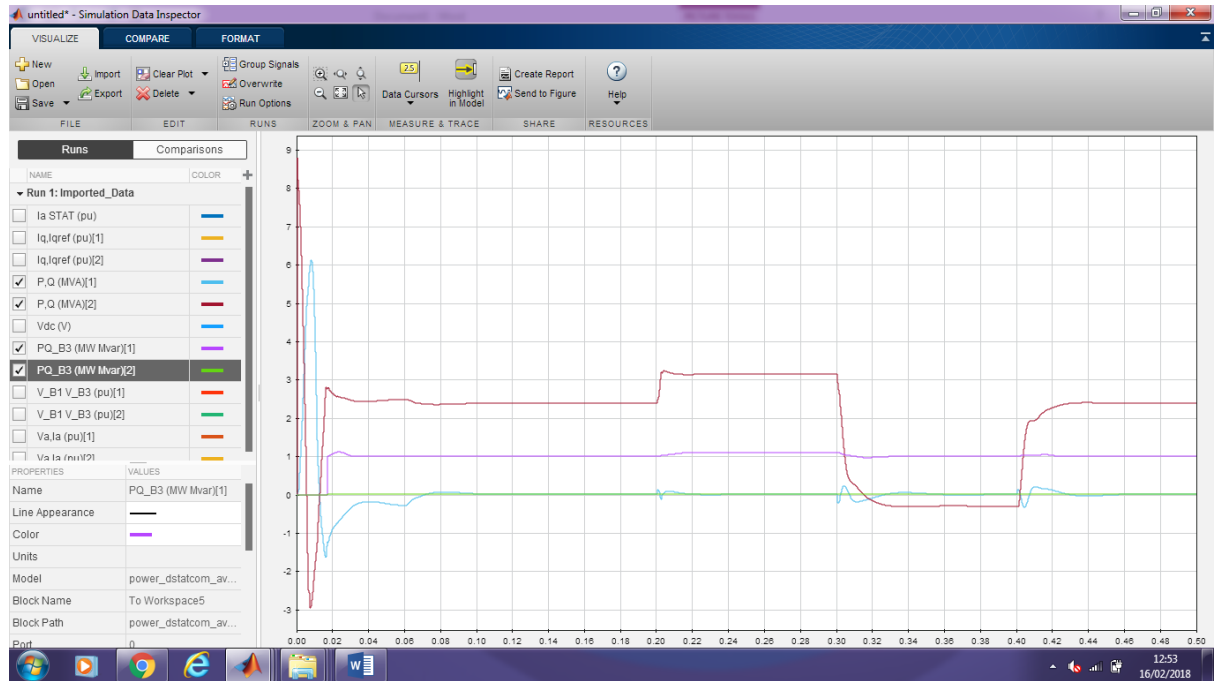


Figure F: Wind Turbine Doubly-Fed Induction Generator (Phasor Type)

SOME SCREENSHOTS OF SIMULATION





APPENDIX B MATLAB C-CODE

```
1  /*
2  * power_dstatcom_avgextraload_data.c
3  *
4  * Code generation for model "power_dstatcom_avgextraload".
5  *
6  * Model version : 1.630
7  * Simulink Coder version : 8.7 (R2014b) 08-Sep-2014
8  * C source code generated on : Fri Feb 16 14:05:55 2018
9  *
10 * Target selection: grt.tlc
11 * Note: GRT includes extra infrastructure and instrumentation for prototyping
12 * Embedded hardware selection: 32-bit Generic
13 * Emulation hardware selection:
14 * Differs from embedded hardware (MATLAB Host)
15 * Code generation objectives: Unspecified
16 * Validation result: Not run
17 */
18 #include "power_dstatcom_avgextraload.h"
19 #include "power_dstatcom_avgextraload_private.h"
20
21 /* Block parameters (auto storage) */
22 P_power_dstatcom_avgextraload T_power_dstatcom_avgextraload P = {
23 4.0E-5,
24 2.0,
25 2.0,
26 2.0,
27 2.0,
28 60.0,
29 60.0,
30 60.0,
31 60.0,
32 60.0,
33 60.0,
34 60.0,
35 60.0,
36 60.0,
37 60.0,
38 60.0,
39 60.0,
40 0.0,
41 376.99111843077515,
```

42 0.0,
43 2500.0,
44 200.0,
45 0.15,
46 0.55,
47 0.001,
48 0.8,
49 60.0,
50 -1.0,
51 -1.0,
52 -1.0,
53 -1.0,
54 4396.8340882958046,
55 3297.6255662218532,
56 1.0,
57 -25.0,
58 35.0,
59 0.0,
60 0.0,
61 2.0,
62 1.0,
63 1.0,
64 1.0,
65 2.0,
66 1.0,
67 1.0,
68 1.0,
69 1.0,
70 1.0,
71 1.0,
72 2.0,
73 2.0,
74 6595.2511324437064,
75 0.0,
76 219841.70441479021,
77 10992.085220739511,
78 4.0,
79 2400.0,
80 1.0,
81 2.0,
82 1.0,
83 2.0,
84 1.0,

85 2.0,
86 1.0,
87 2.0,
88 3.0,
89 2.0,
90 0.000133333333333336367,
91 -0.000666666666666672736,
92 0.000133333333333336367,
93 -0.000666666666666672736,
94 0.000133333333333336367,
95 -0.000666666666666672736,
96 0.000133333333333336367,
97 -0.000666666666666672736,
98 0.000133333333333336367,
99 -0.000666666666666672736,
100 0.000133333333333336367,
101 -0.000666666666666672736,
102 0.000133333333333336367,
103 -0.000666666666666672736,
104 0.000133333333333336367,
105 -0.000666666666666672736,
106 0.000133333333333336367,
107 -0.000666666666666672736,
108 0.000133333333333336367,
109 -0.000666666666666672736,
110 0.000133333333333336367,
111 -0.000666666666666672736,
112 0.000133333333333336367,
113 -0.000666666666666672736,
114 0.000133333333333336367,
115 -0.000666666666666672736,
116 0.000133333333333336367,
117 -0.000666666666666672736,
118 0.000133333333333336367,
119 -0.000666666666666672736,
120 0.000133333333333336367,
121 -0.000666666666666672736,
122 0.000133333333333336367,
123 -0.000666666666666672736,
124 0.000133333333333336367,
125 -0.000666666666666672736,
126 0.000133333333333336367,
127 -0.000666666666666672736,

128 0.000133333333333336367,
129 -0.000666666666666672736,
130 0.000133333333333336367,
131 -0.000666666666666672736,
132 0.000133333333333336367,
133 -0.000666666666666672736,
134 0.000133333333333336367,
135 -0.000666666666666672736,
136 0.000133333333333336367,
137 -0.000666666666666672736,
138 0.00019928995732989486,
139 2.5265371893206812,
140 9.9644978664947432E-5,
141 -1.0,
142 1.0,
143 -1.0,
144 1.0E-6,
145 0.5,
146 0.5,
147 1.0,
148
149 { 1.0, 0.0, 0.5, -0.5, 0.8660254037844386, 0.5, -0.5, -0.8660254037844386, 0.5
150 },
151 0.666666666666666663,
152 8.0E-5,
153 0.0,
154 1.0E+6,
155 2.2204460492503131E-16,
156
157 { 1.0, 1.0 },
158 0.02238222222222223,
159
160 { 1.0, 1.0 },
161 0.00016,
162
163 { 1.0, 1.0 },
164 0.0,
165
166 { 1.0, 1.0 },
167 1.0,
168 0.0,
169 0.016666666666666666,
170 1.0,

171 8.0E-5,
172 0.0,
173 1.0E+6,
174 2.2204460492503131E-16,
175
176 { 1.0, 1.0 },
177 0.022382222222222223,
178
179 { 1.0, 1.0 },
180 0.00016,
181
182 { 1.0, 1.0 },
183 0.0,
184
185 { 1.0, 1.0 },
186 1.0,
187 0.0,
188 0.016666666666666666,
189 0.0,
190 0.0,
191 2.2204460492503131E-16,
192 57.295779513082323,
193 0.5,
194
195 { 0.0, 2.0943951023931953, -2.0943951023931953 },
196
197 { 0.0, -2.0943951023931953, 2.0943951023931953 },
198
199 { 0.0, 0.0, 0.0 },
200
201 { 0.0, 2.0943951023931953, -2.0943951023931953 },
202
203 { 0.0, -2.0943951023931953, 2.0943951023931953 },
204
205 { 0.0, 0.0, 0.0 },
206 0.0,
207 0.0,
208 0.017453292519943295,
209 1.0,
210 0.05,
211 0.0,
212 1.0,
213 3.0,

214 0.0,
215 -1.0,
216 0.017453292519943295,
217 1.0,
218 0.0,
219 0.0,
220 0.017453292519943295,
221 0.0,
222 0.0,
223 0.0,
224 6.2831853071795862,
225 0.0,
226 1.0,
227 2.0,
228 0.5,
229 0.0,
230 0.0,
231 0.0,
232 0.0,
233 0.0,
234
235 { -1.0, 0.0, 0.2, 0.2, 0.3, 0.3, 0.4, 0.4, 1.4 },
236
237 { 21984.170441479022, 21984.170441479022, 21984.170441479022,
238 23303.220667967766, 23303.220667967766, 20665.120214990278,
239 20665.120214990278, 21984.170441479022, 21984.170441479022 },
240 2.0,
241 3.0,
242 4.0,
243 4.0,
244 4.0E-5,
245 0.0,
246 1.0,
247 0.0,
248 1.0,
249 0.0,
250 1.0,
251 4.0E-5,
252 0.0,
253 0.0,
254 0.5,
255 0.5,
256 6.2831853071795862,

257 0.5,
258 0.5,
259 0.5,
260 1.0,
261 0.5,
262 0.5,
263 0.5,
264
265 { 0.0, 0.0, 0.0 },
266 0.0,
267 0.017453292519943295,
268
269 { 0.0, -2.0943951023931953, 2.0943951023931953 },
270 4.0E-5,
271 0.0,
272 6.2831853071795862,
273 0.0,
274 0.5,
275 1.0E-6,
276 -1.0,
277 0.0,
278 0.5,
279 1.0E-6,
280 21984.170441479022,
281 0.5,
282 0.5,
283 60.0,
284 6.2831853071795862,
285 19.0,
286 0.017453292519943295,
287
288 { 0.0, -2.0943951023931953, 2.0943951023931953 },
289 1.0,
290 1.0,
291 1.0,
292 4.8989794855663556E-5,
293 1.0,
294 1.0,
295 1.0,
296 0.010206207261596574,
297 1.0,
298 0.04613357228799779,
299 0.0,

300 6288.2526877556757,
301 0.0,
302 0.09226714457599558,
303
304 { 1.0, 0.0, 0.5, -0.5, 0.8660254037844386, 0.5, -0.5, -0.8660254037844386, 0.5
305 },
306 0.66666666666666663,
307 0.00016,
308 0.064577182323790186,
309 6.2831853071795862,
310 0.04613357228799779,
311 0.0,
312 6288.2526877556757,
313 0.0,
314 0.09226714457599558,
315
316 { 1.0, 0.0, 0.5, -0.5, 0.8660254037844386, 0.5, -0.5, -0.8660254037844386, 0.5
317 },
318 0.66666666666666663,
319 0.00016,
320 0.0,
321 1.0,
322 0.019200000000000002,
323 -0.019200000000000002,
324 0.0,
325 0.0,
326 0.0,
327 0.0,
328 0.0,
329 0.0,
330 0.0,
331 20.412414523193149,
332 0.097979589711327114,
333 2.0,
334 1.5,
335 1.5,
336 1.0,
337 3750.0,
338 2250.0,
339 1.6,
340 -1.6,
341 3000.0,
342 0.04613357228799779,

343 0.0,
344 6288.2526877556757,
345 0.0,
346 0.09226714457599558,
347 0.00016,
348 0.0,
349 1.0,
350 -1.0,
351 0.038400000000000004,
352 -0.038400000000000004,
353 0.0,
354 0.00016,
355 0.0,
356 0.00016,
357 0.0,
358 1.0,
359 1.0,
360 1.0,
361 4.8989794855663556E-5,
362 2.0,
363 0.0,
364 0.015079073236037119,
365 0.99988630431181635,
366 -0.015079073236037119,
367 0.99988630431181635,
368 2.0E-5,
369 0.0,
370 0.01668,
371
372 { 1.0, 1.0 },
373 0.01676,
374
375 { 1.0, 1.0 },
376 4.0E-5,
377
378 { 1.0, 1.0 },
379 0.0,
380
381 { 1.0, 1.0 },
382 1.0,
383 60.0,
384 0.0,
385 1.0,

386 2.0,
387 0.0,
388 0.015079073236037119,
389 0.99988630431181635,
390 0.99988630431181635,
391 0.015079073236037176,
392 2.0E-5,
393 0.0,
394 0.01668,
395
396 { 1.0, 1.0 },
397 0.01676,
398
399 { 1.0, 1.0 },
400 4.0E-5,
401
402 { 1.0, 1.0 },
403 0.0,
404
405 { 1.0, 1.0 },
406 1.0,
407 60.0,
408 0.0,
409 0.0,
410 57.295779513082323,
411 0.017453292519943295,
412 2.0,
413 0.0,
414 0.015079073236037119,
415 0.99988630431181635,
416 -0.015079073236037119,
417 0.99988630431181635,
418 2.0E-5,
419 0.0,
420 0.01668,
421
422 { 1.0, 1.0 },
423 0.01676,
424
425 { 1.0, 1.0 },
426 4.0E-5,
427
428 { 1.0, 1.0 },

429 0.0,
430
431 { 1.0, 1.0 },
432 1.0,
433 60.0,
434 0.0,
435 -0.49999999999999978,
436 2.0,
437 0.0,
438 0.015079073236037119,
439 0.99988630431181635,
440 0.99988630431181635,
441 0.015079073236037176,
442 2.0E-5,
443 0.0,
444 0.01668,
445
446 { 1.0, 1.0 },
447 0.01676,
448
449 { 1.0, 1.0 },
450 4.0E-5,
451
452 { 1.0, 1.0 },
453 0.0,
454
455 { 1.0, 1.0 },
456 1.0,
457 60.0,
458 0.0,
459 -0.86602540378443871,
460 57.295779513082323,
461 0.017453292519943295,
462 2.0,
463 0.0,
464 0.015079073236037119,
465 0.99988630431181635,
466 -0.015079073236037119,
467 0.99988630431181635,
468 2.0E-5,
469 0.0,
470 0.01668,
471

472 { 1.0, 1.0 },
473 0.01676,
474
475 { 1.0, 1.0 },
476 4.0E-5,
477
478 { 1.0, 1.0 },
479 0.0,
480
481 { 1.0, 1.0 },
482 1.0,
483 60.0,
484 0.0,
485 -0.49999999999999978,
486 2.0,
487 0.0,
488 0.015079073236037119,
489 0.99988630431181635,
490 0.99988630431181635,
491 0.015079073236037176,
492 2.0E-5,
493 0.0,
494 0.01668,
495
496 { 1.0, 1.0 },
497 0.01676,
498
499 { 1.0, 1.0 },
500 4.0E-5,
501
502 { 1.0, 1.0 },
503 0.0,
504
505 { 1.0, 1.0 },
506 1.0,
507 60.0,
508 0.0,
509 0.86602540378443871,
510 57.295779513082323,
511 0.017453292519943295,
512 1.0,
513 0.0,
514 0.0,

515 1.0,
516 1.0,
517 1.0,
518 0.030618621784789725,
519 2.0,
520 0.0,
521 0.015079073236037119,
522 0.99988630431181635,
523 -0.015079073236037119,
524 0.99988630431181635,
525 2.0E-5,
526 0.0,
527 0.01668,
528
529 { 1.0, 1.0 },
530 0.01676,
531
532 { 1.0, 1.0 },
533 4.0E-5,
534
535 { 1.0, 1.0 },
536 0.0,
537
538 { 1.0, 1.0 },
539 1.0,
540 60.0,
541 0.0,
542 0.0,
543 2.0,
544 0.0,
545 0.015079073236037119,
546 0.99988630431181635,
547 0.99988630431181635,
548 0.015079073236037176,
549 2.0E-5,
550 0.0,
551 0.01668,
552
553 { 1.0, 1.0 },
554 0.01676,
555
556 { 1.0, 1.0 },
557 4.0E-5,

558
559 { 1.0, 1.0 },
560 0.0,
561
562 { 1.0, 1.0 },
563 1.0,
564 60.0,
565 0.0,
566 0.0,
567 57.295779513082323,
568 0.017453292519943295,
569 2.0,
570 0.0,
571 0.015079073236037119,
572 0.99988630431181635,
573 -0.015079073236037119,
574 0.99988630431181635,
575 2.0E-5,
576 0.0,
577 0.01668,
578
579 { 1.0, 1.0 },
580 0.01676,
581
582 { 1.0, 1.0 },
583 4.0E-5,
584
585 { 1.0, 1.0 },
586 0.0,
587
588 { 1.0, 1.0 },
589 1.0,
590 60.0,
591 0.0,
592 -0.0,
593 2.0,
594 0.0,
595 0.015079073236037119,
596 0.99988630431181635,
597 0.99988630431181635,
598 0.015079073236037176,
599 2.0E-5,
600 0.0,

601 0.01668,
602
603 { 1.0, 1.0 },
604 0.01676,
605
606 { 1.0, 1.0 },
607 4.0E-5,
608
609 { 1.0, 1.0 },
610 0.0,
611
612 { 1.0, 1.0 },
613 1.0,
614 60.0,
615 0.0,
616 -0.0,
617 57.295779513082323,
618 0.017453292519943295,
619 2.0,
620 0.0,
621 0.015079073236037119,
622 0.99988630431181635,
623 -0.015079073236037119,
624 0.99988630431181635,
625 2.0E-5,
626 0.0,
627 0.01668,
628
629 { 1.0, 1.0 },
630 0.01676,
631
632 { 1.0, 1.0 },
633 4.0E-5,
634
635 { 1.0, 1.0 },
636 0.0,
637
638 { 1.0, 1.0 },
639 1.0,
640 60.0,
641 0.0,
642 -0.0,
643 2.0,

644 0.0,
645 0.015079073236037119,
646 0.99988630431181635,
647 0.99988630431181635,
648 0.015079073236037176,
649 2.0E-5,
650 0.0,
651 0.01668,
652
653 { 1.0, 1.0 },
654 0.01676,
655
656 { 1.0, 1.0 },
657 4.0E-5,
658
659 { 1.0, 1.0 },
660 0.0,
661
662 { 1.0, 1.0 },
663 1.0,
664 60.0,
665 0.0,
666 0.0,
667 57.295779513082323,
668 0.017453292519943295,
669 1.0,
670 0.0,
671 0.0,
672 1.5,
673 57.295779513082323,
674 57.295779513082323,
675 0.017453292519943295,
676 0.666666666666666663,
677 1.0,
678 1.0,
679 1.0,
680 4.8989794855663556E-5,
681 2.0,
682 0.0,
683 0.015079073236037119,
684 0.99988630431181635,
685 -0.015079073236037119,
686 0.99988630431181635,

687 2.0E-5,
688 0.0,
689 0.01668,
690
691 { 1.0, 1.0 },
692 0.01676,
693
694 { 1.0, 1.0 },
695 4.0E-5,
696
697 { 1.0, 1.0 },
698 0.0,
699
700 { 1.0, 1.0 },
701 1.0,
702 60.0,
703 0.0,
704 1.0,
705 2.0,
706 0.0,
707 0.015079073236037119,
708 0.99988630431181635,
709 0.99988630431181635,
710 0.015079073236037176,
711 2.0E-5,
712 0.0,
713 0.01668,
714
715 { 1.0, 1.0 },
716 0.01676,
717
718 { 1.0, 1.0 },
719 4.0E-5,
720
721 { 1.0, 1.0 },
722 0.0,
723
724 { 1.0, 1.0 },
725 1.0,
726 60.0,
727 0.0,
728 0.0,
729 57.295779513082323,

730 0.017453292519943295,
731 2.0,
732 0.0,
733 0.015079073236037119,
734 0.99988630431181635,
735 -0.015079073236037119,
736 0.99988630431181635,
737 2.0E-5,
738 0.0,
739 0.01668,
740
741 { 1.0, 1.0 },
742 0.01676,
743
744 { 1.0, 1.0 },
745 4.0E-5,
746
747 { 1.0, 1.0 },
748 0.0,
749
750 { 1.0, 1.0 },
751 1.0,
752 60.0,
753 0.0,
754 -0.49999999999999978,
755 2.0,
756 0.0,
757 0.015079073236037119,
758 0.99988630431181635,
759 0.99988630431181635,
760 0.015079073236037176,
761 2.0E-5,
762 0.0,
763 0.01668,
764
765 { 1.0, 1.0 },
766 0.01676,
767
768 { 1.0, 1.0 },
769 4.0E-5,
770
771 { 1.0, 1.0 },
772 0.0,

773
774 { 1.0, 1.0 },
775 1.0,
776 60.0,
777 0.0,
778 -0.86602540378443871,
779 57.295779513082323,
780 0.017453292519943295,
781 2.0,
782 0.0,
783 0.015079073236037119,
784 0.99988630431181635,
785 -0.015079073236037119,
786 0.99988630431181635,
787 2.0E-5,
788 0.0,
789 0.01668,
790
791 { 1.0, 1.0 },
792 0.01676,
793
794 { 1.0, 1.0 },
795 4.0E-5,
796
797 { 1.0, 1.0 },
798 0.0,
799
800 { 1.0, 1.0 },
801 1.0,
802 60.0,
803 0.0,
804 -0.49999999999999978,
805 2.0,
806 0.0,
807 0.015079073236037119,
808 0.99988630431181635,
809 0.99988630431181635,
810 0.015079073236037176,
811 2.0E-5,
812 0.0,
813 0.01668,
814
815 { 1.0, 1.0 },

816 0.01676,
817
818 { 1.0, 1.0 },
819 4.0E-5,
820
821 { 1.0, 1.0 },
822 0.0,
823
824 { 1.0, 1.0 },
825 1.0,
826 60.0,
827 0.0,
828 0.86602540378443871,
829 57.295779513082323,
830 0.017453292519943295,
831 1.0,
832 0.0,
833 0.0,
834 2.0,
835 0.0,
836 0.015079073236037119,
837 0.99988630431181635,
838 -0.015079073236037119,
839 0.99988630431181635,
840 2.0E-5,
841 0.0,
842 0.01668,
843
844 { 1.0, 1.0 },
845 0.01676,
846
847 { 1.0, 1.0 },
848 4.0E-5,
849
850 { 1.0, 1.0 },
851 0.0,
852
853 { 1.0, 1.0 },
854 1.0,
855 60.0,
856 0.0,
857 1.0,
858 2.0,

859 0.0,
860 0.015079073236037119,
861 0.99988630431181635,
862 0.99988630431181635,
863 0.015079073236037176,
864 2.0E-5,
865 0.0,
866 0.01668,
867
868 { 1.0, 1.0 },
869 0.01676,
870
871 { 1.0, 1.0 },
872 4.0E-5,
873
874 { 1.0, 1.0 },
875 0.0,
876
877 { 1.0, 1.0 },
878 1.0,
879 60.0,
880 0.0,
881 0.0,
882 57.295779513082323,
883 0.017453292519943295,
884 2.0,
885 0.0,
886 0.015079073236037119,
887 0.99988630431181635,
888 -0.015079073236037119,
889 0.99988630431181635,
890 2.0E-5,
891 0.0,
892 0.01668,
893
894 { 1.0, 1.0 },
895 0.01676,
896
897 { 1.0, 1.0 },
898 4.0E-5,
899
900 { 1.0, 1.0 },
901 0.0,

902
903 { 1.0, 1.0 },
904 1.0,
905 60.0,
906 0.0,
907 -0.49999999999999978,
908 2.0,
909 0.0,
910 0.015079073236037119,
911 0.99988630431181635,
912 0.99988630431181635,
913 0.015079073236037176,
914 2.0E-5,
915 0.0,
916 0.01668,
917
918 { 1.0, 1.0 },
919 0.01676,
920
921 { 1.0, 1.0 },
922 4.0E-5,
923
924 { 1.0, 1.0 },
925 0.0,
926
927 { 1.0, 1.0 },
928 1.0,
929 60.0,
930 0.0,
931 -0.86602540378443871,
932 57.295779513082323,
933 0.017453292519943295,
934 2.0,
935 0.0,
936 0.015079073236037119,
937 0.99988630431181635,
938 -0.015079073236037119,
939 0.99988630431181635,
940 2.0E-5,
941 0.0,
942 0.01668,
943
944 { 1.0, 1.0 },

945 0.01676,
946
947 { 1.0, 1.0 },
948 4.0E-5,
949
950 { 1.0, 1.0 },
951 0.0,
952
953 { 1.0, 1.0 },
954 1.0,
955 60.0,
956 0.0,
957 -0.49999999999999978,
958 2.0,
959 0.0,
960 0.015079073236037119,
961 0.99988630431181635,
962 0.99988630431181635,
963 0.015079073236037176,
964 2.0E-5,
965 0.0,
966 0.01668,
967
968 { 1.0, 1.0 },
969 0.01676,
970
971 { 1.0, 1.0 },
972 4.0E-5,
973
974 { 1.0, 1.0 },
975 0.0,
976
977 { 1.0, 1.0 },
978 1.0,
979 60.0,
980 0.0,
981 0.86602540378443871,
982 57.295779513082323,
983 0.017453292519943295,
984 1.0,
985 0.0,
986 0.0,
987 57.295779513082323,

988 57.295779513082323,
989 1.0,
990 1.0,
991 1.0,
992 1.0,
993 1.0,
994 4.8989794855663556E-5,
995 1.0E-6,
996 2.0,
997 0.0,
998 1.0E-6,
999 2.0,
1000 0.0,
1001 0.90773285542400439,
1002 2.7992046745597148E-5,
1003 -4613.35722879979,
1004 0.39960233727985828,
1005 1.3996023372798549E-5,
1006 0.69980116863992914,
1007 0.90773285542400439,
1008 2.7992046745597148E-5,
1009 -4613.35722879979,
1010 0.39960233727985828,
1011 1.3996023372798549E-5,
1012 0.69980116863992914,
1013 0.90773285542400439,
1014 2.7992046745597148E-5,
1015 -4613.35722879979,
1016 0.39960233727985828,
1017 1.3996023372798549E-5,
1018 0.69980116863992914,
1019 0.0,
1020 0.0,
1021 0.0,
1022 0.0,
1023 0.0,
1024 0.0,
1025 0.0,
1026 0.0,
1027 0.0,
1028 0.0,
1029 0.0,
1030 0.0,

1031 60.0,
1032 6.2831853071795862,
1033 0.99980071004267,
1034 0.00015774167103394866,
1035 -2.4911244666256942,
1036 0.97177088792514166,
1037 7.8870835516942073E-5,
1038 0.98588544396257083,
1039 0.0,
1040
1041 { 0.0001, 6.0000000000000008E-5 },
1042 0.0,
1043 0.224,
1044 0.0,
1045 0.0,
1046
1047 { 1.0, 0.0, 0.5, -0.5, 0.8660254037844386, 0.5, -0.5, -0.8660254037844386, 0.5
1048 },
1049 0.66666666666666663,
1050 8.0E-5,
1051 0.0,
1052 1.0E+6,
1053 2.2204460492503131E-16,
1054
1055 { 1.0, 1.0 },
1056 0.02238222222222223,
1057
1058 { 1.0, 1.0 },
1059 0.00016,
1060
1061 { 1.0, 1.0 },
1062 0.0,
1063
1064 { 1.0, 1.0 },
1065 1.0,
1066 0.0,
1067 0.016666666666666666,
1068 0.0,
1069 0.0,
1070 0.0,
1071 0.15915494309189535,
1072 0.0016,
1073 -0.0016,

1074 60.0,
1075 15.196577571617487,
1076 0.99968970233492693,
1077 0.0,
1078 0.00015718208458581496,
1079 -3.8787208134131435,
1080 0.96477605732267058,
1081 7.8591042292908142E-5,
1082 0.98238802866133523,
1083 0.00015514883253652835,
1084 3.9476448422236783,
1085 0.0003102976650730567,
1086 0.0,
1087 0.0,
1088 2.0,
1089 0.0,
1090 0.0,
1091 0.0,
1092
1093 { 0.0, 0.016626666666666672, 0.016626666666666672, 0.083293333333333344,
1094 0.083293333333333344, 1.0832933333333334 },
1095
1096 { 0.0, 0.0, 1.0, 1.0, 0.0, 0.0 },
1097 0.5,
1098 0.0,
1099 1.0,
1100
1101 { 0.0, 999999.99996000016, 999999.99996000016, 1.0000009999600002E+6 },
1102
1103 { 0.0, 0.0, 0.0, 0.0 },
1104 0.5,
1105 1.5,
1106 0.0,
1107 1.0,
1108 0.0,
1109 0.0,
1110 0.0,
1111 2.0,
1112 0.0,
1113 0.0,
1114 1.0,
1115
1116 { 0.0, 999999.99996000016, 999999.99996000016, 1.0000009999600002E+6 },

```

1117
1118 { 0.0, 0.0, 0.0, 0.0 },
1119 0.5,
1120 1.5,
1121 0.0,
1122 1.0,
1123 0.0,
1124 0.0,
1125 0.0,
1126 2.0,
1127 0.0,
1128 0.0,
1129 1.0,
1130
1131 { 0.0, 999999.99996000016, 999999.99996000016, 1.0000009999600002E+6 },
1132
1133 { 0.0, 0.0, 0.0, 0.0 },
1134 0.5,
1135 1.5,
1136 0.0,
1137 1.0,
1138 0.0,
1139 0.0,
1140
1141 /* Start of '<S260>/Subsystem1' */
1142 {
1143 { 0.0, 0.0 }
1144 }
1145 /* End of '<S260>/Subsystem1' */
1146 ,
1147
1148 /* Start of '<S260>/Subsystem - pi//2 delay' */
1149 {
1150 { 0.0, 0.0 }
1151 }
1152 /* End of '<S260>/Subsystem - pi//2 delay' */
1153 ,
1154
1155 /* Start of '<S247>/Subsystem1' */
1156 {
1157 { 0.0, 0.0 }
1158 }
1159 /* End of '<S247>/Subsystem1' */

```

```

1160 ,
1161
1162 /* Start of '<S247>/Subsystem - pi//2 delay' */
1163 {
1164 { 0.0, 0.0 }
1165 }
1166 /* End of '<S247>/Subsystem - pi//2 delay' */
1167 ,
1168
1169 /* Start of '<S225>/Subsystem1' */
1170 {
1171 { 0.0, 0.0 }
1172 }
1173 /* End of '<S225>/Subsystem1' */
1174 ,
1175
1176 /* Start of '<S225>/Subsystem - pi//2 delay' */
1177 {
1178 { 0.0, 0.0 }
1179 }
1180 /* End of '<S225>/Subsystem - pi//2 delay' */
1181 ,
1182
1183 /* Start of '<S219>/Subsystem1' */
1184 {
1185 { 0.0, 0.0 }
1186 }
1187 /* End of '<S219>/Subsystem1' */
1188 ,
1189
1190 /* Start of '<S219>/Subsystem - pi//2 delay' */
1191 {
1192 { 0.0, 0.0 }
1193 }
1194 /* End of '<S219>/Subsystem - pi//2 delay' */
1195 ,
1196
1197 /* Start of '<S67>/Zero Seq. Computation' */
1198 {
1199 0.33333333333333331
1200 }
1201 /* End of '<S67>/Zero Seq. Computation' */
1202 ,

```

```

1203
1204 /* Start of '<S67>/Pos. Seq. Computation' */
1205 {
1206 0.33333333333333331,
1207
1208 { { 1.0, 0.0 }, { -0.49999999999999978, 0.86602540378443871 }, { -
1209 0.49999999999999978, -0.86602540378443871 } }
1210 }
1211 /* End of '<S67>/Pos. Seq. Computation' */
1212 ,
1213
1214 /* Start of '<S67>/Neg. Seq. Computation' */
1215 {
1216 0.33333333333333331,
1217
1218 { { 1.0, 0.0 }, { -0.49999999999999978, -0.86602540378443871 }, { -
1219 0.49999999999999978, 0.86602540378443871 } }
1220 }
1221 /* End of '<S67>/Neg. Seq. Computation' */
1222 ,
1223
1224 /* Start of '<S66>/Zero Seq. Computation' */
1225 {
1226 0.33333333333333331
1227 }
1228 /* End of '<S66>/Zero Seq. Computation' */
1229 ,
1230
1231 /* Start of '<S66>/Pos. Seq. Computation' */
1232 {
1233 0.33333333333333331,
1234
1235 { { 1.0, 0.0 }, { -0.49999999999999978, 0.86602540378443871 }, { -
1236 0.49999999999999978, -0.86602540378443871 } }
1237 }
1238 /* End of '<S66>/Pos. Seq. Computation' */
1239 ,
1240
1241 /* Start of '<S66>/Neg. Seq. Computation' */
1242 {
1243 0.33333333333333331,
1244
1245 { { 1.0, 0.0 }, { -0.49999999999999978, -0.86602540378443871 }, { -

```

```

1246 0.49999999999999978, 0.86602540378443871 } }
1247 }
1248 /* End of '<S66>/Neg. Seq. Computation' */
1249 ,
1250
1251 /* Start of '<S69>/Zero Seq. Computation' */
1252 {
1253 0.33333333333333331
1254 }
1255 /* End of '<S69>/Zero Seq. Computation' */
1256 ,
1257
1258 /* Start of '<S69>/Pos. Seq. Computation' */
1259 {
1260 0.33333333333333331,
1261
1262 { { 1.0, 0.0 }, { -0.49999999999999978, 0.86602540378443871 }, { -
1263 0.49999999999999978, -0.86602540378443871 } }
1264 }
1265 /* End of '<S69>/Pos. Seq. Computation' */
1266 ,
1267
1268 /* Start of '<S69>/Neg. Seq. Computation' */
1269 {
1270 0.33333333333333331,
1271
1272 { { 1.0, 0.0 }, { -0.49999999999999978, -0.86602540378443871 }, { -
1273 0.49999999999999978, 0.86602540378443871 } }
1274 }
1275 /* End of '<S69>/Neg. Seq. Computation' */
1276 ,
1277
1278 /* Start of '<S68>/Zero Seq. Computation' */
1279 {
1280 0.33333333333333331
1281 }
1282 /* End of '<S68>/Zero Seq. Computation' */
1283 ,
1284
1285 /* Start of '<S68>/Pos. Seq. Computation' */
1286 {
1287 0.33333333333333331,
1288

```



```
1289 { { 1.0, 0.0 }, { -0.4999999999999978, 0.86602540378443871 }, { -
1290 0.4999999999999978, -0.86602540378443871 } }
1291 }
1292 /* End of '<S68>/Pos. Seq. Computation' */
1293 ,
1294
1295 /* Start of '<S68>/Neg. Seq. Computation' */
1296 {
1297 0.33333333333333331,
1298
1299 { { 1.0, 0.0 }, { -0.4999999999999978, -0.86602540378443871 }, { -
1300 0.4999999999999978, 0.86602540378443871 } }
1301 }
1302 /* End of '<S68>/Neg. Seq. Computation' */
1303 };
1304
```